The influence of mangroves on coastline stability

MSc thesis

Anais Wens

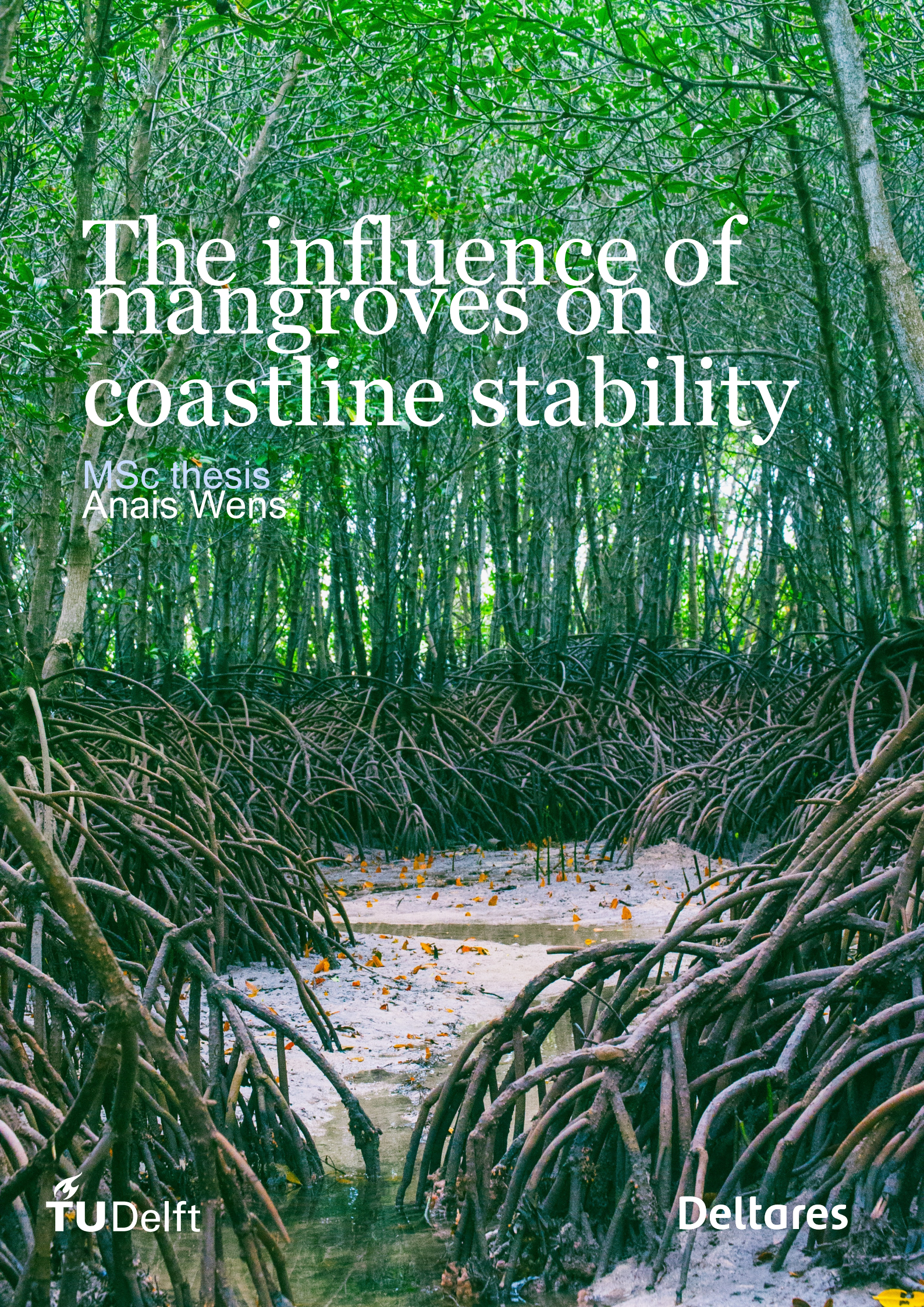

TU Delft

Deltares

The cover image shows a mangrove forest in South America. The photo was found on: https://www.pexels.com/photo/a-mangrove-forest-13035525/.

The influence of mangroves on coastline stability

MSc thesis

by

Anais Wens

to obtain the degree of Master of Science
at the Delft University of Technology,

Student number: 4917049
Project duration: September, 2023 – June, 2024
Thesis committee: Dr. B. van Wesenbeeck, TU Delft/ Deltares (Chair)
Dr. Ir. J. Timmermans, TU Delft
Ir. V. T. M. van Zelst, TU Delft/ Deltares

TU Delft Deltares

Preface

In this report, I present the findings of my research into the effect of mangroves on coastline stability. This thesis was written in order to meet the requirements to obtain the degree of Master of Science in Hydraulic Engineering at Delft University of Technology. The report was conducted in collaboration with Deltares.

Firstly, I would like to express my gratitude to my supervisors, Vincent van Zelst, Bregje van Wesenbeeck, and Joris Timmermans, for their invaluable guidance and support throughout this research. Specifically, I would like to thank Mr. van Zelst for the weekly supervision sessions and the excellent guidance provided during those meetings. I am also deeply grateful to Mrs. van Wesenbeeck for her insightful feedback and her encouragement to think critically and creatively about the research challenges. Lastly, I truly appreciate Dhr. Timmermans for his continuous support and for offering valuable perspectives that significantly enhanced the quality of this work.

I also want to thank my parents for their endless support, patience, and belief in me. Their support and guidance have played a crucial role in my achievements. Furthermore, I want to extend my sincerest thanks to my best friends, Martin and Lucas, for their friendship and motivation and for always being there to lift my spirits. Your support has meant the world to me. Finally, I'm truly grateful to my boyfriend for his constant support and understanding during this journey. His encouragement and love have been a constant source of strength for me.

Anais Wens
Delft, June 2024

Summary

Mangrove ecosystems are dynamic environments that provide numerous ecological, economic, and societal benefits, such as shoreline protection, carbon sequestration, and flood protection. These ecosystems are exclusively found in tropical and subtropical regions and thrive at the interface of land and sea. Despite their many benefits, mangroves face significant threats, leading to substantial losses over the past century. The degradation of mangroves compromises flood protection and shoreline stability, increasing the risk of severe coastline erosion and flooding.

Current research highlights the role of mangroves in flood protection but presents conflicting theories on their impact on coastline stability. Two competing theories exist regarding the effect of mangroves on coastline stability, namely the ”land-builders” and the ”land-consolidators” theory. According to the ”land-builders” theory, mangroves actively accumulate sediment and contribute to the expansion of coastlines. In contrast, the ”land-consolidators” theory suggests that mangroves play a more passive role in stabilizing existing landforms and serve as buffers against erosion. The debate on the primary function of mangroves remains unresolved. Furthermore, existing studies often date back over 50 years and are limited by specific hydrodynamic and geomorphic settings, leaving a gap in understanding broad trends.

This research aims to bridge this gap through a global assessment of the influence of mangroves on coastline development, complemented by a local assessment to explore detailed interactions in specific case study areas. The local assessment will focus on two coastlines of about 15 kilometres. The first case study focuses on a coastline that is mostly experiencing erosion, and the mangrove forest is stable. In contrast, the second case study focuses on a coastline that is mostly eroding, and the mangrove forest is contracting. The study's objective is to explore the dynamic impact of mangroves on coastline stability through an extensive analysis of historical datasets to identify trends and patterns in coastline changes associated with mangrove ecosystems. The focus lies on observing trends between coastline stability and the presence of mangroves, the relationship between coastline stability and mangrove forest width, and the influence of the state of mangrove forests (contracting, expanding, stable) on coastline stability.

Both the global and local assessment rely on two primary datasets: the Muddy Shoreline Monitor, which offers historical coastline position data for muddy coastlines (Hulskamp et al., 2023), and the Global Mangrove Watch, which provides data on the global extent of mangrove ecosystems (Bunting et al., 2022). The Muddy Shoreline Monitor dataset and the Global Mangrove Watch dataset were used to analyze coastline position changes and mangrove width changes, respectively, between 2005 and 2016.

The results found that, globally, mangrove areas exhibit slightly higher accretion rates compared to non-mangrove areas, yet also experience slightly higher erosion rates. Secondly, the relationship between the mangrove width and coastline stability differs between the global assessment and the local assessment. In the global assessment, it was found that larger widths are associated with increased accretion and erosion rates. In contrast, in the local assessment, it was found that widths above 1000 meters are more effective at lowering erosion rates. Finally, it was found that the state of mangrove forests influences coastline stability, with expanding and stable forests contributing to higher accretion rates and lower erosion rates and contracting forests correlating with increased erosion rates and decreased accretion rates.

Although the results, particularly those regarding the effect of the state of the mangrove forest, offer promising insights, it is essential to acknowledge the constraints imposed by data limitations, including spatial and temporal resolutions, as well as methodological challenges. These uncertainties underscore the need for caution in drawing definitive conclusions and emphasize the importance of continued research to refine our understanding. Recommendations for future research include addressing data limitations and enhancing methodological approaches. Furthermore, research should also focus on the effect of the state of the coastline on the stability of a mangrove forest. Finally, factors that could significantly impact the ability of mangroves to stabilize coastlines, such as hydrodynamic conditions, human activities, and sediment availability, should be investigated further. These factors should preferably be investigated by performing local studies and using local data instead of global data, as this data is often more accurate.

Contents

1 Introduction

1.1. Background

Mangrove ecosystems are among Earth's most vital and dynamic environments, providing a multitude of ecological, economic, and societal benefits (McCarthy, 2001 and Fagherazzi et al., 2017). These ecosystems are known for their rich biodiversity and for the diverse range of ecosystem services they offer, including shoreline protection, flood protection, carbon sequestration, improving the water quality, wood provision and facilitating fisheries (T. Worthington and Spalding, 2018 and McCarthy, 2001). Mangrove ecosystems are exclusively found in tropical and subtropical regions and thrive at the interface of land and sea (T. Worthington and Spalding, 2018 and McIvor et al., 2013). To be able to withstand the harsh conditions within this zone, such as significant hydrodynamic forces and extensive ranges of salinity, mangroves exhibit unparalleled morphological and physiological adaptations compared to other vegetation types (Kathiresan and Bingham, 2001 and Hamilton, 2019). Yet, mangrove ecosystems face various threats ranging from deforestation for industrialization and urbanization to climate change, such as rising sea levels and changes in freshwater input (Ashton, 2022). In the previous century, numerous mangrove ecosystems globally were lost, mainly due to the conversion of mangrove forests to aquaculture and agriculture. It is estimated that in the twentieth century, up to 35% of the total global mangrove forest area has been lost. However, providing an exact number is challenging due to limited data available before 1996 (Polidoro et al., 2010 and Ashton, 2022). Over the past decade, there has been a heightened recognition of the value of mangrove forests, leading to a yearly decrease in the rate of mangrove degradation. Nevertheless, the ongoing loss remains substantial, with an estimated disappearance between 0.3% and 0.7% of the total mangrove forest area annually (Hamilton and Casey, 2016 and Friess et al., 2019). The consequences of large-scale losses can be devastating, especially regarding flood protection and shoreline stability. Since mangroves can anchor sediment due to their dense root system, they can protect shorelines from the erosive forces of waves and currents (Kathiresan, 2003 and Gijsman et al., 2023). Without this protection, coastlines become vulnerable to erosion, which can result in the loss of valuable land. Furthermore, mangroves can mitigate flooding during storms. Losing mangroves can elevate the frequency and severity of flooding events, posing a direct threat to humans (Gijón Mancheño et al., 2021). In addition, factors like biodiversity loss, reduced water quality, and the release of carbon make the situation all the more critical (M. Spalding et al., 2014).

Currently, extensive research has been conducted regarding the influence of mangroves on flood protection. It is well established that mangroves can play a crucial role in flood protection (Menéndez et al., 2020; Gijsman et al., 2021; Verhagen and Loi, 2012). Mangroves can effectively attenuate incoming waves and stabilize sediment with their roots. The former stems from two key factors: the shoaling effect due to the presence of vegetation and roots that decrease the water depth and, most significantly, the substantial drag force exerted by the vegetation (Gijón Mancheño et al., 2021 and Horstman et al., 2014).

The latter reduces damages due to erosion, and consequently, since the roots trap the sediment, sediment accumulates, decreasing the water depth. The reduced water depth will, in turn, cause waves to attenuate earlier and thus limit the number of waves that can propagate deep into the mangrove forest (Gijón Mancheño et al., 2021 and Thampanya, 2006). However, many uncertainties remain regarding the effect of mangroves on coastline stability. Two competing theories exist in the literature, namely the ”land-builders” theory and the ”land-consolidators” theory (Friess et al., 2019). According to the ”land-builders” theory, mangroves actively accumulate sediment and contribute to the expansion of coastlines (J. H. Davis, 1946). In contrast, the ”land-consolidators” theory suggests that mangroves play a more passive role in stabilizing existing landforms and serve as buffers against erosion (Swales et al., 2015). Studies on this topic present conflicting evidence, with some indicating exclusive roles for mangroves and others demonstrating their ability to function in both capacities, influenced by various biogeomorphic factors (f.e. the specific species of mangroves present and the sediment availability and the composition of the sediment). However, no consensus exists on what biogeomorphic factor is the most crucial (Friess and McKee, 2021; S. Y. Lee et al., 2014; C. D. Woodroffe et al., 1985; Lovelock et al., 2010; Chapman, 1944; Steers et al., 1940; Bird, 1986; K. Krauss et al., 2003; Moldenke et al., 1960).

Despite the incomplete understanding of the exact nature of the impact of mangroves on coastline protection, it is recognized that mangroves are contributors to soil development and sediment accumulation. Mangroves directly influence soil development through biological processes, such as introducing organic matter into the soil through litter deposition and root growth. Additionally, they indirectly contribute to soil development through physical processes by reducing water velocities, promoting sediment deposition, and capturing sediment (McIvor et al., 2013 and Gijón Mancheño et al., 2021). In the long term, the increase of sediment accumulation due to the presence of mangroves leads to landscape alterations. The slope on the seaward side of the mangroves outside the forest will increase, while the slope within the forest will flatten. The profile becomes more convex-up, resulting in a faster decrease in water depth and reduced velocities towards the end of the flat, as waves break earlier (Friedrichs, 2011; Lovelock et al., 2010; Mullarney et al., 2017). This convex shape also influences the average water depth during high water slack, allowing for increased sediment deposition on the bed. Overall, mangrove forests enhance the flood-dominant behaviour of tidal flats, potentially reducing erosion rates across the entire tidal flat (Bryan et al., 2017).

1.2. Problem Statement

Despite decades of research, the debate on whether mangroves predominantly act as ”land-builders” or ”land-consolidators” remains inconclusive, highlighting the complexities and uncertainties inherent in understanding the diverse ecological roles of these coastal ecosystems (Friess and McKee, 2021 and McIvor et al., 2013). Existing studies provide valuable insights into regional and local assessments of mangrove ecosystems. However, they only hold in specific hydrodynamic and biogeomorphic settings (Besset et al., 2019; Thampanya et al., 2006; S. Das, 2020). Furthermore, a substantial portion of existing research on this topic dates back over 50 years (J. H. Davis, 1946; Steers et al., 1940; Watson, 1928; Egler, 1952). A noticeable void exists in understanding broad patterns and trends across diverse hydrodynamic settings. This research endeavours to bridge this gap by undertaking a global assessment of the influence of mangroves on coastline development. The complex interplay of climate, wave dynamics, and hydrodynamics varies significantly across regions, and a global perspective may prove helpful in capturing the nuanced relationships between mangroves and coastline stability. Combining the global assessment with a local assessment could lead to a more thorough understanding of the effect of mangroves on coastline stability. The local assessment allows exploring the influence of mangroves on coastline stability more closely when hydrodynamic and climatic conditions are similar.

1.3. Research Framework

1.3.1. Objective

This study aims to explore the dynamic impact of mangroves on morphological development, encompassing both global and local perspectives. It will do this through an extensive analysis of big data sources, focusing particularly on historical data sets. The overarching goal of this research is to unveil trends and patterns associated with coastline changes linked to mangrove ecosystems.

1.3.2. Research questions

Main research questions:

1. Can a trend be observed between coastline stability with or without the presence of mangroves globally?

2. Globally, is there a relationship between coastline stability and mangrove forest width?

3. On a global level, does a relationship exist between coastline stability and the state of a mangrove forest (contracting, expanding or stable)?

4. Locally, how do erosion and accretion rates vary between coastlines hosting contracting, stable or expanding mud-mangrove belts?

Sub research questions:

1. To what extent can the impact of mangrove ecosystems on coastline development be assessed using available global data?

2. Do the results of the global assessment and the local assessment align?

1.3.3. Research Object

In this research, only open coast mangrove ecosystems will be discussed. The complex interplay of tidal forces, wave dynamics, and sediment dynamics in lagoonal, deltaic, and estuarine settings presents substantial data collection and interpretation challenges, so they will not be discussed. Furthermore, while mangroves flourish in muddy, sandy and mixed tidal flats, their behaviour and influence on the tidal flats diverge significantly. Due to time and resource constraints, only muddy coastlines will be discussed, as more mangrove habitats are found on muddy coastlines than on sandy ones.

1.3.4. Methodology

This section will give an overview of the method. The research will be divided into four parts: a literature study, a global assessment, a regional assessment, and finally, a local assessment. The four parts of this thesis will be discussed below.

1. Literature study

The literature study aims to gain a comprehensive understanding of the ecosystem services provided by mangroves, the threats they face, and the dynamics of sediment on both bare mudflats and mangrove-covered mudflats.

2. Global assessment (scale 1000 - 2000 km)

In this phase, the objective is to provide a comprehensive overview of the global impact of mangroves on coastline stability. Data from the Muddy Shoreline Monitor is used to obtain historical and current data on coastline development on muddy coastlines (Hulskamp et al., 2023), and data from the Global Mangrove Watch is used to obtain data on the worldwide extent of mangrove ecosystems (Bunting et al., 2022). Using these datasets, the trends in coastline change between mangrove-covered and non-vegetated areas in tropical and sub-tropical regions globally are compared. Furthermore, it will be determined if a global relation exists between the forest's width and coastline stability. Finally, it will be determined if the state of the mangrove forest (stable, expanding or contracting) influences the coastline stability.

3. Local assessment (scale 10 - 100 km)

In the local assessment, the same data will be used as in the global assessment. The local assessment aims to investigate if the changes in coastline positions are influenced by the behaviour of a mangrove forest (contracting, stable, or expanding). In the case studies it is assumed that hydrodynamic and climatic conditions are similar. This analysis will be done for two case study areas considering a coastline of around 15 [km]. The first case study considers a coastline that is mostly experiencing erosion and the mangrove forest is stable. In contrast, the second case study considers a coastline where most of the coastline experiences erosion and the mangrove forest contracts.

1.3.5. Overview

Chapter 2 contains the literature review, which discusses mangrove forests and their effect on coastline stability. Chapter 3 presents the global assessment. In this chapter, the influence of mangroves on coastline stability globally will be researched. Chapter 4 presents the local assessment. In this chapter, two case studies will be discussed to analyse the effect of mangroves on coastline stability when hydrodynamic and climatic conditions are similar. In Chapter 5 the research questions will be answered. Finally, Chapters 6, 7, and 8 present the conclusion, discussion, and recommendations, respectively.

2

Literature study

2.1. Introduction on mangroves

Mangrove ecosystems are unique ecosystems that consist of trees, shrubs and other vegetation that thrive in brackish water and are able to withstand the harsh conditions in the intertidal area (McIvor et al., 2013). Other terms that are frequently used to describe this environment are mangal or tidal forest (Hamilton, 2019). The intertidal area is situated between mean sea level (MSL) and high tide. At low tide, this area is exposed to air and at high tide, this area is partially submerged (J. Ellison, 2009). To be able to thrive in this zone, mangrove trees are adapted to withstand large ranges of salinity, low levels of oxygen in the soil (anaerobic soil) and substrate that is unstable due to the various changes in hydrodynamic forcing (Hamilton, 2019). In literature, the terms 'mangals' and 'mangrove forests' are frequently used interchangeably to describe the ecosystem in which this vegetation thrives. The term 'mangal' typically encompasses the entire plant life found in a swamp within a mangrove forest, while the term 'mangrove forest' specifically denotes those species classified as mangrove trees within mangals. This terminology is the most consistently employed in literature and will also further be used in this research (Macnae, 1968 and Hamilton, 2019).

Mangrove ecosystems are primarily distributed within the latitudinal band spanning 30° north to 30° south of the equator. However, there are exceptions to these geographic boundaries particularly along the eastern coast of South Africa and the southern coast of Australia (M. D. Spalding et al., 1997). The most northern mangrove forest exists in Bermuda at 32°20'N. Conversely, the most southern mangrove forest exists near southern Victoria, Australia, at 38°45'S. It appears that a consistent water temperature above 20°C is important for mangroves to thrive (Hamilton, 2019 and M. D. Spalding et al., 1997).

The total area of mangrove forests in 2020 covered approximately 145,000 km^2 (Bunting et al., 2022). The majority of these mangrove forests are concentrated in Asia, Africa and South America. More specifically, in Indonesia, most mangrove forests are located, followed by Brazil and Australia, respectively. Notably, neither Europe nor Antarctica contains any mangrove ecosystems (Jia et al., 2023 and Bunting et al., 2022). A visual representation of the global distribution of mangroves and their respective sizes can be found in Figure 2.1.

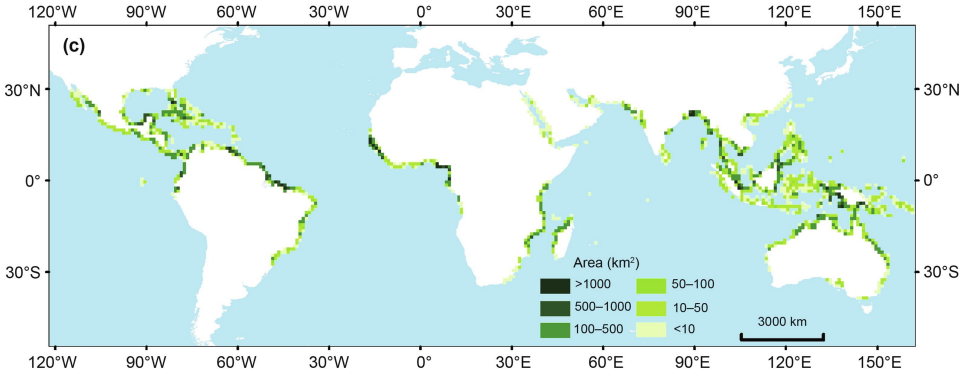

Figure 2.1: Mangrove distribution (Jia et al., 2023)

The distribution of mangroves is often divided into two groups: a western group and an eastern group. The eastern group includes the land surrounding the Atlantic Ocean and the west coast of America (essentially the eastern hemisphere), while the western group includes the land surrounding the Indian Ocean and the Pacific Ocean (except for the west coast of America). The western group is often also referred to as the Indo-West Pacific group (IWP), and the eastern group as the Atlantic East Pacific group (AEP). The eastern group has a considerably larger biodiversity than the western group (M. D. Spalding et al., 1997 and Basha, 2018). Mangrove ecosystems can also further be divided into four categories according to their geomorphological features, namely deltaic mangrove ecosystems, estuarine mangrove ecosystems, open coast mangrove ecosystems and lagoonal mangrove ecosystems. This will further be discussed in section 2.1.3.

Mangrove ecosystems hold immense ecological, economic and social values. However, mangrove ecosystems face an array of threats (T. Worthington & Spalding, 2018). In the past couple of decades, there has been a significant loss and degradation of these vital ecosystems. Just a few decades ago, mangroves were commonly viewed as unproductive wastelands, devoid of intrinsic value, and were actively encouraged for destruction by governments and urban planners (M. D. Spalding et al., 1997). This mindset led to the disappearance of a substantial number of mangrove areas. It is estimated that in the twentieth century up to 35% of the total global mangrove area has been lost, though the exact extent of these losses remains challenging to ascertain due to the limited availability of reliable data (Valiela et al., 2001 and FAO, 2007). At present, mangrove forests continue to face significant rates of degradation, but in comparison to previous decades, this trend has notably decelerated (T. Worthington & Spalding, 2018). It is estimated that every year, between 0.3% and 0.7% of the global mangrove area disappears. Unfortunately, higher rates can be observed in Asia (Hamilton and Casey, 2016 and Friess et al., 2019). In the next sections, the array of ecosystem services of mangrove forests and the threats mangrove forests face will be discussed.

2.1.1. The ecosystem services of mangroves

In this section, some of the key ecosystem services of mangrove forests are discussed.

Biodiversity

Mangrove trees and shrubs constitute a vital and diverse habitat that supports numerous species. These trees create a complex labyrinth of root systems that provide shelter and offer a safe breeding environment for many species (Hutchison et al., 2014). The channels within mangrove ecosystems transport freshwater from inland rivers hereby establishing vital connections with diverse ecosystems, enabling larger creatures to visit or utilize mangroves as nursery areas (Hutchison et al., 2014 and M. D. Spalding et al., 2021).

Mangals are critical habitats for many species. Approximately 340 species that primarily live in mangrove forests are considered to be critically endangered, endangered or threatened-vulnerable. Examples of these species include seahorses and tigers (M. D. Spalding et al., 2021).

Coastal protection

Mangroves play a crucial role in protecting coastlines from coastal hazards such as storm surges and cyclones. Mangroves are able to achieve this by attenuating waves and effectively capturing and stabilizing sediment (Menéndez et al., 2020; Gijsman et al., 2021; Verhagen and Loi, 2012). The influence of mangroves on stabilizing sediment will be discussed in Chapter 2.2. Their effectiveness in wave attenuation stems from two key factors: the shoaling effect due to the presence of vegetation and roots that decrease the water depth and, most significantly, the substantial drag force exerted by the vegetation (Horstman et al., 2014 and Gijón Mancheño et al., 2021). The degree of wave attenuation largely depends on the length of the waves, with short waves, such as wind waves, being dissipated easier than long waves, such as swell waves. Additional factors influencing the capacity of mangroves to dissipate waves include the height of the mangrove trees, the structure of their root systems, the density of the mangrove ecosystem, and the overall size of the mangrove area (Mazda et al., 1997 and Gijón Mancheño et al., 2021). An illustration of the possible role of mangroves in coastal protection can be seen in Figure 2.2.

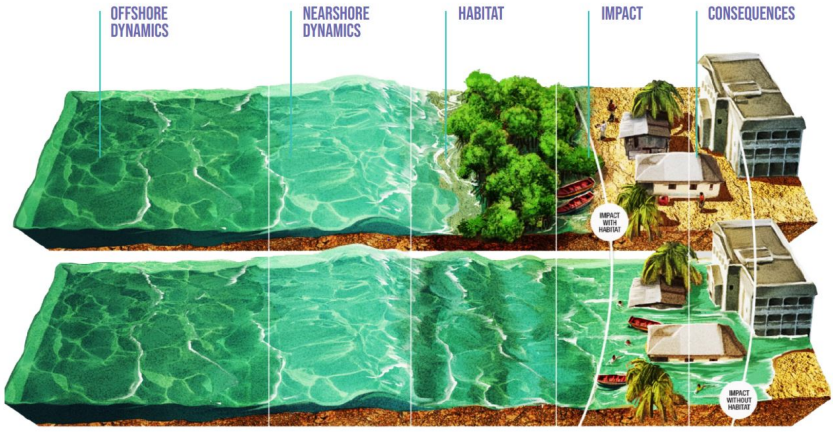

Figure 2.2: The possible role of mangroves in coastal protection (M. D. Spalding et al., 2021)

Carbon sequestration

Like all forests, mangrove trees convert carbon dioxide. Carbon is captured through photosynthesis into the leaves, wood, and roots of the trees. As the trees grow, the carbon reserves in the trees steadily increase (Alongi, 2014 and M. D. Spalding et al., 2021). However, mangroves rank among the most efficient carbon-capturing ecosystems globally. They excel at transforming carbon dioxide into organic carbon at rates surpassing nearly all other habitats on Earth (M. D. Spalding et al., 2021; Sanderman et al., 2018; T. Worthington and Spalding, 2018). Furthermore, in contrast to many other types of forests, the carbon deposited in mangrove soil through litterfall and root growth decomposes exceptionally slowly due to the waterlogged conditions caused by tidal inflows. This results in the gradual accumulation of carbon-rich and highly organic soil over extended periods, often spanning hundreds to thousands of years (Lang'at, 2013; Alongi, 2014; M. D. Spalding et al., 2021).

Improving water quality

Mangroves enhance water quality through pollutant filtration. Their intricate root systems slow down water movement and facilitate the settlement of sediment. Toxins and nutrients often bind to sediment or clay particles, and these contaminants are effectively removed from the water during the sediment settling process (of Australasia, 2015 and Gardner and Finlayson, 2018). Furthermore, due to the ability of mangroves to trap sediments, the turbidity in coastal waters is reduced (online coastal information, n.d.). This means that the water is clearer, which allows for better light penetration, resulting in the increase of photosynthetic activity of plants and algae and better oxygen exchange near the water surface (Lunt & Smee, 2019).

Facilitating fisheries

Mangrove forests function as thriving fish production centres. Their intricate systems of water channels and shallow pools provide shelter and offer a safe breeding environment for many aquatic species (Hutchison et al., 2014 and zu Ermgassen et al., 2020). The remarkable productivity of mangroves ensures a consistent and abundant food source. Every year, over 1,000 trillion commercially valuable fish and invertebrates are introduced into coastal waters across the globe by the current mangrove cover (T. Worthington & Spalding, 2018). At present, many small-scale fisheries rely on the existing stock of these fish and invertebrates, targeting valuable species like anchovies, crabs, and shrimp (T. Worthington and Spalding, 2018 and zu Ermgassen et al., 2020).

2.1.2. Threats facing mangrove forests

The main causes for the global degradation of mangrove forests can be subdivided into two categories, namely direct human threats and indirect human threats or climate change. The most significant direct human threats to mangrove forests, ranked from most to least important, are conversion to aquaculture and agriculture, mining, forest exploitation, urbanization and the impact of civil engineering structures (Ashton, 2022; E. L. Gilman et al., 2008a; S. C. Das et al., 2022). The most important causes of global mangrove forest losses due to climate change are the effect of storms and high-water events, changes in precipitation patterns and sea level rise (Romañach et al., 2018 and S. C. Das et al., 2022).

Conversion to aquaculture and agriculture

It is estimated that the conversion of mangrove forests into suitable land for aquaculture and agriculture is responsible for about 47% of global mangrove loss between 2000 and 2016 (Goldberg et al., 2020). Shrimp farms, in particular, are the primary drivers of this change within the aquaculture sector. During the 1980s and 1990s, many countries encouraged the conversion to aquaculture to enhance food security and improve livelihoods, which caused mangrove destruction on a large scale (Hishamunda et al., 2009). Unfortunately, the immense economic value of the shrimp industry continues to pose a substantial and persistent threat to mangrove ecosystems (Ashton, 2022; Richards and Friess, 2016; FAO Fisheries and Aquaculture Information and Statistics Service, 2021). In Figure 2.3 a picture of mangrove deforestation due to shrimp ponds can be observed.

Figure 2.3: Mangrove deforestation due to shrimp ponds (Laman, 2009)

The primary drivers in the agricultural sector are rice cultivation and palm oil production (Goldberg et al., 2020 and Richards and Friess, 2016). This is particularly evident in Myanmar, where rice farming, and Indonesia, where palm oil cultivation has already led to extensive mangrove loss. Unfortunately, in both countries, the large-scale degradation of mangrove forests is still ongoing (Ashton, 2022 and Richards and Friess, 2016).

Mining

Approximately 12% of the global reduction in mangrove coverage between 2000 and 2016 can be attributed to activities associated with resource mining and petroleum extraction (Goldberg et al., 2020). In both Cameroon and Nigeria, the practices of sand mining and oil drilling have resulted in significant rates of land subsidence and environmental degradation (Ashton, 2022).

These negative impacts extend beyond mere subsidence and include issues such as the increased turbidity and siltation of waterways. Mangroves have been significantly impacted, as mining sediments have covered and suffocated these crucial coastal ecosystems. Furthermore, there are long-lasting indirect pollution effects that persist for many years as a result of these activities (Ashton, 2022 and Ohimain, 2003).

Forest exploitation

Forestry was responsible for an 8.3% worldwide decline in mangroves between 1996 and 2010, with its effects predominantly concentrated in Southeast Asia (Thomas et al., 2017). Mangroves are primarily harvested for fuel wood and charcoal production. Unfortunately, forestry still poses a significant threat to mangroves (Ashton, 2022). However, forestry can be done in a sustainable way. For example, fast-growing timber trees, such as the species Acacia, can be planted in areas adjacent to protected mangroves to discourage the cutting of conservation areas for fuel wood consumption (Ashton, 2022 and Goessens et al., 2014).

Urbanization

One of the most direct ways urbanization threatens mangroves is through the clearing of land for infrastructure development. With the expansion of cities, mangroves often make way for the construction of ports, airports, housing, industrial facilities, and other projects. Many large cities, such as Jakarta (Indonesia) and Mumbai (India), resulted in the large-scale loss of mangrove forests (Ashton, 2022). Fortunately, the impact of this threat has diminished in the past decade, with urbanization accounting for only 3% of mangrove forest loss between 2000 and 2016 (Goldberg et al., 2020).

However, urbanization also indirectly endangers mangrove forests. As urban areas grow, they tend to consume more plastic and generate more waste. Additionally, urbanization frequently leads to heightened industrial and agricultural activities, resulting in the release of pollutants such as heavy metals, pesticides, and chemical fertilizers. The accumulation of these pollutants can adversely affect mangrove vegetation and the species that inhabit these ecosystems (Ashton, 2022 and Harris et al., 2021).

The effect of civil engineering structures

The implementation of civil engineering structures in both marine and river environments can result in significant mangrove ecosystem losses. Seawalls and coastal erosion control structures, designed to safeguard coastal populations, have adverse impacts on mangrove ecosystems by disrupting sediment dynamics and reducing sediment availability (E. L. Gilman et al., 2008a). When these structures are constructed near mangrove ecosystems, they can lead to shoreline erosion directly impacting the mangroves (Tait and Griggs, 1991 and Fletcher et al., 1997). This alteration destabilizes the mangrove habitat, leading to the loss of valuable vegetation and associated wildlife. Similarly, upstream construction of structures like dams in rivers traps sediment, conversely limiting sediment availability in mangrove ecosystems, which can potentially result in vegetation loss (E. L. Gilman et al., 2008a). Additionally, such constructions often lead to a decrease in freshwater availability. Since mangrove ecosystems only thrive in brackish water, reduced freshwater availability can result in excessively saline water, unsuitable for mangrove survival (S. C. Das et al., 2022 and Kathiresan, 2002).

Climate change

Climate change exerts significant pressures that can result in the degradation of mangrove ecosystems. Firstly, an anticipated increase in the frequency and intensity of extreme weather events is expected (Solomon et al., 2007 and Church et al., 2001). These events have already played a substantial role in mangrove loss, contributing to 11% of overall mangrove depletion between 2000 and 2016 (Goldberg et al., 2020). Extreme weather events such as cyclones, storm surges, and tsunamis can inflict direct and indirect damage on mangrove trees. Strong winds, often accompanying these events, can lead to severe mangrove damage or mangroves can even be uprooted. Prolonged inundation from extreme weather events can also cause significant mortality. Additionally, these events can introduce large amounts of sediment, smothering mangrove roots and disrupting their ability to respire and access nutrients, thereby causing mangrove losses on a large scale (Smith et al., 1994; C. Woodroffe and Grime, 1999; Sherman et al., 2001).

Furthermore, precipitation patterns can change due to climate change (E. L. Gilman et al., 2008a). Changes in precipitation, particularly in regions experiencing reduced rainfall, can reduce freshwater availability, elevate salinity levels, and ultimately contribute to the degradation and potential loss of mangrove ecosystems (S. C. Das et al., 2022). Finally, sea level rise can pose a significant threat to mangroves situated in the intertidal zone (Ashton, 2022). The consequences of sea level rise can vary based on local factors like topography, slope, rate of sea level rise, sediment sources, sediment quantity, and land availability for migration (C. D. Woodroffe, 1990 and E. L. Gilman et al., 2008b). In areas with higher elevations and lower tidal ranges, there may be potential for vertical sediment accumulation, aiding mangroves in keeping pace with sea level rise. Conversely, in regions with lower elevations and greater tidal ranges, mangroves may struggle to adapt, potentially leading to widespread tree mortality (Romañach et al., 2018; E. Gilman et al., 2007; J. C. Ellison, 2000; Ward et al., 2016). Figure 2.4 shows a picture of a mangrove ecosystem in the US. Unfortunately, this ecosystem was largely destroyed after the passing of the hurricanes Katrina and Wilma and to this day still struggles to re-establish (Popkin, 2020).

Figure 2.4: Mangroves still struggle to re-establish after the passing of hurricanes Katrina and Wilma (USA) (Popkin, 2020).

2.1.3. Mangrove topologies

Mangrove ecosystems can be classified according to geomorphological and biological factors. Many classifications exist (f.e Thom, 1984 and C. Woodroffe, 1992); however, in this research, the classification proposed by Worthington et al. (2020) will be used. This classification is chosen as Wortington et al (2020) combined many previously designed classifications into one. The classification categorizes mangrove ecosystems based on their geomorphic characteristics, such as deltas and lagoons, together with their sedimentary composition. Initially, the classification distinguishes between mangrove ecosystems situated in areas where either terrigenous sediments or carbonate sediments predominate. Terrigenous sediments primarily result from the weathering of continental rocks and are the most dominant setting. Carbonate sediments are formed from calcium carbonate, often originating from the shells and remains of marine organisms. These sediments can also be referred to as marine sediments (Balke and Friess, 2016 and Bosboom and Stive, 2021). Utilizing their geomorphic features, four main types of mangrove ecosystems can be differentiated namely, deltaic mangrove ecosystems, lagoonal mangrove ecosystems, estuarine mangrove ecosystems, and open coast mangrove ecosystems. In 2016, among all mangrove ecosystems, approximately 40.5% were deltaic, 27.5% were estuarine, 21% were open coast, and the remaining 11% were lagoonal (T. A. Worthington et al., 2020). All four types can be found in areas dominated by terrigenous sediments, but only open coast mangrove systems and lagoonal mangrove systems can be present in regions where carbonate sediments predominate (T. A. Worthington et al., 2020 and Balke and Friess, 2016). The four types will be further discussed below.

Deltaic mangrove ecosystems

Deltaic mangrove ecosystems occur at river-dominated coasts. These coasts are characterized by substantial freshwater input and sediment discharge but experience a low tidal range. The substantial sediment discharge carried by these rivers contributes to the creation of delta formations (Wright, 1985 and C. Woodroffe, 1993). Within a delta two types of plains can be discerned, namely active deltaic plains and abandoned deltaic plains. Active deltaic plains receive a high influx of freshwater, which hinders the growth of salt-tolerant vegetation like mangroves. In the abandoned deltaic plains, the river water flow is less forceful, resulting in a conducive environment where the extensive growth of mangrove ecosystems is possible (Wright and Coleman, 1973 and C. D. Woodroffe, 2000). Due to the large sediment supply coming from the river, continuously new areas are created that are suitable for mangrove colonization (Selvam & Karunagaran, 2019). Figure 2.5 provides a schematic representation of the deltaic mangrove ecosystem.

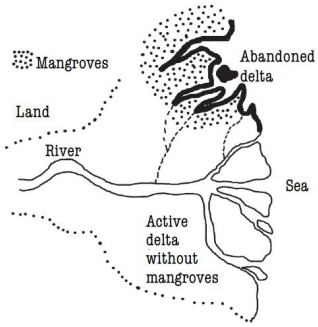

Figure 2.5: Deltaic mangrove ecosystem (Selvam & Karunagaran, 2019)

Estuarine mangrove ecosystems

Estuarine mangrove ecosystems occur at tide-dominated coasts. These coasts are characterized by a significant tidal range and strong bidirectional tidal currents (C. Woodroffe, 1992 and Thom, 1984). This means that during high tide, a large volume of water enters the estuary with a significant velocity, and conversely, at low tide, a large volume of water leaves the estuary with a significant velocity. These tidal currents are able to disperse the large amounts of sediments transported by rivers and often in the process create elongated islands and shoals offshore. These features are able to dampen the wave energy effectively (Selvam & Karunagaran, 2019). Typically, the primary river channels exhibit a funnel-like shape and receive inflow from a network of numerous tidal creeks (Wright et al., 1973). These tidal creeks are separated by expansive tidal flats, which provide habitats for extensive mangrove growth. These tidal flats, along with the elongated islands and shoals, accommodate thriving mangrove ecosystems (Selvam & Karunagaran, 2019). Figure 2.6 provides a schematic representation of an estuarine mangrove ecosystem.

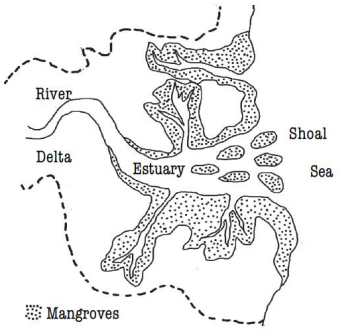

Figure 2.6: Estuarine mangrove ecosystem (Selvam & Karunagaran, 2019)

Lagoonal mangrove ecosystems

Lagoonal mangrove ecosystems occur at wave-dominated coasts. These coasts are characterized by a low volume of river discharge and a high wave energy (Thom, 1984). This high wave energy is able to continually reshape the sediment deposits brought in by rivers and sediments settled on the seabed. This natural process results in the creation of elongated sandy ridges running parallel to the shoreline, alongside the formation of barrier islands. These barrier islands encircle expansive lagoons (Selvam and Karunagaran, 2019 and Thom, 1984). Within the vicinity of these lagoons, mangrove ecosystems flourish (C. Woodroffe, 1992 and C. D. Woodroffe et al., 2016). Figure 2.7 provides a schematic representation of the lagoonal mangrove ecosystem.

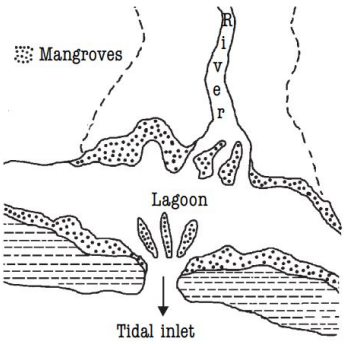

Figure 2.7: Lagoonal mangrove ecosystem (Selvam & Karunagaran, 2019)

Open coast mangrove ecosystems

Open coast mangrove ecosystems occur either at low energy coasts where carbonate sediments are dominant or at sheltered embayments where terrigenous sediments are dominant (C. Woodroffe, 1992 and C. D. Woodroffe et al., 2016). At coasts where carbonate sediments dominate, mangroves can thrive when the coast is protected by carbonate platforms and/or coral reefs. Carbonate platforms are shallow marine areas where carbonate sediments accumulate. Both carbonate platforms and coral reefs are able to dampen wave energy (Twilley and Rivera-Monroy, 2009 and C. Woodroffe, 1992). Mangroves can also thrive on coasts that are protected by mud banks. These mud banks can also dampen wave energy effectively (Spencer et al., 2016). Figure 2.8 provides a schematic representation of an open coast mangrove ecosystem.

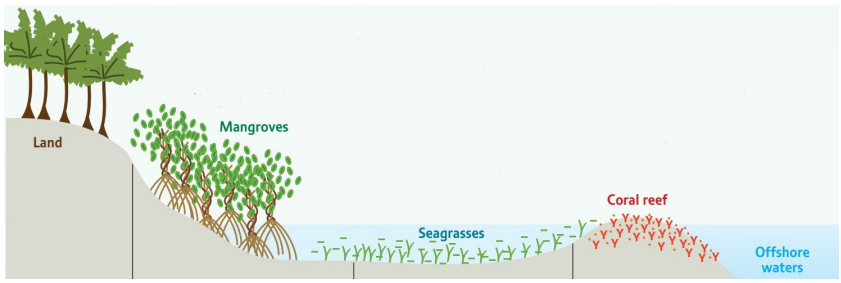

Figure 2.8: Open coast mangrove ecosystem (Silvestri, Kershaw, et al., 2010)

2.2. Sediment dynamics on mudflats

Mangroves colonize mudflats or intertidal flats on muddy coasts, sandy coasts and mixed muddy/sandy coasts (Swales et al., 2021). However, mangroves are primarily present on muddy coasts. Mud is a mixture of (salt)water, silt, clay, fine sands and organic matter (Bosboom & Stive, 2021).

Mangrove forests influence the sediment dynamics along the coastline, yet the precise nature of their impact remains a subject of ongoing research and debate. This debate centres around two primary hypotheses: mangroves as ”land-builders” and mangroves as ”land-consolidators” (Friess & McKee, 2021). According to the hypothesis of mangroves as ”land-builders”, mangroves are able to accumulate sediment and even self-generate new organic soil actively. These processes establish the requisite conditions for the expansion of land either horizontally (toward the sea) or vertically (J. H. Davis, 1946). According to the hypothesis of mangroves as ”land-consolidators”, mangroves inhabit intertidal areas once they reach an elevation where tidal conditions permit the establishment and survival of seedlings (Swales et al., 2015). Once established, mangroves play a role in sediment consolidation, the formation of soil through biogenic processes and the promotion of additional sediment deposition. However, they don’t actively accumulate sediment and build new land (Friess and McKee, 2021 and Swales et al., 2015).

Some studies have presented evidence supporting the idea that mangroves exclusively act as ”land-builders” (J. H. Davis, 1946; Steers et al., 1940), while others propose that mangroves solely act as ”land-consolidators” (Watson, 1928; Egler, 1952; Swales et al., 2015). However, another widely accepted theory is that mangroves can function as both ”land-builders” and ”land-consolidators” depending on the specific biogeomorphic setting, although no consensus exists on what setting causes what behaviour. The term biogeomorphic setting denotes the interplay of biological and geomorphological processes shaping coastal landscapes (Viles, 1988). Some researchers believe that sediment availability is the most important factor. In sediment-rich environments, mangroves will act as ”land-builders”, while mangroves in sediment-poor environments will act as ”land-consolidators” (S. Y. Lee et al., 2014; C. D. Woodroffe et al., 1985; Lovelock et al., 2010). Another theory is that the sedimentary habitat is the crucial factor that determines the behaviour of mangroves. According to this theory, three different sedimentary habitats exist, namely sand-dominated environments, mud-dominated environments and reef-dominated environments (Chapman, 1944). Mangroves in sand-dominated environments will act as ”land-builders” and begin forming peat after colonization. Mangroves in mud-dominated areas rely on the mechanical trapping of silt for land consolidation and will act more like ”land-consolidators”. Similarly, mangroves rooted in reef-dominated settings may not significantly contribute to land development (Chapman, 1944 and Steers et al., 1940). Other researchers say the type of mangrove species and the type of mangrove roots is the determining factor, with some species able to act as ”land-builders”, while some are not able to actively accumulate sediment (Bird, 1986; K. Krauss et al., 2003; Moldenke et al., 1960). It is clear that many uncertainties still exist regarding these coastal ecosystems’ diverse ecological roles.

To better understand the role of mangroves on mudflats, the sediment dynamics on bare mudflats and on mangrove-covered mudflats will be discussed. In Figure 2.9 an overview of all morphodynamic processes that will be discussed in this research can be observed. Many of the processes are present on both bare- and vegetated mudflats. In the following section, an introduction on tidal flats will be given, followed by the sediment dynamics on bare mudflats. Finally, sediment dynamics present on mangrove-covered mudflats will be discussed.

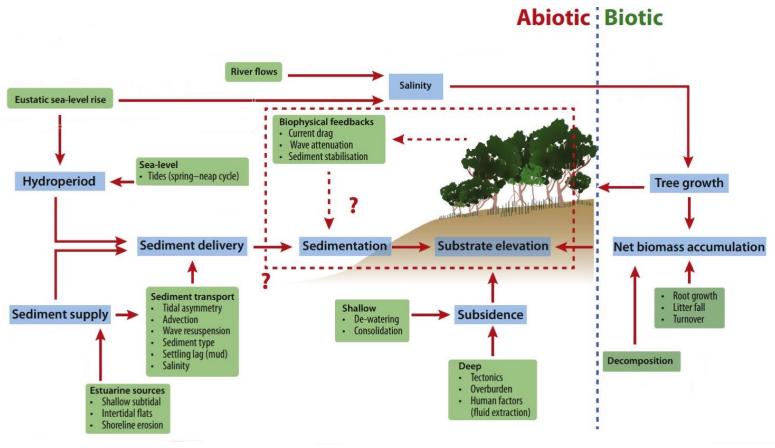

Figure 2.9: Processes influencing soil development and degradation (adapted from Swales et al., 2021)

2.2.1. Introduction on tidal flats

Tidal flats

Tidal flats are areas where sediments, such as sand and mud that are brought in by tides or rivers, accumulate (Balasuriya, 2018). A tidal flat consists of three zones, namely the subtidal zone, the intertidal zone and the supratidal zone. The subtidal zone is located below the mean low water spring tide (MLWS) and is seldom exposed to the air. The supratidal zone is located above mean high water spring tide (MHWS) and is only inundated during extreme conditions. The intertidal zone, as already discussed previously, is the zone between mean low water springs and mean high water springs (Gao, 2019 and Amos, 1995). An overview of the three regions can be seen in Figure 2.10.

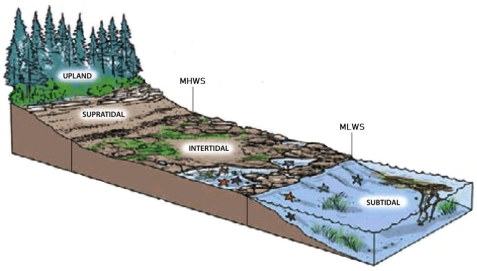

Figure 2.10: The zonation of tidal flats (BC, 2010)

As is the case for mangrove ecosystems, tidal flats can be classified as well. A classification can be seen in Figure 2.11. In this classification, three main types of tidal flats are discerned namely, back-barrier systems, tide-dominated estuary/delta and coastal plain (R. A. Davis & Dalrymple, 2012). Back-barrier tidal flats are found on the inner side of barrier islands, spits, and bars, which act as natural wave buffers (Morales, 2022). Tide dominated estuaries and deltas are tidal flats present near estuaries and deltas. Coastal plain tidal flats can be divided into Chenier plains and Strand plains. Strand plains, also known as beach plains, are coastal landforms that are essentially flat or gently sloping areas adjacent to a shoreline. Chenier plains are elongated, beach ridges made of sand or seashells that run parallel to the shoreline (R. A. Davis and Dalrymple, 2012 and Augustinus, 1989). Mudflats tend to develop near extensive chenier plains and larger river deltas, while sandy tidal flats tend to develop near smaller river deltas and strand plains (Healy et al., 2002). Mudflats and sandy tidal flats generally have a different cross-shore profile. Mudflats typically display an accretional, convex-up cross-shore profile, while sandy tidal flats display an erosional, concave-up cross-shore profile (M.-e. Ren, 1985; Frey et al., 1989; Semeniuk, 1981; Hale and McCann, 1982). A convex-up profile means that the lower flat has a larger slope than the upper flat, while a concave-up profile means the upper flat has a larger slope than the lower flat (Hanssen et al., 2022). In Figure 2.12, a schematization of a convex-up and concave-up profile can be seen.

This research focuses exclusively on open coast mangrove systems. Therefore, the discussion will specifically revolve around coastal plain tidal flats. Among these, Chenier plains are of primary interest due to their muddy substrates, which provide an ideal environment for mangrove ecosystems to thrive.

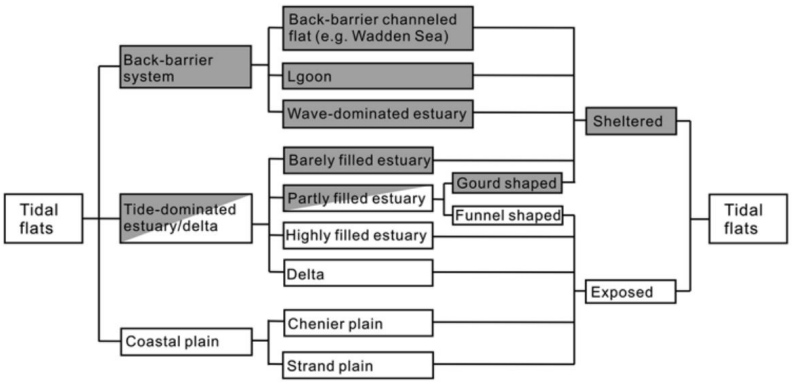

Figure 2.11: Classification tidal flats (R. A. Davis & Dalrymple, 2012)

Tidal flats develop in regions with sufficient fine-grained sediment, such as clay, silts, and fine sands available. The critical factor contributing to the formation of tidal flats is the predominance of tides and tidal currents over other hydrodynamic forces. The tidal action should thus be significant (Klein, 1985). However, this does not mean that wave forces can't exert a dominant influence (King, 1972). Waves break in the surf zone, driving the transportation of fine-grained sediment toward offshore regions. In such instances, if the supply of fine-grained materials is limited, the result is the formation of sandy or gravelly beaches instead of tidal flats. However, when there is a substantial influx of fine-grained sediment, the accumulation of these materials progressively reduces the slope of the intertidal area. This reduction in bed slope enhances tidal currents and the wave energy disperses over the intertidal flat due to bed friction. Therefore, the presence of fine-grained sediment weakens the impact of wave action and amplifies tidal forces (Gao, 2019). Although the impact of wave action weakens, waves still play a crucial role in sediment transport and in shaping the morphology of tidal flats (Christiansen et al., 2006; Friedrichs, 2011; Fan, 2011). Furthermore, the tide-dominated setting can temporarily be changed to wave-dominated conditions during extreme events such as storms and cyclones (Mei-e et al., 1985; M. Ren, 1986; Andersen and Pejrup, 2001).

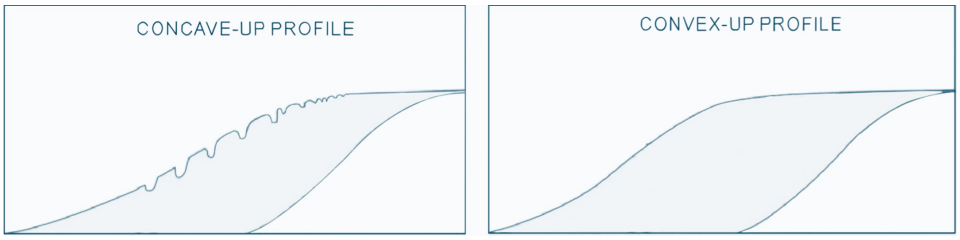

Figure 2.12: Concave-up and convex-up tidal flat after Choi and Jo, 2015

Intertidal flats

To discuss the interplay between mangrove ecosystems and tidal flats, mainly the intertidal zone is important as most mudflats can be found there (Gao, 2019). The intertidal zone is often divided into four zones as can be seen in Figure 2.13. These four zones are the sand flat, mixed flat, mud flat and salt march. Salt marches comprise the top part of the intertidal flat. The salt march consists mainly of clayey or muddy materials, often rich in organic carbon content. Just below this layer, there is a mud layer, consisting of clay and fine silts, that aligns with the elevation close to the high-water mark. This layer exhibits very thin laminae. Laminae are different layers that are less than 10 mm thick (Reineck & Singh, 2012). They are identifiable due to variations in sediment texture and/or composition within and between these thin layers (Bridge, 2003). Subsequently, the mixed flats can be found.

On the mixed flat, a sedimentary structure called tidal bedding can be found. Tidal bedding are alternating layers of mixed sand and mud. This feature is formed as a result of tidal cyclicity, as sand gets deposited during spring tides and mud during neap tides (Shi, 1991 and Gao, 2019). The lowest section is characterized by a layer of sand. This layer corresponds to the lower part of the intertidal zone and extends into the subtidal zone. This zone is characterized by well-sorted sand and bedforms such as bed ripples (Gao, 2019 and Reineck and Singh, 2012). The different zones are not always very distinguishable as on some intertidal flats mud completely covers the flat, while on other intertidal flats mud is only scarcely present (G. Evans, 1965; Amos, 1995; Gao, 2019).

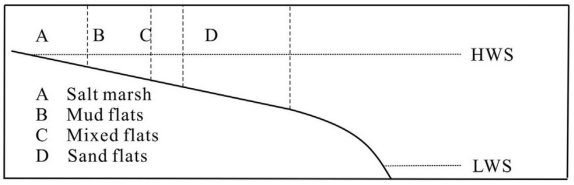

Figure 2.13: The zonation of intertidal flats (Gao, 2019)

On open coast intertidal flats, tidal channels are frequently less developed compared to other types of tidal flats. This is particularly true in the lower section of the intertidal flat (Frey et al., 1989; Fan et al., 2004; Alexander et al., 1991). This phenomenon is attributed to the substantial hydrodynamic forces exerted on the lower part of the intertidal bank. These forces diminish the stability of the creek banks, resulting in a smoothing effect on the creeks (R. A. Davis & Dalrymple, 2012). However, in the upper part of the intertidal flat, where vegetation is often present, tidal creeks, comprising small creeks and larger tidal channels form. The presence of vegetation provides protection from high hydrodynamic forces, fostering the development of more intricate tidal channel networks (R. A. Davis and Dalrymple, 2012; M.-e. Ren, 1985; Froidefond et al., 1988).

2.2.2. Sediment dynamics on bare mudflats

There are four primary morphodynamic processes influencing the development and stability of intertidal flats, namely hydrodynamic forcing, sediment dynamics, morphological changes, and bed properties (Zhu, 2017; Le Hir et al., 2000; Doeke, 2019; Wright et al., 1988; Maa et al., 1998). Hydrodynamic forcing involves wave-induced currents and tidal currents, while sediment dynamics encompass erosion, deposition, and advection (Le Hir et al., 2000 and Holthuijsen, 2010). Figure 2.14 schematizes these processes.

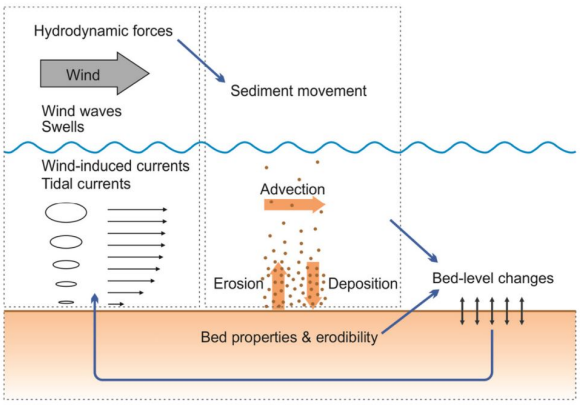

Figure 2.14: The sediment dynamics on tidal flats (Zhu, 2017)

In order for the intertidal flat to be stable, a balance needs to exist between tidal currents and wave-induced currents. Tidal currents generally cause a net-landward transport, while wave-induced currents mostly cause a net-seaward sediment transport (Green & Coco, 2014).

When considering wave-induced currents, it is essential to differentiate between larger waves, such as shallow water waves, and shorter waves, such as capillary waves. Larger waves, characterized by their substantial energy, possess the capability to efficiently stir and re-suspend fine sediments settled on the seabed. These re-suspended sediments can subsequently be carried by tidal currents into the mudflats. In contrast, smaller waves lack the energy required to effectively re-suspend fine sediments. However, both smaller and larger waves have the potential to induce substantial rates of erosion on the mudflats due to the ease with which they can erode the fine sediments (Winterwerp et al., 2005). This erosion is primarily driven by a bed shear stress resulting from the wave orbital velocity (Wiberg & Sherwood, 2008). The magnitude of the wave orbital velocity depends on three variables, namely the wave height, wave period and water depth. The magnitude of the orbital velocity increases with decreasing water depth, increasing wave period and increasing wave height. (Winterwerp et al., 2005 and Zhu, 2017).

The transport of fine sediments is linked to certain lag effects in relation with the tidal currents present. These effects depend on the interplay between sediment properties and hydrodynamic asymmetries (van Maren and Winterwerp, 2013; Hsu et al., 2013, Uncles, 1981). Two types of asymmetries can be discerned. These asymmetries often occur simultaneously in tidal environments. The first type is an asymmetry in the hydrodynamic forcing. These asymmetries are related to variations in the movement of water during tidal cycles. Hydrodynamic asymmetries encompass changes in current velocity, direction, and duration between flood (rising tide) and ebb (falling tide) phases. The second type of asymmetry is associated with the properties and behaviour of sediments. These asymmetries involve how sediment particles settle, re-suspend, and transport under the influence of tidal forces (van Maren & Winterwerp, 2013).

Asymmetry in sediment properties

The asymmetry in sediment properties and behaviour is described using the principle of ”settling-and scour lag”. This concept revolves around the idea that a significant amount of energy is required to displace fine cohesive sediment particles from the bed. This process demands more energy than simply keeping these particles suspended in the water column. Moreover, the timescale for suspending particles is much shorter than the time it takes for them to settle (van Maren & Winterwerp, 2013). To delve more into the specifics, ”settling lag” pertains to the additional time and distance needed for fine sediment particles to settle after the flow velocity has decreased below the critical shear stress necessary for erosion (Postma, 1954 and Van Straaten and Kuenen, 1957). This effect results in a tidally-averaged residual transport directed towards an area with lower energy, as the suspended sediment requires time to fully settle out. As a consequence, the settling-lag effect causes a net transport in the direction of lower maximum bottom stress or tidal velocity. This effect generally causes a net-landward transport (Hsu et al., 2013 and Friedrichs and Aubrey, 1996). Conversely, ”scour lag” is based on the principle that a higher critical shear stress is essential for erosion compared to maintaining fine sediment particles in suspension (Van Straaten & Kuenen, 1957). When scour lag is coupled with variations in hydrodynamic forcing, it can induce both landward or seaward sediment transport (van Maren & Winterwerp, 2013).

Asymmetry in hydrodynamic properties

Asymmetries in hydrodynamic properties can manifest in three distinct ways: temporal asymmetry, vertical asymmetry, and horizontal asymmetry (van Maren & Winterwerp, 2013).

Temporal asymmetry is associated with imbalances in the tidal cycle, particularly during the slack tidal period, a term describing the moment when the direction of tidal flow reverses. In the context of fine sediment particles, the process of landward transport occurs when the duration of high-water slack, the period from flood to ebb, surpasses that of low-water slack, the transition from ebb to flood (Friedrichs and Aubrey, 1988 and Van de Kreeke and Robaczewska, 1993). The tidal regime that occurs most frequently globally is a semi-diurnal tidal regime. This means that two high-waters and two low-waters occur per day (Bosboom & Stive, 2021). Tidal asymmetry arises due to the presence of the M_4 overtide.

The generated asymmetry is often defined by the phase difference between the M_4 overtide and the M_2 tidal component. It is important to note that the specifics of this phenomenon can vary in different tidal regimes around the world, as other tidal components may also influence the asymmetry (Hoitink et al., 2003; Nidzieko, 2010; Song et al., 2011, Van Maren and Gerritsen, 2012). When this phase difference falls within the 90 to 270 degrees range, it induces the landward transport of fine sediment particles, as depicted in Figure 2.15. In this figure, a situation is illustrated where the high water slack is larger than the low water slack, resulting in a net-landward transport of fine sediments (van Maren & Winterwerp, 2013).

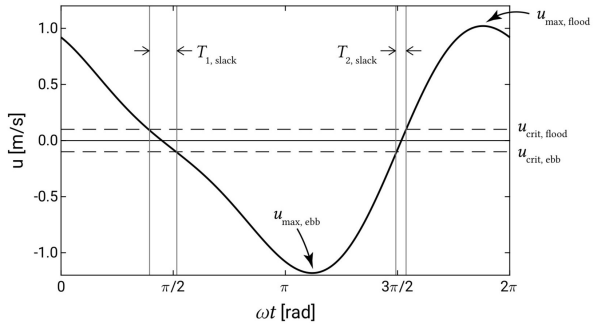

Figure 2.15: The tidal asymmetry for a phase difference of 270 degrees (Bosboom & Stive, 2021)

Vertical asymmetry involves variations in vertical mixing. When the peak velocity is higher during the flood phase than during ebb, the intensity of vertical mixing differs between the two phases. Sediment particles will be able to travel for longer distances during flood due to the higher velocities. Vertical mixing intensity exhibits a non-linear relationship with flow velocity, where slight changes in velocity can yield significant alterations in mixing intensity. If vertical mixing is more significant during the flood phase, sediment particles are actively mixed and transported upward during this period due to higher flow velocities in the upper part of the water column. Flow velocity profile asymmetry can result in net sediment transport in a process referred to as ”differential advection”, leading to sediment transport in one direction more than the other. When peak velocity is higher during flood than ebb, it results in net landward transport (Jay and Musiak, 1994 and van Maren and Winterwerp, 2013). However, fine sediments can sometimes inhibit turbulent mixing due to strong concentration gradients, counteracting the effect described above (Van der Ham & Winterwerp, 2001).

Finally, *the asymmetry in longitudinal direction* is important. On tidal flats, velocities decrease towards the top part of the tidal flat. This can lead to an asymmetry on the timing of slack water at a certain location. This also affects the duration of the slack water (Postma, 1961). Consider two locations, one more at a seaward location (location 1) on the tidal flat and one more landward (location 2). A water particle that starts its journey at the commencement of the flood will first pass location 1 and will arrive at location 2 towards the end of the flood. At location 2, where the flow velocity is less than that at location 1, this water particle encounters a longer period of slack tide. This ”slack tide” signifies the duration during which the water particle experiences flow velocities below a critical threshold. Sediment can thus more easily settle near location 2 than near location 1 (van Maren & Winterwerp, 2013). Furthermore, as the tidal flat often has a convex-up shape, the average water depth is less during high water slack (when the flats are inundated) than during low water slack (when water is confined to the tidal creeks). This means that, during high water slack, the water is shallower over the flats, allowing more sediment to be deposited on the bed. Both asymmetries can explain the flood-dominant behaviour of tidal flats (Van Straaten & Kuenen, 1957).

The previously mentioned asymmetries can all result in a net landward transport, but their relative importance varies depending on the specific tidal flat. In some cases, a particular asymmetry might even lead to a net-seaward transport. Unfortunately, it remains uncertain which type of lag effect is more dominant and under what specific conditions the effect is dominant (van Maren & Winterwerp, 2013).

The morphodynamic behaviour of an intertidal mudflat at different timescales

The fluctuation in bed level on mudflats is a highly dynamic process that undergoes significant changes over time. On a very small scale (minutes to days), the wave-induced currents and tidal currents dominate the fluctuation in bed level (Christie et al., 1999 and Le Hir et al., 2000). As the tide cycle progresses, the strength of tidal currents and their influence on the seabed decrease when moving from the lower intertidal flats toward land. At high tide, these tidal currents nearly come to a standstill. On the other hand, wave processes, including the stresses waves exert on the seabed, become more significant during the rising tide. This happens because, as the tide rises, the water depth increases and consequently influences the wave height (Green et al., 1997; Le Hir et al., 2000; R. A. Davis and Dalrymple, 2012).

On an intermediate time scale (days to weeks), the neap-spring tidal cycle becomes important. During spring tide, the largest amount of sediment is transported into the mudflats. In conditions of low wave energy, this often leads to substantial sediment deposition. However, when higher waves are present, these newly deposited sediments can be easily eroded, especially during the later stages of the receding tide or the initial phases of the subsequent tide. Conversely, during neap tides, when sediment supply is reduced, the impact of wave-induced erosion can be more pronounced. Typically, erosion tends to be more severe during spring tides, primarily because larger waves can penetrate deeper into the mudflat due to the increased water depth (Fan et al., 2006; Kim, 2003; R. A. Davis and Dalrymple, 2012).

Finally, on a longer time scale (monthly to yearly), it becomes evident that seasonal effects exert a significant influence on bed level changes. Seasonal shifts between accretion and erosion are a common feature of tidal flats (B. Yang et al., 2005). These seasonal variations are primarily linked to changes in wind patterns. In many regions, winter storms, which are often more frequent and intense than their summer counterparts, can trigger more pronounced erosion during the winter months. However, this pattern is not uniform across all mudflat ecosystems (R. A. Davis and Dalrymple, 2012 and Whitehouse and Mitchener, 1998).

Other important processes affecting mudflat dynamics

Beyond the influence of tides or waves, other crucial processes affecting mudflat dynamics include consolidation, fluidization, drying and subsidence (van Maren and Winterwerp, 2013; Swales et al., 2021; McIvor et al., 2013).

Consolidation occurs when water is expelled from the soil due to changing pressure conditions. This process strengthens the soil, making it more resistant to sediment erosion. However, it also leads to a lowering of the bed level (Testbook, 2023).

Fluidization occurs when sediments become temporarily suspended or when sediments behave like a fluid, often due to the upward flow of water. This phenomenon can be triggered by factors such as currents or wave action. While fluidization might briefly elevate the bed level, it renders the bed more susceptible to erosion (Soltanpour & Haghshenas, 2009).

The drying of intertidal areas can also lower the bed. As intertidal areas dry out, the pore water content decreases, resulting in reduced particle mobility and fluidity. However, this process also enhances internal cohesion and, consequently, the overall strength of the bed, making the bed less susceptible to erosion (Rinaldi and Casagli, 1999 and van Maren and Winterwerp, 2013).

Subsidence, which can result from various factors like human activities (e.g., gas or groundwater extraction), plate tectonics, or overburden, involves a significant lowering of the bed level (de la Barra et al., 2023). Overburden pressure refers to the force exerted on a soil formation by the material above it, which encompasses the weight of the soil and surrounding earth. When this pressure surpasses the pressure of any fluids within the pore spaces of the soil, the formation will compact, resulting in land subsidence (Baker et al., 2015).

Morphodynamic processes in tidal creeks

The final significant aspect to address in the context of tidal flats is the morphodynamic processes important in tidal creeks. Tidal creeks play a vital role in shaping mudflat morphology. Typically, larger drainage basins are associated with more intricate tidal creek networks (Renshun, 1992). These creeks exhibit varying flow patterns during tidal cycles. During the flood tide, the creek experiences numerous velocity peaks, primarily due to the rapid expansion of the inundated area adjacent to it. In contrast, during the ebb tide, extra water enters the creek, creating an asymmetric water balance with greater discharge during ebb than flood tides (Bayliss-Smith et al., 1979; Pethick, 1980; Wang et al., 1999). Sediment transport within these creeks predominantly moves seaward, particularly during spring tides. This behaviour reduces overall accretion rates on the mudflats (Y. Yang et al., 2003). Both tidal creeks and the mudflats exhibit an upward fining pattern (Gao, 2019 and R. A. Davis and Dalrymple, 2012).

2.2.3. Sediment dynamics on mangrove-covered mudflats

Mangrove trees contribute to soil development and sediment accumulation through two primary mechanisms: (1) direct involvement in biological processes that incorporate organic matter into the soil by depositing litter and growing roots beneath the surface, and (2) indirect contributions through physical processes that reduce water velocities, encourage sediment deposition, and capture and secure sediment (Massel et al., 1999; Henderson et al., 2017; Cahoon, 2006; McKee, 2011). However, on the flip side, mangroves can also facilitate soil degradation and sediment erosion through two primary mechanisms: (1) directly through biological processes like root decomposition and the breakdown of organic matter, and (2) indirectly through physical mechanisms that increase turbulence around the roots and alter groundwater pressure (Mullarney et al., 2017; Fagherazzi et al., 2017; Cahoon et al., 2003).

It is crucial to thoroughly examine the factors influencing both the immediate processes of erosion and accumulation and the long-term processes of soil degradation and development when studying the influence of mangroves on coastline stability. Erosion and accumulation processes are important as they directly impact sediment dynamics, which play a visible role in shaping the coastal landscape. However, the stability of a coastline depends both on short-term and long-term factors. Healthy soil development not only enhances sediment retention and supports mangrove growth but also contributes to the long-term resilience of coastal ecosystems. Conversely, soil degradation can exacerbate vulnerabilities to erosion and compromise the overall health of the coastal area (McIvor et al., 2013 and Fagherazzi et al., 2017).

In the upcoming sections, the factors that have the potential to influence soil development and, subsequently, those influencing soil degradation will be discussed. Aside from the physical and biological factors that will be discussed, faunal processes can also play a role in soil degradation and development, but these will not be covered in this discussion as the importance of these processes varies strongly across regions (Kristensen & Alongi, 2006).

Factors influencing soil development

The processes can be categorized into two divisions: surface processes, which occur at or above the soil surface, and subsurface processes, which take place beneath the soil surface (McIvor et al., 2013).

Surface processes that significantly influence soil development include sedimentation and accretion. Sedimentation involves the deposition of both organic and inorganic materials onto the soil, while accretion pertains to the anchoring of these deposited materials, making them less susceptible to being washed away by waves or tides (McIvor et al., 2013). The incoming material that gets deposited can be categorized as either allochthonous, originating from outside the mangrove area, or autochthonous, produced within the mangrove area. Allochthonous material includes sediment carried in by rivers and tides, while autochthonous material consists of materials generated by the mangroves themselves, such as leaves or branches (C. D. Woodroffe and Davies, 2009; Allison and Lee, 2004; Cahoon, 2006). Two important factors influence sedimentation rates. Firstly, the amount of incoming material is significant. The amount depends on sediment availability, but also on hydrodynamics, such as water currents or flow pathways that are able to transport the sediment into the mangroves (Saad et al., 1999 and Cahoon, 2006).

Secondly, even though there is enough sediment available, favourable conditions are required for sediment to settle. Mangroves have the capacity to reduce tidal and current velocities by increasing drag force. This reduction in particle velocities can facilitate sediment settlement (Massel et al., 1999 and Henderson et al., 2017). This process is closely related to flocculation, where sediment particles with larger diameters tend to settle more easily even in flowing water, while very small sediment particles may struggle to settle even with reduced current velocities (Wolanski et al., 1980).

Accretion is influenced by factors such as the growth of new roots, the development of benthic mats, and sediment consolidation (McIvor et al., 2013). When new mangrove roots grow, they can bind sediments, preventing them from being washed away (Cahoon & Lynch, 1997). Benthic mats consist of a mixture of algae, organic litter, single-celled organisms, and bacteria. These mats, formed on top of newly developed soil, can protect the soil from erosion (McKee, 2011). Finally, the sediment can consolidate which increases the shear strength of the soil, which makes it harder for soil particles to be washed away (Wells & Roberts, 1980). In Figure 2.16 the processes influencing soil development are depicted.

Subsurface processes that significantly impact soil development are the growth of mangrove roots, soil swelling, and soil rebound. The growth of mangrove roots contributes to an increase in the thickness of the soil layer (McKee et al., 2007 and Cahoon, 2006). Soils have the potential to swell as a result of water presence and rising groundwater pressure (Cahoon et al., 2011; Whelan, 2005; Rogers and Saintilan, 2008). Additionally, soils can rebound during consolidation when pressure is alleviated (Cahoon, 2006). While the last two processes typically occur on a shorter timescale, they can also influence long-term processes. For instance, during a drought, soil can undergo significant shrinkage, potentially leading to more frequent and prolonged inundation events. This, in turn, could increase sedimentation by introducing sediment or even erosion if more hydrodynamic forces are able to reach the intertidal flat (McIvor et al., 2013 and Rogers et al., 2005).

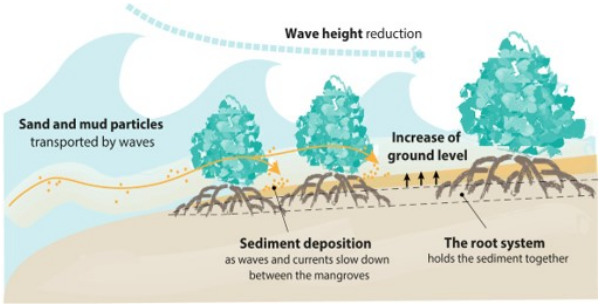

Figure 2.16: Soil development processes (BioManCo, n.d.)

Factors influencing soil degradation

Once again, the processes can be categorized into surface and subsurface processes. The most significant surface process affecting soil degradation is erosion. Surface erosion is mostly caused by wave attack and flow currents (Massel et al., 1999 and Henderson et al., 2017). Furthermore, erosion can also be induced by mangrove trees as turbulent eddies develop around their roots (Mullarney et al., 2017 and Nardin et al., 2016). Finally, the availability of sediment is another crucial factor as insufficient sediment supply can exacerbate natural erosion processes (McIvor et al., 2013).

The most important subsurface processes contributing to soil degradation are essentially the opposite of those involved in soil development, namely the decomposition of mangrove roots, soil shrinkage and consolidation (McIvor et al., 2013). Mangrove root decomposition primarily occurs as a result of tree mortality, but also due to the (excessive) presence of some nutrients such as nitrogen (McKee et al., 2007). Additionally, soil shrinkage can be induced by water scarcity, and soils may undergo compression or consolidation in response to heightened pressure (Cahoon et al., 2011; Cahoon et al., 2006; Whelan, 2005).

The effect of mangroves on the lower tidal flat

Mangroves not only influence the mudflat they grow on, but they also influence the entire tidal flat. As became evident in the previous chapter, the presence of mangrove forests can reduce tidal- and wave-induced currents, which promote sedimentation. The presence of mangroves, if enough sediment is available, will increase the bed level just in front of the forest and within the forest. Over an extended period, this accumulation would result in an elevation increase toward the sea from the mangroves, and a reduction in the slope within the mangrove area (Bryan et al., 2017).

When mangroves first start growing, they have a two-fold effect. They increase water currents, and the outer edges of the mangrove area are flood-dominant. This enhances sediment transport into the forest. However, as mangroves become denser, they effectively reduce these currents, leading to a gradual accumulation of sediment just inside the fringe (near the edge of the mangrove area) (W.-C. Liu et al., 2003; Mazda et al., 1997; Wu et al., 2001). Over time, this sediment accumulation alters the landscape. It increases the slope of the land outside the mangrove forests while flattening the slope inside the mangroves. This change in slope within the mangrove forest decreases the space available within the forest for sediment deposition. In other words, the tidal flat has a stronger convex-up profile (Friedrichs, 2011 and Lovelock et al., 2010). This means the water depth decreases faster than before and, in turn, decreases velocities towards the end of the flat, as waves now break earlier (Mullarney et al., 2017 and Bryan et al., 2017). Moreover, the convex-up shape of the tidal flat results in a reduced average water depth during high water slack. This condition facilitates more sediment deposition on the bed. Mangrove forests contribute to reinforcing the flood-dominant behaviour of tidal flats, potentially mitigating erosion rates across the entire tidal flat (Bryan et al., 2017 and van Maanen et al., 2013).

The effect of mangroves on tidal creeks

When mangroves inhabit mudflats, they change the geometry of the tidal creeks. On bare mudflats the tidal creeks are meandering, however when mangroves inhabit the mudflats, the tidal creeks become more straight. Furthermore, the tidal creeks become more narrow. This increases the velocity in the tidal creeks, and consequently, tidal creeks are able to transport more sediment. As tidal creeks are ebb-dominant, this means more sediment is able to leave the vegetated mudflat, which is necessary in order to maintain the morphological balance on the mudflat (K.-Y. Lee et al., 2022; Doeke, 2019; van Maanen et al., 2013).

Eroding tidal flats and degrading mangrove forests

In the context of coastline erosion, two theories offer insights into the dynamics at play, mirroring the dual theories previously discussed for accretion scenarios (”land-builders” vs. ”land-consolidators” discussion).

The first theory regarding coastal erosion states that the initial trigger is the disappearance of mangrove forests. Mangrove ecosystems, being highly specialized, can exhibit mortality on a large scale in response to even minor variations in their hydrological regimes (Blasco et al., 1996). A small change in, for example, salinity due to a reduced freshwater availability and inundation frequency due to sea level rise can cause mangrove mortality on a large scale (Snedaker, 1993; Pernetta, 1993; Field, 1994). As the mangrove cover diminishes, the fine sediment they once held in place is no longer effectively retained. Subsequently, the tidal flat succumbs to erosion, leading to the degradation of the coastline (Blasco et al., 1996; Bryan et al., 2017).

Contrasting, the second erosion theory suggests a different sequence of events. Here, the process initiates with the transformation of a convex-up tidal flat into a concave-up profile. The development of concave mudflats in mangrove environments can be attributed to an increase in wave-attack and a decrease in sediment availability (Kirby, 2000). As the concave-up profile develops, the water depth on the tidal flat rises. This elevation increases the wave height, allowing waves to penetrate deeper into mangrove forests without breaking. The intensified wave impact sets off an erosional feedback loop, progressively eroding more sediment. This erosion again results in an increased water depth, higher wave height, and a continuous cycle of sediment erosion (van Bijsterveldt et al., 2020 and Kirby, 2000). Mangroves will not be able to survive in these conditions as they will be inundated for too long or will simply be uprooted. Consequently, widespread mangrove mortality leads to the loss of sediment retention capacity, exacerbating coastal erosion even more (Blasco et al., 1996; Bryan et al., 2017).

Environmental factors influencing accretion and erosion rates

As the previous chapter shows, a delicate relationship exists between erosion and sedimentation within mangrove ecosystems. For instance, mangroves can reduce particle velocities, which encourages sedimentation, but they can also introduce highly turbulent zones locally, promoting erosion. Whether mangrove ecosystems primarily facilitate erosion or sedimentation depends on several factors such as the type of species, the type of root, the type of mangrove forest et cetera (McIvor et al., 2013). All factors will be introduced, and afterwards, their role will be explained.

Mangrove species

Different mangrove species can induce different rates of sedimentation. There are approximately 70 distinct species of mangrove trees, classified into roughly 27 different genera and spanning two separate plant divisions (M. D. Spalding et al., 1997). Within these genera, nine are considered true mangroves according to the most strict criteria (Tomlinson, 2016). The identification of true mangrove species relies on physical and ecological characteristics rather than a strict characteristic such as family lineage. Due to this, there is often variability among scientists in identifying which species qualify as true mangroves, leading to an undefined exact count of true mangroves (N. Duke, 1992). Appendix A provides an overview of the 27 genera of mangroves. Species belonging to the genus Avicennia and Rhizophora are the most prevalent and most widespread species along mangroves (N. C. Duke et al., 2002). Together with the genus Acrostichum, these three genera are the only genera present in both the Western and Eastern group. Only one species is present in both the Western and Eastern group, namely the Acrostichum aureum (N. C. Duke & Allen, 2006). Among the most commonly encountered mangrove species are the red mangrove (Rhizophora mangle), black mangrove (Avicennia germinans), and white mangrove (Laguncularia racemosa) (N. Duke, 1992). Images of the red mangrove, black mangrove, and white mangrove can be observed in Figure 2.17a, 2.17b, and 2.17c, respectively.

(a) Red mangrove (Owen, 2014)

(b) Black mangrove (Ndurya, 2017)

(c) White mangrove (Scobel, 2008)

Figure 2.17: The three most common mangrove species

To be able to survive in the intertidal zone, mangrove trees have developed specially adapted roots. Firstly, in order to maintain stability in an unstable substrate, mangrove trees have evolved by developing roots that do not penetrate deeply into the soil but instead spread horizontally. This structural adaptation enhances their overall stability (Polidoro et al., 2014). Secondly, to endure low oxygen levels within the soil, mangroves have also developed aerial roots, which grow above ground. These aerial roots absorb oxygen from the atmosphere and facilitate its transfer through the plant to the submerged roots (Miththapala, 2008). Various types of aerial roots exist, including prop roots, stilt roots, pneumatophores, knee roots and plank roots (Selvam & Karunagaran, 2019). The following section will discuss each of these root types.

Prop roots are roots that emerge from the trunk and lower branches of a mangrove tree. They can develop at a considerable height, sometimes up to 2 meters above ground. These roots extend far away from the trunk, and upon reaching the soil, they give rise to absorptive roots that penetrate vertically into the ground. Occasionally, secondary aerial roots may branch off from the initial prop roots, further extending away from the mangrove's trunk (Tomlinson, 2016).

In certain cases, when a mangrove tree ages, it undergoes changes in its trunk shape, becoming wider at the top and narrower at the bottom (an inverted cone shape). Furthermore, the trunk may even lose contact with the soil. When either or both events happen, the prop roots transition into a different category of roots known as stilt roots (Selvam & Karunagaran, 2019). These roots are now the primary support system of the tree. Prop roots and stilt roots serve the dual purpose of anchoring the mangrove plant securely in its habitat and accumulating water-borne silt and debris, which contributes to the gradual formation of soil beneath the plant. Moreover, they function effectively as a protective barrier against storm surges, surpassing the capabilities of other mangrove species (Srikanth et al., 2016; Laso Bayas et al., 2011; Ohira et al., 2013). Prop roots are characteristic of mangrove species within the Rhizophora genus (Zhang et al., 2015). For a visual representation and schematic depiction of prop roots, see Figure 2.18.

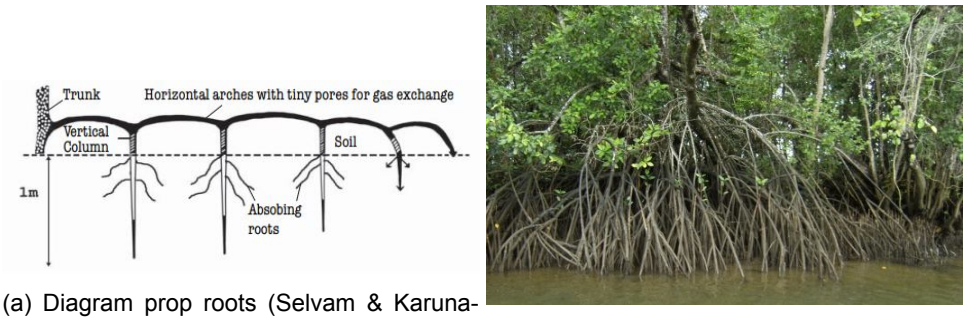

(a) Diagram prop roots (Selvam & Karunagaran, 2019)

(b) Picture prop roots (Alison, 2010)

Figure 2.18: Prop roots

Pneumatophores are vertical roots that emerge as upward extensions of the underground root system. These specialized roots are found in at least five different genera but are most prominently developed in the Avicennia and Sonneratia genera (Tomlinson, 2016). In the Avicennia genus, pneumatophores typically reach a length of around 30 centimeters, whereas in the Sonneratia genus, the pneumatophores can grow much taller, reaching up to 3 meters, although the majority are smaller, typically under 50 centimeters in length. The Avicennia species tend to have a higher number of pneumatophores compared to those of the Sonneratia genus (Selvam & Karunagaran, 2019). Pneumatophores are thought to enhance the flow of oxygen from the aerated portions of the plant to the submerged roots during flooding (Rehem et al., 2012 and Agoramoorthy et al., 2008). Therefore, it is believed that the main function of pneumatophores is to give mangroves the ability to withstand flooding when the trees are deprived of oxygen, however the precise physiological role remains uncertain (Parelle et al., 2006 and Z. Liu et al., 2014). For a visual representation and schematic depiction of pneumatophores, see Figure 2.19.

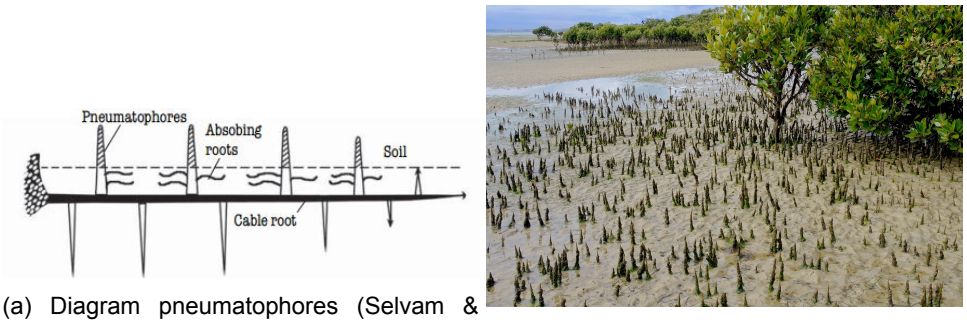

(a) Diagram pneumatophores (Selvam & Karunagaran, 2019)

(b) Picture pneumatophores (Sin, 2014)

Figure 2.19: Pneumatophores

Knee roots occur within species of the Bruguiera and Ceriops genus (Bingham & Kathiresan, 2001). These roots grow underground and periodically grow vertically out of the soil after which they immediately loop back into the soil where they keep growing horizontally (Nguyen et al., 2023). This resembles a bent knee, resulting in the name. This process is repeated and several knee-like structures develop (Selvam & Karunagaran, 2019). Like pneumatophores, it is believed that the primary function of knee roots is to provide oxygen to the mangrove trees when the trees are inundated (Ong & Gong, 2013). For a visual representation of knee roots, see Figure 2.20.

Figure 2.20: Knee roots (Xin, 2010)

Plank roots or buttress roots develop within species of the Xylocarpus genus. These underground roots extend vertically upwards along their entire length from the soil. These roots curve in a serpentine manner (Tomlinson, 2016). Buttress roots form in mangroves exposed to significant forces, primarily the impact of wind. These specialized roots play a crucial role in providing the essential stability required for the survival of trees in such environments (T. P. Young & Perkocha, 1994). For a visual representation, see Figure 2.21.

Figure 2.21: Plank roots (Sevvel, 2017)

The variety of aerial roots and the density of these roots are pivotal factors influencing sedimentation rates. High root densities are generally positive for sedimentation, but if root densities become excessively high, erosion can become the dominant process (B. M. Young & Harvey, 1996). Furthermore, research has shown that vertical sedimentation rates are the highest for plank roots followed by prop roots, pneumatophores and knee roots. However, prop roots, due to their structure, can also have the highest erosional rates, primarily because large turbulent eddies develop behind them (K. Krauss et al., 2003 and Du et al., 2021). Pneumatophores and knee roots are more effectively able to prevent surface erosion (Chen et al., 2023).

Habitat zonation

Within mangrove ecosystems, a clear zonation pattern emerges as one moves from the open sea towards the land. A characteristic of mangroves is that mangroves thrive primarily as a single species in dense concentrations (Selvam & Karunagaran, 2019). Depending on environmental factors such as tidal influence, salinity levels, and soil conditions, different species of mangrove trees emerge. Frequently, the various zones present within mangrove ecosystems are classified according to the inundation frequency or duration. Two classifications are often used in literature, one based on inundation frequency developed by Watson, 1928 and one based on the duration of an inundation developed by van Loon et al., 2007.

The framework based on inundation frequency was designed for mangrove ecosystems found in regions characterized by consistent semi-diurnal tidal patterns and a gently sloping terrain. To this day it is the most commonly used framework for mangrove rehabilitation. One should, however, be cautious in using this framework as only a subset of mangrove ecosystems around the world conforms to these specific criteria (van Loon et al., 2007; van Loon et al., 2016; Te Brake and Van Huijgevoort, 2008).
In areas where these specific criteria don't hold, an alternative approach has been proposed. This approach is not based on the frequency of the inundation but on the duration of the inundation. To get a reliable estimation of the species that are able to grow in a specific area, the duration of inundation is preferred over the frequency of inundation. Only when not enough data is available should one resort to the frequency of inundation (van Loon et al., 2007). In Table 2.1, the zonation based on the frequency of inundation is given, while in Table 2.2, the zonation based on the duration of inundation is given.

In both of these frameworks, the species that may inhabit a specific zone remain consistent. In inundation class 1, few mangroves can survive. In inundation class 2 species belonging to the genus Avicennia or Sonneratia are often present. Furthermore, in inundation class 3 species belonging to the genus Rhizophora or Ceriops can thrive. In inundation class 4 species belonging to the genus Lumnitzera, Bruguiera or Acrostichum can be found. Finally, in inundation class 5, few species can thrive. Occasionally, species belonging to the genus Ceriops or Phoenix are present in this zone (Watson, 1928). As the tidal elevation increases, so does the extent of the mangrove area, leading to the presence of a greater number of zones (Selvam & Karunagaran, 2019).

Table 2.1: Zonation based on the frequency of inundation (Watson, 1928)

Inundation class	**Tidal regime**	**Elevation above MSL [m]**	**Flooding frequency [per month]**
1	All high tides	<0	56 - 62
2	Medium high tides	0 - 0.09	45 - 59
3	Normal high tides	0.9 - 1.5	20 - 45
4	Spring high tides	1.5 - 2.1	2 - 20
5	Equinoctial tides	> 2.1	< 2

Table 2.2: Zonation based on the duration of inundation (van Loon et al., 2007)

Inundation class	**Tidal regime**	**Duration of inundation [min/day]**	**Duration of inundation [min/inundation]**
1	All high tides	> 800	> 400
2	Medium high tides	400 - 800	200 - 400
3	Normal high tides	100 - 400	100 - 200
4	Spring high tides	10 - 100	50 - 100
5	Equinoctial tides	< 10	< 502

It is important to acknowledge that these two frameworks only provide an estimate of the species that might thrive in a certain zone. The zonation of species is a complex interplay influenced by factors including salinity, tidal range, bed morphology, soil composition, and climate conditions, which makes it complicated to predict which species may survive at a certain location (Selvam and Karunagaran, 2019 and van Loon et al., 2016).
Sedimentation rates are heavily influenced by the frequency and duration of flooding events. In conditions where enough sediment is available, and mangroves are regularly flooded, substantial sedimentation rates can occur.

However, if zones experience more frequent and prolonged flooding, higher wave attack and flow currents can contribute to increased erosion (J. C. Ellison and Stoddart, 1991; C. D. Woodroffe, 1995; Cahoon et al., 2003; Lovelock et al., 2011).

Furthermore, a higher species diversity can lead to higher sedimentation rates (MacKenzie et al., 2016; Farnsworth, 1998; Field et al., 1998). This is associated with the width of the intertidal flat and the tidal elevation. As the tidal range expands, the width of the tidal flat also increases, consequently creating more zones on the intertidal flat where various types of mangroves can thrive van Loon et al., 2016; Selvam and Karunagaran, 2019; Cahoon et al., 2006).

Local scale
Mangrove wetlands can not only be categorized on a regional scale into various ecotypes but also on a local scale based on topography and hydrology. Six distinct types were identified by Lugo and Snedaker, 1974, namely, overwash, fringe, riverine, basin, scrub and hammock mangroves.

Overwash mangroves predominantly occupy areas within and adjacent to bays, including small islands, newly formed shoals, and finger-like extensions of larger land masses. These locations are strategically positioned to obstruct the natural flow of tides, resulting in frequent inundation of the mangrove system during high tides. The incoming tidal currents possess enough force to transport loose (organic) debris, which is then deposited in the inner bays as the tidal velocity diminishes. However, the debris that is carried away by the outgoing tides is not brought back, leading to a clear lack of organic matter within these forested regions (Lugo & Snedaker, 1974).

Fringe mangroves are commonly found along the edges of sheltered shorelines and islands. These mangroves are heavily influenced by tides, which play a pivotal role in their dynamics. Unlike other types of mangroves, these forests are not subjected to tidal overwash. Instead, tides export buoyant materials such as leaves, twigs and propagules from the mangrove areas into adjacent shallow water regions. This exportation of organic matter acts as a vital source of nutrition for a diverse range of organisms and contributes to the sustained growth of these mangroves (Lugo & Snedaker, 1974).

Riverine mangroves occur along major river basins that flow into broad mangrove wetlands. Salinity levels fluctuate with the seasons, decreasing during the wet season due to substantial freshwater runoff from precipitation. In the dry season, salinity is increased in the system due to a decrease in freshwater runoff. This seasonal salinity variation can enhance primary production by limiting competition from terrestrial plants. Furthermore, nutrient availability in these ecosystems is highest when salinity is lowest, creating optimal conditions for mangrove growth (Lugo & Snedaker, 1974).

Basin mangrove forests, also known as interior mangroves, are situated on the landward side of a mangrove wetland. These forests are shielded from the impact of waves and experience infrequent inundation by tides. Salinity levels can vary significantly, depending on various factors. In regions with high precipitation or substantial groundwater flow, salinity tends to be relatively low. Conversely, a combination of evaporation and the withdrawal of water by the mangrove trees can lead to elevated salinity levels, with some areas exhibiting distinctly hypersaline soil. Given the low currents, both riverine and tidal, it is likely that the basin type of mangroves serves as a sink for nutrients and sediments (Lugo & Snedaker, 1974).

Scrub mangroves are mangroves that occur in environments that lack nutrients or freshwater. Consequently, these mangroves are very small as they can reach maximum heights of 1.5 meters (Lugo & Snedaker, 1974).

Hammock mangroves only exist in Florida (USA). They resemble basin mangrove forests but exist on soil that is only slightly elevated. The mangrove forest flourishes above a bed of peat that has filled a void within the underlying limestone substrate (Lugo & Snedaker, 1974).

The type of forest is another important factor influencing sedimentation rates. Research has shown that accretion rates tend to be higher for fringe forests compared to overwash forests. This is because fringe forests tend to trap a lot of organic material transported into the forests, which is not carried out again (Cahoon and Lynch, 1997; K. W. Krauss et al., 2010; McKee, 2011).

Furthermore, forest density can be an important factor influencing sedimentation rates. If the mangrove density is too low, the presence of trees can significantly increase turbulence in the water column, leading to high erosional rates and potential damage to the trees. Low-density forests may also fail to dissipate wave and flow currents, exacerbating erosion effectively. It is also observed that higher forest densities correspond to higher sedimentation rates (Fagherazzi et al., 2017; Mullarney et al., 2017; Kumara et al., 2010).

Changing amount of resistance against erosion throughout the lifetime of mangroves
When mangroves are in their initial stages of growth as seedlings and saplings, they do not largely influence the sediment dynamics on the mudflat. The young plants have shallow root systems that do not offer substantial protection against wave and tidal forces. As mangrove trees grow and establish themselves, their root systems become more developed and extensive. This increased root density helps to bind and stabilize the soil and sediments, making the shoreline more resistant to erosion. During this phase of mangrove growth, the spatial distribution of the plants is critical. To stabilize the area, a wide coverage of mangroves needs to be established. As the mangroves continue to grow and mature, the emphasis shifts. In these later stages, the health and density of the vegetation become more important. The root systems of mature mangroves are well-developed and provide strong protection against erosion. As mangrove trees age more, there is an apparent decrease in fine root production in shallow soil layers. The decrease in fine root production is associated with declining tree density as mangroves mature. Both the decrease in fine root production and tree density reduce the ability of mangrove trees to stabilise the mudflat (Beselly et al., 2023; Xiao et al., 2020; Arnaud et al., 2021).

2.3. Conclusion

Ongoing research and debate surround the role of mangroves in coastal ecosystems, with several uncertainties still in place. The debate primarily concerns whether mangroves act as ”land-builders” or ”land-consolidators” (J. H. Davis, 1946; Steers et al., 1940; Watson, 1928; Egler, 1952; Swales et al., 2015). Some studies support that mangroves actively accumulate sediment and foster land expansion (”land-builders”), while others argue that they play a more passive role in sediment consolidation and soil formation (”land-consolidators”). Additionally, there is no consensus on whether mangroves exhibit one specific behaviour or can function as both, depending on various biogeomorphic settings such as sediment availability or the type of mangrove tree (Viles, 1988; S. Y. Lee et al., 2014; C. D. Woodroffe et al., 1985; Lovelock et al., 2010; Chapman, 1944; Bird, 1986; K. Krauss et al., 2003; Moldenke et al., 1960).

In the context of coastline erosion, there are two contrasting theories as well. There is no agreement on whether a particular behaviour is true or both are possible. One theory suggests that the disappearance of mangrove forests triggers erosion. This theory proposes that the loss of sediment retention capacity happens due to the decline of mangrove forests, ultimately leading to coastal degradation (Blasco et al., 1996; Bryan et al., 2017). On the other hand, the second theory proposes a different sequence of events. This theory suggests that the transformation of tidal flats from a convex-up profile to a concave-up profile results in the intensification of wave impact and more erosion. The intensified wave impact sets off an erosional feedback loop, progressively eroding more sediment. This erosion results in an increased water depth, higher wave height, and a continuous cycle of sediment erosion. In these conditions, mangroves will not be able to survive as they will be inundated for too long or simply uprooted, causing even more erosion (Kirby, 2000; van Bijsterveldt et al., 2020; Blasco et al., 1996; Bryan et al., 2017).

Despite uncertainties, certain aspects of mangrove ecology are better understood. Mangroves play a vital role in the development of soil and sediment accumulation through both biological and physical mechanisms. Their participation ranges from direct contributions through organic deposition and root growth, to indirect effects such as reducing water velocities and encouraging sediment deposition (McIvor et al., 2013). Over time, the presence of mangroves significantly impacts the coastal landscape through sediment accumulation. Sediments gather due to the presence of mangroves and produce distinct changes in the topography. The seaward side of mangroves beyond the forested area gradually increases in slope, while within the forest, the slope flattens. This shift produces a more convex-up profile, which affects water dynamics along the coast (Bryan et al., 2017). With a convex-up shape, there is a quicker reduction in water depth, resulting in reduced velocities towards the end of the flat as waves break earlier. This altered shape affects water depth during high water slack, facilitating increased sediment deposition on the bed (W.-C. Liu et al., 2003; Mazda et al., 1997; Wu et al., 2001). Overall, mangrove forests play a pivotal role in enhancing the flood-dominant behaviour of tidal flats, which can potentially reduce erosion rates across the entire tidal flat area (Bryan et al., 2017 and van Maanen et al., 2013). Moreover, the presence of mangroves reshapes the geometry of tidal creeks, especially in mudflat areas. As mangroves colonize mudflats, tidal creeks tend to become straighter and narrower. This transformation increases the velocity within tidal creeks, allowing them to transport more sediment, which is necessary to maintain the morphological balance crucial for the health of these ecosystems (K.-Y. Lee et al., 2022; Doeke, 2019; van Maanen et al., 2013).

Although mangroves play a constructive role in the ecosystem, they can also unknowingly contribute to soil degradation and sediment erosion. Some of the processes that lead to this include root decomposition and changes in groundwater pressure, which can increase turbulence and compromise sediment stability. These negative effects may oppose the positive impacts observed in flood-dominant tidal flat behaviour (McIvor et al., 2013).

It becomes clear that a delicate relationship exists between erosion and sedimentation within mangrove ecosystems. Whether mangrove ecosystems primarily facilitate erosion or sedimentation depends on several factors. Below is a summary of the presumed effects of these factors.

Wave climate
Larger waves can positively impact coastline stability by stirring up sediments offshore and transporting them inland. However, beyond a certain threshold, larger waves may lead to erosion on the tidal flat (Winterwerp et al., 2005).

Tidal range, width tidal flat and inundation frequency
The stability of the coastline, the distribution of species and the movement of water and sediment are interconnected and mutually influence each other. A larger tidal range is expected to be beneficial for the stability of the coastline. It contributes to a wider tidal flat, which allows for a more expansive habitat for species to thrive. This expansion positively affects the distribution of species, ultimately increasing stability. Moreover, a heightened tidal range increases the movement of water and sediment, which helps to transport more sediment into the tidal flat during high tide. This extended tidal range also provides a more prolonged period for sediments to settle out of the water column, thereby contributing to the overall stability of the coastal environment. However, it is important to note that a threshold exists. If the tidal flat experiences excessive and prolonged inundation, the heightened wave attack and flow currents associated with frequent inundation may increase erosion rates (van Loon et al., 2016; Selvam and Karunagaran, 2019; Cahoon et al., 2006).

Sediment availability
Adequate sediment deposition is crucial for mangroves to counter erosive forces and stabilize mudflats; hence, the availability of a large amount of sediment positively influences the ability of mangroves to stabilize the coastline (S. Y. Lee et al., 2014; C. D. Woodroffe et al., 1985; Lovelock et al., 2010).

Freshwater input
Freshwater input is essential for mangrove survival. However, excessive freshwater can lead to widespread mortality, highlighting the delicate balance required (S. C. Das et al., 2022).

Subsidence
Higher rates of subsidence resulting from tectonic or human activities can negatively impact coastline stability as it leads to a relative sea-level rise. This renders shorelines more susceptible to erosion caused by tidal and wave-induced currents (Ashton, 2022).

Density of mangrove forests, width of mangrove forest and mangrove species
The density of mangrove forests, the width of mangrove forests and mangrove species are interconnected and mutually influence each other. An expansion in the width of a mangrove forest along the shoreline is linked to increased coastal stability. A wider belt of mangroves is a more effective barrier against wave energy and tidal forces, thereby reducing their erosive impact on the coastline. A greater cross-shore mangrove width typically indicates a more diverse range of mangrove species, which is highly beneficial for shoreline stability due to their unique characteristics. These attributes collectively enhance the overall effectiveness of mangroves in stabilizing the mudflat and protecting the coastline. Thus, it is expected that an increase in the density of mangrove forests will have a positive correlation with the stability of the coastline. Denser vegetation can effectively increase the drag force, dissipating wave energy and reducing sediment transport, thereby contributing to shoreline protection (Fagherazzi et al., 2017; Mullarney et al., 2017; Kumara et al., 2010; Selvam and Karunagaran, 2019; van Loon et al., 2007; Cahoon et al., 2006).

Human influence
Increased human activity may disturb habitats through deforestation, urbanization, increased waste, and pollution. In addition, it can reduce mangrove resilience by, for example, reducing sediment availability due to the construction of artificial structures (E. L. Gilman et al., 2008b; Tait and Griggs, 1991; Fletcher et al., 1997; Ashton, 2022; Harris et al., 2021).

3

Global assessment

This chapter compares the trends in coastline change between mangrove-covered and non-mangrove-covered areas in tropical and sub-tropical regions globally. Additionally, it aims to determine whether there is a correlation between the width of a mangrove ecosystem and coastline stability worldwide. Finally, this chapter seeks to determine whether there is a relationship between the state of the mangrove forest (contracting, expanding and stable) and the state of the coastline (erosion or accretion).

3.1. Method

3.1.1. Data collection

The global assessment of coastlines is primarily based on data from two sources: the Muddy Shoreline Monitor, which provides historical coastline position data for muddy coastlines (Hulskamp et al., 2023), and the Global Mangrove Watch, which provides data on the global extent of mangrove ecosystems (Bunting et al., 2022).

The Muddy Shoreline Monitor dataset provides detailed information on the positions and change rates of muddy coastlines from 1984 to 2016. The dataset contains 1.8 million cross-shore transects distributed worldwide, each 1500 meters long. These transects run perpendicular to the 2016 global OpenStreetMap coastline (OpenStreetMap, 2021). The spacing of the transects decreases from 500 meters near the equator to 200 meters near the poles. Some transects are visualized in Figure 3.1a. This dataset focuses primarily on muddy coastlines. However, sandy coastlines are included as well. To categorise each transect, a pixel-based multispectral classification and a global coastal geospatial data analysis was used by Hulskamp et al. (2023). In this classifier, each transect is categorized into one of the coastal types, such as sandy, muddy, rocky, vegetated coasts, and others. To classify the coastline into seven categories worldwide (sandy beaches, mudflats, clear water, turbid water, green vegetation, dry vegetation, and other), Hulskamp et al. (2023) utilized a dataset compiled from freely available Sentinel-2 multispectral global Top of Atmosphere (TOA) images. At the same time, an analysis of global coastal geospatial data provides insights into the physical characteristics of coastal environments, including coastal elevation, climatic conditions, mangrove presence, tidal flats, and transition zones, utilizing six freely available coastal geophysical datasets such as the Multi-Error-Removed Improved-Terrain Digital Elevation Model (MERIT DEM) and the Global Mangrove Forests Distribution. Hulskamp et al. (2023) implemented a shoreline detection algorithm using over 1.9 million Landsat images to calculate shoreline change rates for every transect. Dynamic thresholding methods are used to create accurate surface water masks, enhancing the precision of shoreline detection. The Normalized Difference Water Index (NDWI) estimation and edge detection techniques are applied to refine the identification of water-land transitions (Luijendijk et al., 2018 and Hulskamp et al., 2023). The change rate is then calculated using a least-squares linear regression, which will be elaborated on in section 3.1.3.

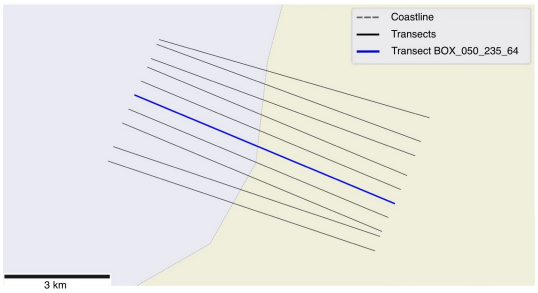

(a) Transects with a length of 1.5 [km] located in Africa

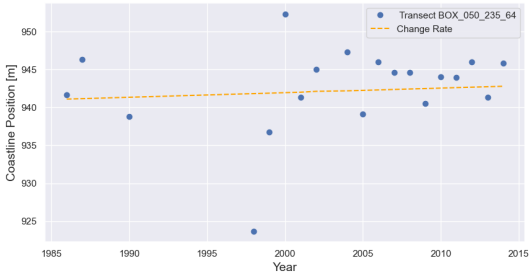

(b) Coastline position and the change rate from 1984 to 2016 for transect BOX_050_235_64

Figure 3.1: The data available in the Muddy Shoreline Monitor dataset

The Global Mangrove Watch (GMW) dataset provides maps of the estimated global extent and changes of mangrove forests. This dataset covers a time period of eleven years, from 1996 to 2020, and includes data from 1996, 2007, 2008, 2009, 2010, 2015, 2016, 2017, 2018, 2019, and 2020. The dataset is useful for determining the geographical extent of mangroves and has a pixel spacing of 25 meters. The dataset distinguishes between mangrove and non-mangrove areas. It is derived from a combination of L-band SAR (JERS-1 SAR, ALOS PALSAR, and ALOS-2 PALSAR-2) and optical (Landsat) satellite data (Bunting et al., 2022 and ALOS, 2021). In this study, the Global Mangrove Watch dataset is not directly utilized. Instead, the dataset provided by Worthington et al. (2020) is employed in the analysis, which utilizes data from the Global Mangrove Watch dataset. The Worthington et al. (2020) dataset is classified into four different mangrove ecosystems, including lagoonal, estuarine, deltaic, or open coast mangrove ecosystems. This classification was overlaid onto the GMW datasets for 1997, 2005, 2010, and 2016. The dataset provided by Worthington et al. (2020) contains polygons and multi-polygons that represent the different mangrove typologies. An example of the (multi-)polygons can be seen in Figure 3.2.

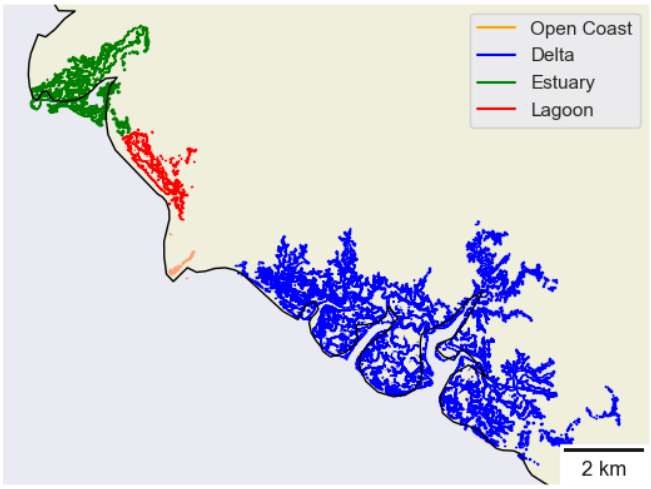

Figure 3.2: Example area with multiple mangrove ecosystems in Africa

The global assessment incorporates two additional datasets. The first one is the OpenStreetMap (OSM) coastline dataset from 2021, which was obtained from the OpenStreetMap project. This dataset has geographical information about coastlines contributed by users and is freely available. The coastlines are split into different line strings (OpenStreetMap, 2021). The second dataset is a global river dataset that contains approximately 2.94 million vector flowlines. These flowlines are precisely defined from a high-accuracy global digital elevation model at 3-arcsec resolution (90 m). This dataset provides accurate information about the geometry and location of the rivers worldwide (Lin et al., 2019).

3.1.2. Data refinement

Spatial refinement through boundary criteria

After analyzing data from the Global Mangrove Watch dataset from 1996, it has been determined that the most northern mangrove forests are located around 32.37 degrees north, while the most southern mangrove forests are found at approximately 38.86 degrees south. To cover all significant geographical zones, it has been decided to include all transects within the latitude range of 33 degrees north to 39 degrees south. The map in Figure 3.3 shows the areas considered in this research.

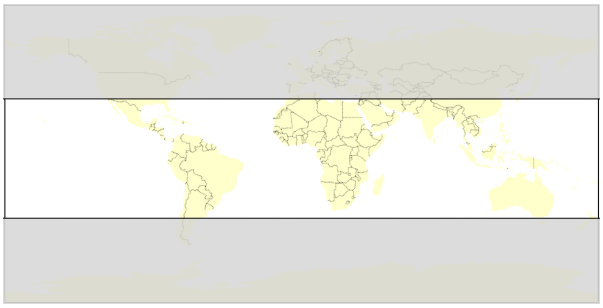

Figure 3.3: Geographical coverage map

The Muddy Shoreline Montor dataset has been categorized based on location into eight distinct clusters: Africa, Asia, Europe, North America, Oceania, Open Sea, South America, and unknowns. Since mangroves are not present in Europe, the Europe cluster includes territories such as Martinique and Mayotte. Similarly, the Open Sea cluster consists of small island nations like the Cook Islands and Papua New Guinea. Data points from the Europe and Open Sea clusters were manually redistributed to the remaining five continents where mangroves are typically found: Africa, Asia, North America, Oceania, and South America. Any unknown data points were also manually assigned to these continents. Figure 3.4 illustrates the various continents and associated islands.

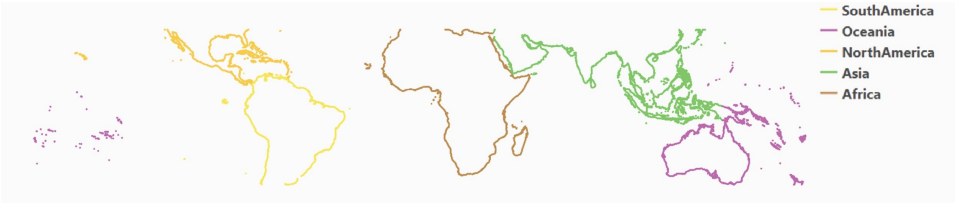

Figure 3.4: Distribution of continents containing mangroves

This study focuses only on the muddy transects found in the Muddy Shoreline Monitor dataset. Among the 791,483 transects within the considered boundaries, those identified as sandy are marked in the dataset and excluded from the analysis. After this exclusion, 500,103 transects remain, which accounts for 64% of all transects within the defined boundaries. Furthermore, transects containing mangrove forests classified as deltaic, estuarine, or lagoonal mangrove ecosystems are also excluded, resulting in a total of 382,704 transects. To help understand the distribution of these transects, a breakdown of the number of transects per continent is provided in Figure 3.5. The analysis shows that most of the transects are located in Asia.

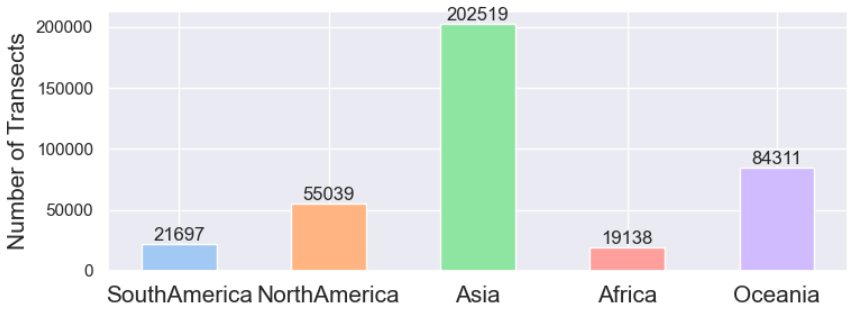

Figure 3.5: Number of transects to be analysed per continent

Temporal extend

The Muddy Coastline Monitor dataset provides annual data on coastline positions spanning over 33 years. However, the dataset by Wortington et al. (2020) only covers 4 years within a 24-year timeframe. To obtain more evenly distributed data on open coast mangrove ecosystems, it has been decided to narrow down the dataset to 12 years, specifically from 2005 to 2016. By adopting this approach, 12 years of coastline position data and 3 years of mangrove data (2005, 2010, and 2016) can be used in the analysis. This allows the optimization of the available data resources and more robust conclusions regarding the dynamics of mangroves and changes in the coastal areas over the selected duration can be derived.

Complex transects

There are situations where a transect from the Muddy Shoreline Monitor dataset intersects with the coastline twice, leading to two potential issues. The first problem is illustrated in Figure 3.11a. In this case, a transect intersects with two mangrove forests on opposite sides of a small island. To address this issue, a gap criterion is implemented to define the cross-shore width along a transect, ensuring that only one mangrove forest is considered. The gap criterion and how the width along a transect is determined, is further discussed in Section 3.1.3. However, if a mangrove forest covers almost the entire length of a transect that intersects twice with the coastline, the entire width may be taken into account, even though the entire width of the mangrove forest only contributes to coastline stability partly. The second problem is demonstrated in Figure 3.6a. In this case, a transect intersects the coastline twice. The mangrove forest is located at the end of the transect on the opposite side of the island. Although the mangrove forest is not situated along the considered coastline, this transect will still be classified as a mangrove transect.

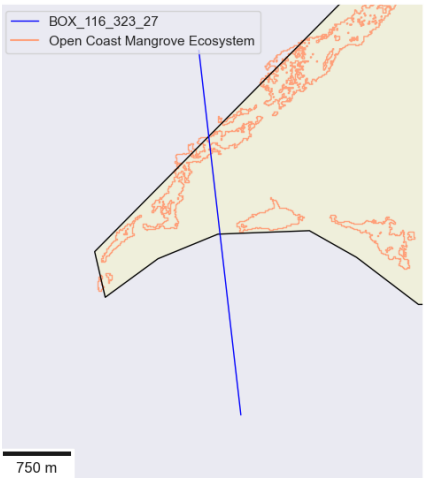

(a) A transect intersecting twice with the coastline

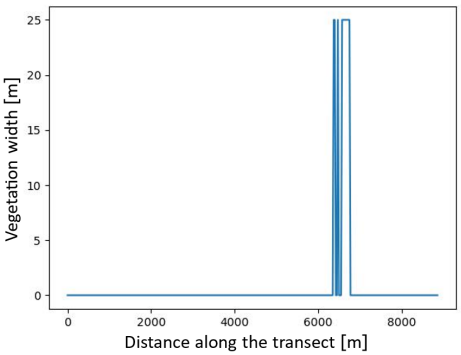

(b) Cross-shore width of a mangrove forest along a transect starting from the most seaward point

Figure 3.6: Visual representation of transect BOX_116_323_27 and its intersections with an open coast mangrove ecosystem

It is difficult to accurately determine the number of transects that could pose challenges when defining the width of mangroves along a transect. Therefore, transects intersecting the coastline more than once will be identified as complex transects. This determination is based on the OSM dataset from 2021 (OpenStreetMap, 2021). If the extended transects intersect with the OSM dataset more than once, they will be classified as complex transects.

Open coast transects

Specific transects are labelled as open coast transects to facilitate global comparisons between similar scenarios among mangrove transects and non-mangrove transects. These transects are located along coastlines that are not sheltered by islands, embayments, or other land masses. However, there is no universally accepted rule to determine how far a landmass should be removed for a coastline to be considered unsheltered. To establish a distance criterion, all open coast mangrove-covered transects were extended seaward by 100 kilometers. For each transect, the distance between the coastline where the transect is defined and the nearest coastline defined by the OSM dataset is calculated. Figure 3.7 shows a histogram displaying the different distances to the nearest coastline. Transects that do not intersect with another coastline within the extended length of the transects are assigned a distance of 100 kilometres. These transects are not included in the histogram. As depicted in this figure, the median value is 6315 km, and the mean is 17897 km. Given the high variability between the median and mean values, two different definitions will be employed in the analysis, depending on the distance. The first definition states that a transect is considered to be an open coast transect if no other coastline is found within 5 kilometres. In comparison, the second definition considers a transect as an open coast transect if no other coastline is found within 15 kilometres. Moreover, the river dataset determines whether the transects intersect with a river within 5 and 15 kilometres, respectively. If so, the transects are not considered open coast transects.

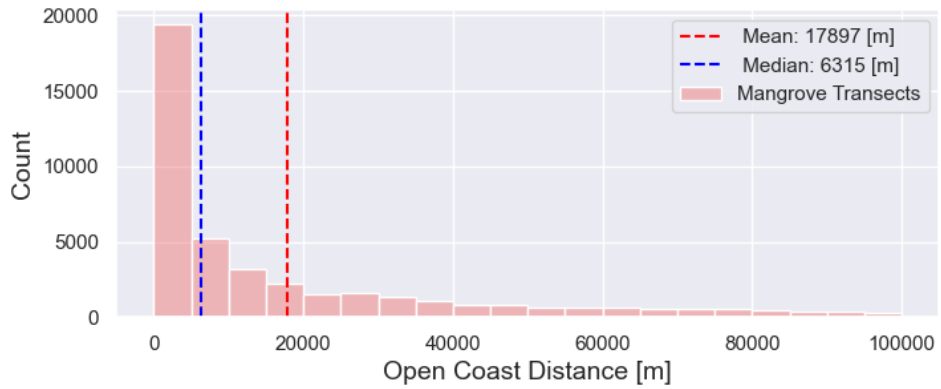

Figure 3.7: Distance to nearest coastline

The four analytical frameworks

The collected data will be analyzed through four different frameworks. Each framework distinguishes between mangrove transects and non-mangrove transects. Mangrove transects intersect with an open coast mangrove ecosystem. In contrast, non-mangrove transects include all transects that do not intersect with any type of mangrove forest (open coast, deltaic, estuarine, or lagoonal). The specifics of each framework are as follows:

Framework 1

Framework 1 serves as the base framework. In this framework, all muddy transects, with or without open coast mangroves, are included in the analysis without additional filters.

Framework 2

Framework 2 applies the same filters as framework 1, adding that only non-complex transects are included.

Framework 3
Framework 3, similar to framework 2, includes only non-complex transects. However, only open coast transects are included. Open coast transects are defined as those that don't intersect with land within 5 kilometres when extended seawards. Additionally, if a transect intersects with a river within 5 kilometres, it is excluded from this framework.

Framework 4
Framework 4 resembles framework 3, including only non-complex and open coast transects. However, in this framework, open coast transects are defined as those that don't intersect with land within 15 kilometres when extended seawards. Additionally, transects that intersect with a river are excluded from this framework.

Figure 3.8 displays the number of transects considered within each framework.

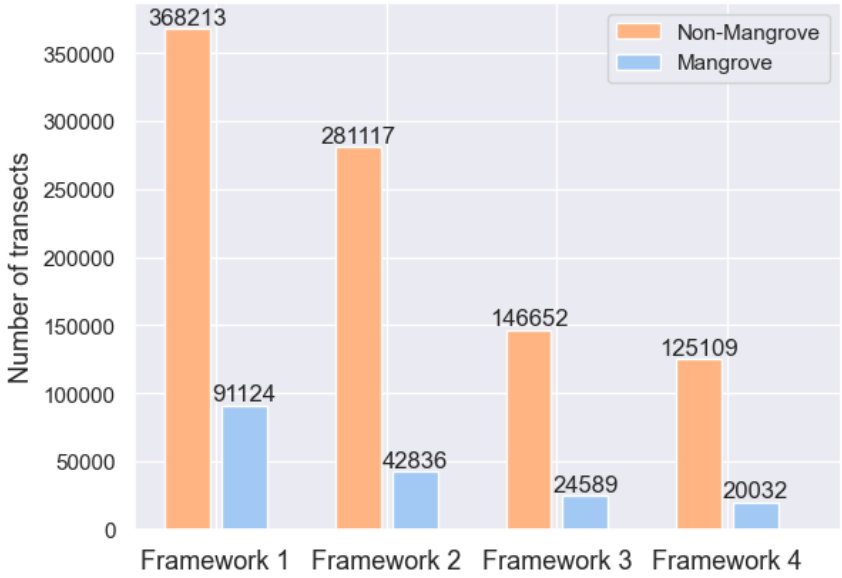

Figure 3.8: Total counts of transects per framework for both mangrove as non-mangrove transects.

This research will discuss and use the main results of framework 4. Framework 4 is selected based on the assumption that applying the filters will eliminate as many uncertainties as possible, yielding the most reliable results.

3.1.3. Data analysis

Determining the coastline position change rate

The Muddy Coastline Monitor dataset provides the change rate from 1984 to 2016. However, for the period between 2005 and 2016, the change rate has been recalculated using the same method as described in Luijendijk et al. (2018), which employs a least squares linear regression approach. During this re-calibration process, certain data points are removed to ensure consistency. In the first method, outliers are identified and eliminated based on their gradients, representing the rate of change in coastline distance per unit of time. Gradients falling outside the predefined range, set to be between -3 times 30 meters (representing a significant decrease in distance) and 3 times 30 meters (representing a significant increase in distance), are deemed outliers and subsequently excluded from further analysis. The second method involves fitting a linear regression line to the dataset using the least squares method, which allows for the identification of outliers based on the deviation of individual data points from the fitted line. After fitting the regression line, an outlier test is conducted using the Bonferroni p-value criterion. Data points with a Bonferroni p-value less than 0.2, indicating a significant deviation from the fitted line, are identified as outliers. If less than 2 data points remain in a transect, that transect is not included in the analysis.

Transects are classified as accreding, eroding, or stable based on their change rate. A transect is considered accreding if the change rate exceeds 0.5 meters per year, eroding if it falls below -0.5 meters per year, and stable if it ranges between -0.5 and 0.5 meters per year. These classifications align with those used in Luijendijk et al. (2018). Figure 3.9 provides an overview of the number of transects per coastal state (accreding, eroding, or stable) for all muddy transects in the Muddy Shoreline Monitor dataset. Globally, the majority of transects are classified as eroding.

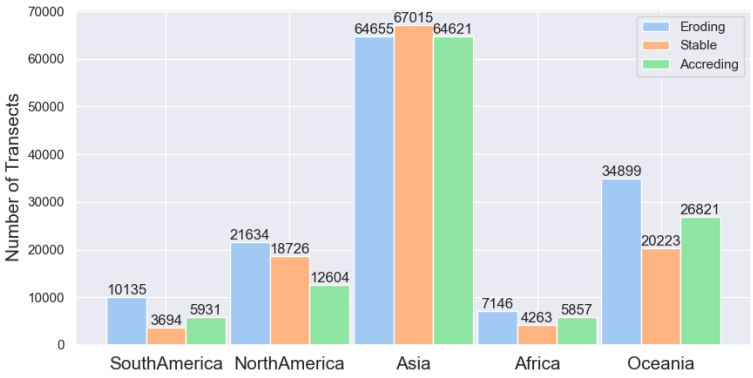

Figure 3.9: Number of transects per coastal state per continent

Framework 4 includes a total of 145,141 transects. However, after filtering out all transects that lack coastline position data, 109,065 transects remain. Of these, 20,032 are mangrove transects, and 89,033 are non-mangrove transects. Figure 3.10 provides a distribution per coastal state for mangrove and non-mangrove transects. Slightly more mangrove transects are eroding compared to non-mangrove transects, while slightly more non-mangrove transects are stable than mangrove transects. However, the differences are relatively small. The percentage of accreding transects is similar for both mangrove and non-mangrove transects.

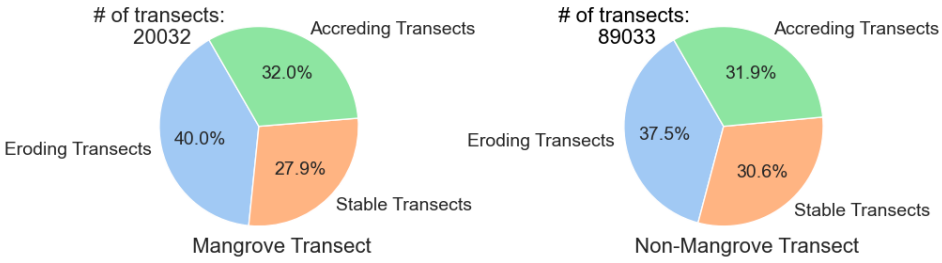

Figure 3.10: The coastal state distribution of mangrove and non-mangrove transect

Determining the cross-shore width of mangrove forests

Along each transect, the cross-shore width of an open coast mangrove forest is computed. Initially, the transects are approximately 1.5 kilometres in length. However, upon visual inspection using QGIS, it was observed that many mangrove forests extend beyond this length, with some spanning up to 20 kilometres. Therefore, it was necessary to expand the original transects. However, overextending the transects leads to a significant increase in computational time. To balance the need for comprehensive coverage of larger mangrove forests with computational efficiency, it was decided to expand the transects to a minimum length of 8 kilometres. Expanding transects to a minimum length of 8 kilometres involves extending them 4 kilometres seaward and 4 kilometres landward. This decision was later validated. It is important to note that due to the utilization of global coordinates, the minimum length of the transects is set to 8 kilometres, with the length increasing proportionally away from the poles, up to a maximum of around 12 kilometres.

The dataset from Worthington et al. (2020) includes polygons and multi-polygons that are made up of cells with a size of 25 [m]. Whenever a cell intersects with the transect, the width of the cell is added to the total mangrove width. Therefore, the cross-shore mangrove width along a transect is calculated by summing up the widths of all the cells intersecting with the transect. However, this approach could potentially overestimate the total width, especially when a transect intersects twice with the coastline. An example of this scenario is depicted in Figure 3.11a. In Figure 3.11b, the mangrove forest's width along the transect is illustrated, with a maximum width of 25 meters corresponding to the pixel size. It can be seen in this figure that the width of the mangrove forest on the opposite side of the island is also included in the calculation. However, this width does not affect the coastline stability on the side of the island where the transect is defined. A gap criterion was established to mitigate this overestimation: if the distance between two mangrove forests exceeds 500 meters, the width measured after that gap will not be added to the total. This criterion ensures a more accurate representation of mangrove coverage by excluding mangrove forests that might not contribute significantly to the overall extent of the ecosystem.

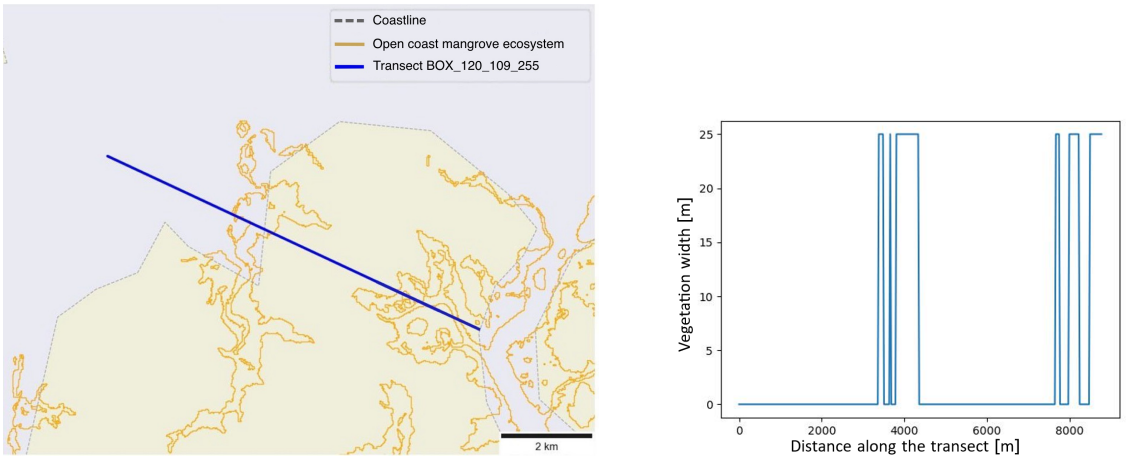

(a) Transect covering two sides of a small island (b) The width of the mangrove forest along the transect

Figure 3.11: Determining the cross-shore width along a transect

After calculating the widths of mangrove forests along all transects, the decision to extend the transects to 8 kilometres is reassessed. Figure 3.12 displays a bar chart of all transects intersecting with open coast mangrove forests. The chart shows that the majority of these mangrove forests are less than 500 meters wide, with very few exceeding 4000 meters in width. The median cross-shore width of all mangrove forests is 300 meters. Extending the transects to 8 kilometres will not significantly affect many mangrove forests, as only a limited number of mangrove forests are expected to exceed this width.

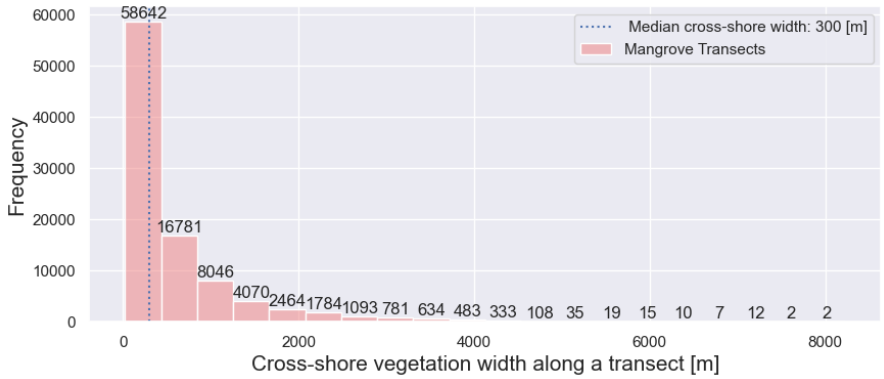

Figure 3.12: Bar plot including all the mangrove-covered transects

The cross-shore widths of open coast mangrove forests along the transects that intersect with these mangrove forests are determined for the three specific time periods considered in this research, namely 2007, 2010, and 2016. Additionally, the cross-shore width of lagoonal, deltaic, and estuarine mangrove forests along transects intersecting with these typologies is calculated using the dataset from 2010. The purpose of this calculation is to allow a fair comparison between open coast mangrove transects and non-mangrove transects. Using the width of these three typologies along a transect, transects containing mangroves can be excluded from the analysis, ensuring that only non-mangrove transects are included in the non-mangrove category.

Determining the cross-shore mangrove width change rate

Similar to the coastline positions, the change rate for the cross-shore width of mangrove forests is calculated using the same method as described previously. Transects with fewer than two values of mangrove widths are excluded from the analysis. Figure 3.13 shows the distribution of change rate values. Only change rates between -10 and 10 [m/year] are displayed, as the majority (96%) of values fall within this range. It can be observed that between 2005 and 2016, most mangrove forests remained stable without significant changes. However, it should be noted that changes of less than 25 meters will not be detected due to the pixel size limitation of 25 meters.

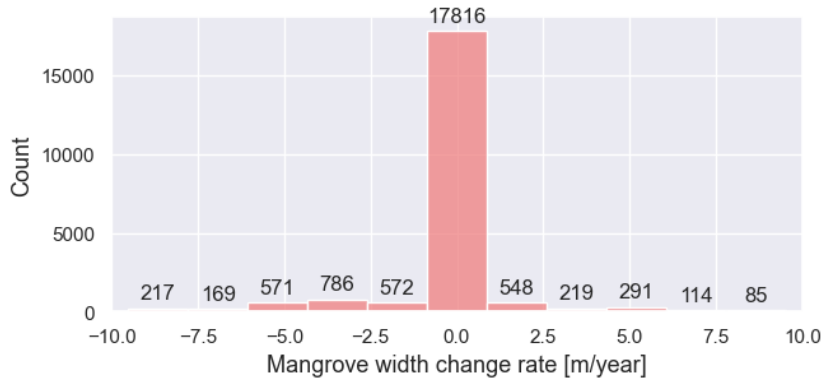

Figure 3.13: Histogram showing the distribution of mangrove width change rates between -10 and 10 [m/year]

In Figure 3.14, the change rates have been classified into three groups: stable, expanding, and contracting. When the change rate is zero, the mangrove forest is considered stable, while it is considered contracting if the change rate is negative and expanding if the change rate is positive. In Figure 3.14, the distribution of contracting, expanding and stable mangrove transects for framework 4 is given. The majority of mangrove transects, namely 72.6%, are stable. Furthermore, 16.6% of mangrove transects are contracting, while only 9.9% of mangrove transects are expanding.

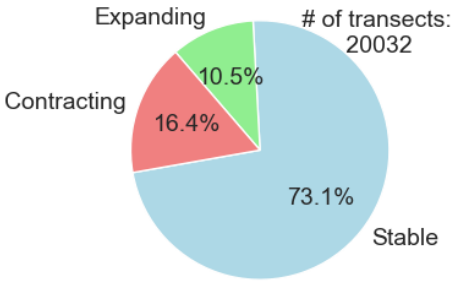

Figure 3.14: Distribution of Mangrove forests into the defined three categories

3.2. Results

As mentioned previously, only the main results of framework 4 will be discussed. Appendix B presents the results for frameworks 1,2 and 3. Furthermore, the results of framework 4 are more thoroughly expanded on in Appendix B. Finally, a comparison of all the frameworks can also be found in the appendix. While only the results from framework 4 are discussed, it should be noted that similar results were found across all frameworks.

The results are categorized into three groups. Firstly, the effect of the presence of mangroves on coastline stability will be investigated. These results compare the coastline position change rates for mangrove and non-mangrove transects. Secondly, the effect of the width of a mangrove forest on coastline stability will be researched. In these results, the coastline position change rates for mangroves with a smaller width will be compared with mangroves with a larger width. Finally, the effect of the state of a mangrove forest (expanding, stable or contracting) on coastline stability will be analysed. These results will compare the coastline position change rates for contracting, expanding and stable mangrove forests.

3.2.1. The influence of the presence of mangroves on coastline stability

In Figure 3.15 boxplots can be seen that represent the distribution of coastline position change rates for both mangrove and non-mangrove transects. The change rates are classified into two groups: transects that are eroding (with a change rate below -0.5 [m/yr]) and transects that are accreding (with a change rate above 0.5 [m/yr]). Each boxplot in this figure shows the interquartile range, median, and standard deviation for each category. After comparing the medians of both mangrove and non-mangrove transects, it was observed that the median value for eroding mangrove transects is slightly lower than that for eroding non-mangrove transects. Additionally, the median value for accreding mangrove transects is higher than accreding non-mangrove transects. Both the standard deviations and interquartile ranges are similar for mangroves and non-mangroves. In Appendix B, it was verified that the difference in sample size between mangroves and non-mangrove transects does not affect these results.

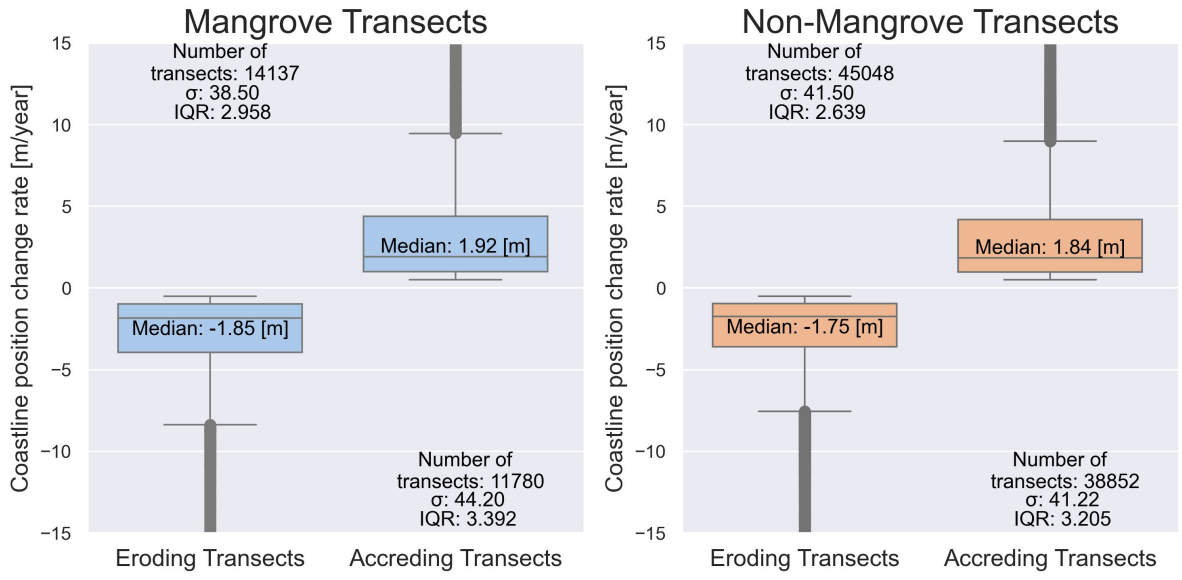

Figure 3.15: Coastline position change rate for mangrove and non-mangrove transects

3.2.2. The influence of the width of a mangrove forest on coastline stability

The scatterplot in Figure 3.16 shows the relationship between the width of open coast mangrove ecosystems along the transects in 2010 and the coastline position change rate. Looking at the figure, it seems that the change rates are centred more around the x-axis for larger mangrove widths, indicating that the coastline is more stable for larger mangrove widths. To investigate this trend further, the data has been divided into bins of 500 meters, and the 15th and 85th percentile for each bin is calculated. These percentiles represent thresholds below which 15% and 85% of the data points fall, offering insights into the range and variability of the dataset. A smaller difference between the 15th and 85th percentile indicates a more consistent pattern in the data, while a larger difference indicates more variability in the data. However, larger mangrove forests are substantially less abundant than smaller mangrove forests. This implies that the first bins include substantially more data points than the last bins. To account for the imbalance in data points per bin, 100 random data points are selected for each bin, and the 15th and 85th percentile is calculated using these data points. Using a least-squares linear regression line, the 15th and 85th percentiles per bin are connected with dotted lines in the figure. The deviation between the 15th and 85th percentiles suggests that for larger mangrove widths, there is an increased variability and a reduced correlation between the variables. To assess the consistency of the observed trends, the slopes of the 85th and 15th percentile lines are calculated 1000 times. The resulting distribution of slopes for the 15th and 85th percentiles is shown in the top right and bottom right figures of the plot, respectively. The analysis indicates that the slope of the 15th percentile is consistently negative, while the 85th percentile is consistently positive. This suggests that the lines across the 1000 runs always diverge. This indicates that there is an increased variability for higher mangrove widths. Furthermore, this indicates that for higher mangrove widths more accretion takes place, however also more erosion takes place. Additionally, when inspecting the 15th and 85th percentiles, it can be seen that the absolute value of the median of the 15th percentile line is higher than the absolute value of the median of the 85th percentile. This indicates that the accretion rate is lower for higher mangrove widths than the erosion rate, which suggests that erosion rates are higher than accretion rates for larger mangrove widths. However, as can be seen, when investigating the dotted line, the relationship per bin is more complex. In Appendix B, there are other methods that are used to support the identified trends.

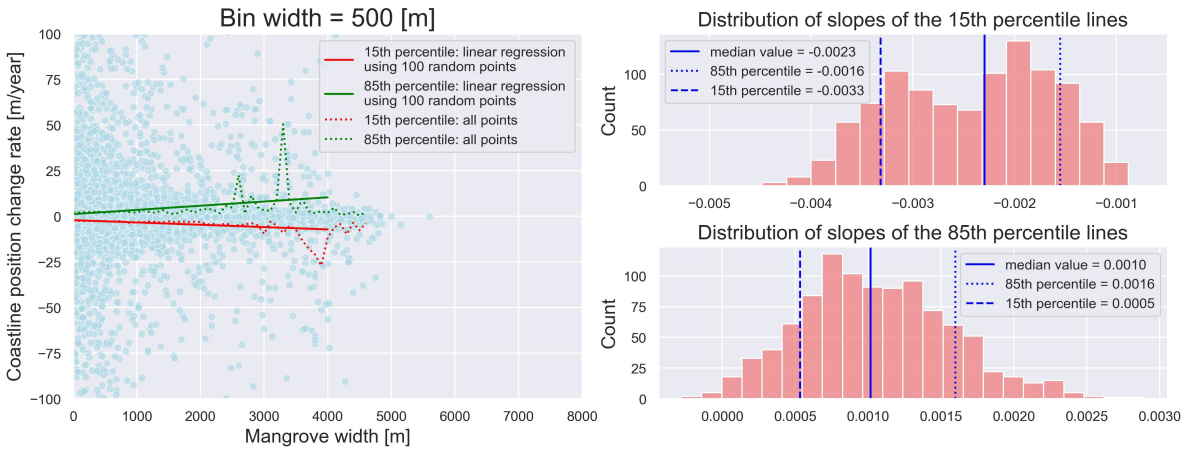

Figure 3.16: Relationship between the cross-shore mangrove width (x-axis) and the coastline position change rate (y-axis)

3.2.3. The influence of the state of a mangrove forest on coastline stability

In Figure 3.17, a scatterplot can be seen that represents the relationship between the mangrove width change rate and the coastline position change rate. The majority of the points on the graph are situated around the y-axis. This suggests that for most transects, the mangrove forest is stable. This could also be seen in Figure 3.14. The scatterplot is divided into four quadrants. Most transects, namely 1,973, are situated in the bottom left quadrant. This indicates that if the mangrove forest is contracting, the coastline is most likely eroding. When the mangrove forest is expanding, marked by a positive mangrove width change rate, most transects, namely 1,151, can be found in the top right quadrant. This suggests that the coastline is most likely experiencing accretion if the mangrove forest is expanding.

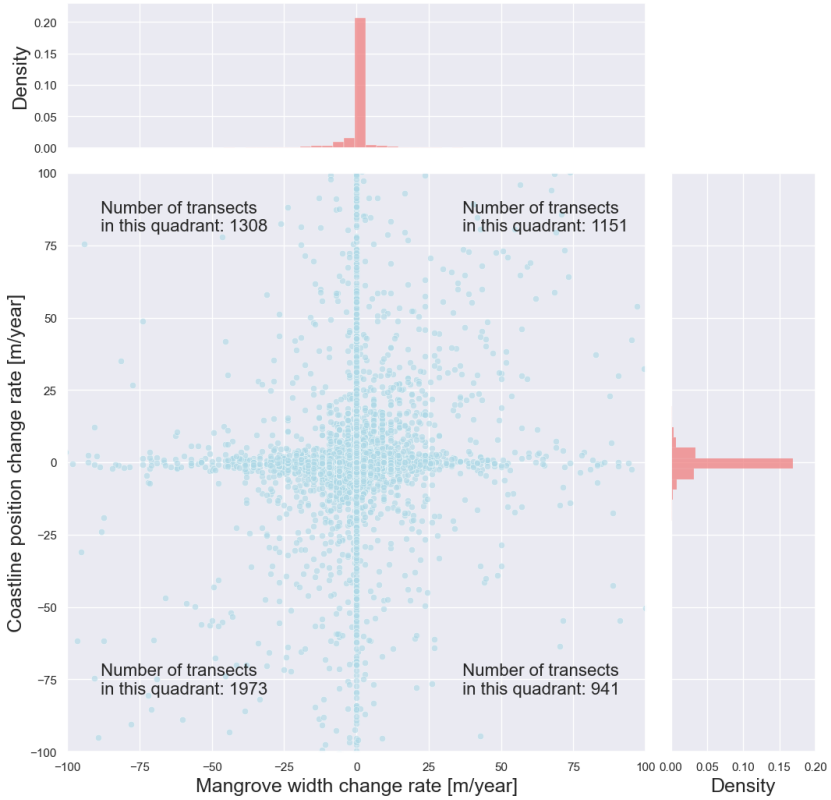

Figure 3.17: Relationship between the mangrove width change rate (x-axis) and the coastline position change rate (y-axis)

In Figure 3.18, the scatterplot is analyzed in more detail by showing the distribution of coastline position change rates for accreding transects with contracting, stable, and eroding mangrove forests. The figure is divided into three parts where the left graph shows the distribution of coastline change rates in the top left quadrant; the middle graph shows the distribution of coastline position change rates on the positive y-axis, and the right graph shows the distribution of coastline position change rates in the top right quadrant. In the graphs, the median value, the 85th percentile and the 15th percentile are presented. In the figure, it can be seen that the distribution is quite similar for contracting and stable mangrove forests. The median value is slightly higher when a mangrove forest is stable, but the difference is minimal. When the mangrove forest is expanding, it can be seen that the median is significantly higher than when it is contracting or stable. This indicates that when a mangrove forest is expanding, the coastline experiences higher accretion rates than when it is contracting or stable. Furthermore, for transects with accreding coastlines, the 85th percentile is considerably higher for expanding mangrove forests than for stable mangrove forests. This suggests that extreme accretion events are more prevalent in expanding mangrove forests than in stable mangrove forests.

Additionally, the 85th percentile is also higher for contracting mangrove forests than for stable mangrove forests, indicating that extreme accretion is also more prevalent in contracting mangrove forests than stable mangrove forests. This shows that when the mangrove forest is stable, less variability exists in coastline position change rates than when the mangrove forest is expanding or contracting. However, it should be noted that there is a substantial difference between the 85th percentile of expanding mangrove forests and contracting mangrove forests, indicating that extreme accretion events are particularly prevalent in expanding mangrove forests.

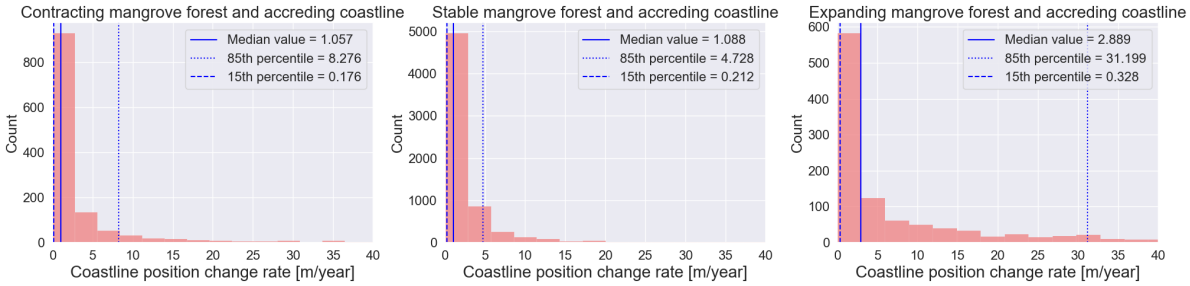

Figure 3.18: The coastline position change rate distribution for accreding transects with contracting, stable and eroding mangrove forests

In Figure 3.19, the distribution of coastline position change rates is shown for eroding transects with contracting, stable, and expanding mangrove forests, respectively. The left graph displays the distribution of coastline change rates in the bottom-left quadrant; the middle graph shows the distribution of coastline position change rates on the negative y-axis, and the right graph shows the distribution of coastline position change rates in the bottom-right quadrant. Examining the median value shows that when a mangrove forest is stable, the median erosion change rate is the least negative. When a mangrove forest is contracting, the median erosion change rate is the most negative. Additionally, more variation exists when a mangrove forest expands or contracts when considering the 15th percentile. This suggests that a stable mangrove forest results in lower erosion rates than when a forest expands or contracts. Moreover, less extreme erosion rates occur when a mangrove forest is stable than when it is expanding or contracting.

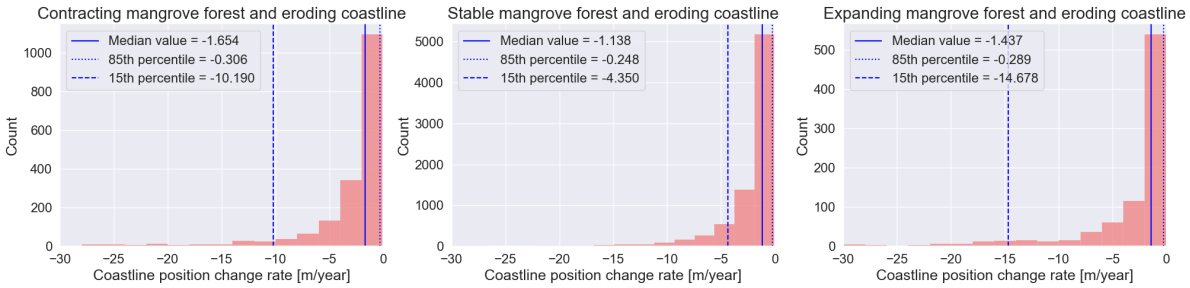

Figure 3.19: The coastline position change rate distribution for eroding transects with contracting, stable and eroding mangrove forests

4

Local assessment

This chapter focuses on the impact of mangroves on the stability of coastlines at a local scale. 15-kilometre stretches of coastline will be investigated to analyse the relationship between coastline position changes and mangrove width changes from 2005 to 2016. Examining smaller stretches of coastlines allows for the closer exploration of the influence of mangroves on coastline stability when hydrodynamic and climatic conditions are similar. The same datasets will be used as in the global assessment. Additionally, the research uses data from the Global Mangrove Watch dataset to determine the extent of open coast mangroves in 2008, 2009, and 2015. This implies that in the local assessment, the width of the mangrove forests along the considered transects is available for six years (2007, 2008, 2009, 2010, 2015 and 2016) between 2005 and 2016 (Bunting et al., 2022). The two local studies investigated in this chapter will be chosen based on Figure 3.17. This figure is repeated in Figure 4.1; however, every quadrant is assigned colours. The blue transects belong to the lower left quadrant, indicating that between 2005 and 2016, the mangrove forest is contracting and the coastline is eroding. The red transects belong to the upper right quadrant, indicating that the mangrove forests is expanding and the coastline is accreding. The yellow transects indicate the lower right quadrant, where the mangrove forests are expanding while the coastline is eroding. The green transects indicate the upper left quadrant, representing transects where the mangrove forest is contracting while the coastline is accreding. Finally, the grey transects are situated along the x-axis- or y-axis, indicating stable mangrove forests or stable coastlines. These colours will continuously be used throughout this chapter.

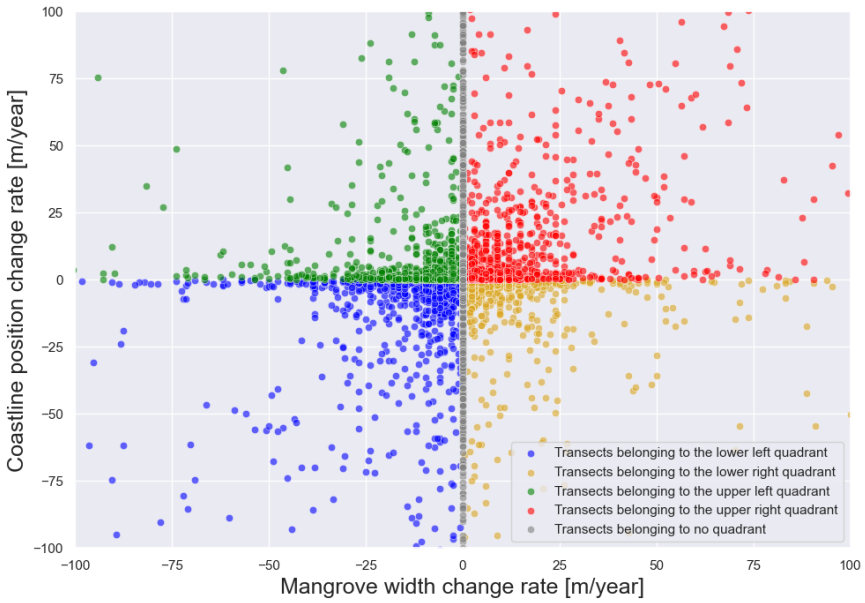

Figure 4.1: Distribution of coastline position change rates versus mangrove width change rates

To select a case study, coastlines were identified where most transects fall within a single quadrant, using Figure 4.1. Unfortunately, due to data availability, only a limited amount of coastlines were found. As can be seen in Figure 3.14 most mangrove forests are stable, while only a small portion are contracting, and even fewer mangrove forests are expanding. Additionally, in Figure 3.10, it can be seen that most coastlines are eroding. Thus, the chances of finding a coastline mostly experiencing accretion or with a mangrove forest that is mainly expanding were slim and such coastlines were not found. Coastlines that were mostly stable were not taken into account as the dynamics of stable coastlines were too minor to properly assess the effect of the state of a mangrove forest on the coastline position. A few coastlines were found where the coastline is eroding and the mangrove forest is stable or contracting. Unfortunately, many of these areas lacked coastline position data in the transects between 2005 and 2016. Areas where too much data was lacking were not considered, and the considered case study areas were chosen as they had the most available data. The first case study will focus on a 15-kilometre coastal stretch that experiences erosion along most of its length and where the mangrove forests are mostly stable. The second case study will focus on another 15-kilometre coastal stretch where most transects experience erosion and the mangrove forest contracts.

The results in the case study areas follow the same structure as the results section in the global assessment. However, only mangrove transects exist in the case study areas, meaning there can be no comparison between mangrove and non-mangrove transects. In addition, significant differences in mangrove widths are only present in case study 1, allowing only for a comparison between smaller and larger mangrove widths in case study 1. Consequently, the most important result is the comparison between the rate of coastline position change and the state of the mangrove forest. In both case studies these results will be discussed first.

4.1. Case Study 1

4.1.1. Site characteristics

The first case study is located on the island of Pulau Siberut (in short, Siberut Island), which is part of the Mentawai islands. Siberut Island is located on the western side of Sumatra at a distance of about 150 kilometres from the mainland (see Figure 4.2). The island has a size of about 3800 square kilometres, and it is located in the Indian Ocean. The island is approximately 100 kilometres long and 35-40 kilometres wide. With a population density of 10.5/km², the island is sparsely populated (Kemp, 2000). The case study focuses on the eastern part of Siberut Island (see Figure 4.2). This area of the island is characterized by a significant amount of swampy forests, and the east coast features an irregular shoreline with multiple small bays, lined with mangroves. Moreover, a few coral islands are located near the coast (Whitten & Whitten, 1982).

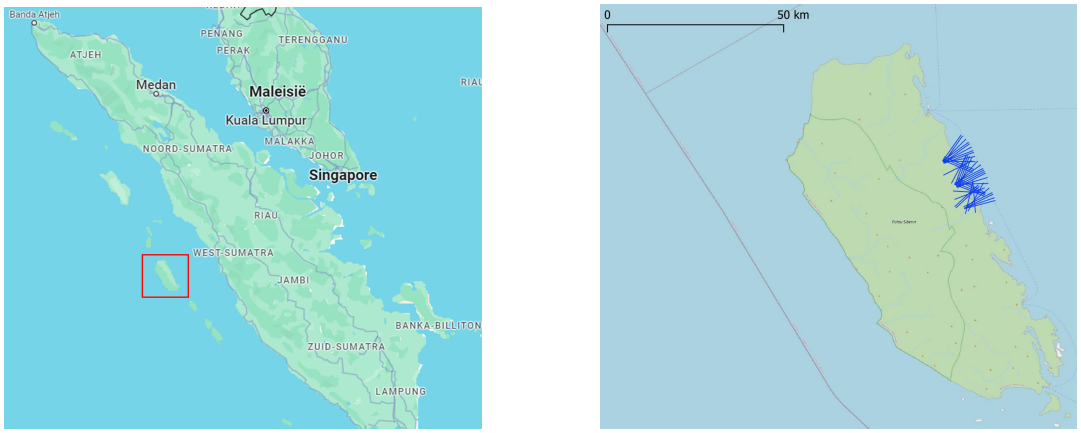

Figure 4.2: The island of Pulau Siberut (Google Maps)

Along the entire coastline on the east side, there are Rhizophora and Bruguiera mangrove forests (Whitten & Whitten, 1982). The whole coastline in the study area is muddy. In the study area, no major rivers flow into the ocean, but just above and below this area, two larger rivers flow into the sea.

Furthermore, several small villages are located within one kilometre of the coast. As a result, some infrastructure, such as roads, extends to the coastline in some places (Kemp, 2000). Analysis of temporal imagery from Google Earth's Timelapse feature revealed that the mangrove forests in the study area remained predominantly stable between 2005 and 2016, with occasional minor disturbances attributed to nearby villages. The coastline is partly sheltered by coral islands, but no landmasses can be found within 100 [km]. This is indicated in Figure 4.3.

Figure 4.3: The island of Pulau Siberut (Google Earth)

The case study area is made up of 43 transects. All transects intersect with mangrove ecosystems. Out of these, 29 transects have stable mangrove forests with eroding coastlines. Eight transects belong to the lower left quadrant, meaning the mangrove width along the transects is contracting and the coastline is eroding. Four transects belong to the lower right quadrant, meaning the mangrove width along the transects is expanding and the coastline is accreding. Finally, two transects have stable mangrove forests with an accreding coastline. This information is shown in Figure 4.4. For more background information on this case study, refer to Appendix C.

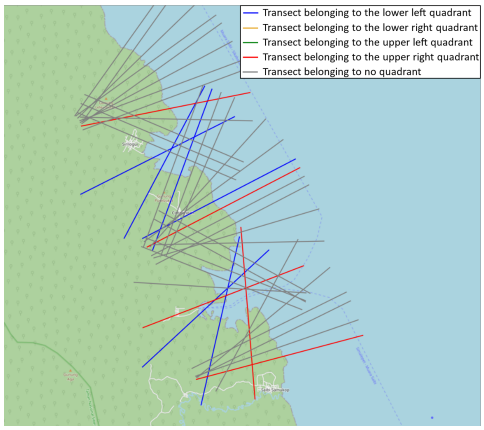

Figure 4.4: The considered study area with colours indicating the different quadrants

The width of the mangrove forest in the case study area varies from about 500 [m] to approximately 2500 [m]. Figure 4.5 depicts the mangrove widths between 2005 and 2016 for all transects. The left graph indicates the transects belonging, where the cross-shore width along the transect contracts while the coastline erodes. The middle graph shows the transects where the cross-shore width along the transect expands while the coastline erodes. Finally, the right graph indicates the transects belonging to no quadrant. In this case, these indicate mostly stable mangrove forest transects with eroding coastlines. As depicted in the figure, two distinct ranges of mangrove widths can be observed, particularly in the left graph. There are transects with smaller mangrove forests (around 500 [m]) and those with larger forests (above 1000 [m]).

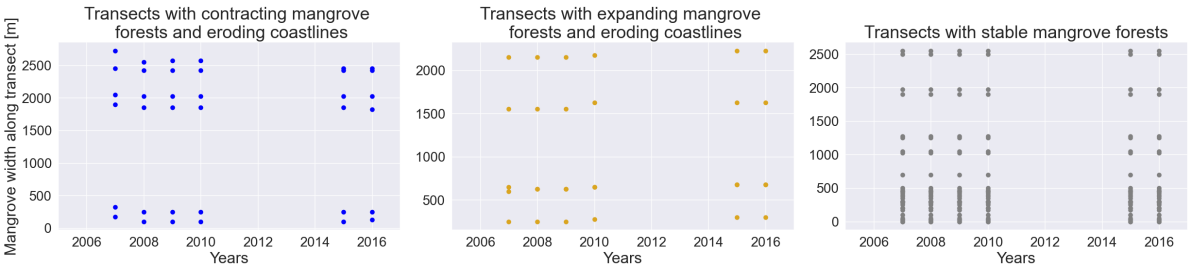

Figure 4.5: Distribution of mangrove widths between 2005 and 2016 for all transects (split according to their respective quadrant)

4.1.2. Results

The influence of the state of a mangrove forest on coastline stability

In Figure 4.6, the distribution of coastline positions between 2005 and 2016 relative to the coastline position in 2005 for all transects is shown. The transects are split according to their respective quadrants. A dotted line indicates the median coastline position per year, and a solid line indicates the total median coastline position for all points. When calculating the median coastline position per year and the total median coastline position, the two transects where the mangrove width is stable but the coastline is accreding are excluded. When the mangrove forest is expanding, the total median coastline position is -24.2 [m], when the mangrove forest is stable, the total median coastline position is -29.3 [m], and finally, when the mangrove forest is contracting, the total median coastline position is -37.1 [m]. When comparing the total median coastline positions, it can be seen that the coastline moves the most inland when the mangrove forest is contracting and the least when the mangrove forest is expanding. This suggests that erosion rates are the lowest when the mangrove forest is expanding and the highest when the mangrove forest is contracting.

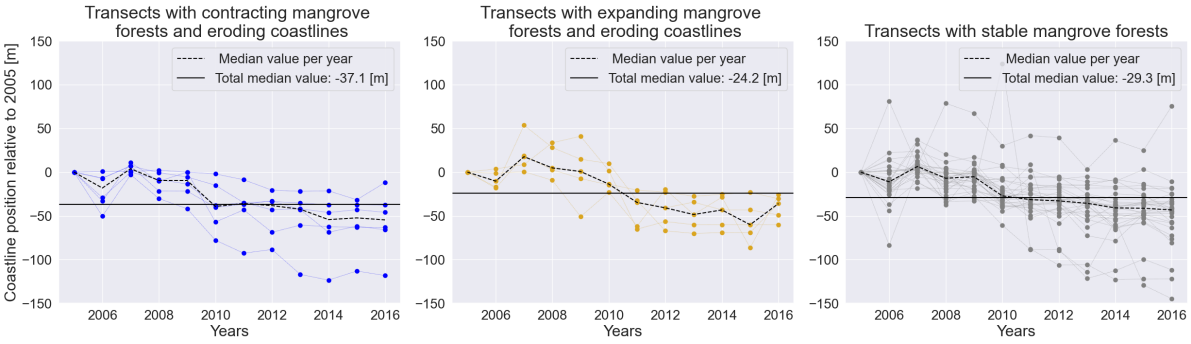

Figure 4.6: Distribution of coastline position between 2005 and 2016 relative to 2005 for all transects (split according to their respective quadrant)

The influence of the width of a mangrove forest on coastline stability

In the analysis presented in Figure 4.5, it is observed that the mangrove widths in the case study area fall into two distinct ranges: smaller widths of around 500 [m] and larger widths above 1000 [m]. To examine the influence of mangrove width on coastline position change rates, the data is divided into two categories based on the width of the mangroves. The first category includes all transects with a mangrove width below 1000 [m], while the second category includes all transects with a mangrove width above 1000 [m]. The coastline position distributions for the two categories between 2005 and 2016 are presented in Figures 4.7 and 4.8. When comparing these figures, it can be observed that when the mangrove forest is stable, the total median value for larger mangrove widths (-17.5 [m]) is substantially lower than for smaller mangrove widths (-29.6 [m]). This indicates that a larger mangrove width can help reduce erosion rates. Unfortunately, there were too few transects with contracting and expanding mangrove forests (less than 2 per category) to properly compare the effect of smaller and larger mangrove widths on coastline stability.

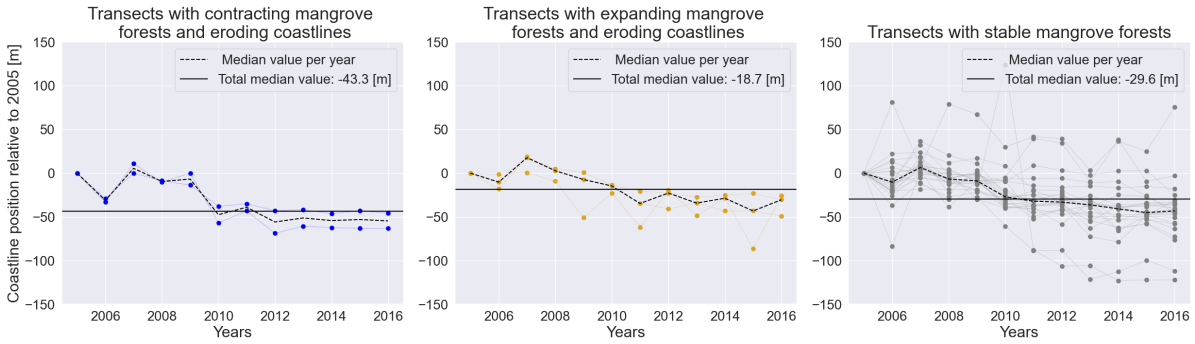

Figure 4.7: Distribution of coastline positions between 2005 and 2016 for all transects with a width below 1000 [m](split according to their respective quadrant)

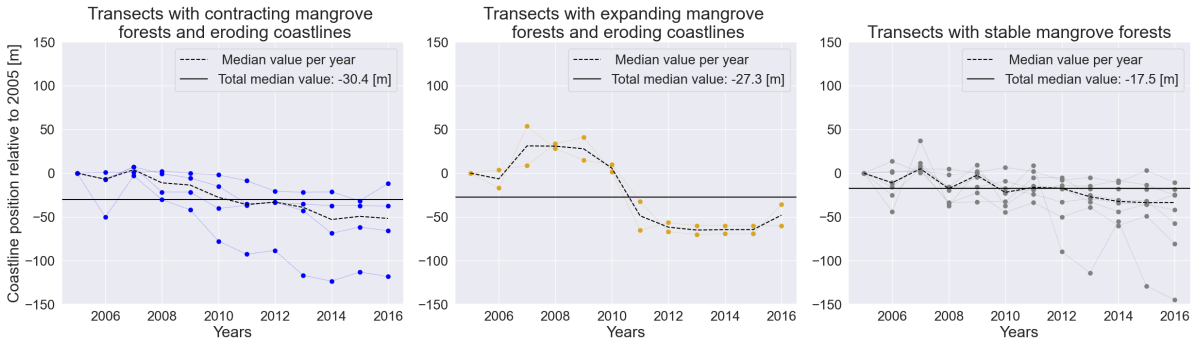

Figure 4.8: Distribution of coastline positions between 2005 and 2016 for all transects with a width above 1000 [m](split according to their respective quadrant)

4.2. Case Study 2

4.2.1. Site characteristics

Case study 2 focuses on a small island just off the coast of Cuba known as Isla de la Juventud. Figure 4.9 shows a map of the island. The island has an area of around 2200 square kilometres and is situated south of Havana in the Caribbean Sea. The Batabanó Gulf separates the island from the mainland of Cuba, and it is approximately 50 kilometres wide (National Office of Statistic and Information, 2017 and Aranda et al., 2020). Despite its relatively small size, the island is home to a large number of mangroves and three major rivers. While these rivers are not located on the northwest side of the island, that area is particularly characterized by inland waterway branches connected to the sea. The largest one is Estero del Pino (Juventud, 2011). Most of the population on the island lives in the capital city, Nueva Gerona. The northwest side of the island is uninhabited. However, there are roads extending all the way to the coast, which disrupt the mangrove forests (National Office of Statistic and Information, 2017). Humans pose a threat to mangrove conservation on the island. The marble industry has caused destruction in Laguna del Capitán, which is located in the study area, and illegal hunting of rodents has also played a significant role in disturbing the mangroves. Paths of destruction caused by hunters have been found in the mangrove forests despite the swamps and difficult access (Borroto-Páez & Ramos García, 2012).

Figure 4.9: Isla de la Juventud (Google Maps)

A coastline of around 15 [km] will be considered in this analysis. The entire coastline is muddy. Analysis of temporal imagery from Google Earth's Timelapse feature revealed a slight reduction of mangrove forests but no major disruptions or changes. Despite being more than 50 kilometres away from mainland Cuba, the coastline near Isla de la Juventud is relatively protected due to the presence of several small islands in the surrounding area. This can be seen in Figure 4.10.

Figure 4.10: Isla de la Juventud (Google Earth)

The study area comprises of 32 transects along the coastline, all of which intersect with open coast mangrove ecosystems and are thus categorized as mangrove transects. Figure 4.11 illustrates the transects that are considered in this study, categorized by quadrants. The majority of the transects (19 in total) belong to the lower left quadrant, indicating a coastline that is eroding and a mangrove forest that is contracting. There are three transects that belong to the upper left and three transects that belong to the lower right quadrants. The upper left quadrant indicates an accreding coastline, while the lower right quadrant indicates an eroding coastline and an expanding mangrove forest. Only one transect belongs to the upper right quadrant, indicating an accreding coastline and an expanding mangrove forest. Six transects belong to no quadrant, in this case they indicate a stable mangrove forest. Out of these, three transects experience and accreding coastline, and three experience an eroding coastline.

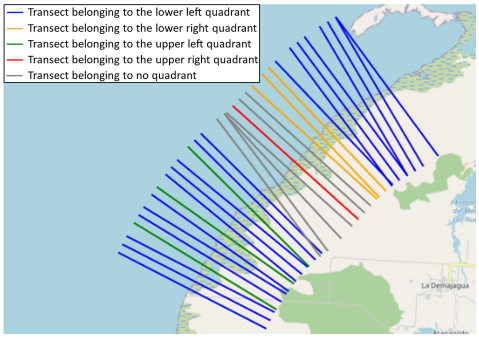

Figure 4.11: Transects ranged according to their quadrant

The mangrove widths along the transects between 2005 and 2016 can be seen in Figure 4.12 for all quadrants except for the transects with stable mangrove forests. The mangroves in this case study are mostly around 500 [m] wide, but some transects have mangroves that reach a width of 2500 [m]. However, there are too few mangroves with a large width to analyse the effect of different widths on coastline stability.

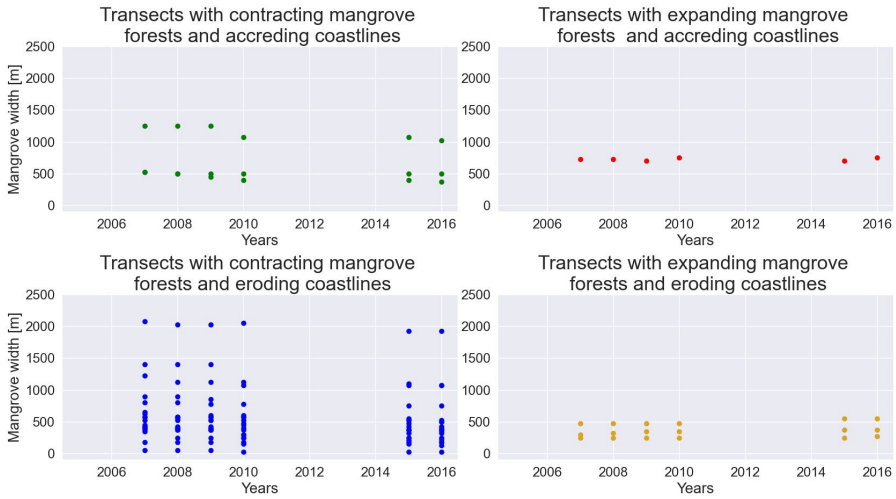

Figure 4.12: Mangrove widths between 2005 and 2016 ranged according to their quadrant

4.2.2. Results

The influence of the state of a mangrove forest on coastline stability

In this case study, the lower left quadrant (blue) and the lower right (yellow) quadrant will be compared as well as the upper left (green) and the transects where the mangrove forest is stable and the coastline is accreding (gray). The transect belonging to the upper right quadrant and the three transects with stable mangrove forests and accreding coastlines will be excluded from the analysis as too little data is available for comparison.

In Figure 4.13, the coastline positions relative to the coastline position in 2005 for the lower left and lower right quadrants can be seen. As can be seen in this figure, a clear difference can be seen between both graphs. The total median coastline position for transects with a contracting mangrove forest equals -5.9 [m]. In contrast, the total median coastline position for transects with an expanding contracting mangrove forest equals -0.5 [m]. It seems that when the mangrove forest is expanding, the erosion rates are lower than when the mangrove forest is contracting.

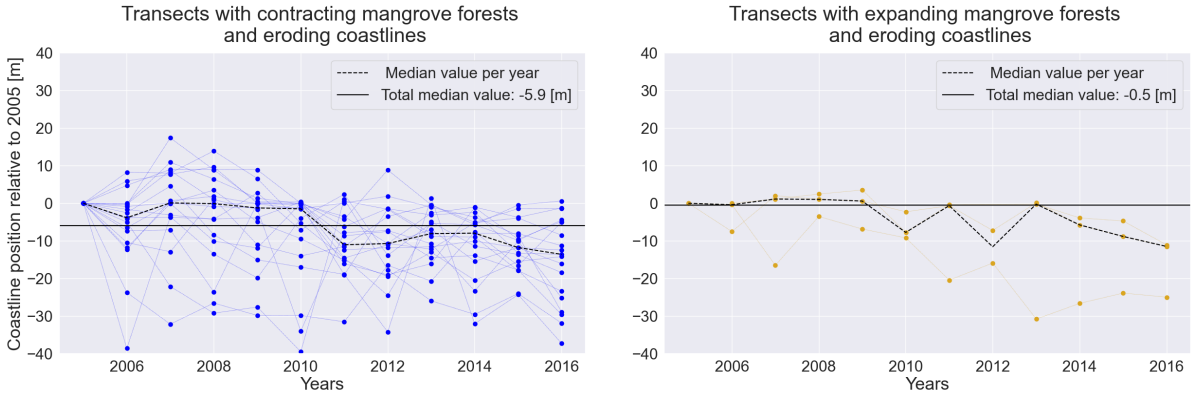

Figure 4.13: Distribution of coastline position between 2005 and 2016 relative to 2005 for transects in the lower left and lower right quadrant

In Figure 4.14, the coastline positions between 2005 and 2016 are plotted for all transects belonging to the top right quadrant, indicating transects with contracting mangrove forests and accreding coastlines and all transects with accreding coastlines and stable mangrove forests. By comparing the coastline positions for the two situations, it can be observed that the median coastline position for a stable forest, which equals 11.6 [m], is slightly higher than that of a contracting forest, which equals 11.2[m]. However, the difference is minimal.

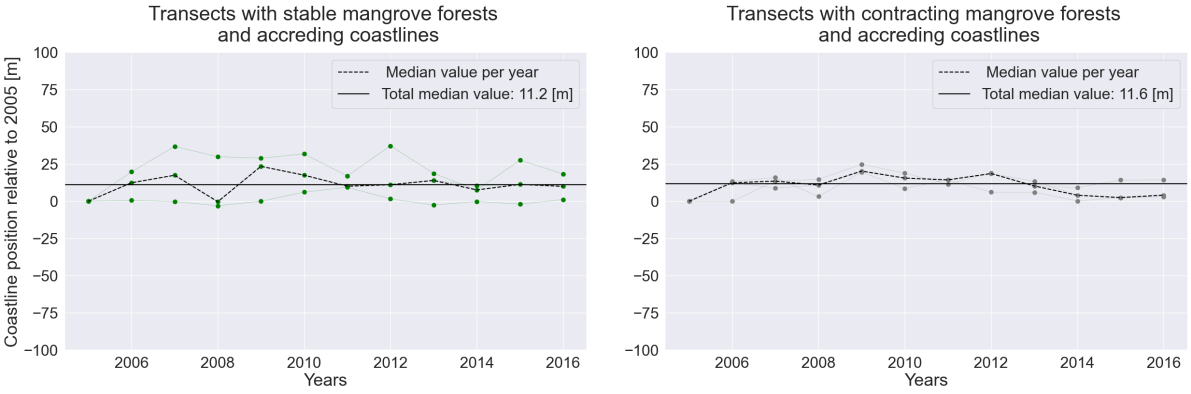

Figure 4.14: Distribution of coastline position between 2005 and 2016 relative to 2005 for the transects in the top right quadrant and transects with a stable mangrove forest and eroding coastline

5

Highlights

This research performed a global and local assessment using historical datasets to explore the impact of mangroves on coastline stability. In this chapter, the research questions will be answered.

1. Can a trend be observed between coastline stability with or without the presence of mangroves globally?

In order to answer this question, a study was conducted to compare the rate of coastline position changes between transects with mangroves and those without (see Section 3.2.1). Only open coast non-complex muddy transects were included in the analysis. Transects are called open coast transects if the nearest landmass is more than 15 kilometres away from the considered coastline.

The research suggests that areas covered with mangroves experience slightly higher sedimentation rates (median value: 1.92 [m/year]) than non-mangrove areas (median value: 1.84 [m/year]). However, despite the benefits of sedimentation, mangrove transects globally also demonstrate slightly higher erosion rates (median value: -1.85 [m/year]) than non-mangrove transects (median value: -1.75 [m/year]). The standard deviations and interquartile ranges are similar for mangrove and non-mangrove transects. For a visual representation of these results, see Figure 3.15.

2. Globally, is there a relationship between coastline stability and mangrove forest width?

To answer the question, the coastline position change rates across several mangrove widths were compared (see Section 3.2.2).

At larger mangrove widths, the accretion and erosion rates increase. Moreover, for larger mangrove widths, the erosion rates are larger than the accretion rates. Finally, it has been found that for larger mangrove widths, the variability in the dataset is larger than for smaller mangrove widths. For a visual representation of these results, see Figure 3.16.

3. On a global level, does a relationship exist between coastline stability and the state of a mangrove forest (contracting, expanding or stable)?

In order to answer this question, the coastline position change rates and the mangrove width change rates were compared (see Section 3.2.3).

It was found that the accretion rate is higher when a mangrove forest is expanding, as opposed to when it is contracting or stable. The lowest accretion rates are observed when the forest is contracting. Furthermore, it was observed that the 85th percentile is significantly higher for expanding and contracting mangrove forests than for stable ones, indicating the occurrence of more extreme accretion events. Furthermore, it has been found that erosion rates are highest when a mangrove forest is contracting and lowest when it is stable. The 15th percentile suggests that erosion rates are less extreme when a mangrove forest is stable than when it is expanding or contracting. For both accreding and eroding coastlines, the lowest variability in coastline position change rates was observed when the mangrove forest is stable, but the highest variability when the mangrove forest is expanding. For a visual representation of these results, see Figures 3.18 and 3.19.

The research also found a negative correlation between the change rates of mangrove width and coastline position. This means the mangrove width tends to reduce as the coastline shifts inward. Furthermore, it was found that as the coastline shifts seaward, the mangrove forest tends to expand correspondingly. For a visual representation of these results, see Figure 3.17.

4. Locally, how do erosion and accretion rates vary between coastlines hosting contracting, stable or expanding mud-mangrove belts?

In order to answer this question, two case study areas were selected (see Section 4.1 and Section 4.2). Both case studies considered a 15-kilometre coastline. It is assumed that hydrodynamic and climatic conditions are similar among the transects in the case studies. In the first case study, the coastline is mostly experiencing erosion and the mangrove forest is stable. In the second case study, the coastline is mostly experiencing erosion and the mangrove forest is contracting. The first case study compared the median coastline positions of the eroding transects with a contracting, stable and expanding mangrove forest. The second case study compared the median coastline positions of the eroding transects with a contracting and expanding mangrove forest. Additionally, the median coastline positions of accreding transects with contracting and stable mangrove forests were compared.

Both case studies found that when the coastline is eroding, an expanding mangrove forest causes the coastline to erode less than when a mangrove forest is contracting (see Figure 4.6 and Figure 4.13). Additionally, case study 1 found that a stable forest causes less erosion than when a mangrove forest is contracting (see Figure 4.6). In case study 2, it was discovered that an expanding mangrove forest causes more accretion than a stable mangrove forest. However, the difference is not substantial (see Figure 4.14).

6

Discussion

This chapter will discuss the data, the methods used to analyse the data, and the results. Firstly, the results of the global and local assessment in relation to the literature study will be discussed. Secondly, the limitations of the data used in the global and local assessment will be discussed. Finally, the limitations of the methods used to analyse the data will be discussed.

6.1. The value of mangroves on coastline stability

In Chapter 2, the influence of mangroves on coastline stability was investigated using a literature study. It was found that a delicate relationship exists between erosion and accretion processes within mangrove ecosystems. Mangrove forests trap and stabilize sediments and can also alter the tidal flat to become more flood-dominant, promoting sedimentation. However, mangrove forests can also promote soil degradation and erosion by, for example, an increase in turbulence around the roots. The results showed that mangrove transects caused slightly higher accretion and erosion rates than non-mangrove transects. However, the differences between mangrove and non-mangrove transects are not substantial. These findings suggest that relying solely on global data may not provide precise insights into the effect of the presence of mangrove ecosystems on coastline stability. Aside from data limitations, which will be discussed in Section 6.2, two factors might contribute to this lack of precision. Firstly, coastal regions exhibit significant variability in geological, climatic, and hydrodynamic conditions. These variations were not taken into account in the global assessment. Secondly, human activities such as coastal development, land-use changes, and pollution can significantly alter coastline dynamic. The degree of human influences also was not taken into account in the global assessment. Additionally, from the literature study, it was expected that mangroves would predominantly facilitate accretion and not erosion. This mismatch between the results in the global assessment and the literature could be caused by the fact that other factors, such as sediment availability or the type of mangrove species, heavily influence the results.

In Chapter 2, it was discovered that a wider belt of mangroves leads to increased coastline stability. This is because a larger width of mangroves is a more effective barrier against wave energy and tidal forces, reducing their erosive impact on the coastline. The global assessment showed that a larger mangrove width resulted in higher accretion- and erosion rates than smaller widths. Furthermore, at larger mangrove widths, erosion rates were higher than accretion rates. In case study 1, a larger mangrove width resulted in smaller erosion rates than a lower mangrove width. In the global and local assessment, contrasting results were thus found. The results in the local assessment align with the literature study, but the results in the global assessment do not. It is expected that the results of the global assessment are heavily influenced by the significant difference in data points for larger widths compared to smaller widths. With the methods used to find the trend previously described (see Appendix B), extreme outliers will more likely be included in the higher mangrove widths than the lower mangrove widths, which can result in a higher variability for larger mangrove widths.

According to literature (see Chapter 2), the state of mangrove forests (expanding, contracting, and stable) is related to coastline stability, but the exact nature of the relationship is not known. It remains unclear whether mangrove ecosystems primarily stabilize the coastline, or if the stability of the coastline predominantly supports the mangrove ecosystems. This ambiguity is central to the land-consolidators vs. land-builders theory, which describes differing roles for mangroves in coastal dynamics. In the results, it seems that a mangrove forest should at least be stable, but even better be expanding in order to keep erosion rates low and accretion rates high. Additionally, it was found that the mangrove width typically decreases as the coastline shifts inward. Moreover, in frameworks 3 and 4, it was found that as the coastline expands, the mangrove forest tends to expand as well. While these results do show a correlation between the state of the mangrove forest and coastline stability, the influence of the state of the coastline on the stability of a mangrove forest and which correlation is the strongest is not investigated. In Appendix D, it was investigated if a correlation exists between yearly mangrove change rates and coastline position change rates and vice versa. However, no correlations were found on this small time scale. A clear answer on whether the state of the coastline influences the mangrove forest the most or vice versa can not be given.

6.2. Data limitations

Data limitations in this research can introduce significant uncertainties, affecting the precision and accuracy of results. The factors influencing the robustness of the results will be summarized below.

One of the primary challenges arises from the spatial resolution of the datasets, with mangrove data collected at 25-meter intervals and coastline position data at 30-meter intervals. This introduces limitations in capturing fine-scale coastal features and mangrove dynamics. This coarse resolution may overlook subtle changes and nuances in coastal processes, potentially leading to underestimation or misinterpretation of the interactions between mangrove ecosystems and coastline stability. Secondly, in the coastline position dataset, varying degrees of missing data is observed. This introduces uncertainties, especially in areas with limited satellite coverage or sparse survey efforts. Missing data leads to the loss of valuable information and can bias results. In order to address the previous challenges, a systematic approach was used. This approach employed four distinct frameworks that were designed to mitigate these issues. Each framework progressively reduced the complexity of the data used, providing insights into the robustness of the findings despite uncertainties. Despite the reduction in dataset complexity across the four frameworks, the results remained remarkably consistent, underscoring the reliability of the findings. However, it is essential to recognize that while these frameworks enhance the reliability of the results, uncertainties may still persist. Factors such as incomplete coverage, spatial resolution limitations, and potential misclassifications can continue to influence the outcomes to some extent.

The third challenge lies in the temporal resolution of the datasets. The mangrove forest change rate is derived from just three years within a nine-year timeframe (2007, 2010, 2016) in the global assessment and six years within a nine-year timeframe (2007, 2008, 2009, 2010, 2015, 2016) in the local assessment. Increasing the temporal coverage of the mangrove forest change rate data would provide a more comprehensive understanding of long-term mangrove dynamics and their impact on coastline stability. Given the significant fluctuations in coastline position throughout the year, relying on annual data points may overlook important short-term variations and complexities in coastal dynamics. Increasing the temporal coverage of both mangrove forests data and coastline position data would offer a more comprehensive understanding of long-term mangrove dynamics and their impact on coastline stability while capturing the nuanced short-term fluctuations in coastline position. Efforts were made to optimize the time span investigated to maximize the availability of mangrove data and enhance the comprehensiveness of the analysis. This resulted in selecting the time span from 2005 to 2016. In the global assessment, only the mangrove datasets from 2007, 2010 and 2016 were added due to computational limitations and time constraints. The other mangrove datasets between 2007 and 2016 were added to the local assessment to understand long-term mangrove dynamics more comprehensively.

Furthermore, muddy, sandy, and mixed transects can be misclassified, which can influence the results. This is critical because muddy, sandy, and mixed coastlines behave differently in relation to the effects of mangrove ecosystems. Misclassifications can lead to inaccurate assessments of the effect of mangroves on coastline stability. However, it should be noted that in the Muddy Shoreline Monitor dataset, the muddy transects are classified with an accuracy of 86.5% (Hulskamp et al., 2023). Therefore, only a small number of transects are likely to be affected.

Finally, in the local assessment, two separate datasets were utilized to evaluate mangrove width changes over a six-year period. The analysis involved using the Global Mangrove Watch dataset for 2008, 2009 and 2015 and the Worthington et al. (2020) dataset, which is derived from the Global Mangrove Watch (GMW), for 2007, 2010 and 2016. Notably, the Worthington et al. (2020) dataset exhibited a higher level of detail compared to the GMW dataset, resulting in variations in mangrove width measurements between the two datasets. Despite similarities in the observed trends in mangrove width changes, the mangrove widths differed substantially between both datasets. While the trends calculated from the GMW dataset were applied to the Worthington et al. (2020) dataset to maintain consistency, this approach may still introduce uncertainties.

6.3. Limitations in the data analysis

Aside from data limitations, the methods used in the data analysis can also introduce uncertainties. This section will outline the primary limitations encountered in the analysis.

The first limitations occur when calculating the mangrove width. Firstly, the width is measured along transects, which may not fully capture the true extent of mangrove forests. This approach could result in inaccuracies of mangrove width, particularly in areas where mangrove forests exhibit irregular shapes or great width variability. This is because transect-based measurements only provide data along specific lines and do not capture the full spatial complexity of the forest. As a result, variations in width that occur between transects may be missed, leading to an incomplete or distorted representation of the forest's actual dimensions. Secondly, the criterion for defining gaps between mangrove patches, set at 500 meters, is somewhat arbitrary. This criterion could cause inaccuracies in defining the real extend of mangrove forests that influence the coastline stability.

Other limitations occur when calculating the mangrove width change rates. The methodology that is now employed does not differentiate between larger and smaller mangrove forests, potentially overlooking the varying degrees of impact associated with changes in width. For example, a decrease in width of 25 meters may have a more significant effect on smaller forests than larger ones. Yet, this distinction is not accounted for in the analysis. Furthermore, one important consideration that was not accounted for is the location at which the width increases or decreases. While the analysis focused on quantifying changes in mangrove width, the specific location of these changes, particularly in relation to the coastline, was not included in the assessment. This exclusion can be significant because an increase or decrease in mangrove width near the coastline will have more impact on coastline stability than similar changes occurring at the end of the forest. The analysis may overlook important nuances in mangrove dynamics and their influence on coastline stability by not considering the spatial distribution of width changes, particularly near the coastline.

Finally, when examining the case studies, it is assumed that consistent hydrodynamic conditions prevail throughout the study areas. However, particularly in case study 1, this assumption may not entirely hold true. Transects within the study area vary in their degree of exposure to the open sea. While some are positioned directly along the open sea, others are more sheltered within embayments. This variability in transect locations introduces potential differences in local hydrodynamic conditions, which could impact mangrove dynamics and coastline stability differently across the study area. For instance, areas near the open sea may experience stronger wave action and tidal currents than areas within embayments, leading to variations in sediment transport and vegetation growth dynamics. Acknowledging that these differences in hydrodynamic conditions may introduce uncertainties when interpreting results is important.

7

Conclusion

This chapter combines the key results from the global and local assessment, which are divided into three groups: the effect of the presence of mangroves on coastline stability, the effect of the width of a mangrove forest on coastline stability, and the effect of the state of a mangrove forest (expanding, stable, or contracting) on coastline stability.

First, the impact of mangrove presence on coastline stability was examined. Due to limited data availability, the coastline position change rates for mangrove and non-mangrove transects were only compared in the global assessment. It was found that mangroves experience slightly higher sedimentation rates than non-mangrove areas. However, mangrove transects globally also demonstrate slightly higher erosion rates than non-mangrove transects. The variability for both datasets is similar. The results thus indicate a difference between mangrove and non-mangrove transects globally, although this difference is not substantial.

Next, the influence of mangrove forest width on coastline stability was investigated. In the global assessment, it was found that for larger mangrove widths, the accretion and erosion rates increase. Furthermore, the erosion rates are higher than the accretion rates for larger mangrove widths. It was also found that the variability in the dataset is greater for larger mangrove widths than for smaller mangrove widths. Conversely, in the local assessment, it was found that larger mangrove widths (above 1000 meters) prevent erosion more effectively than smaller ones (below 1000 meters). Thus, contrasting results emerged between the local and global assessments.

Lastly, the effect of the state of a mangrove forest on coastline stability was investigated. In the global assessment, higher accretion rates were observed when a mangrove forest is expanding and stable compared to when a mangrove forest is contracting. The highest accretion rates were observed when a mangrove is expanding and the lowest when a mangrove forest is contracting. Conversely, erosion rates are the highest when a mangrove forest is contracting and are lowest when the forest is stable. The most extreme accretion and erosion events occur when a mangrove forest is expanding. Stable mangrove forests exhibited the least extreme coastline position change rates, regardless of whether they were accreding or eroding. Furthermore, when the coastline is accreding, mangrove forests tend to expand, while when the coastline is eroding, mangrove forests tend to contract. Similar trends were observed in the local assessment. The highest erosion rates were found when a forest is contracting, while the lowest erosion rates were found when a forest is expanding. Additionally, slightly higher accretion rates were found in stable mangrove forests compared to contracting ones, although this difference was minimal. It can be concluded that stable and expanding mangrove forests are better at promoting accretion and mitigating erosion than contracting mangrove forests.

8

Recommendations

8.1. Implications for governmental policies

The findings of this study emphasize the influence of mangrove forest conditions (expanding, stable, or contracting) on coastal dynamics and stability. Specifically, it was observed that expanding and stable mangrove forests are associated with higher accretion rates and lower erosion rates compared to contracting forests. This highlights the importance of maintaining or promoting the stability and expansion of mangrove forests for coastal protection and resilience. However, this research did not explore the potential reciprocal effect of coastline stability on the health and stability of mangrove forests. While measures should include protecting existing mangrove forests from anthropogenic pressures such as deforestation, pollution, and urban development, and initiatives to restore degraded mangrove areas, further research is needed to determine the most effective strategies. Understanding and enhancing coastline stability should also be a focus to support the mutual benefits between mangroves and coastal environments. This can be achieved by allocating sufficient resources for comprehensive research on the effect of mangroves on coastline stability but also by enhancing data accessibility by f.e. making historical records and field research data openly available.

8.2. Implications for scientists

The findings of this study underscore the complex and nuanced relationship between mangrove forests and coastline stability. While this research suggests a link between the state of mangrove forests (expanding, stable, or contracting) and coastline stability, the reciprocal influence of coastline stability on the stability of a mangrove forest remains unexplored. This gap, therefore, presents a significant opportunity for future research to better understand the interactions between coastline stability and mangrove ecosystems. It is advised to first perform this analysis on a global level to identify if broad trends exist across different climatic and hydrodynamic conditions before conducting local studies. By focusing on localized studies, regional variations, and factors influencing mangrove-coastline interactions can be explored in depth. When selecting local study areas, it is recommended to choose sites with minimal anthropogenic influences to better isolate natural processes affecting mangrove-coastline interactions.

Additionally, the research highlights contrasting results concerning the impact of mangrove forest width on coastline stability. These results may be biased due to differences in sample sizes between larger and smaller forests. To mitigate this bias, researchers should utilize statistical techniques such as weighted analysis and bootstrapping to ensure more balanced and robust results. The inconsistencies in the findings also suggest that the factors influencing mangrove effectiveness in stabilizing coastlines are more complex, potentially involving a combination of biophysical, ecological, and geomorphological variables. Future studies should aim to unravel these complexities by examining a broader range of environmental conditions and mangrove characteristics, such as sediment availability, forest density, and different types of root structures. As global data might be insufficiently precise, these studies should preferably be conducted on a local level using detailed local data.

Moreover, when comparing transects with and without mangroves on a global scale, only minor differences were detected. These findings suggest that relying solely on global data may not provide precise insights into the precise effect of the presence of mangroves on coastline stability. This can be caused by not accounting for the significant heterogeneity in terms of geological, climatic, and hydrodynamic conditions in coastal environments. To address this limitation, one approach is to split the dataset according to coastline regimes based on specific environmental characteristics. For instance, coastal areas can be categorized into different regimes based on factors such as tidal range, wave height, storm frequency, and sediment composition. By categorizing coastlines into distinct regimes, researchers can better capture the diversity of coastal environments and assess how different conditions affect mangrove-coastline interactions. The same approach can be used to categorize coastlines according to anthropological influences.

When utilizing global data, it is advised to enhance the reliability of the results by decreasing the uncertainty in the datasets and increasing the temporal coverage. Firstly, efforts should be directed towards reducing incomplete coverage and missing data, especially in remote or poorly surveyed areas. One approach to improve data accuracy is using Sentinel-2 data, which offers a spatial resolution of 10 meters or other advanced remote sensing techniques. On a global scale, Sentinel-2 data is considered one of the most reliable remote sensing sources. In addition to using global datasets, local studies can improve data precision. Conducting site investigations can help refine the spatial resolution of both mangrove and coastline stability datasets, allowing for capturing fine-scale coastal features and mangrove dynamics with greater accuracy. Additionally, efforts should be directed to minimize misclassifications of muddy, sandy and mixed transects to reduce uncertainty in dataset interpretation. By implementing more precise classification methodologies and validation techniques, the reliability of dataset interpretations can be enhanced.

Furthermore, efforts should also be directed at increasing the temporal coverage of mangrove forest data and coastline position data. Including more datasets within the time frame beyond the current three-year interval (2007, 2010, 2016) regarding mangrove width datasets would offer valuable insights into temporal trends and variability in mangrove ecosystems. Additionally, by acquiring multiple readings of coastline position throughout the year, researchers can gain a more detailed insight into the temporal variability of coastal features and rule out seasonal bias. This higher temporal resolution enables the detection of short-term changes, such as erosion events, accretion processes, and seasonal fluctuations, which may not be adequately captured by annual readings alone. This expanded temporal resolution in both mangrove width and coastline position can enhance the accuracy and reliability of analyses.

8.3. Suggestions for further research

Based on the findings of this study, there are several areas where further research could improve our understanding of mangrove ecosystems and coastline stability. The following recommendations provide directions for refining methods and broadening the scope of analysis.

When using the Global Mangrove Watch dataset and the dataset by Worthington et al. (2020), efforts should be directed at minimizing the disparities between both datasets. One key approach could involve validating both datasets using Sentinel-2 data. By comparing mangrove width measurements derived from Sentinel-2 imagery with those from the existing datasets, discrepancies and inaccuracies can be identified and addressed.

Furthermore, further research should concentrate on enhancing the methods for measuring the mangrove width. Enhancing the precision of the data is crucial. However, considering irregular shapes present in mangrove forests, by avoiding a transect-based calculation or refining the criteria for identifying gaps between mangrove patches can substantially improve the accuracy of the analysis.

To address the limitations associated with calculating the mangrove width change rates, future studies should refine the methodology to differentiate between larger and smaller mangrove forests. By making this distinction, researchers can better understand how changes in mangrove width affect different forest sizes. Additionally, there should be a focus on incorporating spatial information into the analysis. Specifically, the research should consider the location of width changes in relation to the coastline, as changes occurring near the coastline are likely to have a more pronounced impact on coastline stability. Incorporating these improvements into future analyses will enhance the accuracy of the results.

Moreover, further research should also focus on expanding the scope of analysis to include other types of mangrove forests, such as lagoonal, deltaic, and estuarine mangroves and include sandy- and mixed coastlines. This can enrich the understanding of mangrove dynamics and their influence on coastline stability. These diverse mangrove ecosystems exhibit unique characteristics and interactions with their surrounding environments, which may have varying implications for coastline stability.

Finally, when conducting local studies, both eroding and accreding coastlines should be further researched. Exploring fully eroding coastlines through further investigation can offer valuable insights into the persistence of observed trends across diverse locations and environmental conditions. Similarly, exploring accreding coastlines can unveil potential divergent patterns in contrast to eroding coastlines.

Glossary

accretion Accretion pertains to anchoring deposited materials onto the soil or substrate, reducing their susceptibility to erosion by waves or tides. Accretion contributes to the gradual buildup of landforms (McIvor et al., 2013). 19

biogeomorphic Biogeomorphology focuses on understanding the intricate relationships between ecological and geomorphological processes. It explores how living organisms, such as plants and animals, interact with and influence the shaping of landscapes (Viles, 1988). 2

brackish water Brackish water is a mixture between freshwater and seawater. Water is defined to be brackish water if the total dissolved solids (TDS) in the water is between 1-25 [g/L]. This range is higher than that of freshwater (< 1 [g/L]) and lower than that of salt water (> 35 [g/L]) (Tian et al., 2021). 5

carbonate sediments Carbonate sediments are derived from marine environments. They are formed from calcium carbonate, which most often originates from shells or the remains of marine organisms (Bosboom & Stive, 2021). 10

concave-up A concave-up profile is characterized by a shape that slopes downward. This means that the upper tidal flat has a larger slope than the lower tidal flat (Hanssen et al., 2022). 14

convex-up A convex-up profile is characterized by a shape that bulges upward. This means that the lower tidal flat has a larger slope than the upper tidal flat (Hanssen et al., 2022). 2

ebb-dominant An ebb-dominant system indicates that the ebb tide has a higher velocity and lower duration than the flood tide. Therefore, an ebb-dominated system tends to export sediment (Bosboom & Stive, 2021). 22

flood-dominant A flood-dominant system indicates that the flood tide has a higher velocity and lower duration than the ebb tide. Therefore, a flood-dominated system tends to import sediment (Bosboom & Stive, 2021). 2

geomorphological Geomorphology is the scientific study of the origin, evolution, and classification of landforms on the Earth's surface. The discipline encompasses the study of landforms such as mountains, valleys, plains, rivers, and coastal features, providing insights into the dynamic processes that shape the Earth's surface (I. S. Evans, 2012). 6

intertidal area The intertidal area is situated between mean sea level (MSL) and high tide. At low tide, this area is exposed to air and at high tide, this area is partially submerged (J. Ellison, 2009). 5

mangals The term "Mangals" is used to refer to the entire ecosystem of plant life found in a swamp within a mangrove forest. It encompasses all the vegetation, including various species of plants that thrive in the intertidal area (Macnae, 1968 and Hamilton, 2019). 5

mangrove forests The term "mangrove forest" specifically denotes those species classified as mangrove trees within mangals (Macnae, 1968 and Hamilton, 2019). 5

morphodynamic Morphodynamics is the process by which the interaction between landforms (morphology) and physical forces such as hydrodynamics (tides, currents, waves) influences the ongoing evolution of those landforms. This dynamic interplay involves sedimentation, erosion, and sediment transport processes, which continuously reshape the landscape over time (Flanders Marine Institute (VLIZ), 2021 and Friedrichs, 2011). 13

morphological Coastal morphology is the study of the form and structure of coastal systems or their components. Examples include the morphology of deltas, estuaries, beaches, and bedforms ((Flanders Marine Institute (VLIZ), 2024). 1

sedimentation Sedimentation is the process of depositing both organic and inorganic materials onto the soil surface, often facilitated by natural forces such as water movement, wind, or gravity (McIvor et al., 2013). 20

terrigenous sediments Terrigenous sediments are sediments that result from the weathering of continental rocks (terrestrial rocks) (Balke & Friess, 2016). 10

tidal creeks A tidal creek is a dynamic stream that drains the tidal flat. It undergoes flushing during each tidal cycle, allowing for the exchange of water and nutrients. These creeks exhibit significant temporal variations in their physical conditions, influenced by tidal movements and seasonal changes (Hackney et al., 1976). 11

A

Mangrove genera

There are approximately 27 genera of mangroves in total. According to the most strict criteria outlined by Tomlinson, 2016, only 9 of these genera are considered to be true mangroves. However, it's important to note that the classification of true mangroves can be contentious among researchers due to the inherent challenges in precisely defining what species qualify as a true mangrove. The list of these 27 mangrove genera is provided below, with those designated as true mangroves by Tomlinson, 2016 underlined.

Table A.1: List of the 27 different genera of mangroves (N. Duke, 1992)

Number	Genus	Number	Genus
1	Acrostichum	**15**	Bruguiera
2	Aegialitis	**16**	Ceriops
3	Pelliciera	**17**	Kandelia
4	Heritiera	**18**	Rhizophora
5	Diospyros	**19**	Excoecaria
6	Aegiceras	**20**	Aglaia
7	Cynometra	**21**	Xylocarpus
8	Mora	**22**	Avicennia
9	Conocarpus	**23**	Acanthus
10	Lumnitzera	**24**	Dolichandrone
11	Pemphis	**25**	Scyphiphora
12	Osbornia	**26**	Nypa
13	Sonneratia	**27**	Laguncularia
14	Camptostemon		

B

Global assessment

This appendix discusses the results of the global assessment for each framework. The results are divided into four categories. The first category includes results that only show the change rates in the coastline position. The second category includes results that show the cross-shore width of the mangroves. The third category includes the results that compare the cross-shore width of the mangroves to the coastline position change rates. The final category includes the results that compare the mangrove cross-shore width change rates to the coastline position change rates.

B.1. Framework 1

Coastline position change rates

The histogram shown in Figure B.1 compares the distribution of coastline position change rates for two types of transects - those inside mangrove areas (represented in red) and those outside mangrove areas (represented in blue). The histogram focuses on change rates between -15 and 15 [m/yr] to visualise the most common values better. The distribution of mangrove transects and non-mangrove transects is found to be highly similar. Both distributions exhibit a slightly negative median value, which stays within the stable range (-0.5 and 0.5), indicating a tendency towards coastline stability. Further examination reveals that the median rate for accreding transects (above 0.5) is slightly higher for mangrove transects than non-mangrove transects. However, for eroding transects (below -0.5), the median is slightly lower for mangrove transects than non-mangrove transects. These differences, however, are minor.

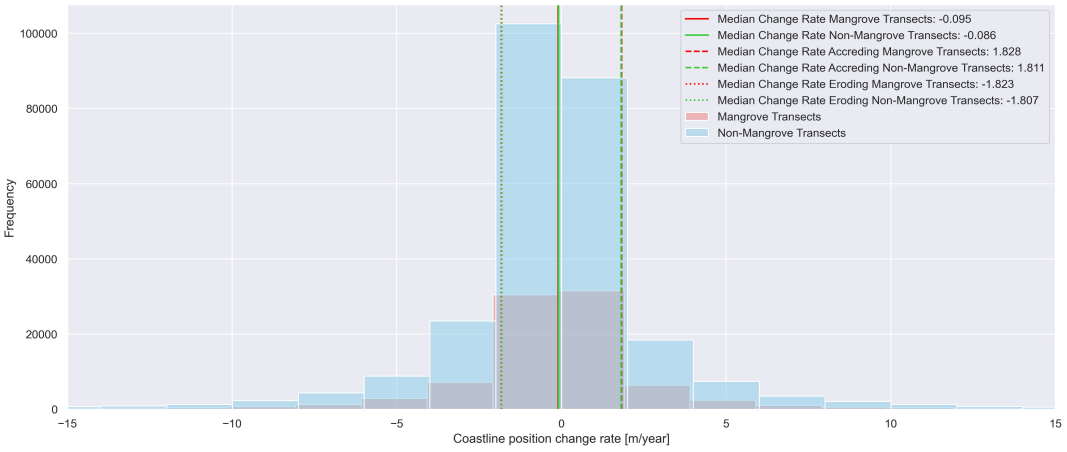

Figure B.1: Coastline position change rates for mangrove and non-mangrove transects

The study analyzed the rates of change in the position of coastlines for both mangrove and non-mangrove transects. The rates were then grouped into four categories: transects that were eroding (change rate below -0.5), transects that were accreding (change rates above 0.5), transects with a negative change rate, and transects with a positive change rate. Figure B.2 shows boxplots that present the median, standard deviation, and interquartile range for each category. The results indicate that mangrove transects tend to move closer to the stability range (around -0.5 and 0.5) than non-mangrove transects when considering all negative and positive values. Additionally, mangrove transects exhibit lower standard deviations, suggesting a lower overall variability than non-mangrove transects. However, the interquartile range is similar for both mangrove and non-mangrove transects.

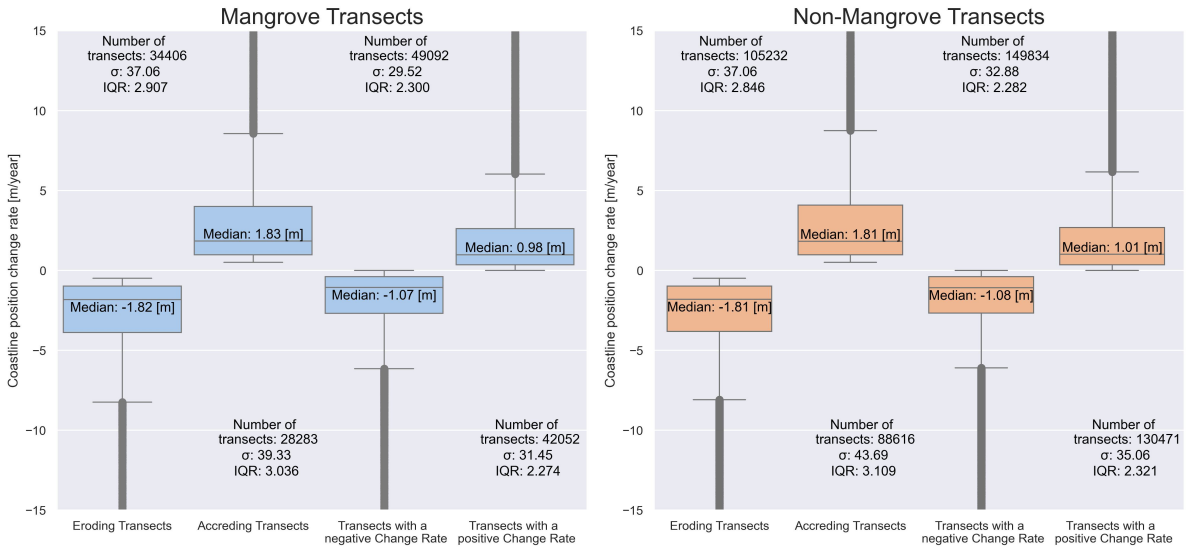

Figure B.2: Coastline position change rates for mangrove and non-mangrove transects

The sample sizes between mangrove and non-mangrove transects are imbalanced, as shown in Figure B.2 and B.1. There are over four times as many non-mangrove transects as there are mangrove transects in this framework. A specific approach was used to evaluate whether this disparity influenced the observed behaviour. Data points were randomly selected within eroding and accreding non-mangrove transect categories, with the number of points chosen matching the count of mangrove transects within their respective eroding and accreding categories. Specifically, 34406 non-mangrove transects within the eroding category and 28283 non-mangrove transects within the accreding category were randomly chosen. This process was repeated 1000 times, and the median and standard deviation of the randomly selected data points were recorded each time. Histograms in Figures B.3 and B.4 depict each run's calculated medians and standard deviations. Figures B.3a and B.3b showcase the distribution of medians and standard deviations across 1000 runs for eroding non-mangrove transects. These figures also highlight the median, 85th, and 15th percentiles, along with the median value and standard deviation of mangrove transects, consistent with Figure B.2 and Figure B.3a shows a similar trend to that in Figure B.2. Most non-mangrove transect medians exceed that of mangrove transects, with only a small fraction (<15%) falling below the median. Furthermore, the standard deviations of mangrove and non-mangrove transects are very similar. This reaffirms the earlier observation that mangrove transects erode slightly more than non-mangrove transects.

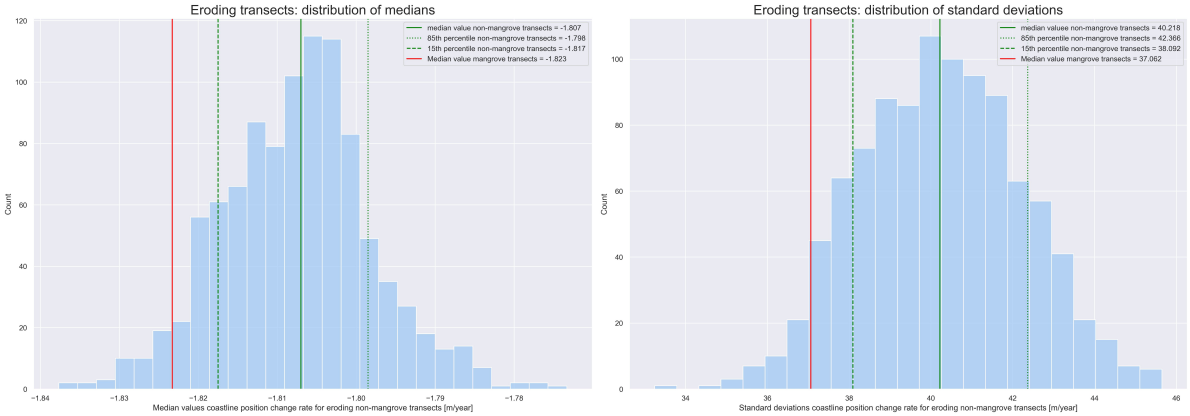

(a) Distribution of medians (b) Distribution of standard deviations

Figure B.3: Eroding non-mangrove transects

In Figure B.3b, the distribution of standard deviations for eroding non-mangrove transects is depicted. It is clear from the figure that the standard deviations among non-mangrove transects are mostly higher (>85%) than those of mangrove transects. This suggests that the variability in change rates among non-mangrove transects is slightly broader than among mangrove transects, consistent with the conclusion drawn from Figure B.2. Moving to Figure B.4a, the distribution of medians for accreding non-mangrove transects can be seen. It is apparent from this figure that most medians (>85%) are lower than the median value of mangrove transects. This reaffirms the observation in Figure B.2 that mangrove transects accrede slightly more than non-mangrove transects. Additionally, Figure B.4b indicates that the majority of non-mangrove transects (>85%) exhibit a higher standard deviation than mangrove transects. This suggests that the variability in change rates among non-mangrove transects is higher compared to mangrove transects, consistent with the findings from Figure B.2.

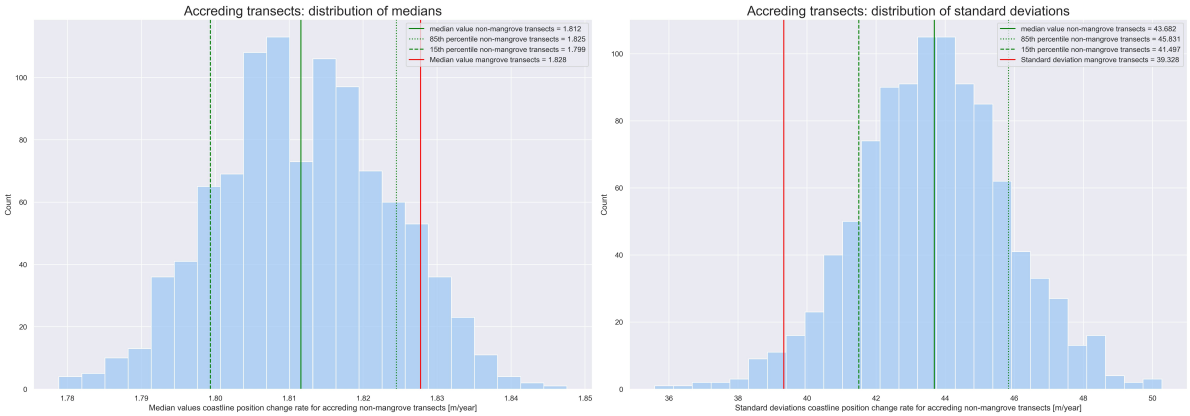

(a) Distribution of medians (b) Distribution of standard deviations

Figure B.4: Accreding non-mangrove transects

In the pie chart shown in Figure B.5, the distribution of coastal states (accreding, eroding, and stable transects) for mangrove and non-mangrove transects is depicted. Overall, there are minimal differences between the two categories. Mangrove transects appear to be slightly more stable than non-mangrove transects. However, they also exhibit a somewhat higher proportion of eroding transects and a slightly lower proportion of accreding transects.

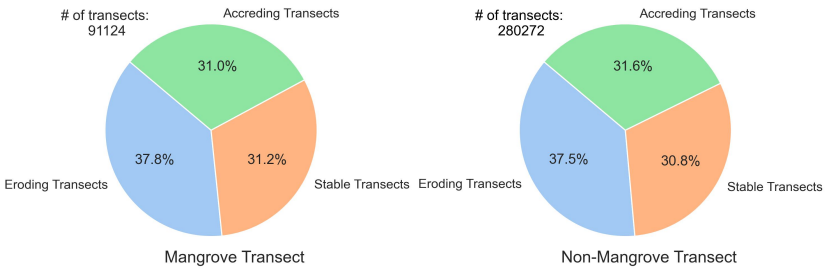

Figure B.5: The coastal state distribution for mangrove and non-mangrove transects

Mangrove cross-shore width

In Figure B.6, an overview of contracting, expanding, and stable mangrove forests is shown for a total of 91124 mangrove transects. The figure illustrates that nearly 73% of the transects are stable. Furthermore, approximately 17% of the transects are contracting, while a very small proportion, around 10%, is expanding.

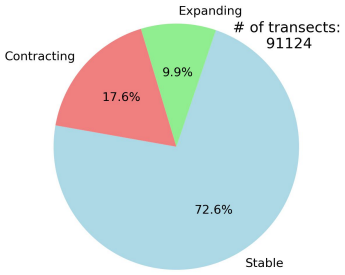

Figure B.6: The distribution of contracting, expanding and stable mangrove forests

Mangrove cross-shore width compared to coastline position change rate

Figure B.7 displays the relationship between the cross-shore mangrove width along the transects and the change rate of the coastline position. The scatterplot on the graph has a wide variety of points for mangrove widths below 4000 meters. However, beyond this threshold, the change rate of the coastline position tends to cluster around the horizontal axis, indicating a more stable situation. The graph also includes two histograms. The first shows the distribution of mangrove widths, which mostly range between 0 and 1000 meters. The second histogram shows the distribution of coastline position change rates, mostly around zero.

The clustered data points around the horizontal axis of the scatterplot for values above 4000 meters can be attributed to the limited number of data points available in that range. Two methods are employed to investigate the observed trend further. In the first method, two bin widths are selected, namely 100 [m] and 500 [m]. Within these bin widths, the 15th and 85th percentile are calculated. These percentiles indicate the thresholds below which 15% and 85% of the data points fall, providing insights into the range and variability of the dataset. If the difference between the 15th and 85th percentile is smaller, it may indicate a more consistent pattern or reduced variability for a certain mangrove width. A more consistent pattern between mangrove width and coastline position suggests a stronger correlation or relationship between these variables. To account for the imbalance in data points per bin, 100 points per bin are chosen, and the 15th and 85th percentiles are calculated using these data points. The 15th and 85th percentiles per bin are then connected using a least-squares linear regression line. For the second method, a bin width of 500 [m] is chosen, and within each bin, 100 random points are selected to create a boxplot. Only bins containing more than 100 data points are considered. A linear regression line is then drawn using the median values from each boxplot.

To summarize, the first method calculates percentiles to provide insights into the range and variability of the dataset. In contrast, the second method employs boxplots and linear regression lines to visualize the relationship between mangrove width and coastline position.

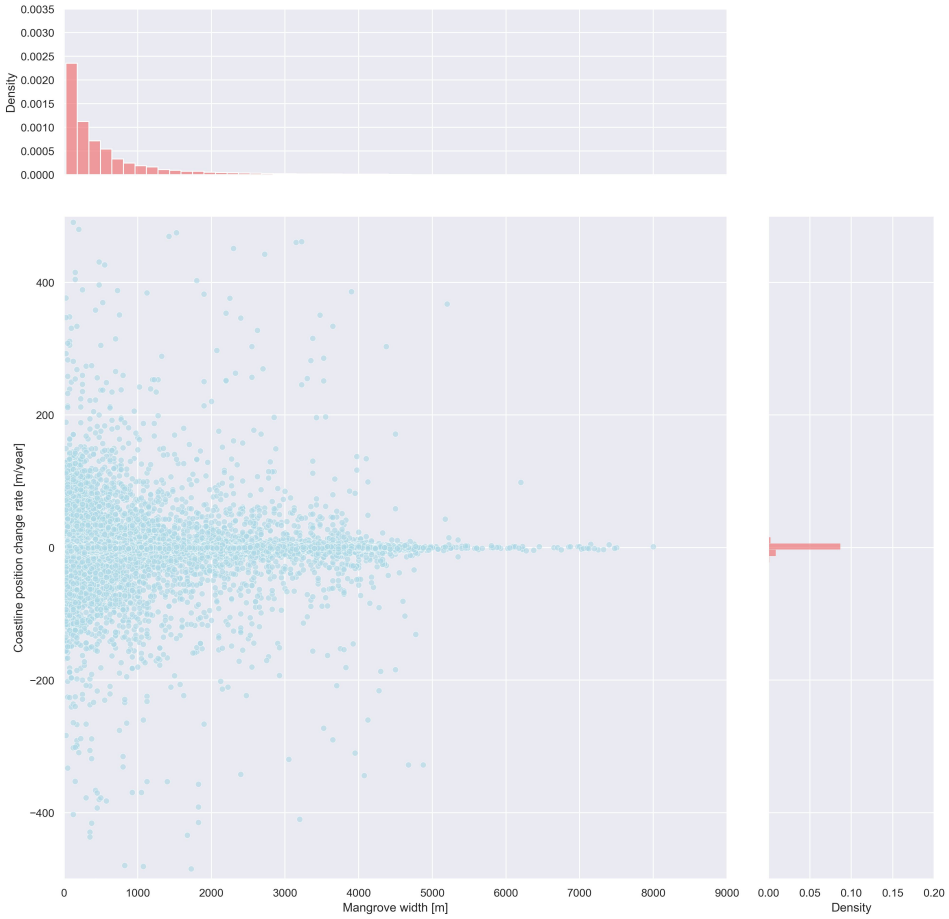

Figure B.7: scatterplot depicting the cross-shore mangrove width versus the coastline position change rate

In Figures B.8 and B.9, the cross-shore mangrove width is compared with the change rate of the coastline position for bin widths of 500 and 100 meters, respectively. When a bin width of 500 meters is used to sample the data, each bin covers a broader range of mangrove widths. This broader range can help smooth out small-scale fluctuations that influence the results. However, when using a smaller bin size of 100 meters, the data within each bin can show more variability, leading to fluctuations in the 15th and 85th percentiles as mangrove width increases. This increased variability can obscure the overall trend and make it harder to discern the relationship between mangrove width and coastline change rate. On the other hand, narrower bins may highlight more localized variability within specific width ranges.

In Figure B.8, the 15th and 85th percentiles are depicted using a specific method. Initially, 100 data points are sampled per bin, and the 15th and 85th percentiles are computed for each bin. Subsequently, a linear regression is performed. The dashed lines in the figure represent the ”raw data,” which incorporates all the data points per bin. The 15th and 85th percentiles are computed per bin and then connected for these lines. Analysis of the linear regression lines reveals that the separation between the 85th and 15th percentiles widens with increasing mangrove width. Notably, the raw data closely aligns with the linear regression line. Beyond 4500 meters, the linear regression lines cease, leaving only the raw data lines. This change showcases that the percentile lines converge, suggesting reduced variability and increased correlation between the variables.

However, this observed trend might also be influenced by limited values in bins after 4500 meters (fewer than 100). To assess the consistency of the observed trends, the slopes of the 85th and 15th percentiles are calculated 1000 times. The resulting distribution of slopes for the 15th and 85th percentiles is shown in the top right and bottom correct figures of Figure B.8, respectively. Analysis indicates that the slope of the 15th percentile is consistently (slightly) negative across the 1000 runs. Conversely, the slope of the 85th percentile tends to centre around zero. This implies that the 85th percentile line can exhibit slight positive, slight negative, or stable slopes, while the 15th percentile line consistently exhibits a negative slope. Consequently, making definitive statements regarding changes in variability for higher mangrove widths is challenging.

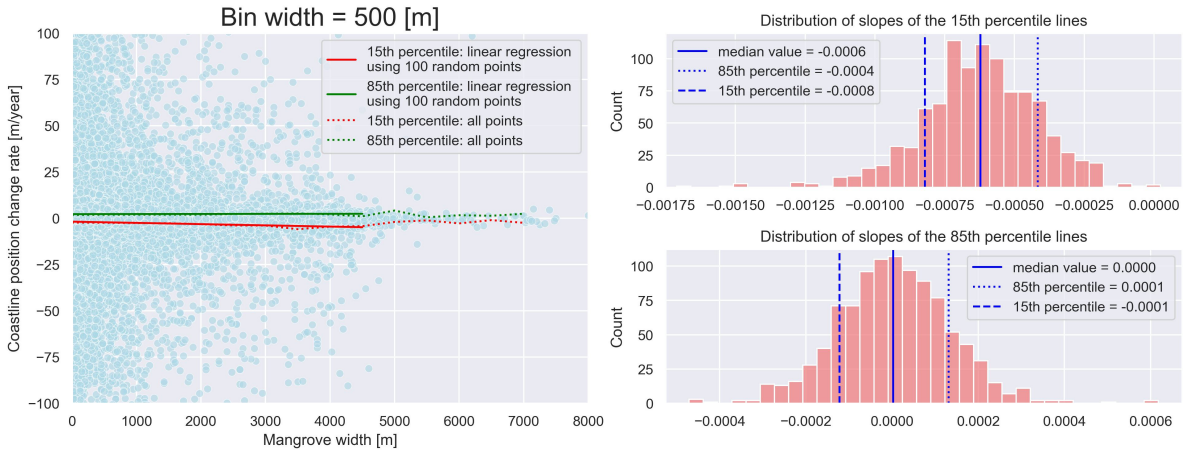

Figure B.8: Bin width of 500 [m]

Figure B.9 shows lines similar to those in Figure B.8, but with a bin width of 100 meters. Upon examining the lines derived from linear regression, it becomes clear that the gap between the 85th and 15th percentiles widens as the mangrove width increases. This trend is reflected in the raw data, which closely resembles the linear regression line. However, the linear regression lines terminate beyond 3750 meters, leaving only those derived from raw data. This suggests a convergence of percentile lines, indicating reduced variability and heightened correlation between the variables. However, this observed trend may be influenced by the limited values within bins after 3750 meters (less than 100). The distribution of calculated slopes for the 15th and 85th percentiles across 1000 runs is illustrated in the top right and bottom right figures of Figure B.8, respectively. In these 1000 runs, the slope of the 15th percentile consistently manifests as negative. Conversely, the slope of the 85th percentile consistently appears positive across these runs. This suggests that the gap between the 15th and 85th percentiles widens for greater mangrove widths, indicative of increasing variability.

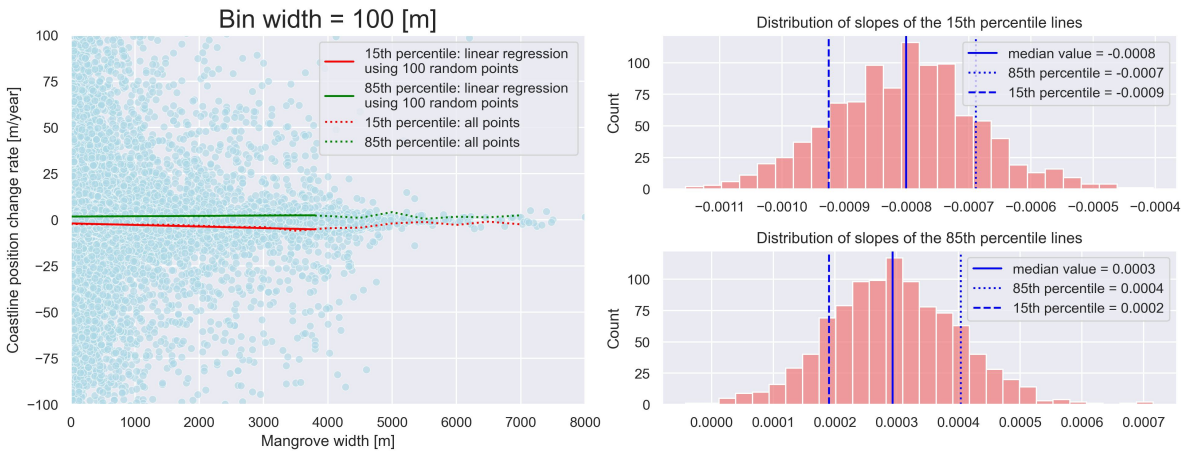

Figure B.9: Bin width of 100 [m]

Figures B.10 and B.11 display the results of method 2 for accreding change rates and eroding change rates, respectively. Upon close examination of the boxplots, several patterns emerge. Firstly, the interquartile range appears relatively narrow for mangrove widths up to 1500 meters, suggesting consistent data within this range. However, numerous outliers are present within this interval. Between 1500 and 4000 meters, the interquartile range significantly expands, indicating increased variability in the data around the median. Moreover, the prevalence of numerous outliers persists. Finally, the interquartile range narrows again in the higher range (> 4000 meters), and the outliers are more concentrated towards the median. This could imply that the variability in the data decreases beyond a certain threshold of mangrove width, and the observations become more uniform. However, there isn't enough data to confirm this hypothesis above a width of 4000 meters. To verify the persistence of the observed trend, the analysis is repeated 1000 times, with the slope of the linear regression line calculated and recorded in each iteration. The distribution of these slopes is visualized in the right subplot of Figure B.10. Notably, most (>85%) of these slopes exhibit a positive trend. This indicates that for wider mangrove widths, accretion rates tend to increase.

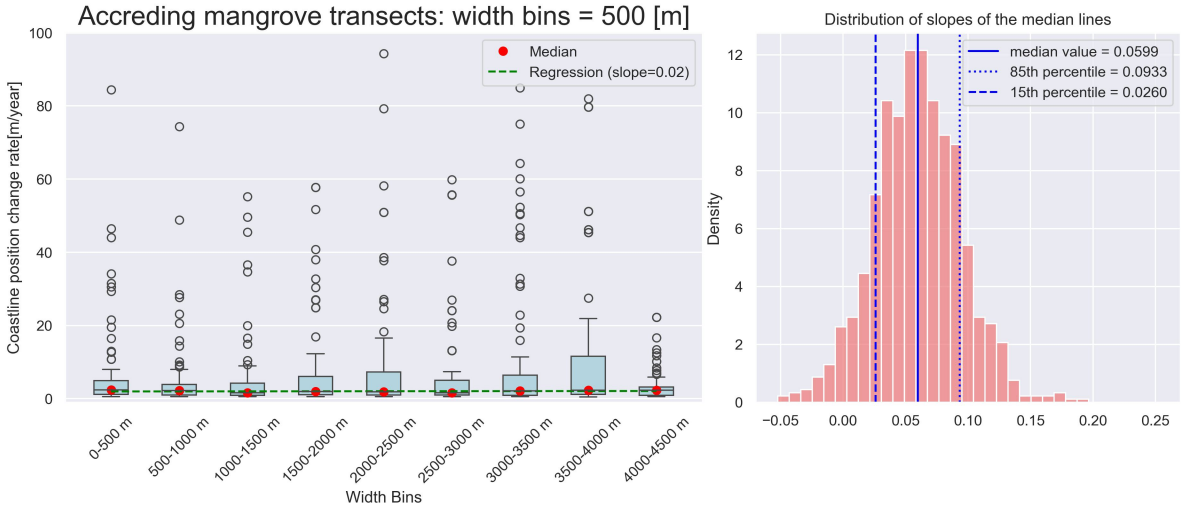

Figure B.10: Random sampling within accreding change rates (> 0.5 [m])

In Figure B.11, representing eroding change rates, an inverse trend compared to that observed in Figure B.10 is evident. Specifically, the linear regression line exhibits a slight downward slope, suggesting that with increasing mangrove width, there is a tendency for more significant erosion. Furthermore, upon closer examination, it is noticeable that in the higher range of mangrove widths (>2000 meters), the interquartile range widens compared to the lower ranges. This suggests a broader dispersion of data points around the median, indicating increased variability in erosion rates as mangrove width increases. These trends remain consistent when alternative random data points are selected. To assess the stability of the observed pattern regarding the slope of the linear regression line, 1000 iterations are conducted. The analysis reveals that most slopes are negative, with only a few positive slopes. This indicates that for wider mangrove widths, erosion rates tend to increase.

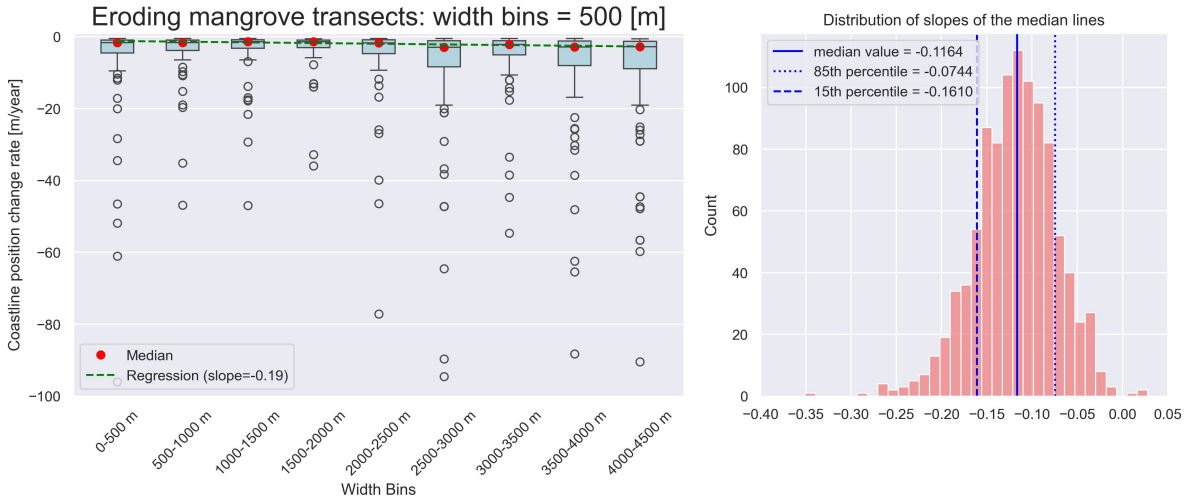

Figure B.11: Random sampling within eroding change rates (< -0.5 [m])

The change rate of the cross-shore mangrove width compared to the coastline position Change Rate

In Figure B.12, a scatterplot illustrates the comparison between the cross-shore mangrove width change rate and the change rate of the coastline position. Most transects are situated on the y-axis, indicating stable mangrove forests. The second-highest concentration of mangrove transects is found in the bottom left quadrant. This observation implies a negative correlation between the change rates of mangrove width and coastline position. Specifically, as the coastline shifts inland (demonstrated by a negative change rate), there is a tendency for mangrove forests to contract. No similar trend is observed on the right side of the graph, which indicates situations where the mangrove forest expands. The distribution of points in the quadrants representing an erosional coastline versus an accreding coast appears relatively balanced, suggesting comparable erosion and accretion along the coastline when a mangrove forest is expanding.

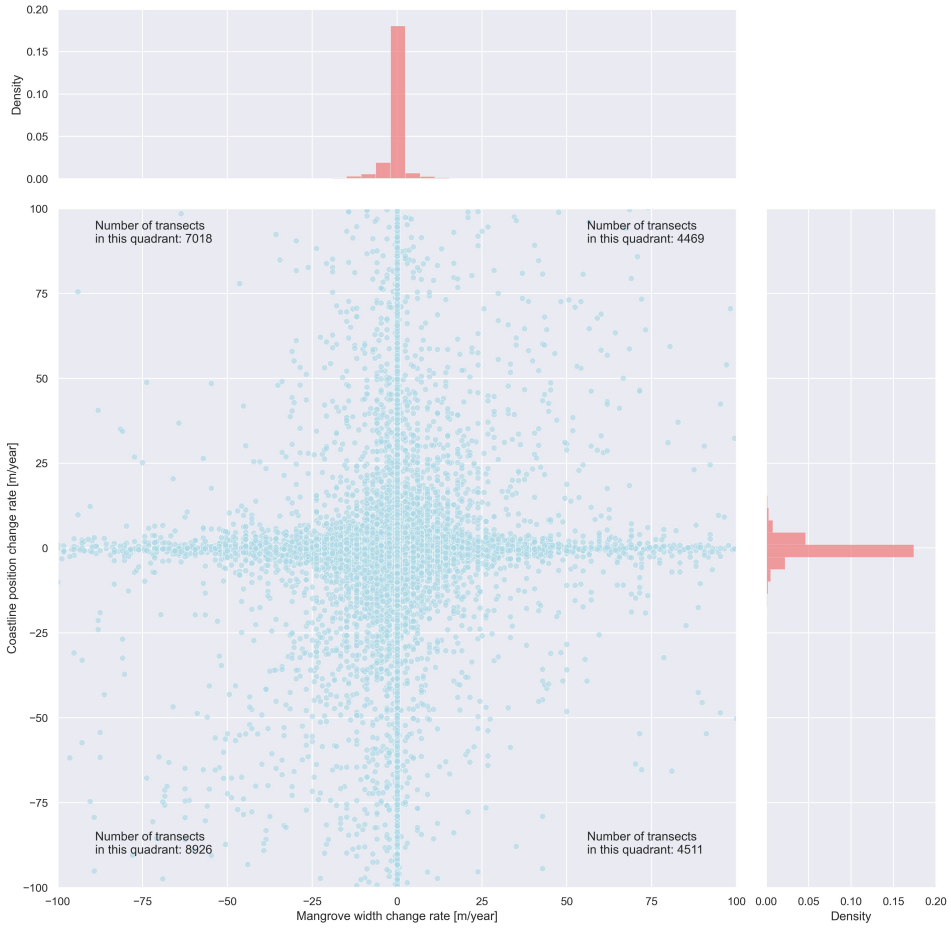

Figure B.12: Scatterplot cross-shore mangrove width change rate versus the coastline position change rate with bin width 50

It is shown in Figure B.6 that most mangrove ecosystems are considered stable. To further examine the distribution of coastline position change rates, mainly when the cross-shore mangrove change rate is zero meters per year, a histogram that illustrates the distribution of coastline position change rates is displayed in Figure B.13. This figure shows that the median coastline position change rate is slightly negative (-0.094), indicating that the coastline is shifting slightly inland, reflecting a negative change rate when the mangrove width remains constant. However, this value still falls within the stable range. Furthermore, the 15th percentile coastline position change rate is around -2.25, while the 85th percentile is approximately 1.83. These percentiles suggest that the likelihood of the coastline eroding is higher when the mangrove width stays constant.

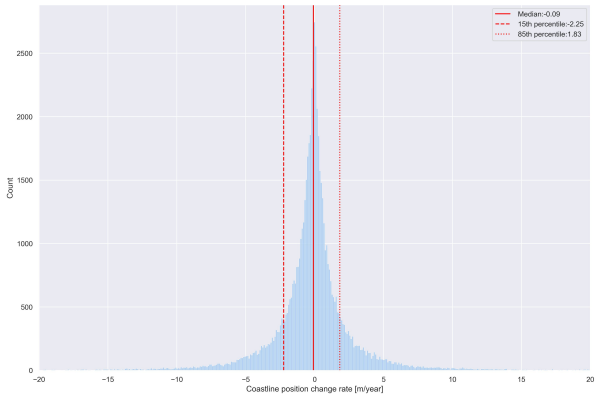

Figure B.13: Histogram coastline position Change Rate for a Mangrove Width Change Rate of 0

The scatterplot in Figure B.14 is analyzed in detail by showing the distribution of coastline position change rates for accreding transects with contracting, stable, and eroding mangrove forests. The figure is divided into three parts: the left graph shows the distribution of coastline change rates in the top left quadrant, the middle graph shows the distribution of coastline position change rates on the positive y-axis, and the right graph shows the distribution of coastline position change rates in the top right quadrant. Upon observing the figure, it is evident that the distribution is quite similar for contracting and stable mangrove forests. Although the median value is slightly higher when a mangrove forest is stable, the difference is minimal. However, when the mangrove forest is expanding, the median is substantially higher than when it is contracting or stable. This suggests that when a mangrove forest is expanding, the coastline experiences higher accretion rates than when it is contracting or stable. Furthermore, in expanding mangrove forests, the 85th percentile is considerably higher than for stable and contracting mangrove forests. This indicates that extreme accretion events are more prevalent in expanding mangrove forests than in stable and contracting mangrove forests.

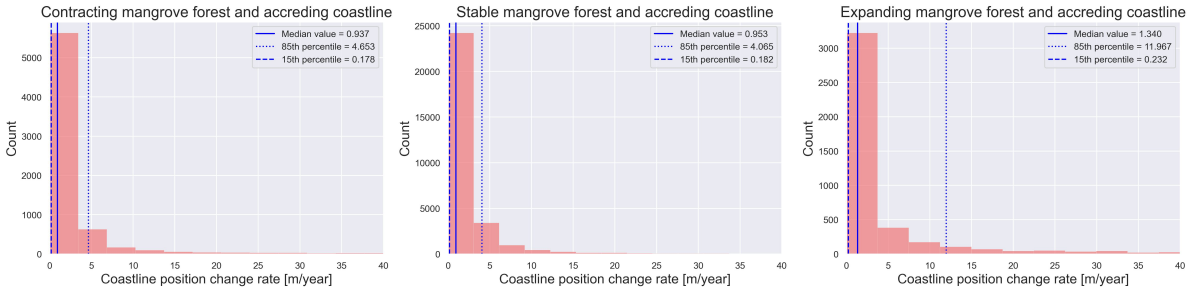

Figure B.14: The coastline position change rate distributions for accreding transects with contracting, stable and eroding mangrove forests, respectively

Figure B.15 displays coastline position change rates distribution for eroding transects where mangrove forests are contracting, stable, or expanding. The figure is divided into three parts: the left graph shows the distribution of coastline change rates in the bottom-left quadrant, the middle graph shows the distribution of coastline position change rates on the negative y-axis, and the right graph shows the distribution of coastline position change rates in the bottom-right quadrant. The median value of the coastline position change rates indicates that when a mangrove forest is stable, the median erosion change rate is the least negative. Conversely, the median erosion change rate is the most negative when a mangrove forest is contracting. Furthermore, there is more variation in erosion rates when a mangrove forest expands or contracts than when it is stable, as indicated by the 15th percentile. This suggests that a stable mangrove forest results in lower erosion rates than when a forest expands or contracts. In addition, when a mangrove forest is stable, less extreme erosion rates occur compared to when it is expanding or contracting.

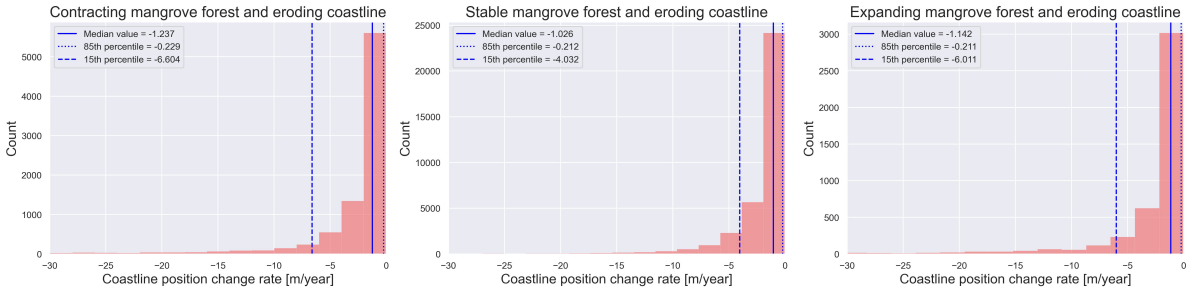

Figure B.15: The coastline position change rate distributions for eroding transects with contracting, stable and eroding mangrove forests, respectively

In the previous results, it was observed that there is a significant difference in sample sizes between expanding, stable, and contracting transects. Specifically, there are 30422 transects with an accreding coastline and stable mangrove forests, 7018 transects with an accreding coastline and contracting mangrove forest, and 4469 transects with an accreding coastline and expanding mangrove forest. Similarly, there are 35459 transects with an eroding coastline and stable mangrove forests, 8926 transects with an eroding coastline and contracting mangrove forest, and 4511 transects with an eroding coastline and expanding mangrove forest. It should be noted that there are the least number of expanding mangrove forests for transects with both eroding and accreding coastlines. The following approach was used to investigate whether the difference in sample size influences the results. Data points for transects with an accreding coastline were randomly selected for transects with both contracting and stable mangrove forests. The number of selected points matched the count of mangrove transects with expanding mangrove forests. Specifically, 4469 transects with a stable and contracting mangrove forest were randomly selected. This process was repeated 1000 times, and the median of the randomly selected data points was recorded each time. The results of this process can be seen in Figure B.16. The red line in the figure indicates the median value of transects with an expanding mangrove forest. Similarly, this process was repeated for transects with an eroding coastline. However, 4511 transects with stable and contracting mangrove forests were randomly selected. The results of this process can be seen in Figure B.17.

In Figure B.16, it can be seen that the median for expanding mangrove forests is substantially higher than the median for stable and contracting mangrove forests. The results for contracting and stable mangrove forests are quite similar. The difference in sample size does not influence the results.

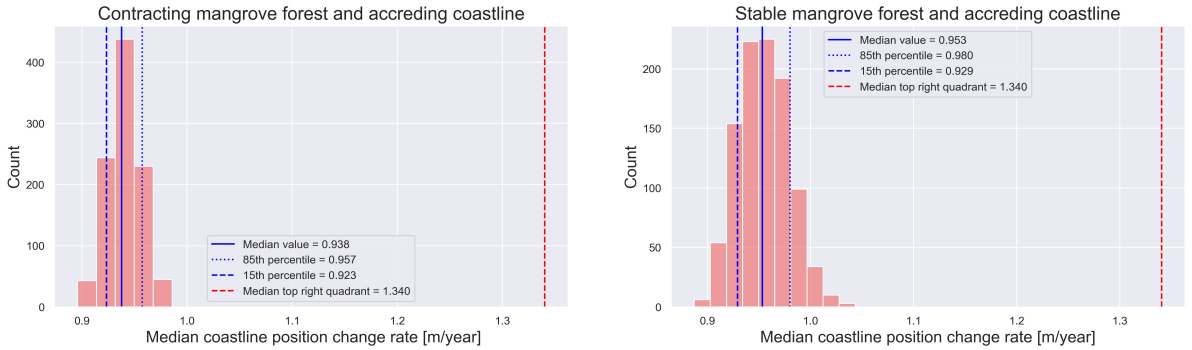

Figure B.16: The median coastline position change rates for accreding transects with contracting and stable forests, respectively, using random sampling

In Figure B.17, it can be seen that the median for stable mangrove forests is substantially higher than the median for expanding and contracting mangrove forests. The difference in sample size does not influence the results.

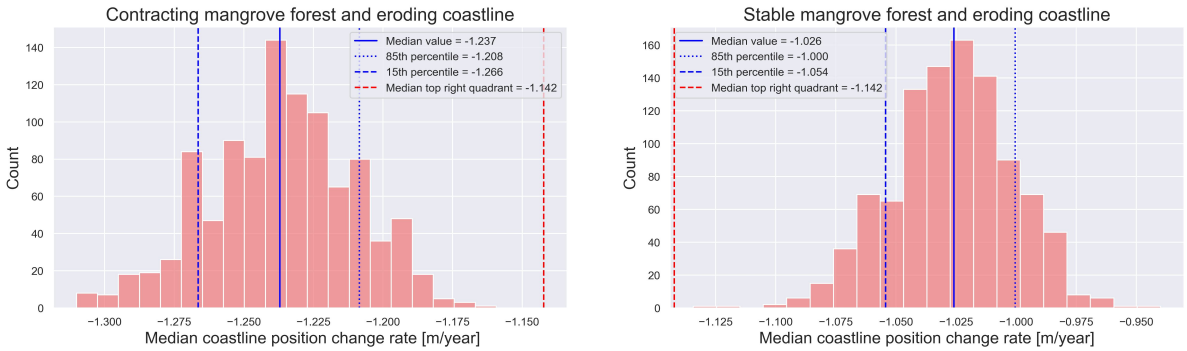

Figure B.17: The median coastline position change rates for eroding transects with contracting and stable forests, respectively, using random sampling

B.2. Framework 2

Coastline position change rates

The distribution of coastline position change rates is illustrated in Figure B.18. It can be observed from the figure that both mangrove and non-mangrove transects are mostly stable, with median change rates of -0.158 and -0.107, respectively. However, accreding mangrove transects have a median change rate of 2.006, higher than accreding non-mangrove transects. This indicates mangrove transects are more likely to experience accreding at higher rates than non-mangrove transects. On the other hand, the opposite trend is observed for eroding mangrove and non-mangrove transects. The median value for eroding mangrove transects is lower than that for eroding non-mangrove transects, suggesting that mangroves are more prone to deteriorate at higher rates than non-mangrove transects.

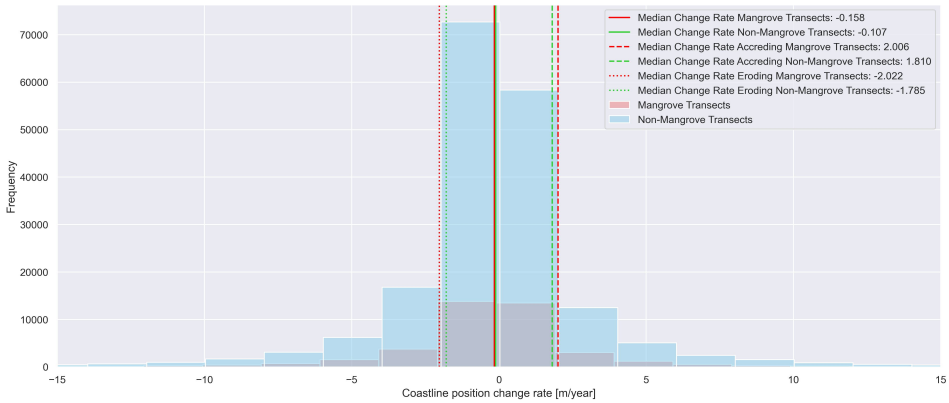

Figure B.18: distribution of the coastline position change rates between -15 and 15

The histogram in Figure B.19 illustrates the change rates of coastline position for mangrove and non-mangrove transects, divided into four categories. The data shows that mangrove transects tend to accrete more than non-mangrove transects when focusing on positive values. Conversely, mangrove transects experience more erosion for negative values than non-mangrove transects. Moreover, mangrove transects exhibit higher standard deviations than non-mangrove transects, indicating more significant overall variability. Additionally, the interquartile range is slightly more comprehensive for mangrove transects than non-mangrove transects, indicating a broader distribution of data points around the median for mangroves.

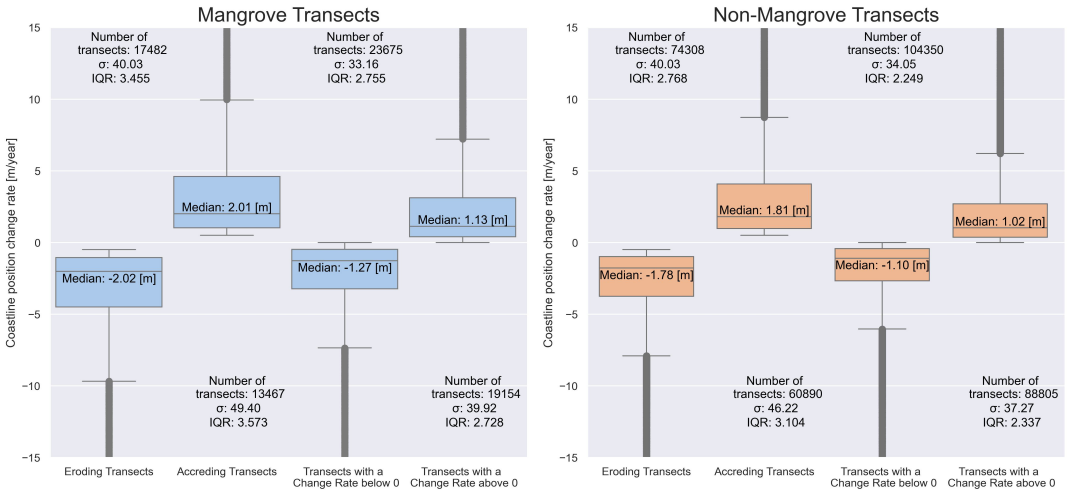

Figure B.19: Boxplots of coastline position change rate for mangrove and non-mangrove transects

There is a significant difference between the number of non-mangrove transects and mangrove transects, with almost seven times more non-mangrove transects than mangrove transects. To balance this, random data points will be selected from eroding and accreding non-mangrove categories, matching the count of mangrove transects within their respective eroding and accreding categories. Specifically, 17,482 eroding non-mangrove transects and 13,467 accreding non-mangrove transects will be chosen randomly. This process will be repeated 1000 times, and the median and standard deviation of the set will be stored in each iteration. Figures B.20 and B.21 illustrate the distribution of medians and standard deviations of those 1000 runs for eroding and accreding transects, respectively. According to Figure B.20a, mangrove transects experience more erosion than non-mangrove transects. However, across the performed runs, the calculated medians for eroding non-mangrove transects do not approach the median value of mangrove transects. Looking at Figure B.20b, it is evident that the standard deviation for both mangrove and non-mangrove transects is comparable.

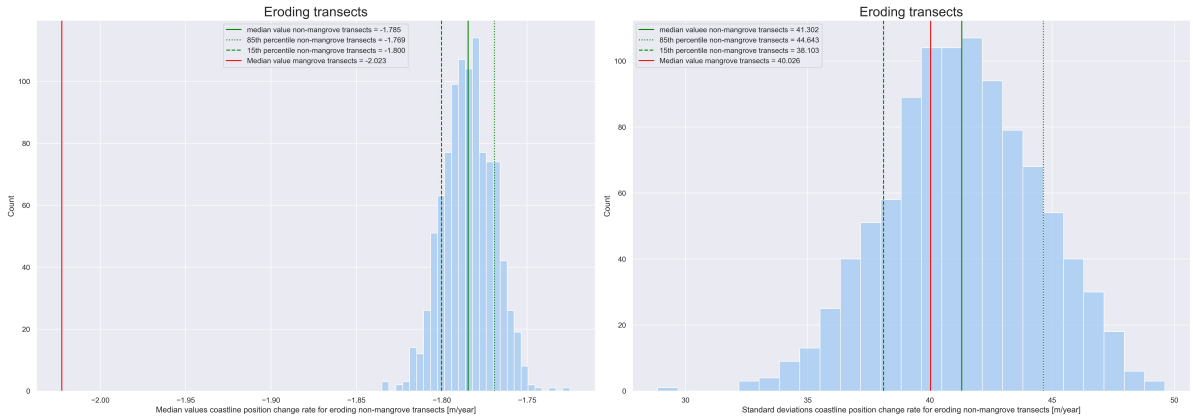

(a) Distribution of medians

(b) Distribution of standard deviations

Figure B.20: Eroding non-mangrove transects

Upon examining Figure B.21a, it is evident that mangrove transects exhibit substantially more accretion than non-mangrove transects. The median of non-mangrove transects in all 1000 runs never approaches the median of mangrove transects. Moreover, upon inspection of Figure B.21b, it is clear that the standard deviations of both mangrove and non-mangrove transects are comparable.

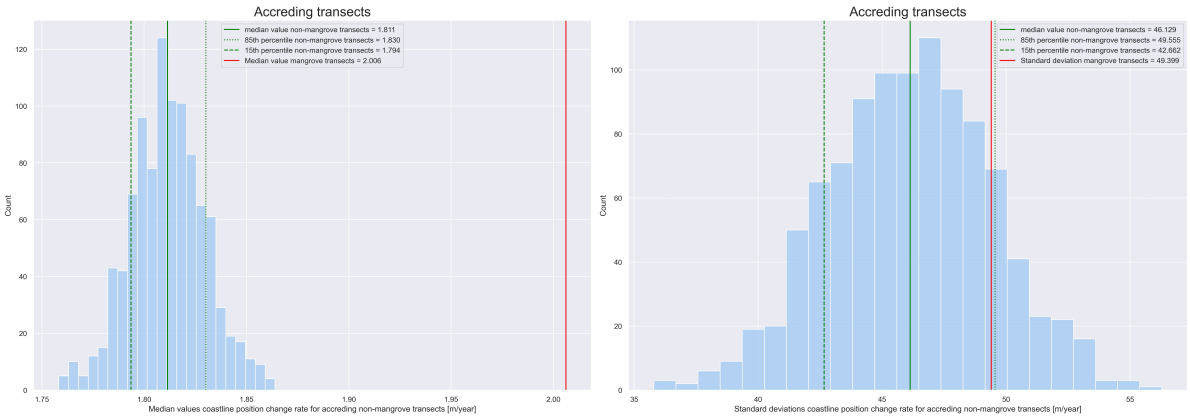

(a) Distribution of medians (b) Distribution of standard deviations

Figure B.21: Accreding non-mangrove transects

Figure B.22 illustrates the distribution of accreding, eroding, and stable transects in coastal states for both mangrove and non-mangrove transects. Non-mangrove transects display more excellent stability than mangrove transects. However, a higher proportion of mangrove transects erode than non-mangrove transects.

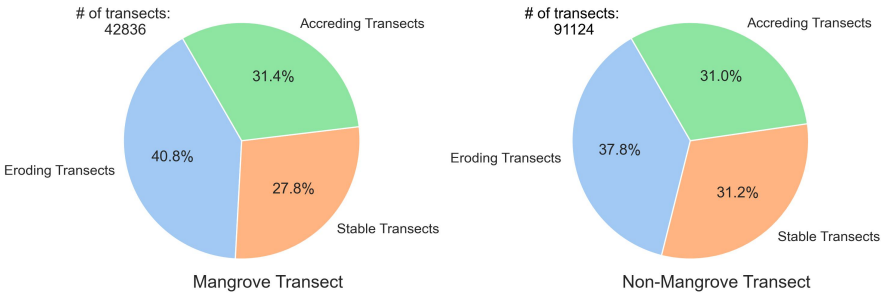

Figure B.22: The coastal state distributions for mangrove and non-mangrove transects

Mangrove cross-shore width

Figure B.23 shows an overview of the contracting, expanding, and stable mangrove forests for 42836 muddy transects where only non-complex transects are included. The majority of transects, 73.8% to be exact, are stable, while 16.6% are expanding, and 9.6% are contracting.

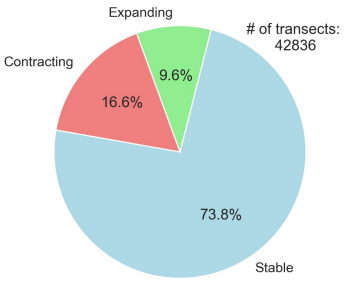

Figure B.23: The distribution of contracting, expanding and stable mangrove forests

Mangrove width compared to change rate of the coastline position

The overview Figure B.24 shows the mangrove cross-shore mangrove width along the transects compared to the change rate of the coastline position. The scatterplot depicts a wide spread of points for a mangrove width below approximately 5000 meters. For higher mangrove widths, the coastline position change rate clusters around the scatterplot's horizontal axis, approaching zero or in a stable situation. The same methods used for framework 1 will be used to investigate this figure.

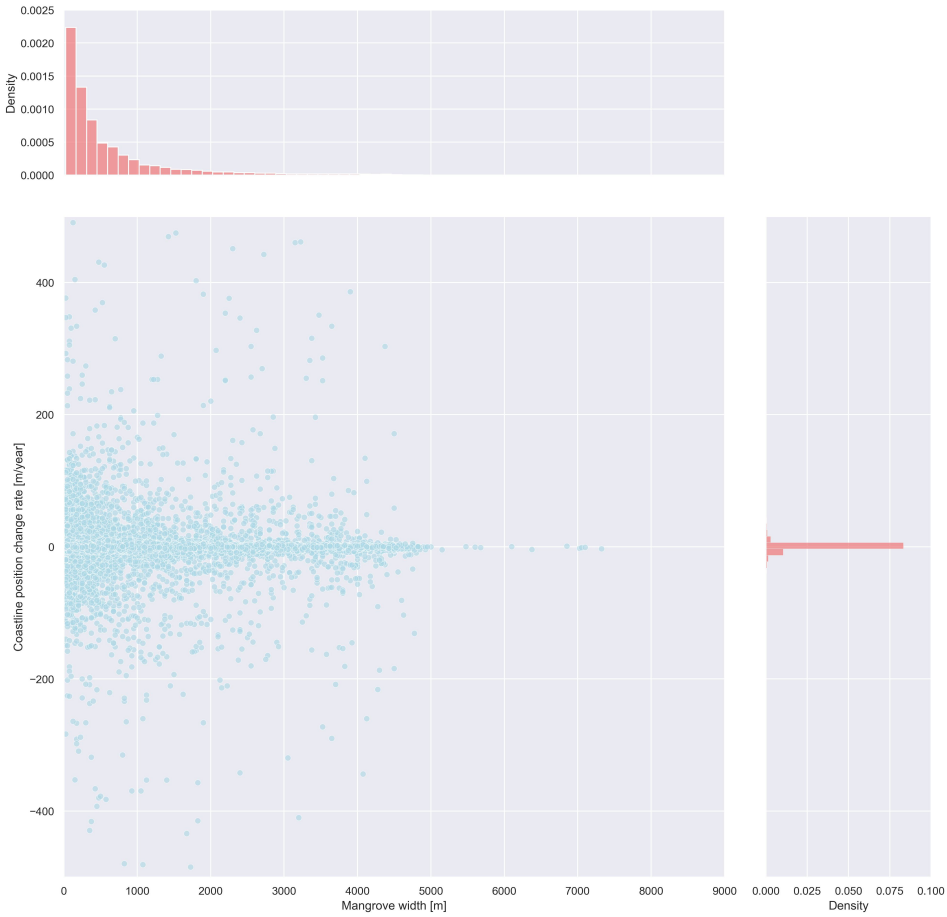

Figure B.24: Scatterplot cross-shore mangrove width versus the coastline position change rate

Figures B.25 and B.26 show the results of method 1. They display scatterplots of the cross-shore mangrove width against the coastline position change rates for bin sizes of 500 and 100, respectively. Both figures show that the difference between the 15th and 85th percentiles becomes larger as the mangrove width increases. This suggests that the erosion and accretion rates are greater for wider mangroves. On the right side of the figures, the behaviour of the 85th and 15th percentile lines can be observed when the slope of those lines is calculated 1000 times by selecting 100 random values per bin. Looking at the graphs on the right of Figure B.25, it can be observed that the 15th percentile line is negative while the 85th percentile line is positive. It can also be seen that the median value of the 15th percentile line is slightly more negative than the 85th percentile line is positive. This indicates that the wider the mangrove width, the higher the accretion and erosion rates. The absolute value of the negative 15th percentile slope that is higher than the absolute value of the positive 75th percentile slope indicates that erosion rates are higher than accretion rates. When looking at the graphs on the right of Figure B.26, the same trends as in Figure B.25 can be observed.

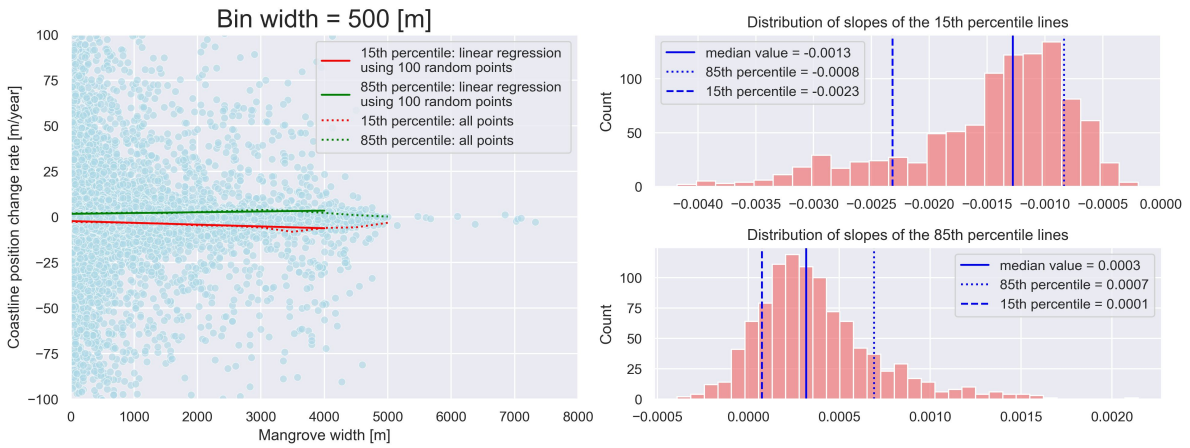

Figure B.25: Bin width of 500 [m]

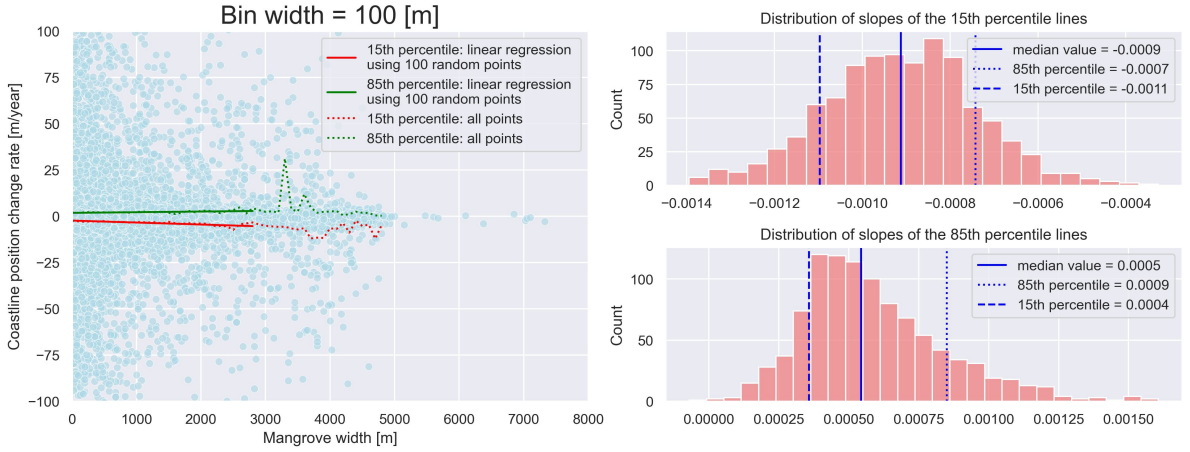

Figure B.26: Bin width of 100 [m]

Figures B.27 and B.28 display the results of method 2. Figure B.27 represents the accreding change rates, which show an upward trend in the medians. This suggests that higher accretion rates are observed with increasing mangrove width. To investigate if this trend remains consistent even with other data points, the slope of the medians is recalculated 1000 times with 100 different data points to form the mean. The right graph of Figure B.27 shows the distribution of the slopes, indicating an upward trend across all these runs. The boxplots in the Figure change significantly when choosing different random points, except for the more significant interquartile distance at a distance of 2000 [m] compared to the zone before.

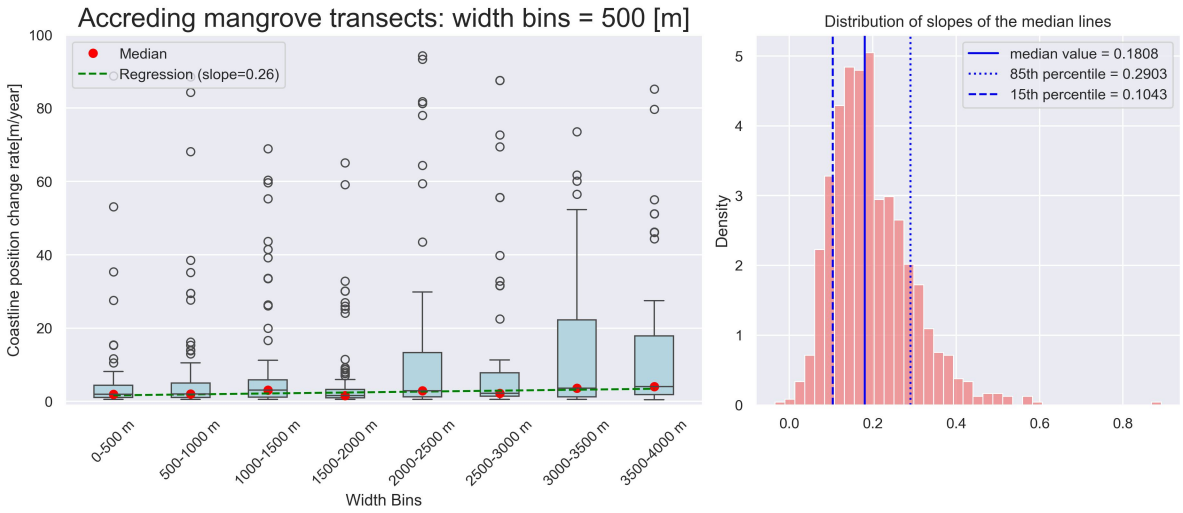

Figure B.27: Random sampling within accreding change rates (> 0.5 [m])

Figure B.28 illustrates the coastline position change rates for eroding coastlines. In this Figure, it can be seen that an opposite pattern prevails compared to Figure B.27. The linear regression line shows a downward trend, indicating that as the width of the mangrove increases, there is a tendency for more erosion to occur. The graph on the right side shows the slope distribution when 1000 times 100 random data points are chosen to calculate the mean. We can see that the downward trend remains consistent across all runs. However, it should be noted that compared to the accreding transects, the absolute value of the median is lower for eroding transects. This suggests that for higher mangrove widths, erosion rates are lower than accretion rates. The difference between the two indicates that more outliers are present in the eroding dataset than in the accreding dataset. However, similar to the accreding boxplots, the interquartile range is relatively small when mangrove widths are small (< 2000). In the higher mangrove width range (> 2000 [m]), the interquartile range is more comprehensive compared to the lower ranges. This indicates a greater spread of data points around the median, suggesting increased variability in erosion rates as mangrove width increases. This trend does not change when choosing other random data points.

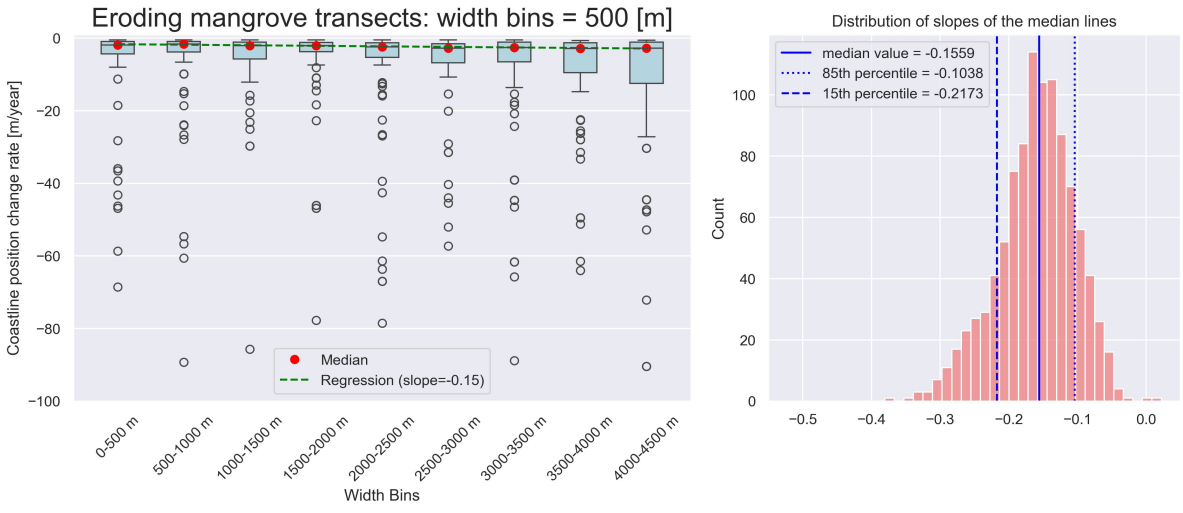

Figure B.28: Random sampling within eroding change rates (< -0.5 [m])

The change rate of the cross-shore mangrove width compared to the coastline position change rate

The histogram depicted in Figure B.29 shows the cross-shore mangrove width change rate distribution about the coastline position. Most data points are in the bottom left quadrant, indicating that mangrove width and coastline positions are decreasing. This suggests a negative correlation between the change rates of mangrove width and coastline position. In other words, as the coastline shifts inland (shown by a negative change rate), the width of mangrove forests tends to decrease. On the other hand, there is no clear trend when it comes to mangrove forest expansion. The distribution of points in the quadrants representing an erosional coast versus an accreding coast appears to be relatively balanced, indicating comparable occurrences of erosion and accretion along the coastline when a mangrove forest is expanding.

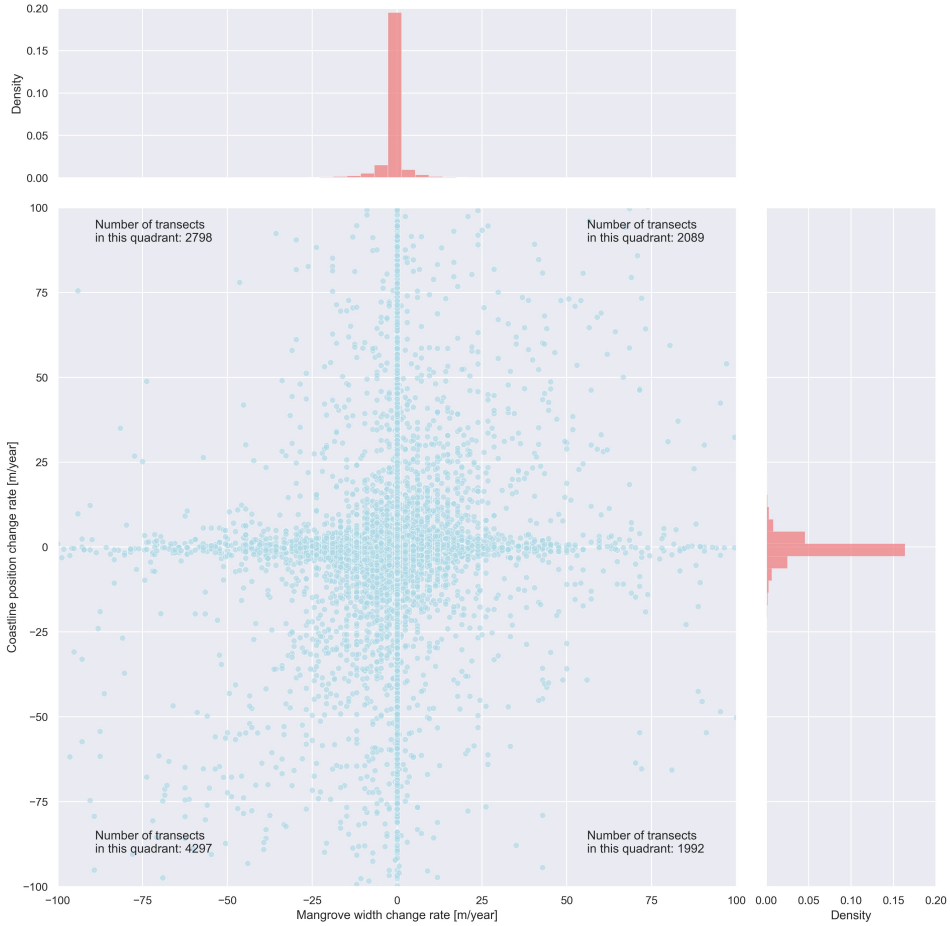

Figure B.29: Scatterplot of cross-shore mangrove width change rate versus the coastline position change rate

In Figure B.30, the change rate of the coastline position for a mangrove with a change rate of zero is depicted. The median change rate of the coastline position is -0.14 meters per year, which is still within the stable region. The 15th percentile of the coastline position change rate is -2.55, while the 85th percentile is 1.97. This suggests a slight tendency towards erosion as the mangrove width remains stable.

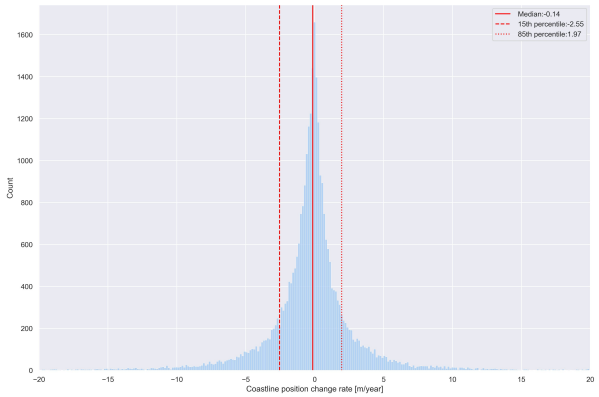

Figure B.30: Histogram coastline position change rate for a mangrove width change rate of zero

The scatterplot displayed in Figure B.31 is thoroughly analyzed by presenting the distribution of coastline position change rates for accreding transects with contracting, stable, and eroding mangrove forests. The figure is divided into three parts: the left graph represents the distribution of coastline change rates in the top left quadrant, the middle graph denotes the distribution of coastline position change rates on the positive y-axis, and the right graph displays the distribution of coastline position change rates in the top right quadrant. Upon observing the figure, it is apparent that the distribution is quite similar for contracting and stable mangrove forests. Although the median value is slightly higher when a mangrove forest is stable, the difference is minimal. However, when the mangrove forest is expanding, the median is substantially higher than when it is contracting or stable. This suggests that when a mangrove forest is expanding, the coastline experiences higher accretion rates than when it is contracting or stable. Furthermore, in expanding mangrove forests, the 85th percentile is considerably higher than for stable and contracting mangrove forests. This indicates that extreme accretion events are more prevalent in expanding mangrove forests than in stable and contracting mangrove forests.

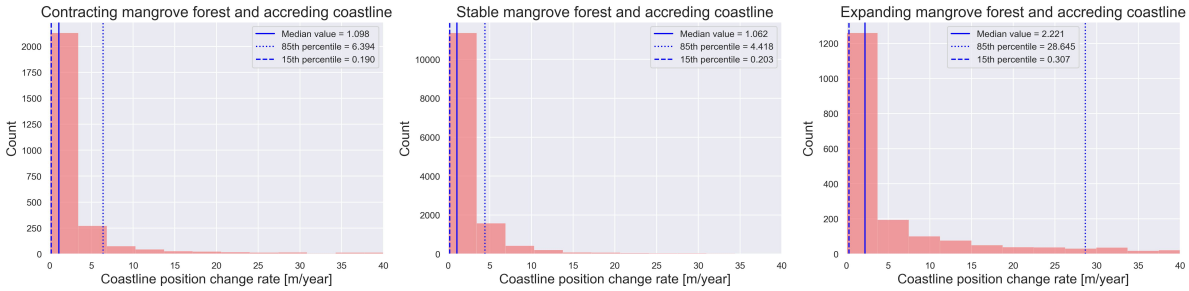

Figure B.31: The coastline position change rate distributions for accreding transects with contracting, stable and eroding mangrove forests, respectively

Figure B.32 displays the distribution of coastline position change rates for eroding transects in areas where mangrove forests are contracting, stable, or expanding. The Figure is split into three sections: the left graph shows the distribution of coastline change rates in the bottom-left quadrant, the middle graph shows the distribution of coastline position change rates on the negative y-axis, and the right graph shows the distribution of coastline position change rates in the bottom-right quadrant. The median value of the coastline position change rates shows that the erosion change rate is the least negative when a mangrove forest is stable. On the other hand, when a mangrove forest is contracting, the erosion change rate is the most negative. Furthermore, there is more significant variation in erosion rates when a mangrove forest expands or contracts than when it is stable, as indicated by the 15th percentile. This suggests that a stable mangrove forest results in lower erosion rates than when a forest expands or contracts. Additionally, less extreme erosion rates occur when a mangrove forest is stable than when it is expanding or contracting.

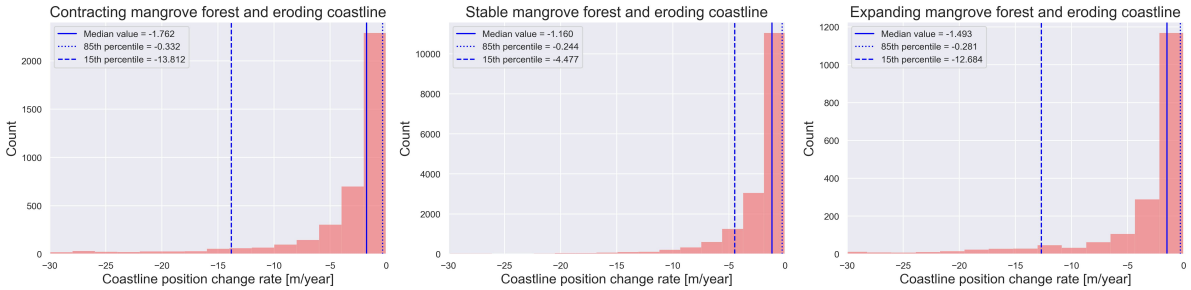

Figure B.32: The coastline position change rate distributions for eroding transects with contracting, stable and eroding mangrove forests, respectively

It was observed in the previous findings that there is a significant difference in the sample sizes of expanding, stable, and contracting transects. Specifically, there are 14202 transects with an accreding coastline and stable mangrove forests, 2798 transects with an accreding coastline and contracting mangrove forest, and 2089 transects with an accreding coastline and expanding mangrove forest. Similarly, there are 17276 transects with an eroding coastline and stable mangrove forests, 4297 transects with an eroding coastline and contracting mangrove forest, and 1992 transects with an eroding coastline and expanding mangrove forest. It should be noted that transects with both eroding and accreding coastlines have the least number of expanding mangrove forests. The following approach was used to investigate whether the difference in sample size affects the results. Data points for transects with an accreding coastline were randomly selected for transects with both contracting and stable mangrove forests. The number of selected points matched the count of mangrove transects with expanding mangrove forests. Specifically, 2089 transects with stable and contracting mangrove forests were randomly selected. This process was repeated 1000 times, and the median of the randomly selected data points was recorded each time. The results of this process can be seen in Figure B.33. The red line on the figure indicates the median value of transects with an expanding mangrove forest. Similarly, this process was repeated for transects with an eroding coastline. However, 1992 transects with stable and contracting mangrove forests were randomly selected. The results of this process can be seen in Figure B.34.

The graph shown in Figure B.33 highlights that the median value for expanding mangrove forests is significantly higher than that of stable and contracting mangrove forests. The outcomes for stable and contracting mangrove forests are relatively alike. The results imply that the difference in sample size does not impact the findings.

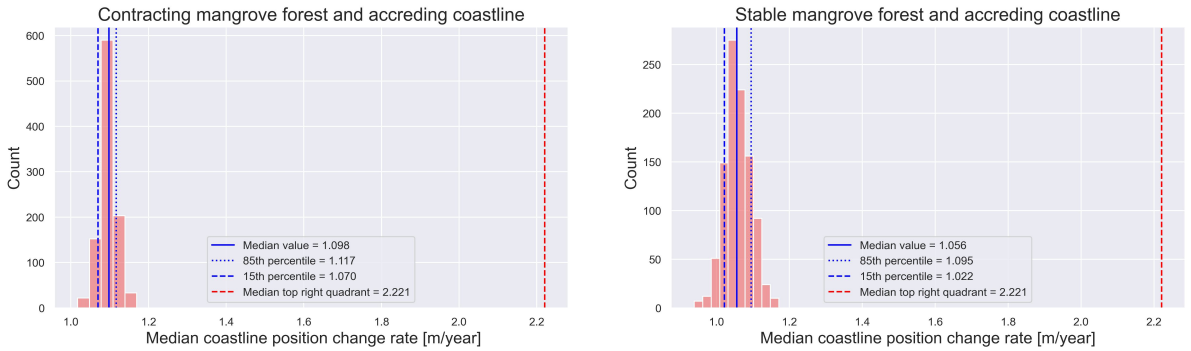

Figure B.33: The median coastline position change rates for accreding transects with contracting and stable forests, respectively, using random sampling

In Figure B.34, it can be seen that the median for stable mangrove forests is substantially higher than the median for expanding and contracting mangrove forests. The difference in sample size does not influence the results.

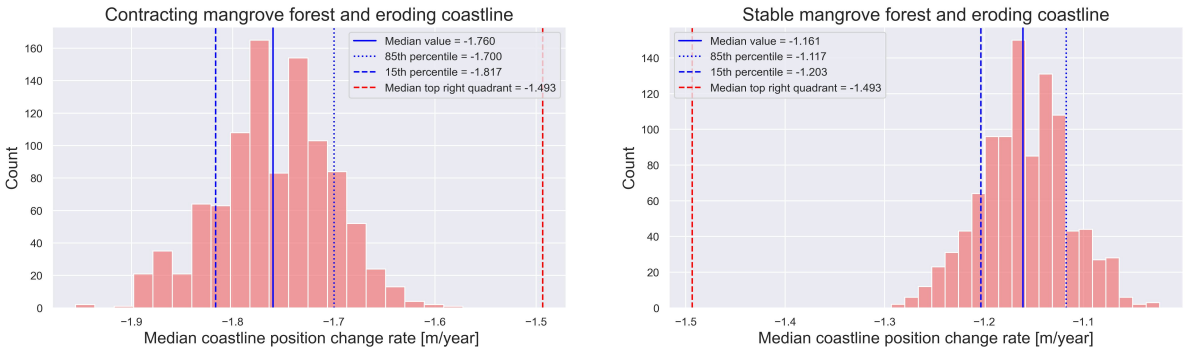

Figure B.34: The median coastline position change rates for eroding transects with contracting and stable forests, respectively, using random sampling

B.3. Framework 3

Coastline position change rates

In Figure B.35, the coastline position change rate distribution is depicted. The median change rate for mangrove transects is slightly lower than that for non-mangrove transects, yet both medians fall within the stable region. However, there is a higher median change rate for accreding mangrove transects than non-mangrove transects. Additionally, when examining the median change rate for eroding transects, it becomes evident that mangrove areas experience a higher rate of coastal erosion than non-mangrove areas.

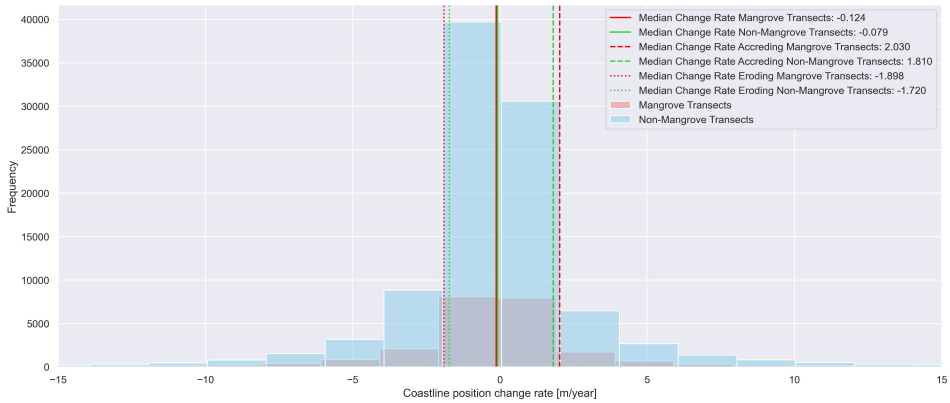

Figure B.35: Coastline position change rate for mangrove and non-mangrove transects

In the histogram presented in Figure B.36, the coastline position change rates for mangrove and non-mangrove transects have been sorted into four groups. It is apparent that when all positive values are considered, mangrove transects tend to experience more accretion than non-mangrove transects. Conversely, when all negative values are examined, mangrove transects erode more than non-mangrove transects. Moreover, mangrove transects exhibit higher standard deviations than non-mangrove transects, indicating a more significant overall variability. Additionally, the interquartile range is marginally higher for mangrove transects than for non-mangroves, suggesting a wider spread of data points around the median for mangroves.

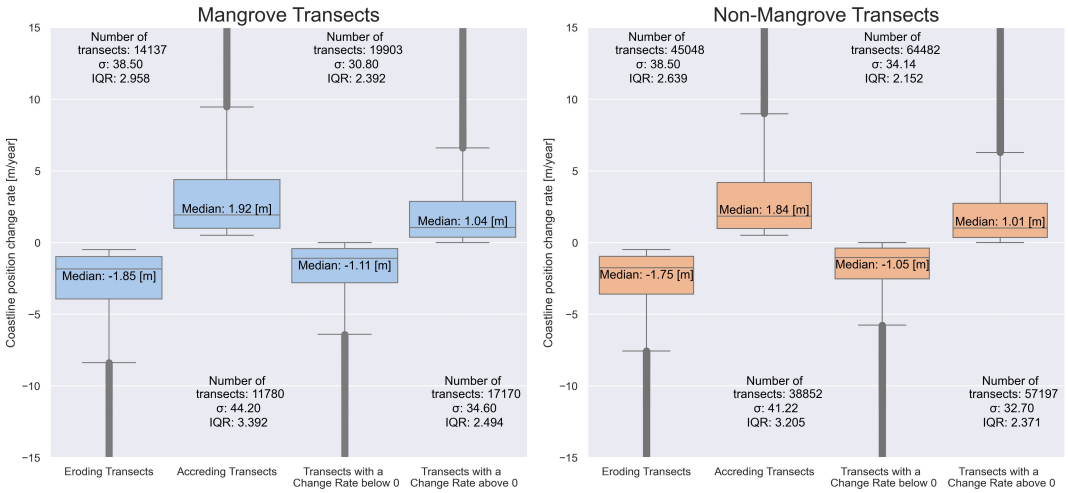

Figure B.36: Coastline position change rate for mangrove and non-mangrove transects

It has been observed that there is a significant difference in the number of non-mangrove and mangrove transects, similar to frameworks 1 and 2. Specifically, there are almost four times more non-mangrove transects than mangrove transects, which creates an imbalance. To address this, a random selection of data points will be made from both accreding and eroding non-mangrove categories, matching the count of mangrove transects within their respective accreding and eroding categories. This process will be repeated 1000 times, storing the median and standard deviation of the set in each iteration. The distribution of medians and standard deviations of those 1000 runs for eroding and accreding transects are illustrated in Figures B.37 and B.38, respectively. Figure B.37a shows that mangrove transects experience more erosion than non-mangrove transects. Across the performed runs, the calculated medians for eroding non-mangrove transects do not approach the median value of mangrove transects. Looking at Figure B.37b, it is evident that the standard deviation for both mangrove and non-mangrove transects is comparable.

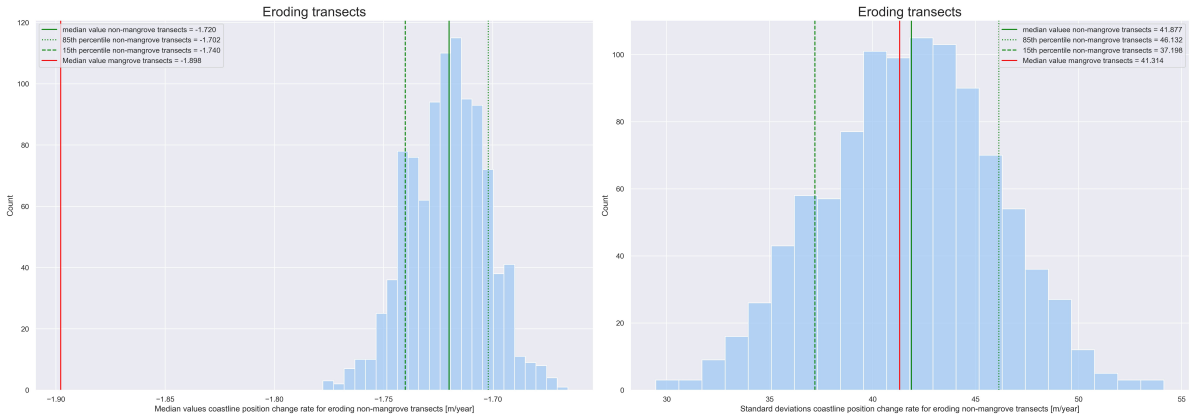

(a) Distribution of medians

(b) Distribution of standard deviations

Figure B.37: Eroding non-mangrove transects

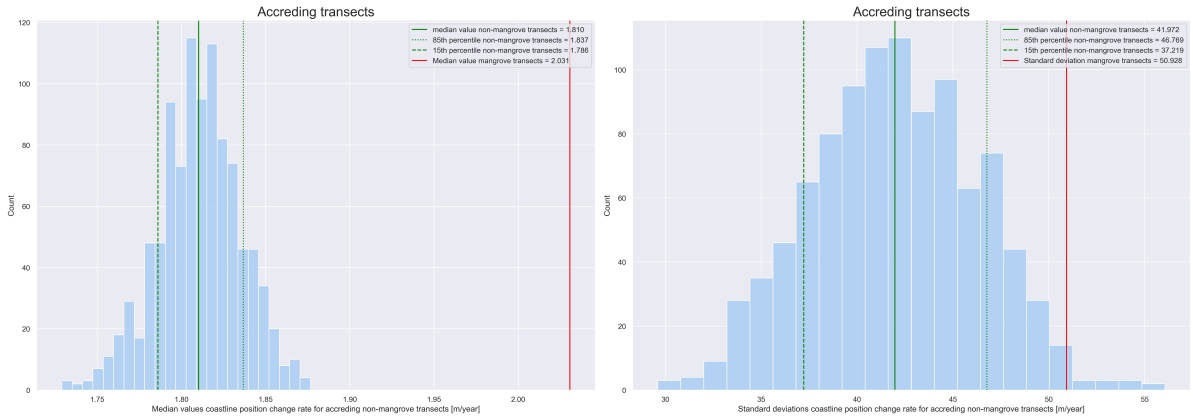

(a) Distribution of medians (b) Distribution of standard deviations

Figure B.38: Accreding non-mangrove transects

Figure B.39 displays the distribution of accreding, eroding, and stable transects for mangrove and non-mangrove areas. The graph illustrates that mangrove transects are more prone to erosion, while non-mangrove regions tend to be more stable.

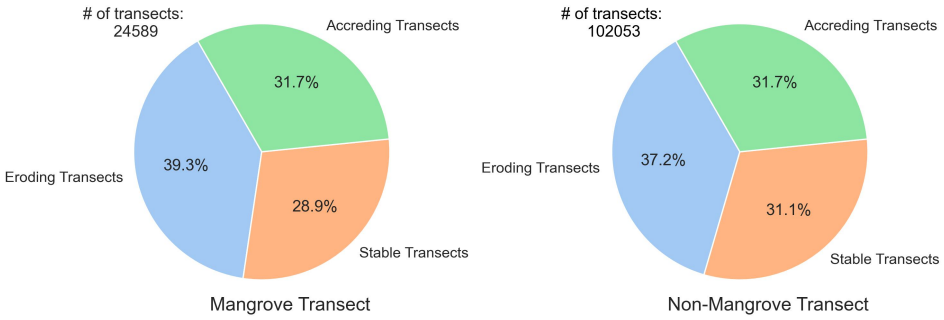

Figure B.39: The coastal state distribution for mangrove and non-mangrove transects

Mangrove cross-shore width

Figure B.40 displays a pie chart presenting the distribution of contracting, expanding and stable mangrove forests. Approximately 75% of the 24589 observations exhibit stability.

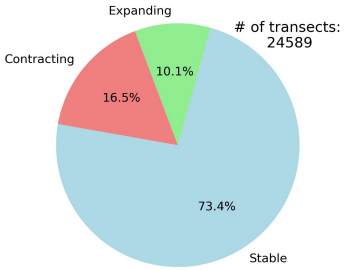

Figure B.40: The distribution of contracting, expanding and stable mangrove forests

The change rate of the cross-shore mangrove width compared to the coastline position change rate

In Figure B.41, the cross-shore width of the mangroves along the transects is compared to the rate of change of the coastline position. The scatterplot shows a wide distribution of points but tends to stabilize when the mangrove width becomes larger.

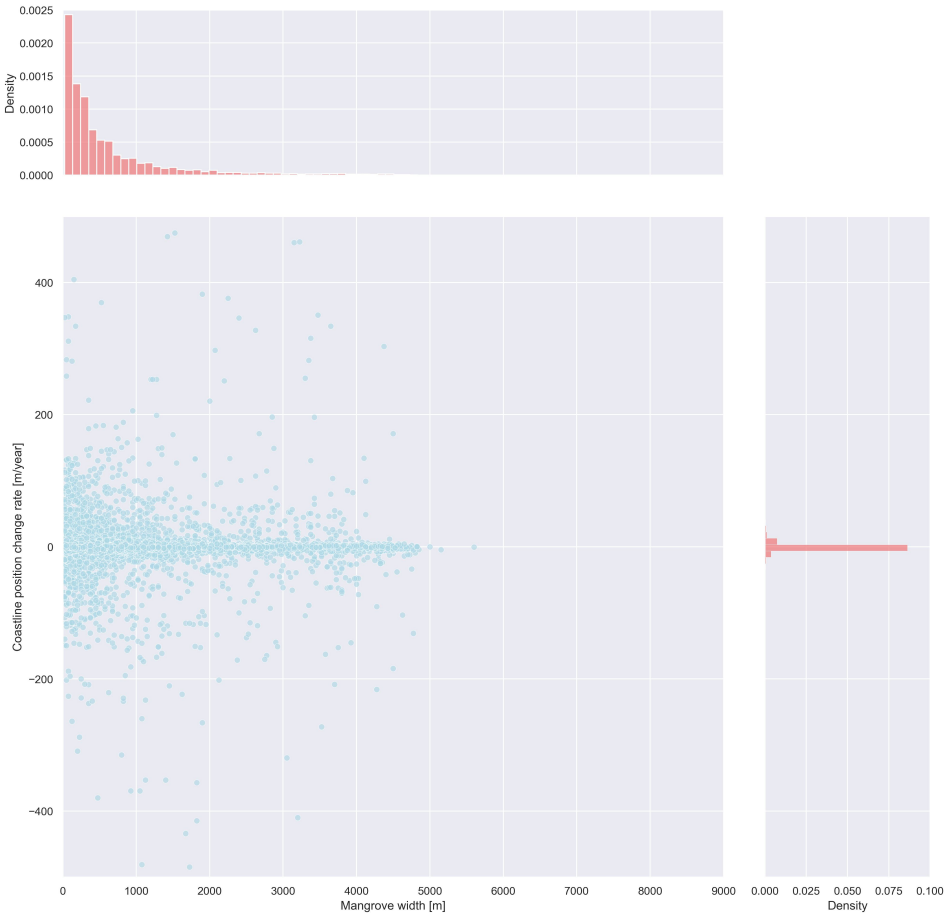

Figure B.41: Scatterplot cross-shore mangrove width versus the coastline position change rate

Figures B.42 and B.43 show the results of method 1. Scatterplots are used to compare the cross-shore mangrove width with the coastline position change rates for bin sizes 500 and 100, respectively. In both figures, it is noticeable that the difference between the 15th and 85th percentiles increases as the mangrove width increases. This suggests that erosion and accretion rates also increase with the size of the mangrove width. The behaviour of the 85th and 15th percentile lines can be observed on the right side of the Figure. The slope of these lines is calculated 1000 times by selecting 100 random values per bin. In the right graphs of Figure B.42, it can be seen that the 15th percentile line is negative, while the 85th percentile line is positive. Additionally, the median value of the 15th percentile line is double the negative value of the 85th percentile line. These findings suggest that the wider the mangrove width, the higher the accretion and erosion rates. Furthermore, the higher absolute value of the negative 15th percentile slope than the positive 85th percentile slope indicates that erosion rates are higher than accretion rates. In the right graphs of Figure B.43, similar trends to Figure B.42 can be observed. However, the absolute distribution of the 85th and 15th percentiles are similar. This indicates that while both lines increase or decrease, they do so at the same rate.

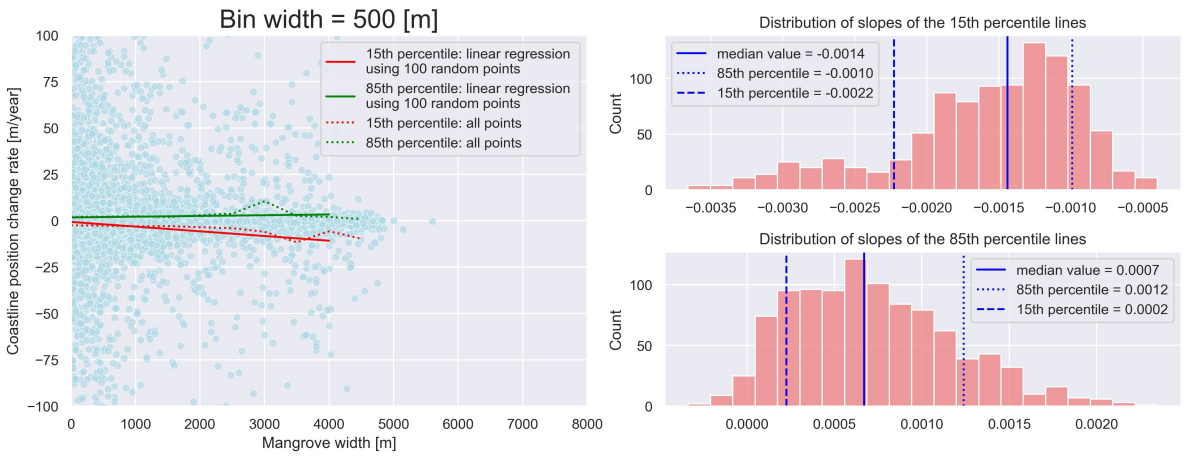

Figure B.42: Bin width of 500 [m]

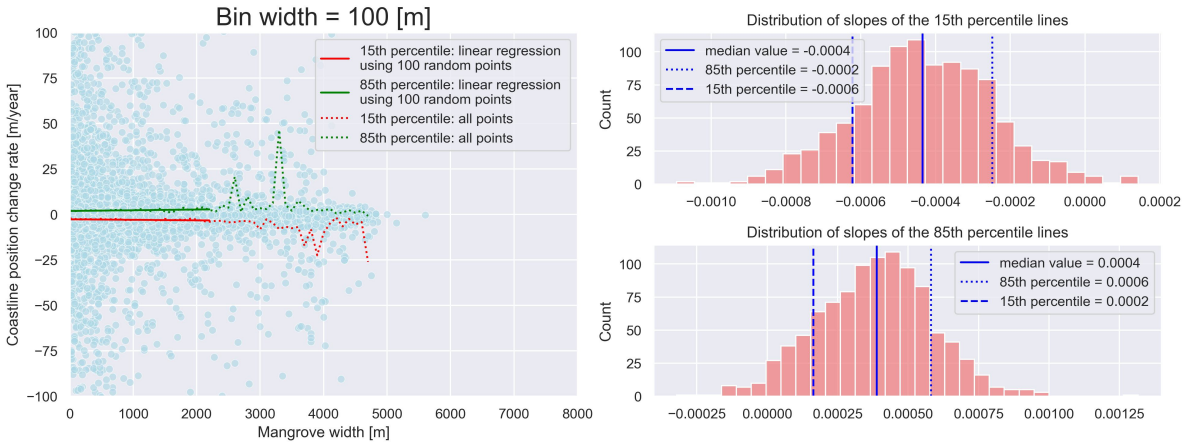

Figure B.43: Bin width of 100 [m]

In Figure B.44 the results of method 2 are depicted. An upward trend in the medians can be observed when examining the accreding change rates. This suggests a tendency for higher accretion rates with increasing mangrove width. Figure B.45 illustrates the eroding change rates; an opposite pattern to that observed in Figure B.44 is evident. Specifically, the linear regression line demonstrates a strong downward trend, indicating that as the mangrove width increases, there is a tendency for more erosion to occur.

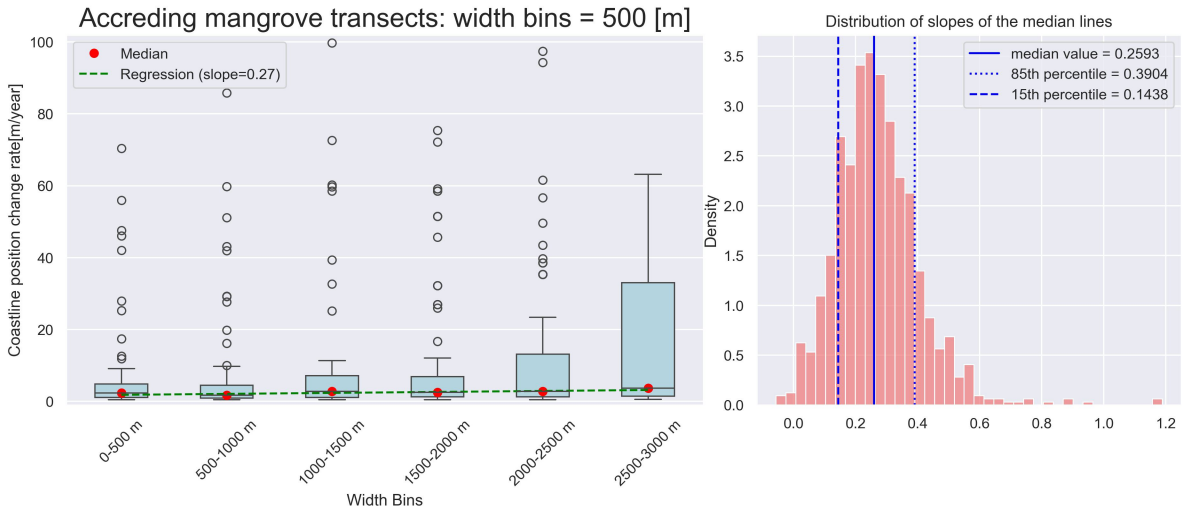

Figure B.44: Random sampling within accreding change rates (> 0.5 [m])

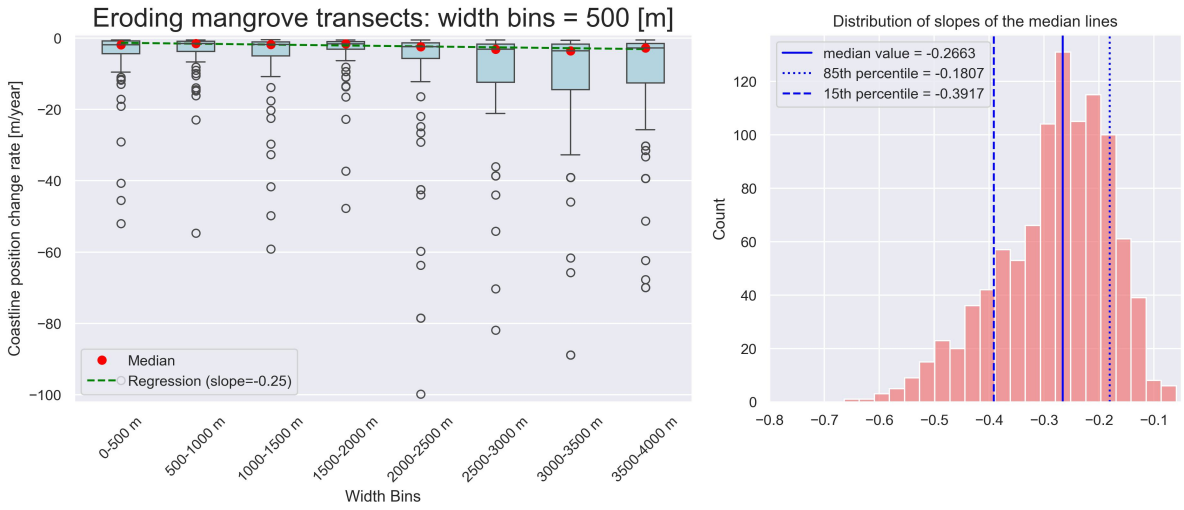

Figure B.45: Random sampling within eroding change rates (< -0.5 [m])

The change rate of the cross-shore mangrove width compared to the coastline position change rate

The histogram shown in Figure B.46 provides valuable insights into the relationship between the change rate of mangrove width and coastline position. The negative quadrant in the graph contains the highest number of transects, indicating the areas where mangrove width and coastline position are decreasing. This suggests a negative correlation between the mangrove width and the coastline position change rate in these areas. On the other hand, the right side of the figure shows more transects in the quadrant where both mangrove width and coastline position are increasing. This indicates that the coastline is more likely to develop if mangrove forests expand.

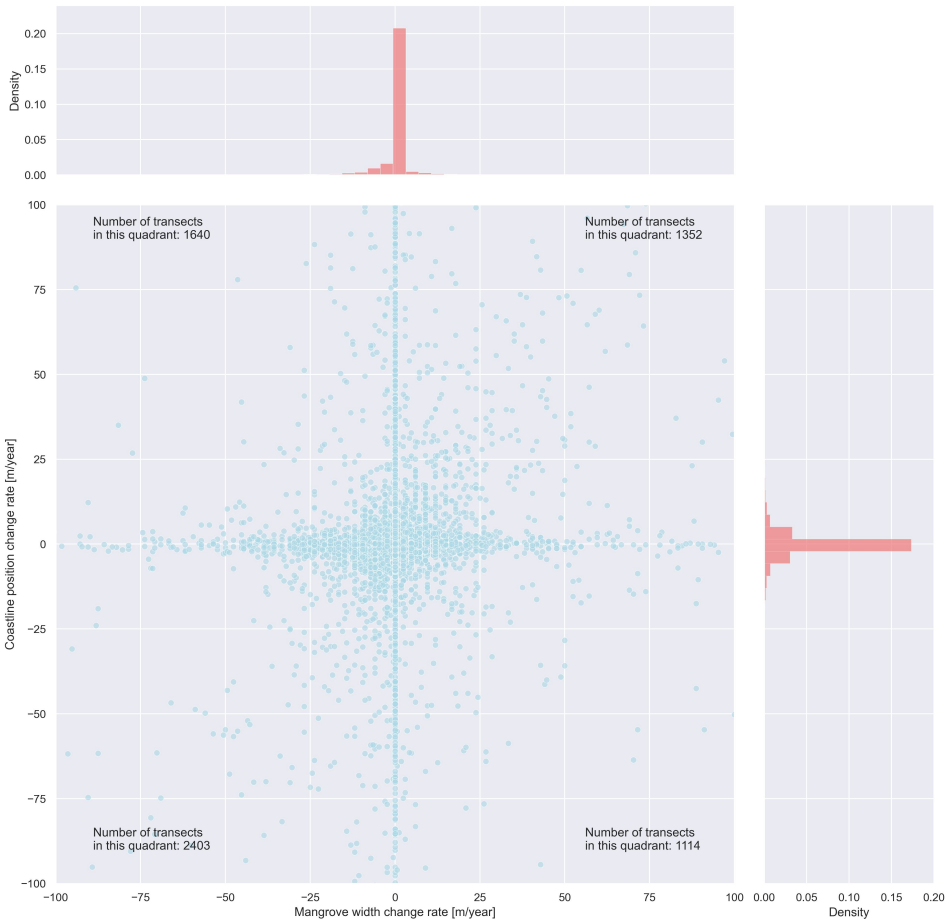

Figure B.46: Scatterplot of cross-shore mangrove width change rate versus the coastline position change rate

Figure B.47 shows the change rate of the coastline position for a constant mangrove width over time. The median of the data is observed to be slightly negative, indicating a slight tendency towards erosion. However, the median value remains within a stable range. Furthermore, the 15th percentile of the coastline position change rate is -2.38, while the 85th percentile is 1.96. This suggests that there is a small but notable risk of erosion.

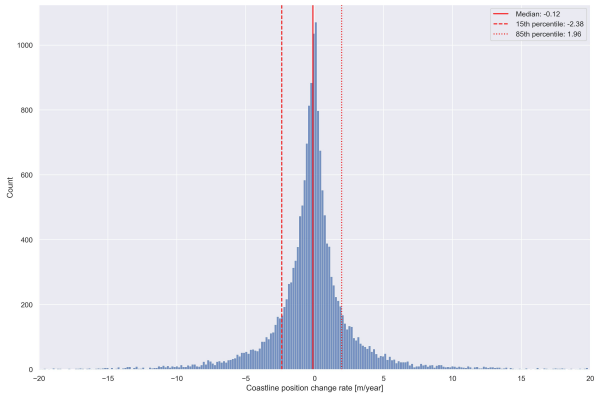

Figure B.47: Histogram coastline position change rate for a mangrove width change rate of 0

The analysis of the scatterplot shown in Figure B.31 is based on the distribution of coastline position change rates for accreding transects that have contracting, stable, and eroding mangrove forests. The figure is divided into three parts: the left graph represents the distribution of coastline change rates in the top left quadrant, the middle graph denotes the distribution of coastline position change rates on the positive y-axis, and the right graph displays the distribution of coastline position change rates in the top right quadrant. Upon observing the figure, it is evident that the distribution is quite similar for contracting and stable mangrove forests. Although the median value is slightly higher when a mangrove forest is stable, the difference is minimal. However, when the mangrove forest is expanding, the median is substantially higher than when it is contracting or stable. This suggests that when a mangrove forest increases, the coastline experiences higher accretion rates than when it is contracting or stable. Moreover, in expanding mangrove forests, the 85th percentile is considerably higher than for stable and contracting mangrove forests. This indicates that extreme accretion events are more prevalent in expanding mangrove forests than in stable and contracting mangrove forests.

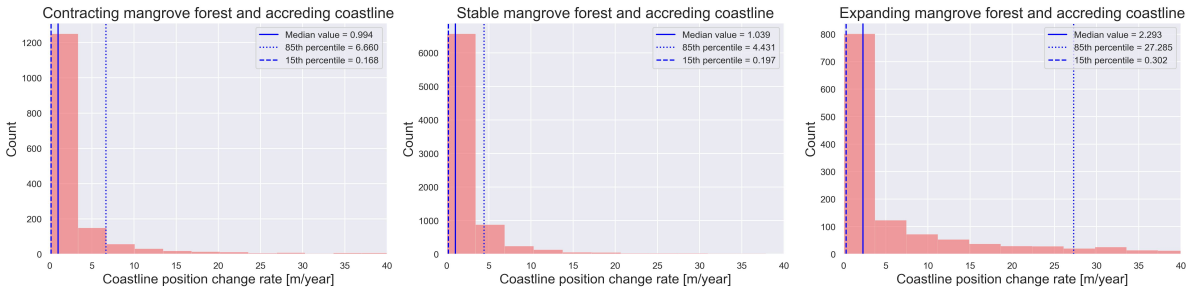

Figure B.48: The coastline position change rate distributions for accreding transects with contracting, stable and eroding mangrove forests, respectively

Figure B.49 illustrate the distribution of coastline position change rates in areas where mangrove forests are either stable, expanding, or contracting. The graph is divided into three sections, each representing a different quadrant. The left graph shows the distribution of coastline change rates in the bottom-left quadrant; the middle graph shows the distribution of coastline position change rates on the negative y-axis; and the right graph shows the distribution of coastline position change rates in the bottom-right quadrant. The median value of the coastline position change rates indicates that the erosion change rate is the least negative when a mangrove forest is stable. In contrast, the erosion change rate is the most negative when a mangrove forest is contracting. Furthermore, there is more significant variation in erosion rates when a mangrove forest expands or contracts than when it is stable, as indicated by the 15th percentile. This suggests that a stable mangrove forest results in lower erosion rates than when a forest expands or contracts. Additionally, less extreme erosion rates occur when a mangrove forest is stable than when it is expanding or contracting. Transects with stable mangrove forests and an eroding and accreding coastline exhibit minor variability in their coastline position change rates.

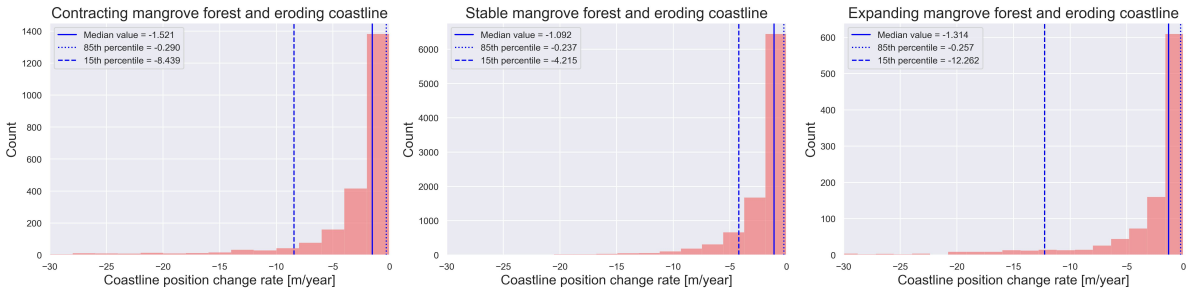

Figure B.49: The coastline position change rate distributions for eroding transects with contracting, stable and eroding mangrove forests, respectively

It was observed in the previous findings that there is a significant difference in the sample sizes of expanding, stable, and contracting transects. Specifically, there are 8200 transects with an accreding coastline and stable mangrove forests, 1640 transects with an accreding coastline and contracting mangrove forest, and 1352 transects with an accreding coastline and expanding mangrove forest. Similarly, there are 9793 transects with an eroding coastline and stable mangrove forests, 2403 transects with an eroding coastline and contracting mangrove forest, and 1114 transects with an eroding coastline and expanding mangrove forest. It should be noted that for transects with both eroding and accreding coastlines, there are the least number of expanding mangrove forests. The following approach was used to investigate whether the difference in sample size affects the results. Data points for transects with an accreding coastline were randomly selected for transects with both contracting and stable mangrove forests. The number of selected points matched the count of mangrove transects with expanding mangrove forests. Specifically, 2089 transects with stable and contracting mangrove forests were randomly selected. This process was repeated 1000 times, and the median of the randomly selected data points was recorded each time. The results of this process can be seen in Figure B.50. The red line on the figure indicates the median value of transects with an expanding mangrove forest. Similarly, this process was repeated for transects with an eroding coastline. However, 1992 transects with stable and contracting mangrove forests were randomly selected. The results of this process can be seen in Figure B.51.

The graph displayed in Figure B.50 indicates that the median value for expanding mangrove forests is considerably greater than that of stable and contracting mangrove forests. The results for stable and contracting mangrove forests are pretty similar. The findings suggest that the variation in sample size does not affect the conclusions.

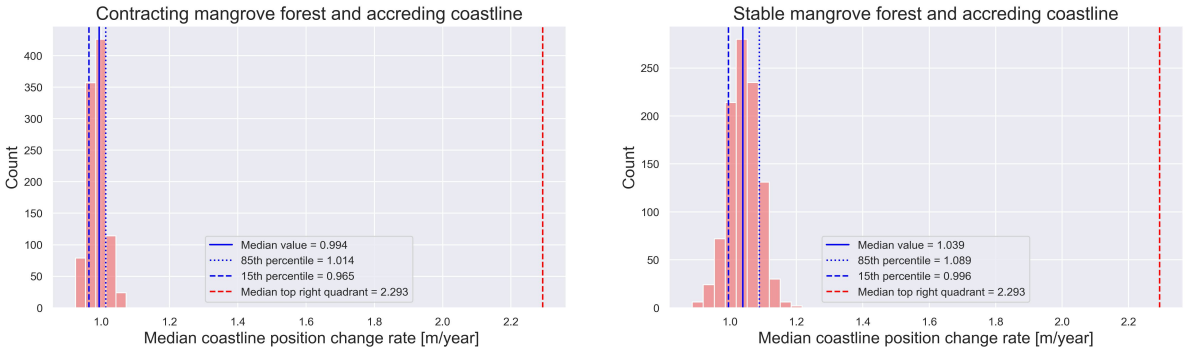

Figure B.50: The median coastline position change rates for accreding transects with contracting and stable forests, respectively, using random sampling

In Figure B.51, the median for stable mangrove forests is higher than for expanding and contracting mangrove forests. The difference in sample size does not affect the results.

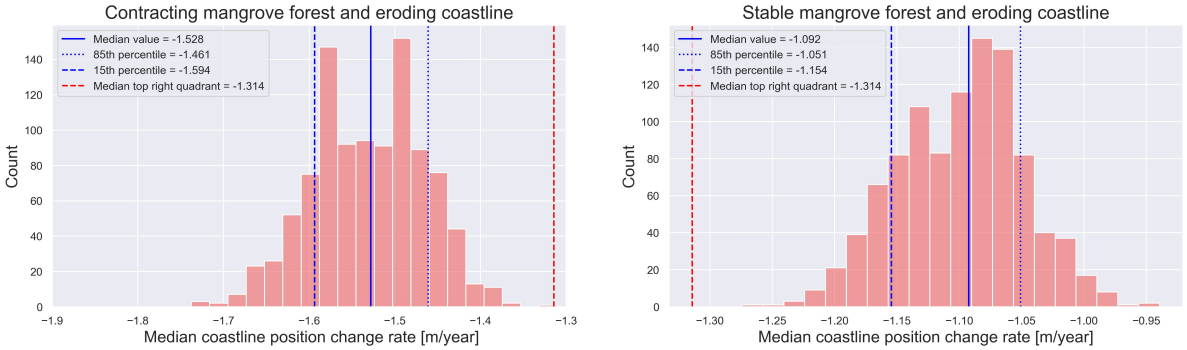

Figure B.51: The median coastline position change rates for eroding transects with contracting and stable forests, respectively, using random sampling

B.4. Framework 4

Coastline position change rates

Figure B.52 shows the distribution of the coastline position change rate in a histogram. The median change rate for mangrove transects is -0.141, while for non-mangrove transects, it is -0.086. Both medians fall within the stable range, but the median mangrove value is more negative than the median non-mangrove value. This suggests that mangrove transects are more prone to experience accretion at higher ranges. On the other hand, the median change rate of eroding transects is higher for non-mangrove transects. Since the median change rate is lower for mangrove transects than for non-mangrove transects, it indicates that mangrove transects are more prone to erode at higher ranges.

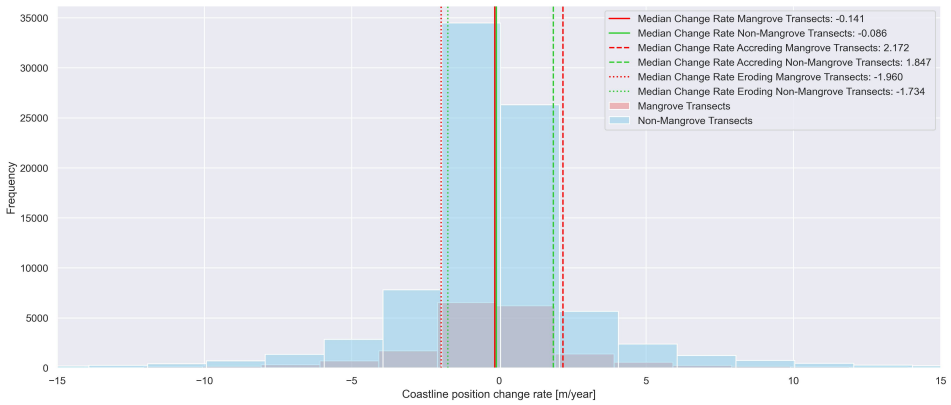

Figure B.52: Coastline position change rate for mangrove and non-mangrove transects

In Figure B.53, multiple boxplots are shown presenting the coastline position change rates for mangrove and non-mangrove transects. These transects are categorized into four groups, namely: all eroding transects (change rate below -0.5), all accreding transects (change rate above 0.5), all transects with a negative change rate, and all transects with a positive change rate. It can be observed that when considering all positive values, mangrove transects tend to accrete more than non-mangrove transects. However, when we examine all negative values, mangrove transects erode more than non-mangrove transects. Moreover, mangrove transects exhibit higher standard deviations than non-mangrove transects, indicating greater variability overall. Additionally, the interquartile range is slightly higher for mangrove transects than for non-mangroves, suggesting a wider spread of data points around the median for mangroves. Although there are some differences in standard deviations and interquartile ranges, they are minimal.

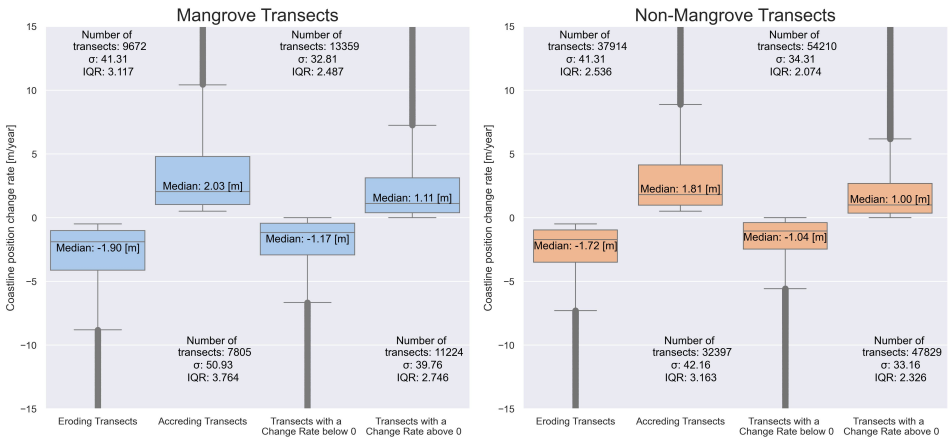

Figure B.53: Coastline position change rate for mangrove and non-mangrove transects

There is a significant imbalance between the number of non-mangrove transects and mangrove transects in frameworks 1, 2, and 3. There are almost four and a half times more non-mangrove transects than mangrove transects. To address this imbalance, random data points will be selected from both accreding and eroding non-mangrove categories, matching the count of mangrove transects within their respective accreding and eroding categories. Specifically, 9672 eroding non-mangrove transects and 7805 accreding non-mangrove transects will be chosen randomly. This process will be repeated 1000 times, and the median and standard deviation of the set will be stored in each iteration. Figures B.54 and B.55 illustrate the distribution of medians and standard deviations of those 1000 runs for eroding and accreding transects, respectively. From Figure B.54a, it is evident that mangrove transects experience more erosion than non-mangrove transects. Across the performed runs, the calculated medians for eroding non-mangrove transects do not approach the median value of mangrove transects. Looking at Figure B.54b, it is clear that the standard deviation for both mangrove and non-mangrove transects is comparable.

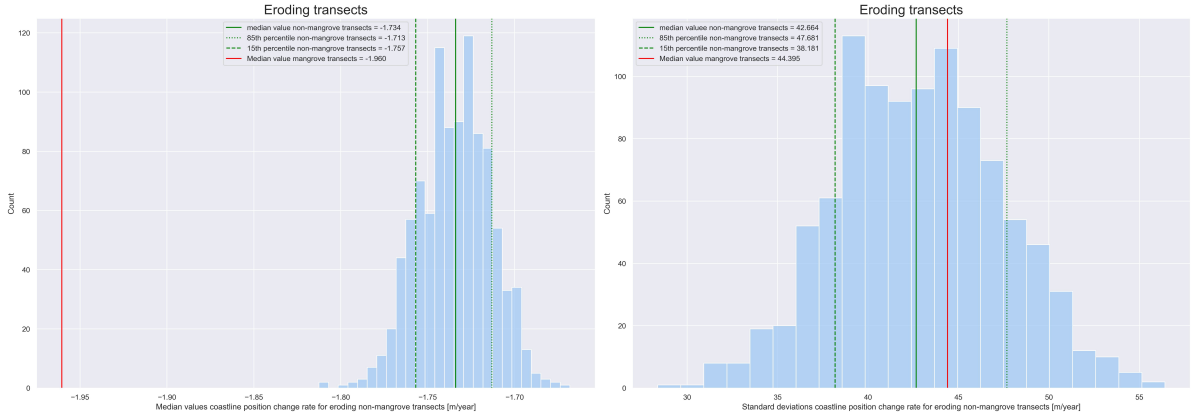

(a) Distribution of medians

(b) Distribution of standard deviations

Figure B.54: Eroding non-mangrove transects

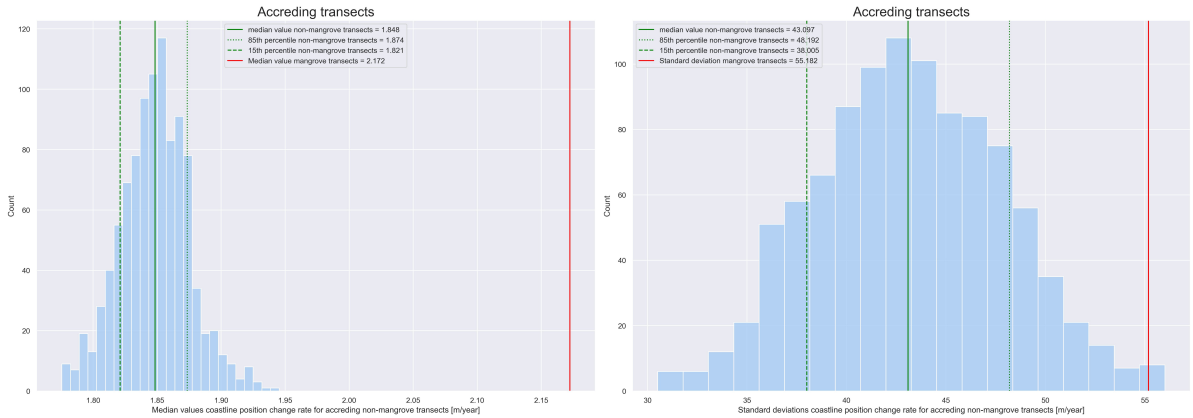

(a) Distribution of medians

(b) Distribution of standard deviations

Figure B.55: Accreding non-mangrove transects

The pie charts shown in Figure B.56 display the distribution of mangrove and non-mangrove transects. The mangrove transects are categorized as accreding, eroding, and stable. There are a total of 20032 mangrove transects and 89033 non-mangrove transects. The non-mangrove transects have a higher proportion of stable transects than the mangrove ones. Additionally, the number of eroding mangrove transects is higher than that of eroding non-mangrove transects.

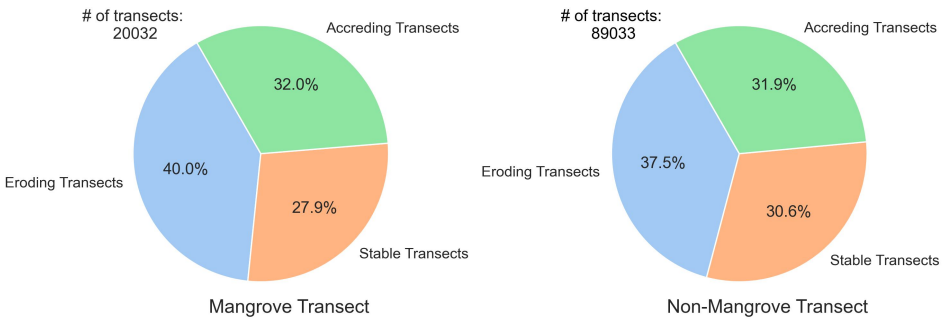

Figure B.56: The coastal state distribution for mangrove and non-mangrove transects

Mangrove cross-shore width

Figure B.57 displays the distribution of contracting, expanding, and stable mangrove forests for non-complex and open coast transects. Approximately 75% of the total transects are stable.

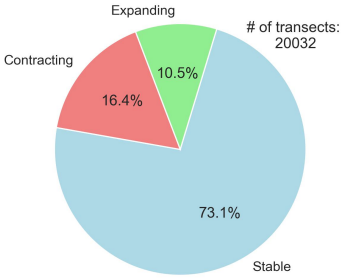

Figure B.57: The distribution of contracting, expanding and stable mangrove forests

The change rate of the cross-shore mangrove width compared to the coastline position change rate

Figure B.58 displays the relationship between the width of the mangrove forest and the rate of change in the coastline position. The scatterplot reveals a wide distribution of points, with fewer outliers as the cross-shore mangrove width increases.

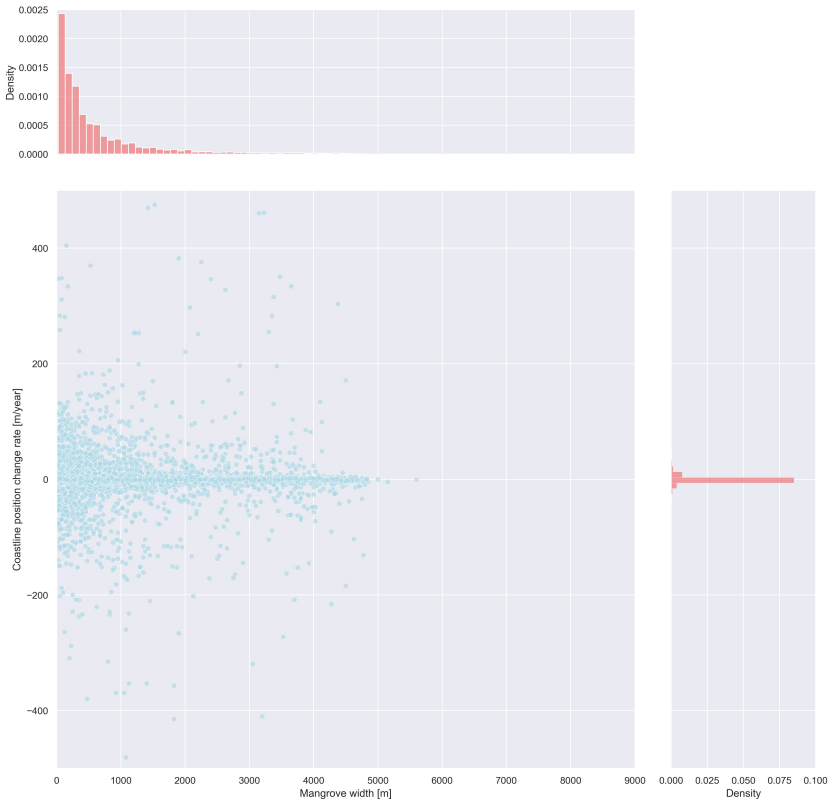

Figure B.58: Scatterplot of cross-shore mangrove width versus the coastline position change rate

In Figure B.59 and B.60, the results of method 1 for framework four are presented. The analysis indicates for both Figures that the slope of the 15th percentile is consistently negative, while the 85th percentile is consistently positive. This suggests that the lines across the 1000 runs always diverge. Furthermore, the 15th percentile is generally slightly more negative than the 85th percentile, which indicates that for higher mangrove widths, the change rate has a higher probability of being more negative than positive. Furthermore, for higher widths, the variability is thus higher.

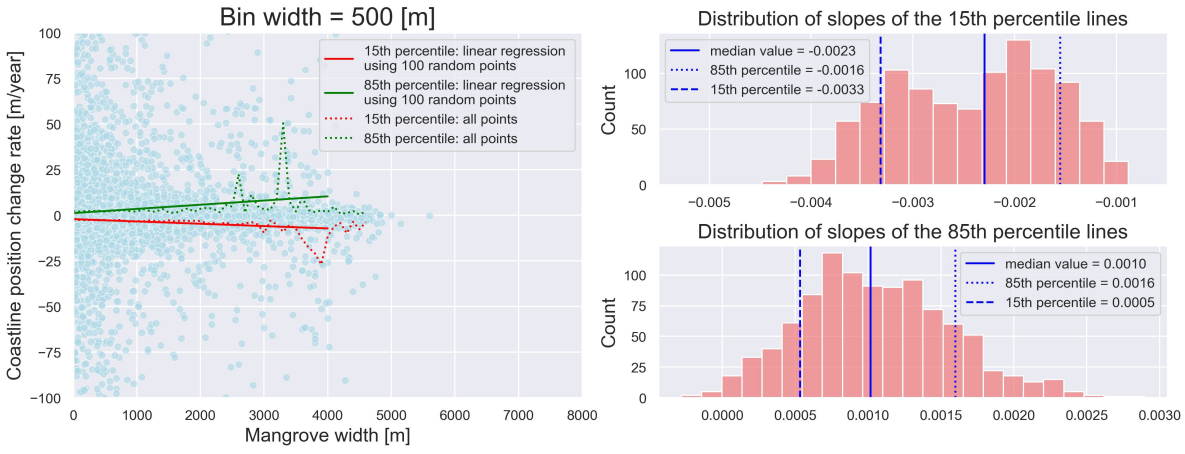

Figure B.59: Bin width of 500 [m]

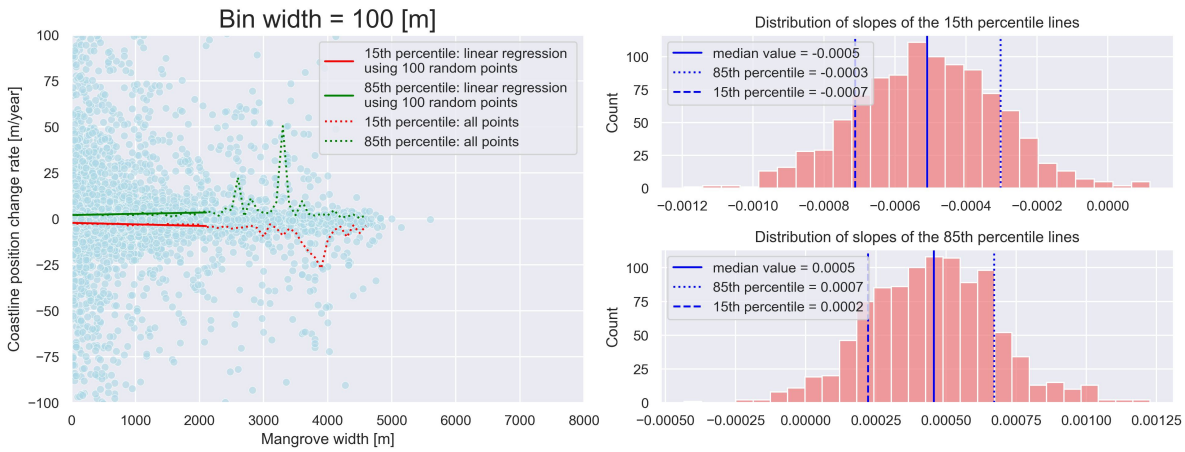

Figure B.60: Bin width of 100 [m]

In Figures B.61 and B.62 the results of method 2 are depicted. An upward trend in the medians can be observed when examining the accreding change rates, represented by Figure B.61. This suggests a tendency for higher accretion rates with increasing mangrove width. In Figure B.62, which illustrates the eroding change rates, an opposite pattern is evident to that observed in Figure B.61. Specifically, the linear regression line demonstrates a strong downward trend, indicating that as the mangrove width increases, there is a tendency for more erosion to occur.

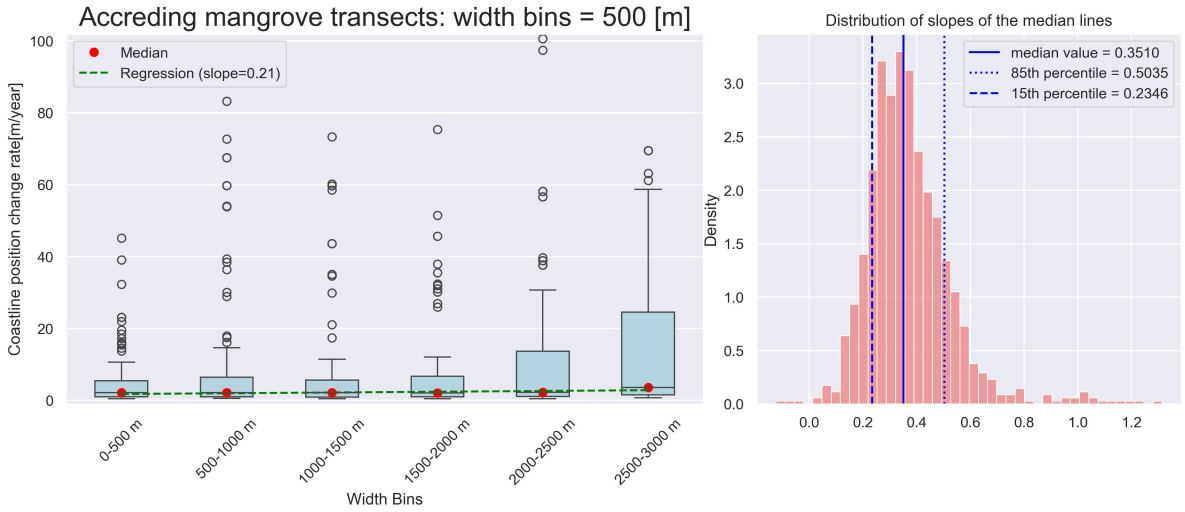

Figure B.61: Random sampling within accreding change rates (> 0.5 [m])

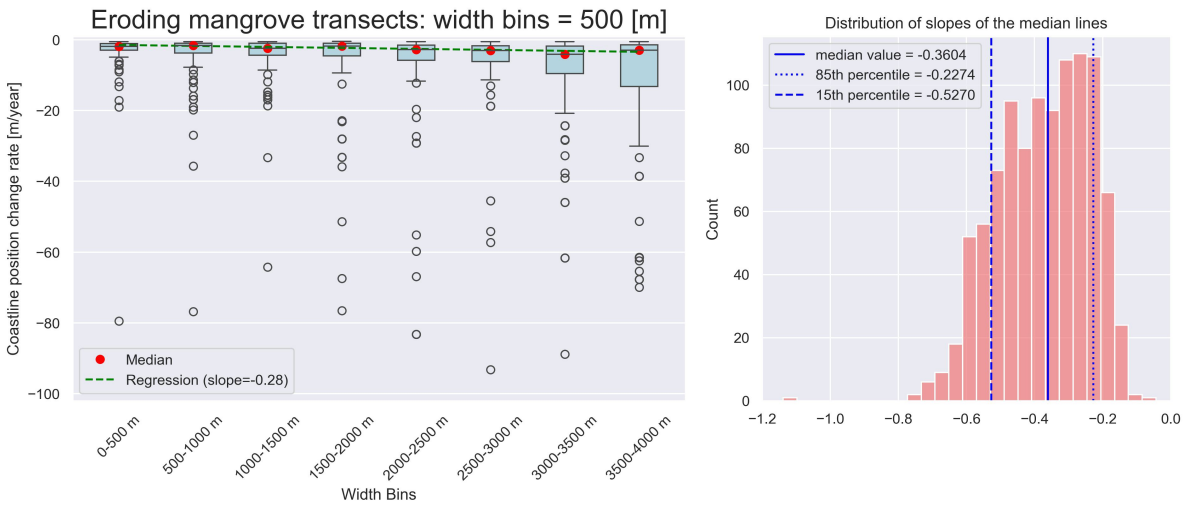

Figure B.62: Random sampling within eroding change rates (< -0.5 [m])

The change rate of the cross-shore mangrove width compared to the coastline position change rate

The scatterplot in Figure B.63 shows how the change rate of mangrove width is related to the change rate of coastline position. The scatterplot is divided into four quadrants, with most transects in the bottom left quadrant. On the right side of the plot, where the mangrove width is expanding, the upper quadrant has the most transects. This indicates that mangrove forests and coastlines tend to expand simultaneously. In other words, the coastline also expands if a mangrove forest increases.

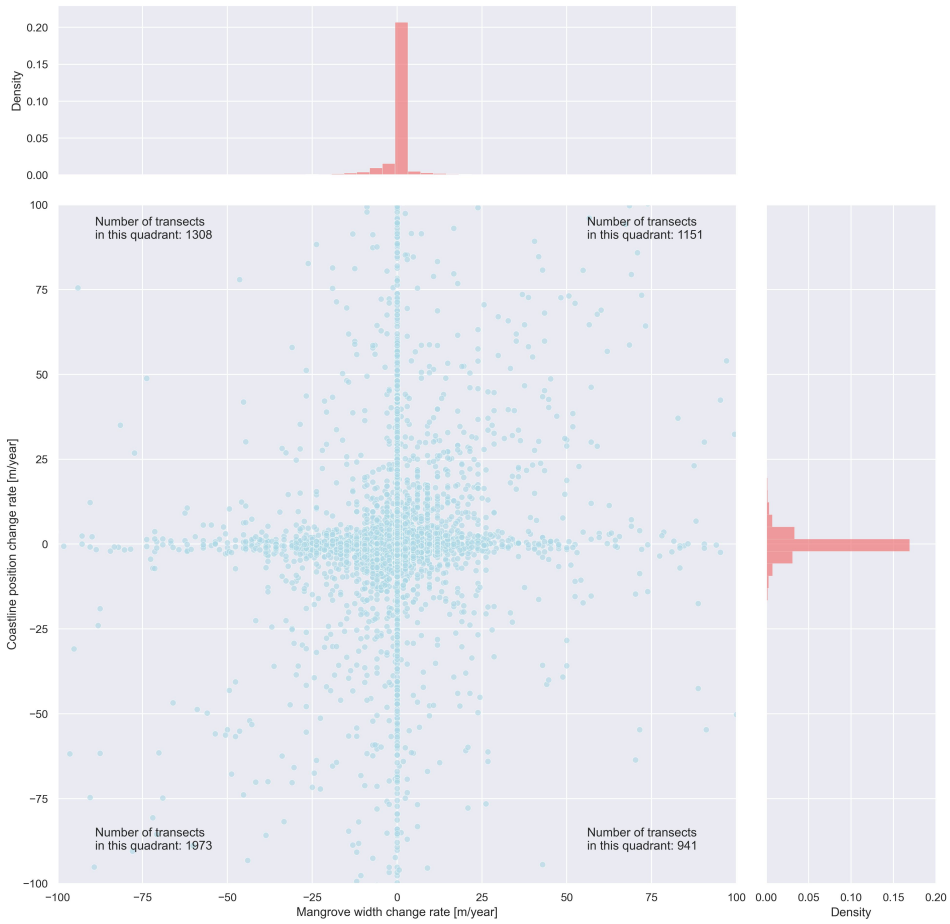

Figure B.63: Scatterplot cross-shore mangrove width change rate versus the coastline position change rate with bin width 50

In Figure B.64, a histogram is displayed, which shows the distribution of the change rate of coastline position per year. The histogram shows that most data points are clustered around zero, indicating that there is only a small noticeable change in the coastline position over time for many observations. This implies that the coastline is relatively stable for these observations. The median change rate is slightly negative, suggesting that, on average, the coastline is receding with a small amount each year, but it still falls within the stable region. The 15th and 85th percentiles are -2.47 m/year and 2.05 m/year, respectively, indicating that the coastline is more likely to erode if the mangrove width remains constant.

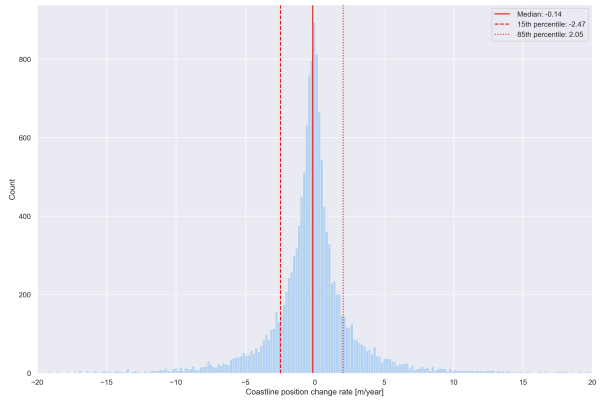

Figure B.64: Histogram coastline position change rate for a mangrove width change rate of 0

In Figure B.65, the scatterplot is analyzed in more detail by showing the distribution of coastline position change rates for accreding transects with contracting, stable, and eroding mangrove forest. The Figure is divided into three parts: where the left graph shows the distribution of coastline change rates in the top left quadrant; the middle graph shows the distribution of coastline position change rates on the positive y-axis, and the right graph shows the distribution of coastline position change rates in the top right quadrant. When observing the Figure, it can be seen that the distribution is quite similar for contracting and stable mangrove forests. The median value is slightly higher when a mangrove forest is stable, but the difference is minimal. When the mangrove forest is expanding, it can be seen that the median is significantly higher than when it is contracting or stable. This indicates that when a mangrove forest is expanding, the coastline experiences higher accretion rates than when it is contracting or stable. Furthermore, in expanding mangrove forests, the 85th percentile is considerably higher for expanding mangrove forests than for stable mangrove forests. This suggests that extreme accretion events are more prevalent in expanding mangrove forests than in stable mangrove forests. However, the 85th percentile is considerably higher for contracting mangrove forests than for stable mangrove forests, indicating that extreme accretion is also more prevalent in contracting mangrove forests than expanding mangrove forests. This shows that when the mangrove forest is stable, a more uniform pattern exists in coastline position change rates than when the mangrove forest is expanding or contracting.

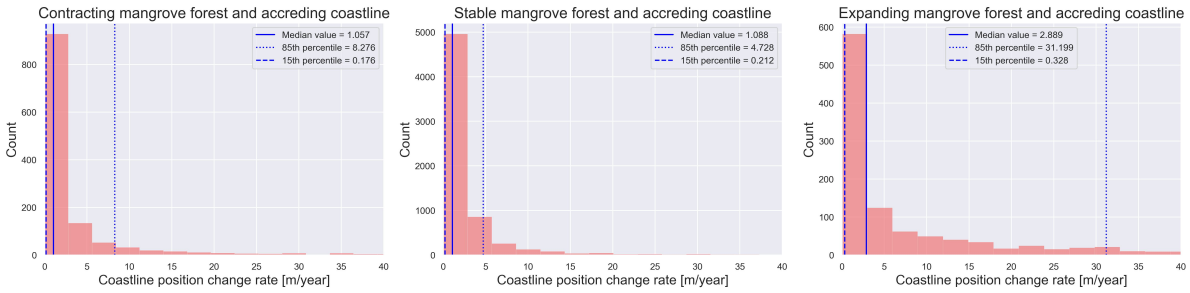

Figure B.65: The coastline position change rate distribution for accreding transects with contracting, stable and eroding mangrove forests

In Figure B.66, the distribution of coastline position change rates is shown for eroding transects with contracting, stable, and expanding mangrove forests. The left graph displays the distribution of coastline change rates in the bottom-left quadrant; the middle graph shows the distribution of coastline position change rates on the negative y-axis, and the right graph shows the distribution of coastline position change rates in the bottom-right quadrant. Examining the median value shows that when a mangrove forest is stable, the median erosion change rate is the least negative. On the other hand, when a mangrove forest is contracting, the median erosion change rate is the most negative. Additionally, more variation exists when a mangrove forest expands or contracts when considering the 15th percentile. This suggests that a stable mangrove forest results in lower erosion rates than when a forest expands or contracts. Moreover, less extreme erosion rates occur when a mangrove forest is stable than when it is expanding or contracting.

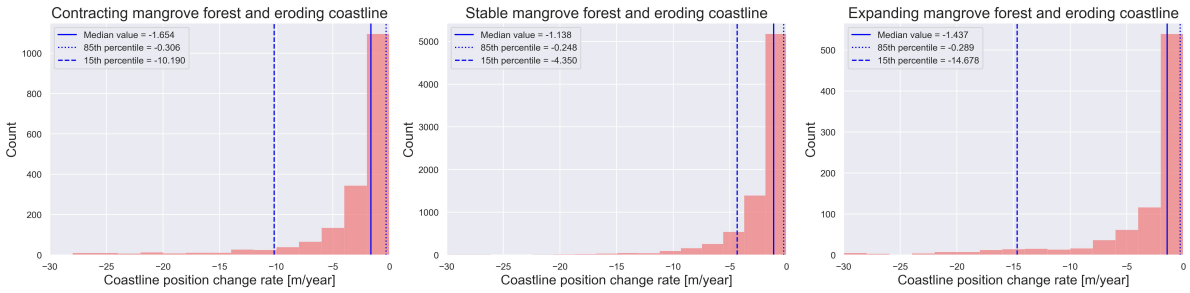

Figure B.66: The coastline position change rate distribution for eroding transects with contracting, stable and eroding mangrove forests

It was observed in the previous findings that there is a significant difference in the sample sizes of expanding, stable, and contracting transects. Specifically, there are 6610 transects with an accreding coastline and stable mangrove forests, 1308 transects with an accreding coastline and contracting mangrove forest, and 1151 transects with an accreding coastline and expanding mangrove forest. Similarly, there are 7974 transects with an eroding coastline and stable mangrove forests, 1973 transects with an eroding coastline and contracting mangrove forest, and 941 transects with an eroding coastline and expanding mangrove forest. It should be noted that for transects with both eroding and accreding coastlines, there are the least number of expanding mangrove forests. The following approach was used to investigate whether the difference in sample size affects the results. Data points for transects with an accreding coastline were randomly selected for transects with both contracting and stable mangrove forests. The number of selected points matched the count of mangrove transects with expanding mangrove forests. Specifically, 2089 transects with stable and contracting mangrove forests were chosen randomly. This process was repeated 1000 times, and the median of the randomly selected data points was recorded each time. The results of this process can be seen in Figure B.67. The red line on the figure indicates the median value of transects with an expanding mangrove forest. Similarly, this process was repeated for transects with an eroding coastline. However, 1992 transects with stable and contracting mangrove forests were randomly selected. The results of this process can be seen in Figure B.68.

The graph displayed in Figure B.67 indicates that the median value for expanding mangrove forests is considerably greater than that of stable and contracting mangrove forests. The results for stable and contracting mangrove forests are pretty similar. The findings suggest that the variation in sample size does not affect the conclusions.

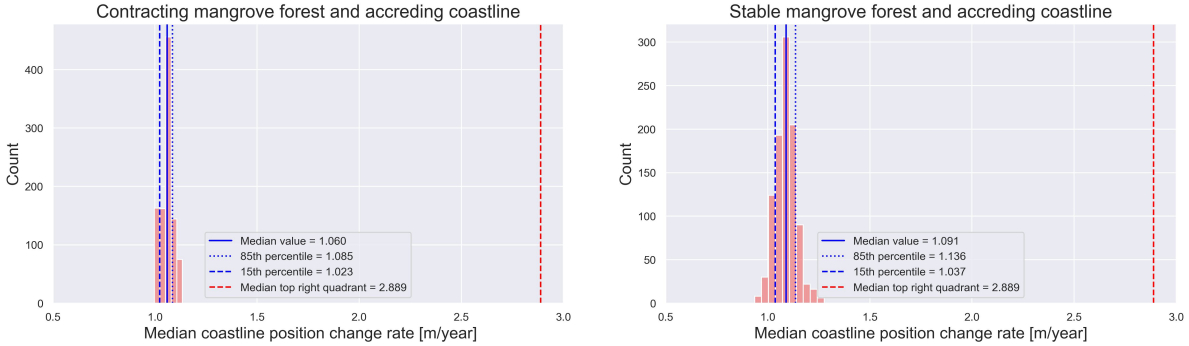

Figure B.67: The median coastline position change rates for accreding transects with contracting and stable forests, respectively, using random sampling

In Figure B.68, the median for stable mangrove forests is higher than for expanding and contracting mangrove forests. The difference in sample size does not affect the results.

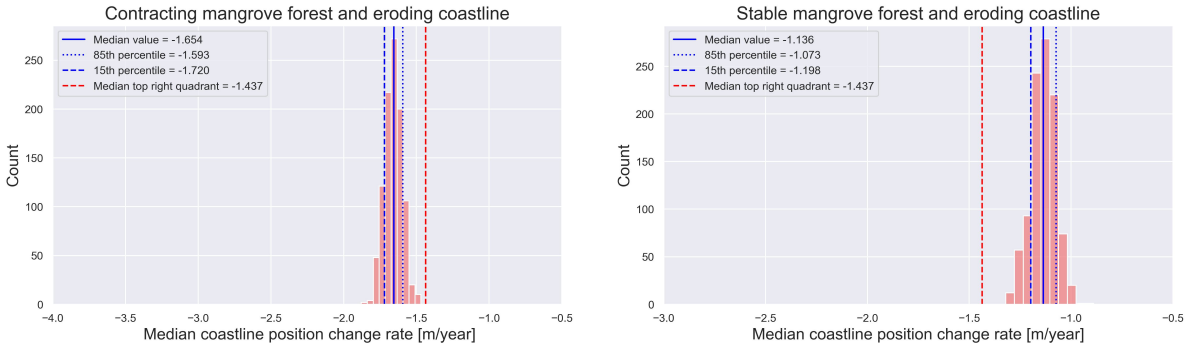

Figure B.68: The median coastline position change rates for eroding transects with contracting and stable forests, respectively, using random sampling

B.5. Comparing the frameworks

When comparing frameworks 1, 2, 3, and 4, many similarities emerge from the analysis. All similarities and differences will be discussed below.

Examining the distribution of coastline position change rates across the frameworks reveals a consistent pattern. Mangrove transects exhibit a greater tendency to erode in all frameworks than non-mangrove transects. Additionally, mangrove transects tend to accrede more than non-mangrove transects across all frameworks. However, the magnitude of these trends varies among the framework. Framework 1 shows minimal distinction between the medians of mangrove and non-mangrove transects, with the trends present but not as pronounced. In contrast, framework 2 exhibits the most significant eroding trend among mangrove transects, indicating a substantial erosion rate compared to non-mangrove transects. Conversely, framework 4 demonstrates the most prominent accreding trend, where mangrove transects exhibit much stronger accretion than non-mangrove transects. These discrepancies could be explained by examining the distribution of coastal states within each framework. For instance, framework 2 displays the highest proportion of eroding mangrove transects, with 40.8% eroding compared to 37.8% of non-mangrove transects. The probability for extreme eroding transects is thus higher. Conversely, framework 1 shows slightly different eroding percentages between mangrove (37.8%) and non-mangrove (37.5%) transects. The exclusion of complex transects alters the distribution, potentially contributing to a lower median change rate. Furthermore, frameworks 3 and 4 exhibit a slight reduction in the prevalence of eroding mangrove transects compared to framework 2, which could, in turn, explain the less extreme median values observed. Frameworks 2, 3, and 4 notably demonstrate higher standard deviations and interquartile ranges than framework 1. This discrepancy suggests greater variability in the data, particularly in mangrove transects, across these frameworks. The substantial difference between frameworks 1 and 4 in standard deviation and interquartile range can be attributed to the transect disparity. The smaller dataset in framework 4 may lead to less effective smoothing of extreme values.

Examining the distribution of mangrove cross-shore widths reveals varying patterns across the framework. Framework 1 includes the highest proportion of expanding mangrove forests, while Framework 4 demonstrates the most expansive forests. The percentage of transects with stable mangrove forests is relatively consistent across all frameworks.

Analyzing the relationship between cross-shore width and coastline position change rate reveals an interesting trend. Across all frameworks, a tendency emerges for values to cluster around the horizontal axis for higher widths, particularly above 4000 meters. However, this pattern is more pronounced in Framework 1 and less so in Framework 4. However, the opposite is found true when analysing the trend more thoroughly. For higher mangrove widths, it is found that there is substantially more variation in the dataset. More accretion takes place for higher mangrove widths; however, more erosion also occurs. However, the trend towards erosion is more pronounced, indicating that for higher mangrove widths, larger erosion rates occur than accretion rates.

When comparing the change rates of the cross-shore widths of mangroves with the change rates of the coastline positions, similar trends across all frameworks are found. Most data points for all frameworks are clustered in the bottom left quadrant. This clustering signifies that as mangrove forests degrade, there is a corresponding likelihood of coastal erosion. However, in frameworks 3 and 4, an additional trend becomes apparent. When examining the quadrant representing expanding mangrove forests (right side), a notable concentration of data points appears in the upper right quadrant. This clustering suggests that as mangrove forests expand, there is a tendency for the coastline position to develop as well. In frameworks 1 and 2, a similar amount of data points are found in the upper right and lower right quadrants.

Furthermore, consistent trends are observed across all frameworks when assessing the change rates of coastline positions where mangrove forests remain stable. Here, the median values fall within a stable range. However, the 15th and 85th percentiles indicate a slight preference towards erosion. This suggests that the coastline is more likely to erode even in scenarios where mangrove forests are stable.

Finally, across all frameworks, it was found that when a coastline is accreding, an expanding mangrove forest causes the most considerable accretion rates compared to stable and contracting mangrove forests. A contracting mangrove forest causes the lowest accretion rates. Transects with an accreding coastline and expanding mangrove forests experience more extreme accretion rates than transects with stable and contracting mangrove forests. The variability in accretion rates is the lowest for transects with a stable mangrove forest. When considering all transects with eroding coastlines, it was found that transects with stable mangrove forests cause the smallest erosion rates. Transects with contracting mangrove forests cause the most significant erosion rates. Both transects with contracting and expanding mangrove forests experience extreme erosion rates. The variability in erosion rates is the lowest for transects with a stable mangrove forest.

C

Case studies

In this appendix, more background information is given about the case studies handled in Chapter 4.

C.1. Case study 1

The area considered in case study 1 includes mostly transects that contain stable mangrove forests but have eroding coastlines. In Figures C.1a and C.1b the distribution of the transects within the coastline and mangrove categories is given. As can be seen in Figure C.1a, most transects contain a stable mangrove forest (74.4%). Furthermore, in Figure C.1b the coastline erodes in most transects (93%).

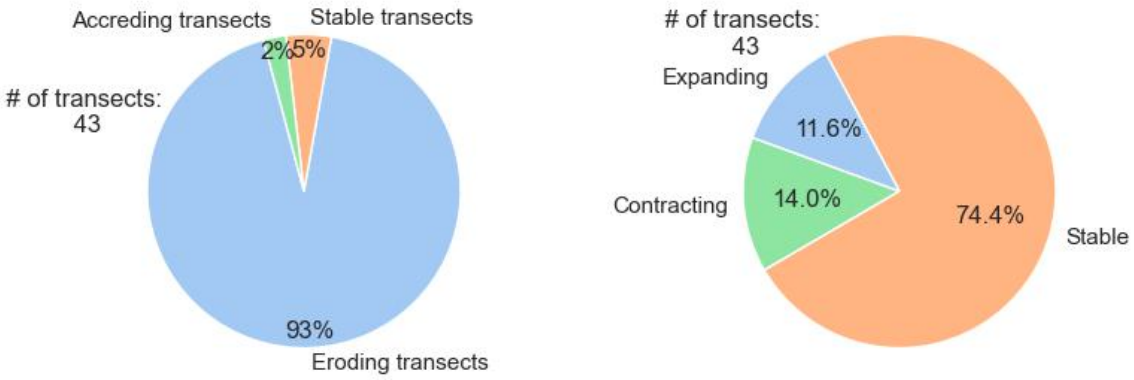

(a) Distribution of coastal states

(b) Distribution of mangrove forest categories

Figure C.1: Distribution of coastal states and mangrove forest categories

In Figure C.2, a scatterplot can be seen where the distribution of mangrove change rates (x-axis) is plotted against the distribution of coastline position change rates. As can be seen in this figure most coastline position change rates are situated between 0 and -7 [m/yr]. There is an outlier situated at around -16 [m/yr]. This indicates the coastline is heavily eroding, but not at extreme rates.

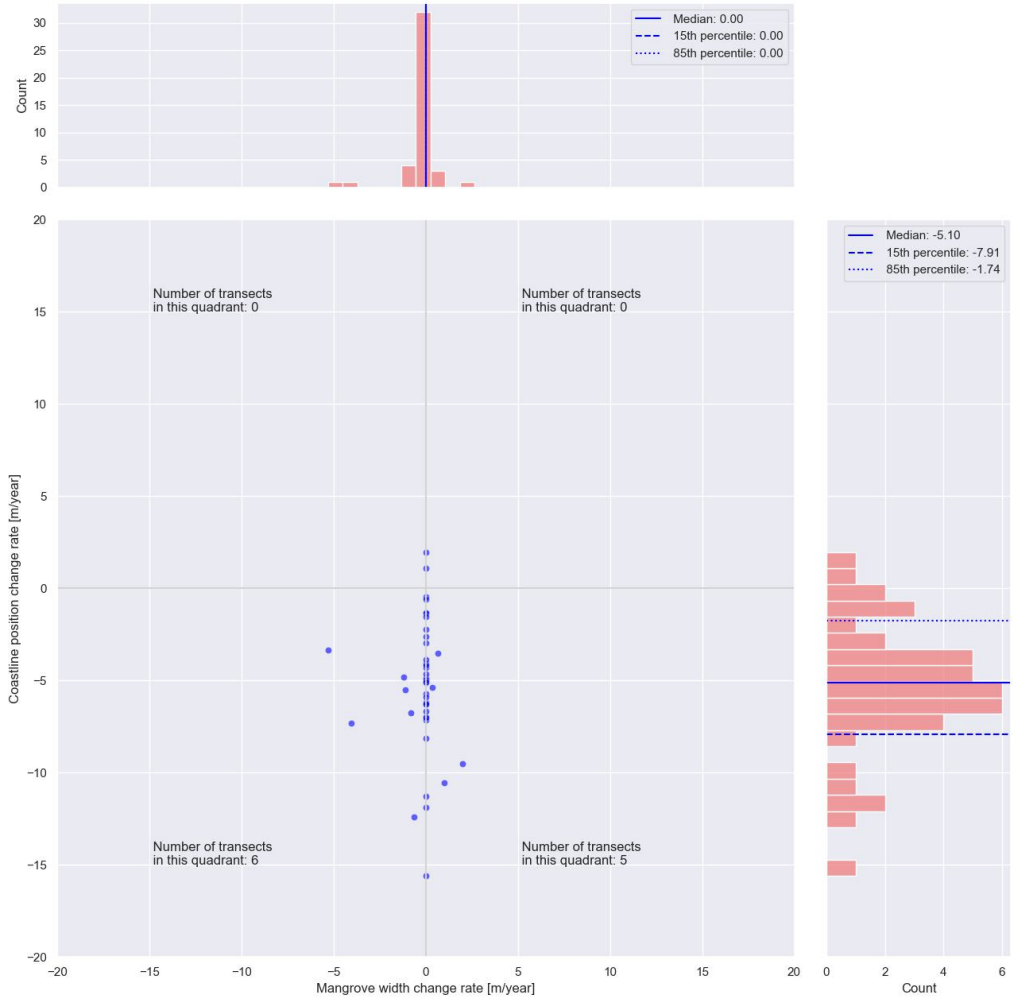

Figure C.2: The distribution of mangrove change rates plotted against the distribution of coastline position change rates

In Figure C.3 the cross-shore mangrove widths in 2010 are plotted against the coastline position change rates. In this Figure it can be seen that most widths are below 500 [m], however the mangrove forest situated in this area can reach a width of more than 2500 [m].

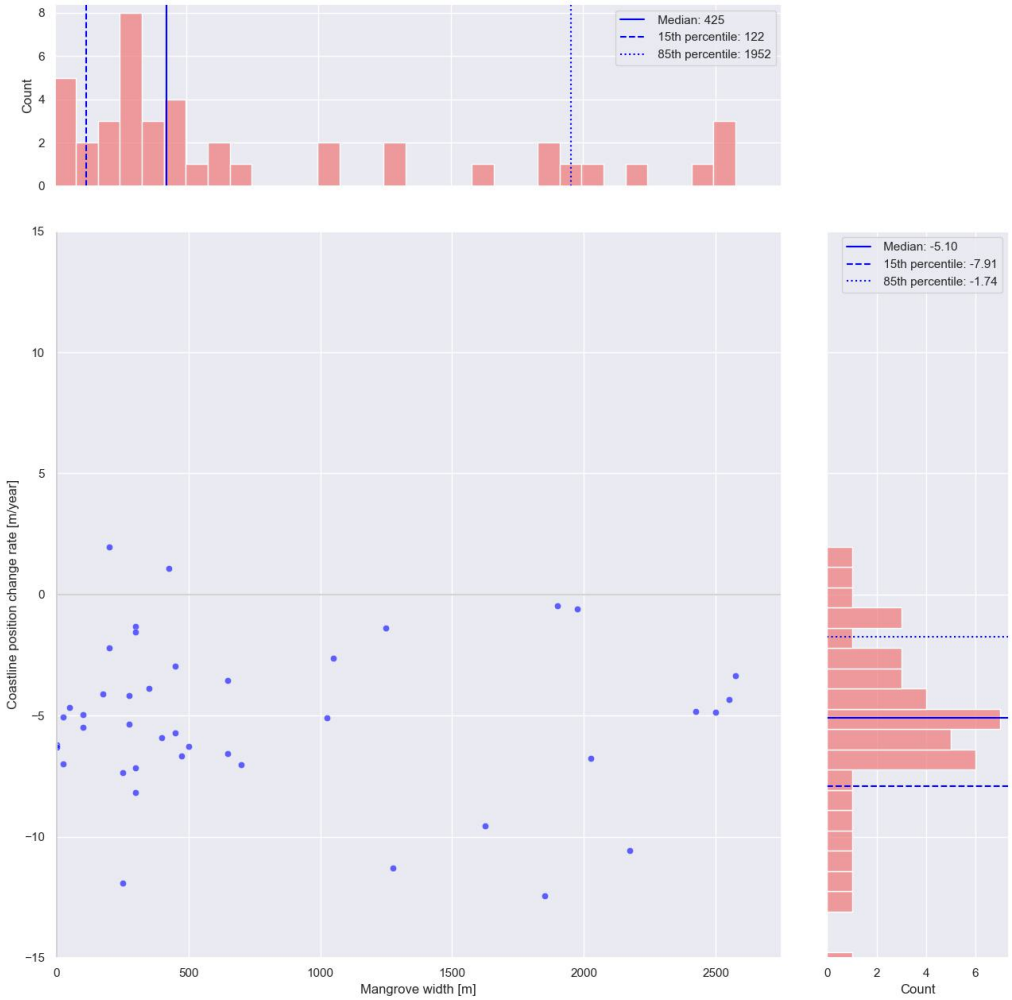

Figure C.3: The distribution of mangrove widths from 2010 plotted against the distribution of coastline position change rates

C.2. Case study 2

In case study 2 most transects are part of the lower left quadrant. This can also be seen in Figure C.4. In this figure, a scatterplot is made that represents the mangrove width change rate on the x-axis versus the coastline position change rate. The fact that most transects are part of the lower left quadrant indicates that in this region, a strong correlation exists between the mangrove width change rate and the coastline position change rate. More specifically, the coastline will most likely erode if a mangrove forest is contracting. Other trends cannot be observed in this figure.

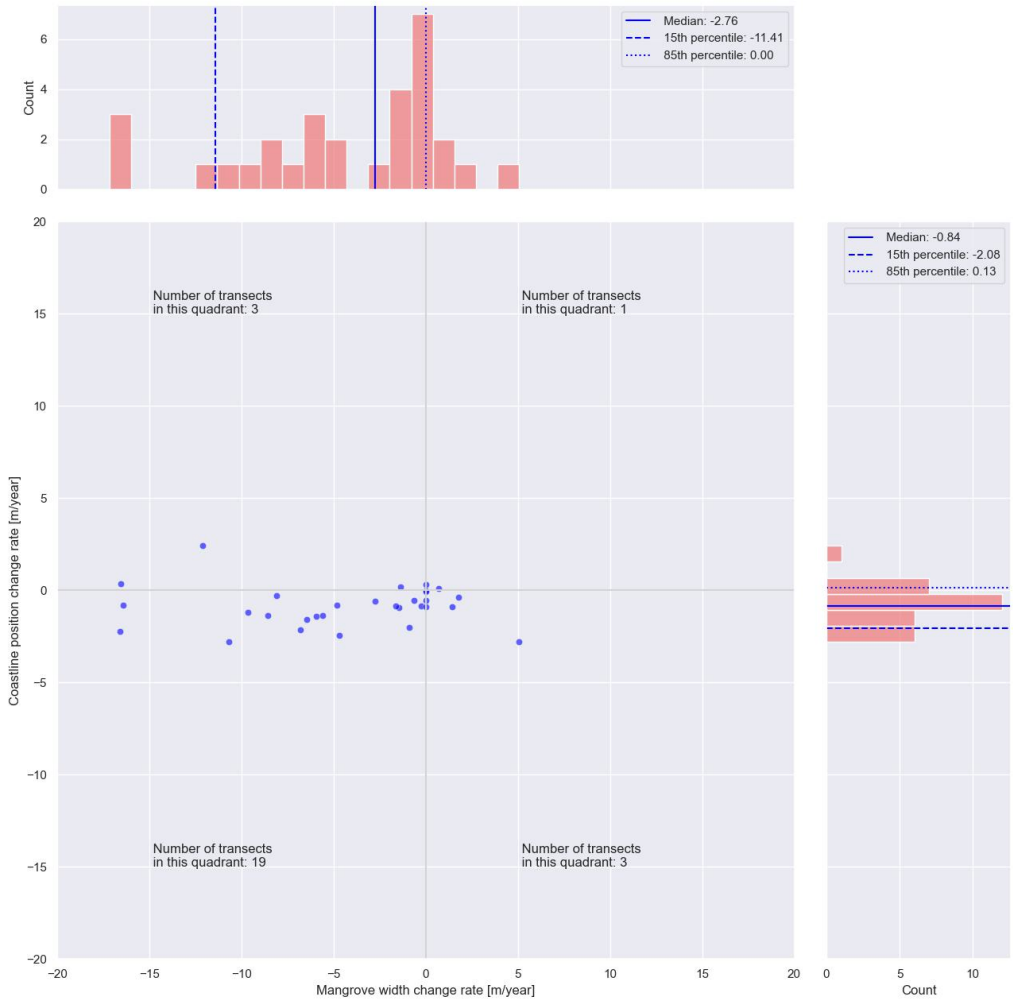

Figure C.4: Scatterplot indicating the spread of coastline position change rate versus mangrove width change rate.

In Figure C.5 two pie charts can be observed. The first one represents the distribution of the transects into the categories: stable, accreding and eroding. The second one represents the distribution of mangroves along transects into the three categories: contracting, expanding and stable. It can be seen that the distribution of eroding transects and contracting mangroves is the highest. The distribution of accreding transects and expanding mangrove transects is the lowest.

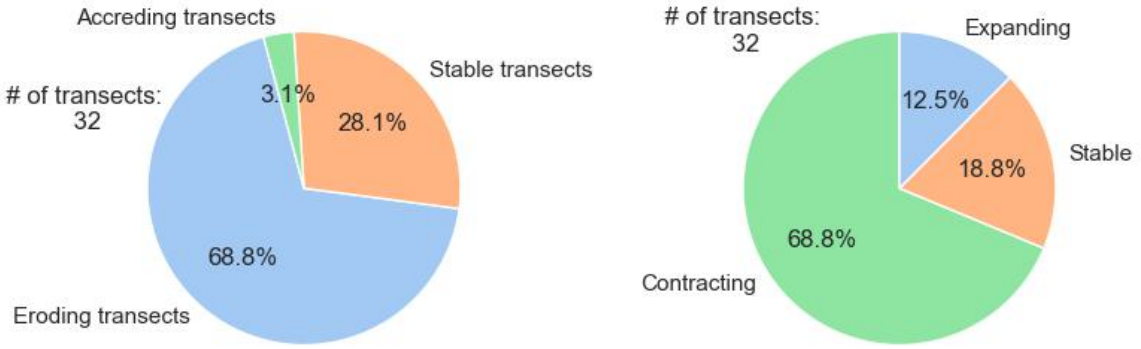

(a) Distribution of transect categories (b) Distribution of mangrove categories

Figure C.5: Distribution of both mangrove and transect categories

In Figure C.6 the mangrove width in 2010 is plotted against the coastline position change rate. In this Figure, no trend is seen.

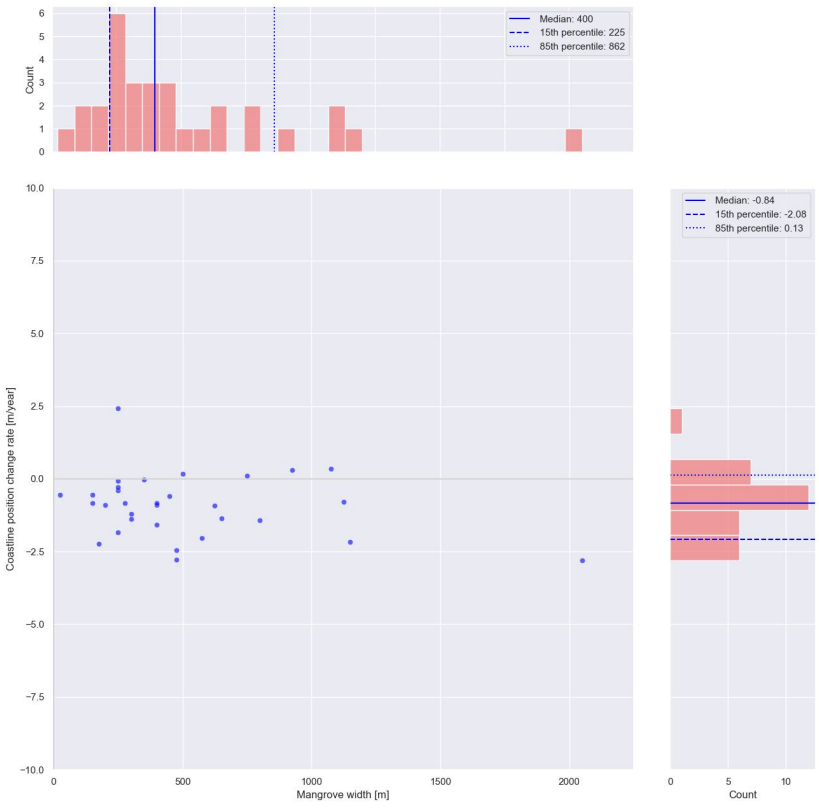

Figure C.6: Scatterplot indicating the mangrove width in 2010 versus the coastline position change rate

D

Analysing correlations between yearly mangrove width and coastline position change rates

This section checks if a correlation exists between yearly mangrove change rates and coastline position change rates. From the literature study, it is expected that there is a correlation between coastline position change rates and mangrove change rates. If the coastline moves land inwards, the mangrove forest is expected to contract as well. If the coastline moves seaward, the mangrove forest is expected to expand. Also, a delay in reaction time of a year is included. This means that it is checked if a correlation exists between the coastline position change rate and the mangrove width change rate the following year and vice versa. This analysis will be done for four extreme transects and the transects in the two case studies.

D.1. Extreme transects

Transects with a coastline position change rate higher than 20 [m/year] or lower than -20 [m/year] and a mangrove width change rate higher than 20 [m/year] or lower than -20 [m/year] are defined as extreme transects. The areas that meet these criteria are highlighted in Figure D.1.

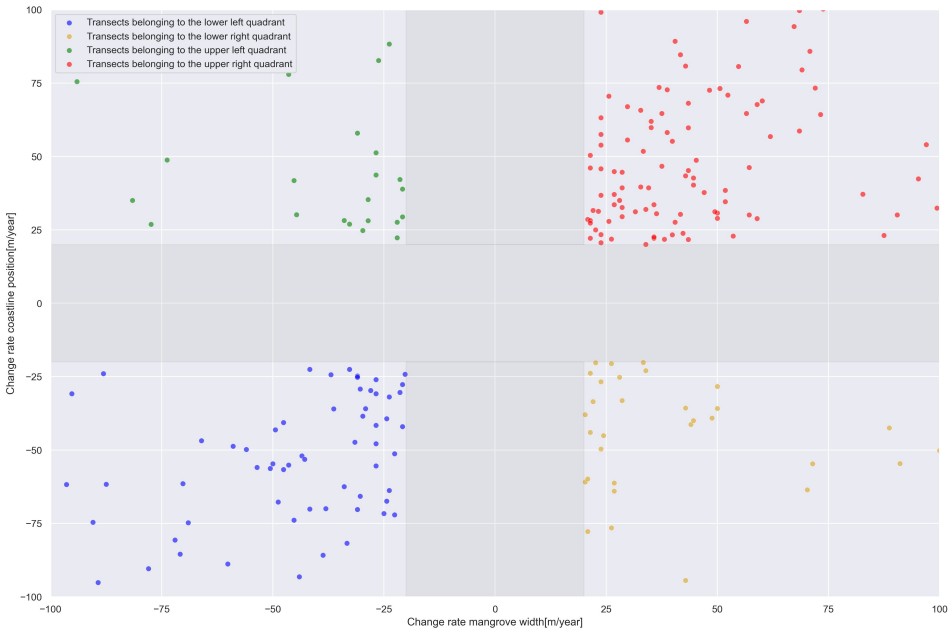

Figure D.1: Zones that are considered to be extreme

In total, there are 606 extreme transects distributed globally. The majority of these transects (353) are located in South America. Figure D.2 provides an overview of these transects.

Figure D.2: Distribution of extreme transects

In this section, four extreme transects globally will be chosen. These transects are determined based on the quadrants in Figure 4.1. One transect will be randomly selected per quadrant. However, a transect can only be chosen if all coastline position data is available between 2005 and 2016. Refer to Figure D.3 for illustrating the chosen quadrants.

Figure D.3: Chosen Distribution of extreme transects

Site characteristics

Transect 1

Transect one is located on Maracá Island near the northern coast of Brazil. Transect one belongs to the upper left quadrant, which indicates that this quadrant has an accreding coastline and a contracting mangrove forest. The shorelines are almost completely covered by mangrove forests, which consist mainly of mangroves of the genus Avicennia germinans (black mangrove), Rhizophora mangle, R. Harrison (red mangroves) and Laguncularia racemose (white mangrove) (Schaeffer-Novelli & Cintron, 1986). The area is strongly influenced by the Amazon River and by a variety of other secondary rivers that are bent northwestward by the flow of the Guyana current. The entire coastline of Maracá island is muddy (Schaeffer-Novelli & Cintron, 1988). The temporal imagery from Google Earth's Timelapse

feature revealed significantly reduced mangrove forests over time. Maracá Island experiences heavy rains and storms during the wet season, often inundating mangrove forests for more extended periods. This could be the reason for the substantial decrease in mangrove forests throughout the years. Maracá Island is a Conservation Unit protected area by the Brazilian government. As a result, there are no significant human disturbances in the area (Fernandes, 2000).

Figure D.4: Transect 1 (Google Earth)

The second extreme transect is located on the western coast of Malaysia in the state of Selangor. Transect two belongs to the upper right quadrant, which indicates that this transect has an accreding coastline and an expanding mangrove forest. The mangroves located in Malaysia can be found mostly on the west coast as it is calmer from waves and winds. This is also where the transect can be found. About 70 per cent of the west coasts of the peninsula consist of mud coasts while the other coasts mostly have sandy beaches (”Rahman & Asmawi, 2016). Since 1980, mangroves have been declining for several reasons, with aquaculture practices being a major factor during those years. Additionally, this coastline is located in a tsunami-prone area, which affects the mangrove forests. While many other parts of the peninsula are experiencing a decrease in mangrove forest, the study area is actually seeing an increase. This is due to the efforts of the Ministry of Natural Resources and Environment of Malaysia, who have been planting mangroves along the coastline (Abd Rahman & Asmawi, 2016).

Figure D.5: Transect 2 (Google Earth)

The third extreme transect is located in the southern part of Sulawesi island, which is a part of Indonesia. Transect three belongs to the lower left quadrant, which indicates that this transect has an eroding coastline and a contracting mangrove forest. The south Sulawesi forests, where the study area is located, contain a large variety of plants. The forests located on the island are a valuable source of firewood and various other products, which, unfortunately, has led to a significant decrease in the width of the mangrove forests. Additionally, many mangrove forests have been converted into brackish water fish ponds for shrimp and milkfish (Nurkin, 1994). The major concern is the rapidly increasing rate of exploitation. Prior to 1965, it was estimated that there were at least 110000 hectares of mangrove

forests along the coast of South Sulawesi, but today only about 30000 hectares remain (Barkey, 1990). It is worth noting that the coastline primarily consists of mud.

Figure D.6: Transect 3 (Google Earth)

Extreme transect four is situated in the southeastern part of Sulawesi island. Transect four belongs to the lower right quadrant, which indicates that this transect has an eroding coastline and an expanding mangrove forest. The area of mangrove forest in this part of the island has increased from 29000 hectares in 1982 to 64000 hectares in 2003 (Nurkin, 1994). Although locally around the studied transect the mangrove forest is expanding, on a larger scale, there has actually been a significant decrease over the years. his decline has been mainly attributed to mangrove logging and aquaculture exploitation (Nurkin, 1994 and Malik et al., 2017. The coastline is muddy.

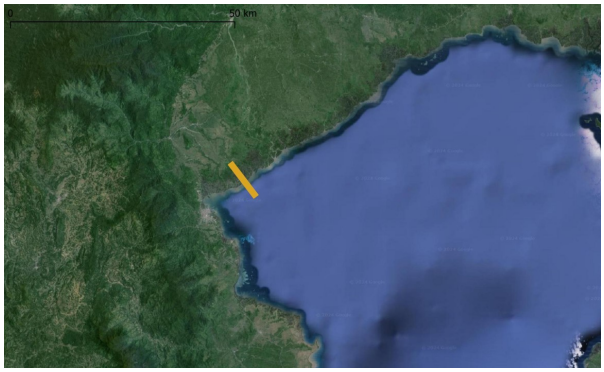

Figure D.7: Transect 4 (Google Earth)

In Figure D.8 the cross-shore mangrove width along the transect for all four transects is illustrated. As can be seen in this Figure, the four chosen transects exhibit a variety of mangrove widths. Transect three has the widest mangrove forest with a width of about 4000 [m], while Transect four has the narrowest mangrove forest with a width of about 300 [m].

Figure D.8: Cross-shore mangrove width along the transect (divided per quadrant)

Results

In Figure D.9, the coastline position, together with the cross-shore mangrove width along the transect, is plotted for all four transects. Both the coastline position and mangrove width are relative to their respective first data points. The coastline position is relative to 2005, while the mangrove width is relative to 2007. It is important to note that some of the coastline position data points are missing. These points were excluded when using the method explained in Section 3.1.3. Upon quick inspection of the figure, there appears to be no clear correlation between the coastline position and mangrove width, even when considering the extreme changes in coastline position between 2010 and 2015.

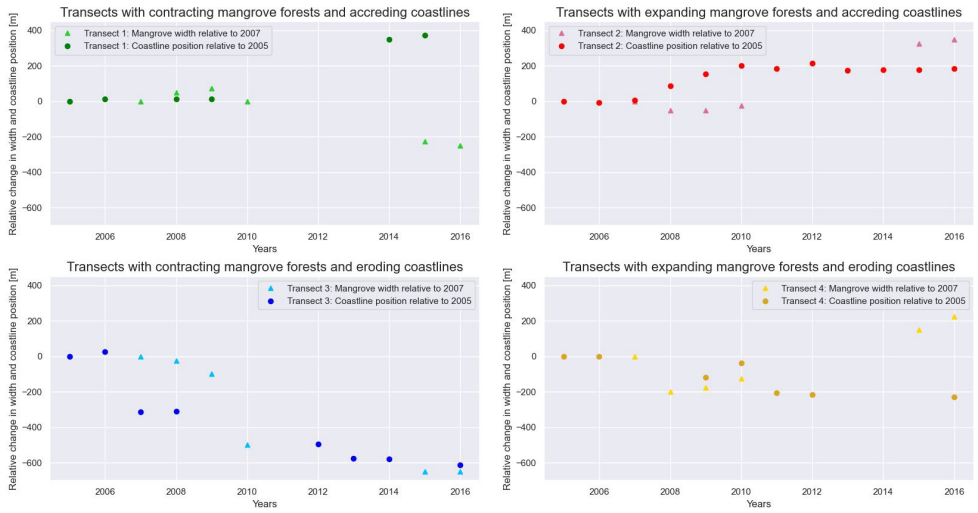

Figure D.9: Cross-shore mangrove width along the transect relative to 2007 and coastline position relative to 2005 (divided per quadrant)

To further analyse this data, yearly change rates for both mangrove width and coastline position are calculated. Ideally, if all data were available in every transect, there would be 11 yearly coastline position change rates and 4 yearly mangrove position change rates between 2005 and 2016 per transect.

Unfortunately, due to the sometimes significant unavailability of coastline position data, only 6 change rates in total can be compared. Table D.10 presents data on the relationship between yearly changes in mangrove width (contracting or expanding) and changes in coastline position (eroding and accreding). The change rate is analysed for both concurrent and one-year delayed correlations splitting the data into three dataframes. The first column compares the yearly coastline position change rate with the yearly mangrove width change rate in the following year. The second column compares the yearly coastline position change rate and yearly mangrove width change rate in the same year. The third column compares the yearly mangrove width change rate with the yearly coastline position change rate in the following year. Each row represents a distinct scenario, indicating whether the coastline is eroding or accreding, and the correlation (ρ) and sample size (n) for each observation. Figure D.10 shows that no clear patterns are found. As can be seen, when comparing the yearly mangrove change rates and yearly coastline position change rates, mostly a negative correlation between coastline position and mangrove width is found. In other words, it is mostly found that when the coastline experiences accretion, the mangrove width decreases. However, when looking at the correlations, the relationship is very weak.

	The coastline position changes first, the mangrove width follows the following year				**The coastline position and mangrove width change simultaneously**				**The mangrove width changes first, the coastline position follows the following year**			
	Mangrove width increases		Mangrove width decreases		Mangrove width increases		Mangrove width decreases		Mangrove width increases		Mangrove width decreases	
	ρ	n	ρ	n	ρ	n	ρ	n	ρ	n	ρ	n
Coastline erodes	/	0	/	1	/	0	/	0	/	0	/	2
Coastline accredes	/	0	-0.04	5	/	0	-0.34	6	/	0	-0.51	4

Figure D.10: The yearly change rates in mangrove width compared to the yearly change rates in coastline position

D.2. Case studies

Case study 1

In Figure D.11 and D.12 the coastline position relative to 2005 is plotted with the mangrove width relative to 2007. The distribution over time of the total 6 blue transects (eroding coastline and contracting mangrove forest) and the 5 yellow transects (eroding coastline and expanding mangrove forest) is split into two graphs for clarity. In the graph, it can be seen that the direction of some yearly change rates in mangrove width and coastline position align, however a clear pattern is unclear. The grey transects (stable mangrove width) are not plotted, as the mangrove width does not change over time.

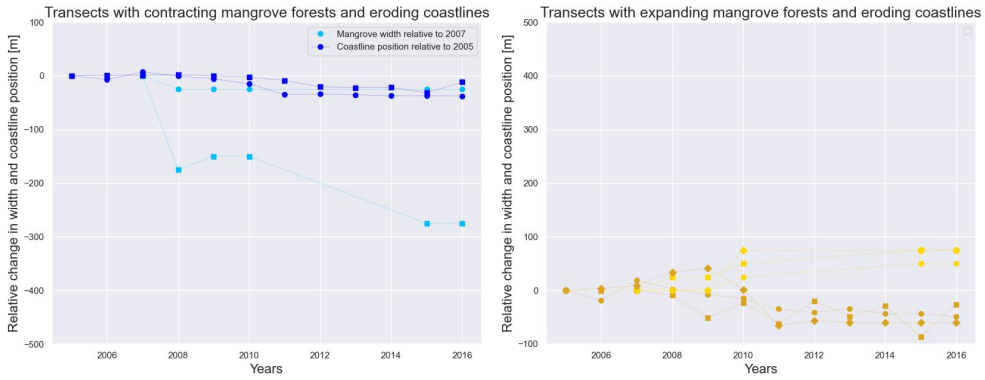

Figure D.11: The coastline position relative to 2005 plotted with the mangrove width relative to 2007

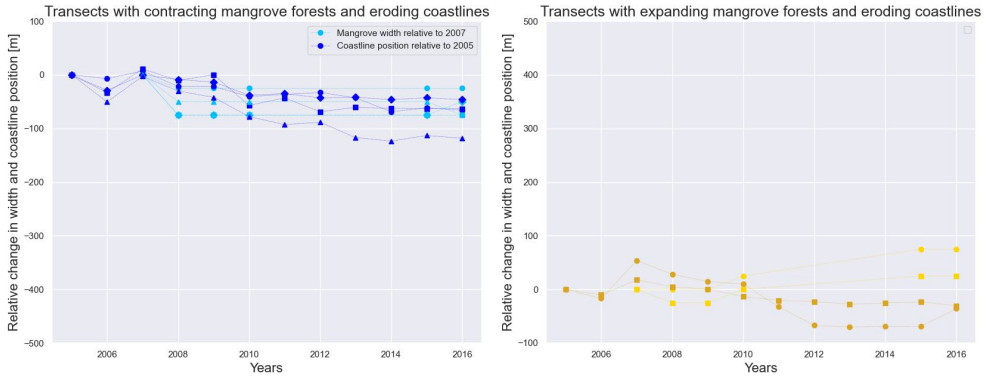

Figure D.12: The coastline position relative to 2005 plotted with the mangrove width relative to 2007

To further analyse this data, yearly change rates for mangrove width and coastline position are calculated. All data is present in the transect. Tables D.13 and D.14 present data on the relationship between yearly changes in mangrove width (contracting or expanding) and changes in coastline position (eroding and accreding). The change rate is analysed for concurrent and one-year delayed correlations, and the data is split into three dataframes. Table D.13 compares the yearly coastline position change rate with the yearly mangrove width change rate in the following year and compares the yearly coastline position change rate and yearly mangrove width change rate in the same year. Table D.14 compares the yearly mangrove width change rate with the yearly coastline position change rate in the following year. In Table D.13, each row represents a distinct scenario, indicating whether the coastline is eroding, accreding or stable, and the correlation (ρ) and sample size (n) for each observation. In Table D.14, each row represents a distinct scenario, indicating whether the mangrove width is increasing, decreasing or stable, and the correlation (ρ) and sample size (n) for each observation. In Table D.13, when analysing the coastline position changes and mangrove width changes in the same year, it can be seen that in this case study it is most likely that when the mangrove width remains stable, the coastline erodes. This coincides with the long-term behaviour of the coastline, as most transects have stable mangrove widths and an eroding coastline. When not looking at the transects where the mangrove width remains stable, most data can be found in the column where the mangrove width increases and the coastline erodes. However, the correlation is very weak. Aside from observing the same behaviour in the yearly change rates as in the long-term behaviour, no relationship is found when comparing the change rates in the same year. The same conclusion can be drawn when analysing the yearly coastline position changes with the yearly mangrove width change rate in the following year. The same behaviour is found in the yearly change rates as in the long-term behaviour. However, no relationship is found when comparing the yearly coastline position change rates with the yearly mangrove width change rates in the following year. This same conclusion can be drawn for table D.14.

	In the same year						In the following year					
	Mangrove width increases		Mangrove width decreases		Mangrove width remains stable		Mangrove width increases		Mangrove width decreases		Mangrove width remains stable	
	ρ	n	ρ	n	ρ	n	ρ	n	ρ	n	ρ	n
Coastline accredes	-0.65	3	/	2	/	37	-0.46	6	0.64	7	/	65
Coastline erodes	0.09	15	-0.03	8	/	93	0.31	10	nan	3	/	66
Coastline remains stable	/	2	/	0	/	11	0.33	4	/	0	/	10

Figure D.13: The yearly change rates in mangrove width compared to the yearly change rates in coastline position

	In the following year					
	Coastline accredes		Coastline erodes		Coastline remains stable	
	ρ	n	ρ	n	ρ	n
Mangrove width increases	/	2	-0.33	10	/	0
Mangrove width decreases	/	2	-0.53	9	/	0
Mangrove width remains stable	/	40	/	60	/	6

Figure D.14: The yearly change rates in mangrove width compared to the yearly change rates in coastline position

Case study 2

Yearly change rates for mangrove width and coastline position are calculated to analyse if a correlation exists. Most data is present in the transects. Tables D.13 and D.14 present data on the relationship between yearly changes in mangrove width (contracting or expanding) and changes in coastline position (eroding and accreding). The change rate is analysed for concurrent and one-year delayed correlations, and the data is split into three data frames. Table D.13 compares the yearly coastline position change rate with the yearly mangrove width change rate in the following year and compares the yearly coastline position change rate and yearly mangrove width change rate in the same year. Table D.16 compares the yearly mangrove width change rate with the yearly coastline position change rate in the following year. In Table D.15, each row represents a distinct scenario, indicating whether the coastline is eroding, accreding or stable, and the correlation (ρ) and sample size (n) for each observation. In Table D.16, each row represents a distinct scenario, indicating whether the mangrove width is increasing, decreasing or stable, and the correlation (ρ) and sample size (n) for each observation. In Table D.15, when analysing the coastline position changes and mangrove width changes in the same year, it can be seen that in this case study it is most likely that when the mangrove width decreases, the coastline erodes. However, the correlation is very weak. The highest correlation is found between when the coastline remains stable and the mangrove width increases. However, compared to the other categories, only limited data is found in this category. When analysing the yearly coastline position changes with the yearly mangrove width change rate in the following year, it is found that most data is found in the category where the coastline erodes and the mangrove width remains stable the following year. However, the correlation can not be determined for this category, so the strength of the relation can not be determined. When comparing the yearly mangrove width change rates with the yearly coastline position change rates in the following year (see Table D.14), it is found that most data is found when the mangrove width decreases and the coastline erodes. However, the relationship is very weak. The highest correlation can be found when the mangrove width increases and the coastline remains stable. However, only limited data is found in this category compared to the other categories.

	In the same year						In the following year					
	Mangrove width increases		Mangrove width decreases		Mangrove width remains stable		Mangrove width increases		Mangrove width decreases		Mangrove width remains stable	
	ρ	n	ρ	n	ρ	n	ρ	n	ρ	n	ρ	n
Coastline accredes	0.19	5	0.19	9	/	21	-0.33	6	0.25	13	/	14
Coastline erodes	-0.05	19	0.01	32	/	21	0	14	0.23	13	/	23
Coastline remains stable	0.96	6	-0.45	6	/	6	-1	2	0.36	7	/	2

Figure D.15: The yearly change rates in mangrove width compared to the yearly change rates in coastline position

	In the following year					
	Coastline accredes		Coastline erodes		Coastline remains stable	
	ρ	n	ρ	n	ρ	n
Mangrove width increases	0.66	13	0.43	12	-0.87	5
Mangrove width decreases	-0.05	25	-0.11	17	0.8	5
Mangrove width remains stable	/	21	/	24	/	3

Figure D.16: The yearly change rates in mangrove width compared to the yearly change rates in coastline position

D.3. Conclusion

This section aimed to discover if a correlation exists between when the mangrove width changes and when the coastline position changes.

In this research, when analysing the extreme transects and case studies, no clear patterns emerge. Also, no clear patterns emerge when including a delay of a year.

Bibliography

Abd Rahman, M. A., & Asmawi, M. Z. (2016). Local residents' awareness towards the issue of mangrove degradation in kuala selangor, malaysia. *Procedia-Social and Behavioral Sciences*, *222*, 659–667.

Agoramoorthy, G., Chen, F.-A., & Hsu, M. J. (2008). Threat of heavy metal pollution in halophytic and mangrove plants of tamil nadu, india. *Environmental pollution*, *155*(2), 320–326.

Alexander, C. R., Nittrouer, C. A., Demaster, D. J., Park, Y.-A., & Park, S.-C. (1991). Macrotidal mudflats of the southwestern korean coast; a model for interpretation of intertidal deposits. *Journal of Sedimentary Research*, *61*(5), 805–824.

Alison. (2010, January). Trees on stilts. https://blog.waikato.ac.nz/bioblog/2010/01/trees-on-stilts/

Allison, M. A., & Lee, M. T. (2004). Sediment exchange between amazon mudbanks and shore-fringing mangroves in french guiana. *Marine Geology*, *208*(2-4), 169–190.

Alongi, D. M. (2014). Carbon cycling and storage in mangrove forests. *Annual review of marine science*, *6*, 195–219.

ALOS. (2021). The k and c global mangrove watch.

Amos, C. L. (1995). Siliciclastic tidal flats. In *Developments in sedimentology* (pp. 273–306, Vol. 53). Elsevier.

Andersen, T., & Pejrup, M. (2001). Suspended sediment transport on a temperate, microtidal mudflat, the danish wadden sea. *Marine Geology*, *173*(1-4), 69–85.

Aranda, E., Viñola-López, L. W., & Álvarez-Lajonchere, L. (2020). New insights on the quaternary fossil record of isla de la juventud, cuba. *Journal of South American Earth Sciences*, *102*, 102656. https://doi.org/https://doi.org/10.1016/j.jsames.2020.102656

Arnaud, M., Morris, P. J., Baird, A. J., Dang, H., & Nguyen, T. T. (2021). Fine root production in a chronosequence of mature reforested mangroves. *New Phytologist*, *232*(4), 1591–1602.

Ashton, E. C. (2022). Threats to mangroves and conservation strategies. In S. C. Das, Pullaiah, & E. C. Ashton (Eds.), *Mangroves: Biodiversity, livelihoods and conservation* (pp. 217–230). Springer Nature Singapore. https://doi.org/10.1007/978-981-19-0519-3_10

Augustinus, P. G. E. F. (1989). Cheniers and chenier plains: A general introduction. *Marine Geology*, *90*(4), 219–229.

Baker, R. O., Yarranton, H. W., & Jensen, J. (2015). *Practical reservoir engineering and characterization*. Gulf Professional Publishing.

Balasuriya, A. (2018). Chapter 25 - coastal area management: Biodiversity and ecological sustainability in sri lankan perspective. In C. Sivaperuman, A. Velmurugan, A. K. Singh, & I. Jaisankar (Eds.), *Biodiversity and climate change adaptation in tropical islands* (pp. 701–724). Academic Press. https://doi.org/https://doi.org/10.1016/B978-0-12-813064-3.00025-9

Balke, T., & Friess, D. A. (2016). Geomorphic knowledge for mangrove restoration: A pan-tropical categorization. *Earth Surface Processes and Landforms*, *41*(2), 231–239.

Barkey, R. (1990). Ekosistim mangrove di sulawesi selatan ditinjau dari aspek konservasinya. In M. Zierren, Y. Rusila Nur, & PHPA (Eds.), *Proseding seminar keterpaduan antara konservasi dan tataguna lahan basah di sulawesi selatan*. Ditjen PHPA/Kanwil Dephut Prop. Sulsel.

Basha, S. (2018). An overview on global mangroves distribution.

Bayliss-Smith, T., Healey, R., Lailey, R., Spencer, T., & Stoddart, D. (1979). Tidal flows in salt marsh creeks. *Estuarine and Coastal Marine Science*, *9*(3), 235–255.

BC, B. (2010, January). Ecological concepts, principles and application to conservation. http://www.biodiversitybc.org/EN/main/where/131.html

Beselly, S., Grueters, U., van Der Wegen, M., Reyns, J., Dijkstra, J., & Roelvink, D. (2023). Modelling mangrove-mudflat dynamics with a coupled individual-based-hydro-morphodynamic model. *Environmental Modelling & Software*, *169*, 105814.

Besset, M., Gratiot, N., Anthony, E. J., Bouchette, F., Goichot, M., & Marchesiello, P. (2019). Mangroves and shoreline erosion in the mekong river delta, viet nam. *Estuarine, Coastal and Shelf Science*, *226*, 106263.

Bingham, B., & Kathiresan, K. (2001). Biology of mangroves and mangrove ecosystems. *Advances in marine biology*, *40*(8), 1–25.

BioManCo. (n.d.). Causes of mangrove loss. https://www.biomanco.org/category/causes-of-mangrove-loss/

Bird, E. (1986). Mangroves and intertidal morphology in westernport bay, victoria, australia. *Marine Geology*, *69*(3-4), 251–271.

Blasco, F., Saenger, P., & Janodet, E. (1996). Mangroves as indicators of coastal change. *Catena*, *27*(3-4), 167–178.

Borroto-Páez, R., & Ramos García, I. (2012). *STATUS OF THE HUTIAS (RODENTIA: CAPROMYIDAE) IN LOS CANARREOS ARCHIPELAGO, CUBA* (tech. rep.). https://www.researchgate.net/profile/Rafael-Borroto-Paez/publication/273831292_STATUS_OF_THE_HUTIAS_RODENTIA_CAPROMYIDAE_IN_LOS_CANARREOS_ARCHIPELAGO_CUBA/links/550e38170cf2752610STATUS-OF-THE-HUTIAS-RODENTIA-CAPROMYIDAE-IN-LOS-CANARREOS-ARCHIPELAGO-CUBA.pdf

Bosboom, J., & Stive, M. J. (2021). Coastal dynamics.

Bridge, J. S. (2003). Planar and parallel lamination. In G. V. Middleton, M. J. Church, M. Coniglio, L. A. Hardie, & F. J. Longstaffe (Eds.), *Encyclopedia of sediments and sedimentary rocks* (pp. 534–537). Springer Netherlands. https://doi.org/10.1007/978-1-4020-3609-5_161

Bryan, K. R., Nardin, W., Mullarney, J. C., & Fagherazzi, S. (2017). The role of cross-shore tidal dynamics in controlling intertidal sediment exchange in mangroves in cù lao dung, vietnam [Sediment- and hydro-dynamics of the Mekong Delta: from tidal river to continental shelf]. *Continental Shelf Research*, *147*, 128–143. https://doi.org/https://doi.org/10.1016/j.csr.2017.06.014

Bunting, P., Rosenqvist, A., Hilarides, L., Lucas, R. M., Thomas, N., Tadono, T., Worthington, T. A., Spalding, M., Murray, N. J., & Rebelo, L.-M. (2022). Global mangrove extent change 1996–2020: Global mangrove watch version 3.0. *Remote Sensing*, *14*(15), 3657.

Cahoon, D. R. (2006). A review of major storm impacts on coastal wetland elevations. *Estuaries and coasts*, *29*, 889–898.

Cahoon, D. R., Hensel, P., Rybczyk, J., McKee, K. L., Proffitt, C. E., & Perez, B. C. (2003). Mass tree mortality leads to mangrove peat collapse at bay islands, honduras after hurricane mitch. *Journal of ecology*, *91*(6), 1093–1105.

Cahoon, D. R., Hensel, P. F., Spencer, T., Reed, D. J., McKee, K. L., & Saintilan, N. (2006). Coastal wetland vulnerability to relative sea-level rise: Wetland elevation trends and process controls. *Wetlands and natural resource management*, 271–292.

Cahoon, D. R., & Lynch, J. C. (1997). Vertical accretion and shallow subsidence in a mangrove forest of southwestern florida, usa. *Mangroves and Salt Marshes*, *1*, 173–186.

Cahoon, D. R., Perez, B. C., Segura, B. D., & Lynch, J. C. (2011). Elevation trends and shrink–swell response of wetland soils to flooding and drying. *Estuarine, Coastal and Shelf Science*, *91*(4), 463–474.

Chapman, V. J. (1944). 1939 cambridge university expedition to jamaica.-part 1. a study of the botanical processes concerned in the development of the jamaican shore-line. *Journal of the Linnean Society of London, Botany*, *52*(346), 407–447.

Chen, G., Hong, W., Gu, X., Krauss, K. W., Zhao, K., Fu, H., Chen, L., Wang, M., & Wang, W. (2023). Coupling near-surface geomorphology with mangrove community diversity at the estuarine scale: A case study at dongzhaigang bay, china. *Sedimentology*, *70*(1), 31–47.

Choi, K., & Jo, J. (2015). Morphodynamics of tidal channels in the open coast macrotidal flat, southern ganghwa island in gyeonggi bay, west coast of korea. *Journal of Sedimentary Research*, *85*, 582–595. https://doi.org/10.2110/jsr.2015.44

Christiansen, C., Vølund, G., Lund-Hansen, L. C., & Bartholdy, J. (2006). Wind influence on tidal flat sediment dynamics: Field investigations in the ho bugt, danish wadden sea. *Marine Geology*, *235*(1-4), 75–86.

Christie, M., Dyer, K., & Turner, P. (1999). Sediment flux and bed level measurements from a macro tidal mudflat. *Estuarine, Coastal and Shelf Science*, *49*(5), 667–688.

Church, J. A., Gregory, J. M., Huybrechts, P., Kuhn, M., Lambeck, K., Nhuan, M. T., Qin, D., & Woodworth, P. L. (2001). Changes in sea level. In *, in: Jt houghton, y. ding, dj griggs, m. noguer, pj van der linden, x. dai, k. maskell, and ca johnson (eds.): Climate change 2001: The scientific*

basis: Contribution of working group i to the third assessment report of the intergovernmental panel (pp. 639–694).
Das, S. (2020). Does mangrove plantation reduce coastal erosion? assessment from the west coast of india. *Regional Environmental Change*, *20*(2), 58.
Das, S. C., Pullaiah, T., & Ashton, E. C. (2022). *Mangroves: Biodiversity, livelihoods and conservation*. Springer.
Davis, J. H. (1946). *The peat deposits of florida, their occurrence, development and uses* (Vol. 30). Published for the Florida Geological survey.
Davis, R. A., & Dalrymple, R. W. (2012). *Principles of tidal sedimentology* (Vol. 625). Springer.
de la Barra, P., Aarts, G., & Bijleveld, A. (2023). Gas extraction under intertidal mudflats is associated with declines in sediment grain size and minor changes in macrozoobenthic community composition. *bioRxiv*. https://doi.org/10.1101/2023.05.09.539962
Doeke, E. (2019). *Intertidal deposits: River mouths, tidal flats, and coastal lagoons*. CRC press.
Du, Q., Qin, Z., Ming, S., & Zhang, C. (2021). Differences in the vertical accretion of sediment among mangrove species with different aerial root types. *Estuarine, Coastal and Shelf Science*, *256*, 107375.
Duke, N. (1992). Mangrove floristics and biogeography. *In: Tropical Mangrove Ecosystems. American Geophysical Union*, 63–100. https://doi.org/10.1029/CE041p0063
Duke, N. C., & Allen, J. A. (2006). Rhizophora mangle, r. samoensis, r. racemosa, r.× harrisonii (atlantic–east pacific red mangrove). *Species profiles for pacific island agroforestry*, *10*, 1–18.
Duke, N. C., Lo, E., & Sun, M. (2002). Global distribution and genetic discontinuities of mangroves–emerging patterns in the evolution of rhizophora. *Trees*, *16*, 65–79.
Egler, F. E. (1952). Southeast saline everglades vegetation, florida and its management: With 16 figs., 8 photographs, 4 plates and 1 table. *Vegetatio*, *3*, 213–265.
Ellison, J. (2009). Geomorphology and sedimentology of mangroves.
Ellison, J. C. (2000). How south pacific mangroves may respond to predicted climate change and sea-level rise. *Climate change in the South Pacific: impacts and responses in Australia, New Zealand, and small island states*, 289–300.
Ellison, J. C., & Stoddart, D. R. (1991). Mangrove ecosystem collapse during predicted sea-level rise: Holocene analogues and implications. *Journal of Coastal research*, 151–165.
Evans, G. (1965). Intertidal flat sediments and their environments of deposition in the wash. *Quarterly Journal of the Geological Society*, *121*(1-4), 209–240.
Evans, I. S. (2012). Geomorphometry and landform mapping: What is a landform? [Geospatial Technologies and Geomorphological Mapping Proceedings of the 41st Annual Binghamton Geomorphology Symposium]. *Geomorphology*, *137*(1), 94–106. https://doi.org/https://doi.org/10.1016/j.geomorph.2010.09.029
Fagherazzi, S., Bryan, K. R., & Nardin, W. (2017). Buried alive or washed away: The challenging life of mangroves in the mekong delta. *Oceanography*, *30*(3), 48–59.
Fan, D. (2011). Open-coast tidal flats. In *Principles of tidal sedimentology* (pp. 187–229). Springer.
Fan, D., Guo, Y., Wang, P., & Shi, J. Z. (2006). Cross-shore variations in morphodynamic processes of an open-coast mudflat in the changjiang delta, china: With an emphasis on storm impacts. *Continental Shelf Research*, *26*(4), 517–538.
Fan, D., Li, C., Wang, D., Wang, P., Archer, A. W., & Greb, S. F. (2004). Morphology and sedimentation on open-coast intertidal flats of the changjiang delta, china. *Journal of Coastal Research*, 23–35.
FAO. (2007). The world's mangroves 1980-2005, fao forestry paper 153.
FAO Fisheries and Aquaculture Information and Statistics Service. (2021). *Aquaculture production: Quantities 1950–2021*. Food and Agriculture Organization of the United Nations. http://www.fao.org/fi/statist/FISOFT/FISHPLUS.asp4
Farnsworth, E. (1998). Issues of spatial, taxonomic and temporal scale in delineating links between mangrove diversity and ecosystem function. *Global Ecology & Biogeography Letters*, *7*(1), 15–25.
Fernandes, M. (2000). Structural analysis of rhizophora, avicennia, and laguncularia forests on maracá island, amapá, brazil.
Field, C. (1994). Assessment and monitoring of climate change impacts on mangrove ecosystems. *UNEP Regional Seas Reports and Studies*, *154*, 62.

Field, C., OSBORN, J., HOFFMAN, L., POLSENBERG, J., ACKERLY, D., BERRY, J., BJÖRKMAN, O., Held, A., MATSON, P., & MOONEY, H. (1998). Mangrove biodiversity and ecosystem function. *Global Ecology & Biogeography Letters*, *7*(1), 3–14.

Flanders Marine Institute (VLIZ). (2021). Coastal morphodynamics [The mutual interaction of coastal morphology with hydrodynamic agents (tides, currents, waves). This interaction takes place through sedimentation, erosion, and sediment transport processes.]. https://www.coastalwiki.org/wiki/Coastal_morphodynamics

Flanders Marine Institute (VLIZ). (2024). Coastal morphology. https://www.coastalwiki.org/wiki/Coastal_morphology#:~:text=Definition%20of%20Coastal%20morphology%3A,the%20morphology%20of%20a%20bedform.

Fletcher, C. H., Mullane, R. A., & Richmond, B. M. (1997). Beach loss along armored shorelines on oahu, hawaiian islands. *Journal of Coastal Research*, 209–215.

Frey, R. W., Howard, J. D., Han, S.-J., & Park, B.-K. (1989). Sediments and sedimentary sequences on a modern macrotidal flat, inchon, korea. *Journal of Sedimentary Research*, *59*(1), 28–44.

Friedrichs, C. T. (2011). Tidal flat morphodynamics: A synthesis.

Friedrichs, C. T., & Aubrey, D. G. (1988). Non-linear tidal distortion in shallow well-mixed estuaries: A synthesis. *Estuarine, Coastal and Shelf Science*, *27*(5), 521–545.

Friedrichs, C. T., & Aubrey, D. (1996). Uniform bottom shear stress and equilibrium hyposometry of intertidal flats. *Mixing in estuaries and coastal seas*, *50*, 405–429.

Friess, D. A., & McKee, K. L. (2021). Chapter 7 - the history of surface-elevation paradigms in mangrove biogeomorphology. In F. Sidik & D. A. Friess (Eds.), *Dynamic sedimentary environments of mangrove coasts* (pp. 179–198). Elsevier. https://doi.org/https://doi.org/10.1016/B978-0-12-816437-2.00007-0

Friess, D. A., Rogers, K., Lovelock, C. E., Krauss, K. W., Hamilton, S. E., Lee, S. Y., Lucas, R., Primavera, J., Rajkaran, A., & Shi, S. (2019). The state of the world's mangrove forests: Past, present, and future. *Annual Review of Environment and Resources*, *44*, 89–115.

Froidefond, J., Pujos, M., & Andre, X. (1988). Migration of mud banks and changing coastline in french guiana. *Marine Geology*, *84*(1-2), 19–30.

Gao, S. (2019). Geomorphology and sedimentology of tidal flats. In *Coastal wetlands* (pp. 359–381). Elsevier.

Gardner, R. C., & Finlayson, C. (2018). Global wetland outlook: State of the world's wetlands and their services to people. *Ramsar convention secretariat*, 2020–5.

Gijón Mancheño, A., Herman, P. M., Jonkman, S. N., Kazi, S., Urrutia, I., & van Ledden, M. (2021). Mapping mangrove opportunities with open access data: A case study for bangladesh. *Sustainability*, *13*(15), 8212.

Gijsman, R., Horstman, E. M., Swales, A., MacDonald, I. T., Bouma, T. J., van der Wal, D., & Wijnberg, K. M. (2023). Mangrove forest drag and bed stabilisation effects on intertidal flat morphology. *Earth Surface Processes and Landforms*.

Gijsman, R., Horstman, E. M., van der Wal, D., Friess, D. A., Swales, A., & Wijnberg, K. M. (2021). Nature-based engineering: A review on reducing coastal flood risk with mangroves. *Frontiers in Marine Science*, *8*, 702412.

Gilman, E., Ellison, J., & Coleman, R. (2007). Assessment of mangrove response to projected relative sea-level rise and recent historical reconstruction of shoreline position. *Environmental monitoring and assessment*, *124*, 105–130.

Gilman, E. L., Ellison, J., Duke, N. C., & Field, C. (2008a). Threats to mangroves from climate change and adaptation options: A review [Mangrove Ecology – Applications in Forestry and Costal Zone Management]. *Aquatic Botany*, *89*(2), 237–250. https://doi.org/https://doi.org/10.1016/j.aquabot.2007.12.009

Gilman, E. L., Ellison, J., Duke, N. C., & Field, C. (2008b). Threats to mangroves from climate change and adaptation options: A review. *Aquatic botany*, *89*(2), 237–250.

Goessens, A., Satyanarayana, B., Van der Stocken, T., Quispe Zuniga, M., Mohd-Lokman, H., Sulong, I., & Dahdouh-Guebas, F. (2014). Is matang mangrove forest in malaysia sustainably rejuvenating after more than a century of conservation and harvesting management? *PloS one*, *9*(8), e105069.

Goldberg, L., Lagomasino, D., Thomas, N., & Fatoyinbo, T. (2020). Global declines in human-driven mangrove loss. *Global change biology*, *26*(10), 5844–5855.

Green, M. O., Black, K. P., & Amos, C. L. (1997). Control of estuarine sediment dynamics by interactions between currents and waves at several scales. *Marine geology*, *144*(1-3), 97–116.
Green, M. O., & Coco, G. (2014). Review of wave-driven sediment resuspension and transport in estuaries. *Reviews of Geophysics*, *52*(1), 77–117.
Hackney, C., Burbanck, W., & Hackney, O. (1976). Biological and physical dynamics of a georgia tidal creek. *Chesapeake Science*, *17*(4), 271–280.
Hale, P., & McCann, S. (1982). Rhythmic topography in a mesotidal, low-wave-energy environment. *Journal of Sedimentary Research*, *52*(2), 415–429.
Hamilton, S. E. (2019). *Mangroves and aquaculture: A five decade remote sensing analysis of ecuador's estuarine environments* (Vol. 33). Springer.
Hamilton, S. E., & Casey, D. (2016). Creation of a high spatio-temporal resolution global database of continuous mangrove forest cover for the 21st century (cgmfc-21). *Global Ecology and Biogeography*, *25*(6), 729–738.
Hanssen, J. L. J., van Prooijen, B. C., Volp, N. D., de Vet, P. L. M., & Herman, P. M. J. (2022). Where and why do creeks evolve on fringing and bare tidal flats? *Geomorphology*, *403*, 108182. https://doi.org/https://doi.org/10.1016/j.geomorph.2022.108182
Harris, P. T., Westerveld, L., Nyberg, B., Maes, T., Macmillan-Lawler, M., & Appelquist, L. R. (2021). Exposure of coastal environments to river-sourced plastic pollution. *Science of The Total Environment*, *769*, 145222. https://doi.org/10.1016/j.scitotenv.2021.145222
Healy, T., Wang, Y., & Healy, J.-A. (2002). *Muddy coasts of the world: Processes, deposits and function*. Elsevier.
Henderson, S. M., Norris, B. K., Mullarney, J. C., & Bryan, K. R. (2017). Wave-frequency flows within a near-bed vegetation canopy. *Continental Shelf Research*, *147*, 91–101.
Hishamunda, N., Ridler, N. B., Bueno, P., & Yap, W. G. (2009). Commercial aquaculture in southeast asia: Some policy lessons. *Food Policy*, *34*(1), 102–107.
Hoitink, A., Hoekstra, P., & Van Maren, D. (2003). Flow asymmetry associated with astronomical tides: Implications for the residual transport of sediment. *Journal of Geophysical Research: Oceans*, *108*(C10).
Holthuijsen, L. H. (2010). *Waves in oceanic and coastal waters*. Cambridge university press.
Horstman, E., Dohmen-Janssen, C., Narra, P., van den Berg, N., Siemerink, M., & Hulscher, S. (2014). Wave attenuation in mangroves: A quantitative approach to field observations. *Coastal Engineering*, *94*, 47–62. https://doi.org/https://doi.org/10.1016/j.coastaleng.2014.08.005
Hsu, T.-J., Chen, S.-N., & Ogston, A. S. (2013). The landward and seaward mechanisms of fine-sediment transport across intertidal flats in the shallow-water region—a numerical investigation [Hydrodynamics and sedimentation on mesotidal sand- and mudflats]. *Continental Shelf Research*, *60*, S85–S98. https://doi.org/https://doi.org/10.1016/j.csr.2012.02.003
Hulskamp, R., Luijendijk, A., van Maren, B., Moreno-Rodenas, A., Calkoen, F., Kras, E., Lhermitte, S., & Aarninkhof, S. (2023). Global distribution and dynamics of muddy coasts. *Nature Communications*, *14*(1), 8259.
Hutchison, J., Spalding, M., & zu Ermgassen, P. (2014). The role of mangroves in fisheries enhancement. *The Nature Conservancy and Wetlands International*, *54*, 434.
Jay, D. A., & Musiak, J. D. (1994). Particle trapping in estuarine tidal flows. *Journal of Geophysical Research: Oceans*, *99*(C10), 20445–20461.
Jia, M., Wang, Z., Mao, D., Ren, C., Song, K., Zhao, C., Wang, C., Xiao, X., & Wang, Y. (2023). Mapping global distribution of mangrove forests at 10-m resolution. *Science Bulletin*.
Juventud, I. d. l. (2011). Isla de la juventud - cuba. a paradise to discover. https://isladelajuventud-cuba.com/nature3.html#:~:text=Its%20hydrography%20is%20made%20up,20%20m%20above%20sea%20level.
Kathiresan, K. (2002). Why are mangroves degrading? *Current Science*, 1246–1249.
Kathiresan, K. (2003). How do mangrove forests induce sedimentation? *Revista de biologia tropical*, *51*(2), 355–360.
Kathiresan, K., & Bingham, B. (2001). Biology of mangroves and mangrove ecosystems. Academic Press. https://doi.org/https://doi.org/10.1016/S0065-2881(01)40003-4
Kemp, N. (2000). The birds of siberut, mentawai islands, west sumatra. *Kukila*, *11*, 73–96.
Kim, B. (2003). Tidal modulation of storm waves on a macrotidal flat in the yellow sea. *Estuarine, Coastal and Shelf Science*, *57*(3), 411–420.

King, C. A. (1972). Beaches and coasts. *(No Title)*.

Kirby, R. (2000). Practical implications of tidal flat shape. *Continental Shelf Research*, *20*(10-11), 1061–1077.

Klein, G. d. (1985). Intertidal flats and intertidal sand bodies. In *Coastal sedimentary environments* (pp. 187–224). Springer.

Krauss, K. W., Cahoon, D. R., Allen, J. A., Ewel, K. C., Lynch, J. C., & Cormier, N. (2010). Surface elevation change and susceptibility of different mangrove zones to sea-level rise on pacific high islands of micronesia. *Ecosystems*, *13*, 129–143.

Krauss, K., Allen, J., & Cahoon, D. (2003). Differential rates of vertical accretion and elevation change among aerial root types in micronesian mangrove forests. *Estuarine, Coastal and Shelf Science*, *56*(2), 251–259. https://doi.org/https://doi.org/10.1016/S0272-7714(02)00184-1

Kristensen, E., & Alongi, D. M. (2006). Control by fiddler crabs (uca vocans) and plant roots (avicennia marina) on carbon, iron, and sulfur biogeochemistry in mangrove sediment. *Limnology and Oceanography*, *51*(4), 1557–1571.

Kumara, M., Jayatissa, L. P., Krauss, K. W., Phillips, D., & Huxham, M. (2010). High mangrove density enhances surface accretion, surface elevation change, and tree survival in coastal areas susceptible to sea-level rise. *Oecologia*, *164*, 545–553.

Laman, T. (2009, November). Aerial view of mangrove forest and shrimp ponds in the sarawak mangrove reserve area, sarawak. https : / / www . naturepl . com / stock - photo - aerial - view - of - mangrove-forest-and-shrimp-ponds-in-the-sarawak-nature-image01245173.html

Lang'at, J. K. S. (2013). *Impacts of tree harvesting on the carbon balance and functioning in mangrove forests.* [Doctoral dissertation].

Laso Bayas, J. C., Marohn, C., Dercon, G., Dewi, S., Piepho, H. P., Joshi, L., Van Noordwijk, M., & Cadisch, G. (2011). Influence of coastal vegetation on the 2004 tsunami wave impact in west aceh. *Proceedings of the National Academy of Sciences*, *108*(46), 18612–18617.

Le Hir, P., Roberts, W., Cazaillet, O., Christie, M., Bassoullet, P., & Bacher, C. (2000). Characterization of intertidal flat hydrodynamics. *Continental shelf research*, *20*(12-13), 1433–1459.

Lee, K.-Y., Shih, S.-S., & Huang, Z.-Z. (2022). Mangrove colonization on tidal flats causes straightened tidal channels and consequent changes in the hydrodynamic gradient and siltation potential. *Journal of Environmental Management*, *314*, 115058.

Lee, S. Y., Primavera, J. H., Dahdouh-Guebas, F., McKee, K., Bosire, J. O., Cannicci, S., Diele, K., Fromard, F., Koedam, N., Marchand, C., et al. (2014). Ecological role and services of tropical mangrove ecosystems: A reassessment. *Global ecology and biogeography*, *23*(7), 726–743.

Lin, P., Pan, M., Beck, H. E., Yang, Y., Yamazaki, D., Frasson, R., David, C. H., Durand, M., Pavelsky, T. M., Allen, G. H., et al. (2019). Global reconstruction of naturalized river flows at 2.94 million reaches. *Water resources research*, *55*(8), 6499–6516.

Liu, W.-C., Hsu, M.-H., & Wang, C.-F. (2003). Modeling of flow resistance in mangrove swamp at mouth of tidal keelung river, taiwan. *Journal of waterway, port, coastal, and ocean engineering*, *129*(2), 86–92.

Liu, Z., Cheng, R., Xiao, W., Guo, Q., & Wang, N. (2014). Effect of off-season flooding on growth, photosynthesis, carbohydrate partitioning, and nutrient uptake in distylium chinense. *PloS one*, *9*(9), e107636.

Lovelock, C. E., Bennion, V., Grinham, A., & Cahoon, D. R. (2011). The role of surface and subsurface processes in keeping pace with sea level rise in intertidal wetlands of moreton bay, queensland, australia. *Ecosystems*, *14*, 745–757.

Lovelock, C. E., Sorrell, B. K., Hancock, N., Hua, Q., & Swales, A. (2010). Mangrove forest and soil development on a rapidly accreting shore in new zealand. *Ecosystems*, *13*, 437–451.

Lugo, A. E., & Snedaker, S. C. (1974). The ecology of mangroves. *Annual review of ecology and systematics*, *5*(1), 39–64.

Luijendijk, A., Hagenaars, G., Ranasinghe, R., Baart, F., Donchyts, G., & Aarninkhof, S. (2018). The state of the world's beaches. *Scientific reports*, *8*(1), 6641.

Lunt, J., & Smee, D. L. (2019). Turbidity alters estuarine biodiversity and species composition. *ICES Journal of Marine Science*, *77*(1), 379–387. https://doi.org/10.1093/icesjms/fsz214

Maa, J. P.-Y., Sanford, L., & Halka, J. P. (1998). Sediment resuspension characteristics in baltimore harbor, maryland. *Marine Geology*, *146*(1-4), 137–145.

MacKenzie, R. A., Foulk, P. B., Klump, J. V., Weckerly, K., Purbospito, J., Murdiyarso, D., Donato, D. C., & Nam, V. N. (2016). Sedimentation and belowground carbon accumulation rates in mangrove forests that differ in diversity and land use: A tale of two mangroves. *Wetlands Ecology and Management*, *24*, 245–261.

Macnae, W. (1968). A general account of the flora and fauna of mangrove swamps in the indio-west pacific region. *Advances Mar. Biol*, *6*, 73–270.

Malik, A., Mertz, O., & Fensholt, R. (2017). Mangrove forest decline: Consequences for livelihoods and environment in south sulawesi. *Regional Environmental Change*, *17*, 157–169. https://doi.org/10.1007/s10113-016-0989-0

Massel, S., Furukawa, K., & Brinkman, R. (1999). Surface wave propagation in mangrove forests. *Fluid Dynamics Research*, *24*(4), 219.

Mazda, Y., Wolanski, E., King, B., Sase, A., Ohtsuka, D., & Magi, M. (1997). Drag force due to vegetation in mangrove swamps. *Mangroves and salt marshes*, *1*, 193–199.

McCarthy, J. J. (2001). *Climate change 2001: Impacts, adaptation, and vulnerability: Contribution of working group ii to the third assessment report of the intergovernmental panel on climate change* (Vol. 2). Cambridge University Press.

McIvor, A. L., Spencer, T., Möller, I., & Spalding, M. (2013). *The response of mangrove soil surface elevation to sea level rise* (tech. rep.). The Nature Conservancy and Wetlands International. http://coastalresilience.org/science/mangroves/surface-elevation-and-sea-level-rise

McKee, K. L. (2011). Biophysical controls on accretion and elevation change in caribbean mangrove ecosystems. *Estuarine, Coastal and Shelf Science*, *91*(4), 475–483.

McKee, K. L., Cahoon, D. R., & Feller, I. C. (2007). Caribbean mangroves adjust to rising sea level through biotic controls on change in soil elevation. *Global Ecology and Biogeography*, *16*(5), 545–556.

Mei-e, R., Ren-shun, Z., & Ju-hai, Y. (1985). Effect of typhoon no. 8114 on coastal morphology and sedimentation of jiangsu province, people's republic of china. *Journal of Coastal Research*, 21–28.

Menéndez, P., Losada, I. J., Torres-Ortega, S., Narayan, S., & Beck, M. W. (2020). The global flood protection benefits of mangroves. *Scientific reports*, *10*(1), 1–11.

Miththapala, S. (2008). *Mangroves* (Vol. 2). IUCN.

Moldenke, H., et al. (1960). Materials towards a monograph of the genus avicennia. i, ii & iii. *Phytologia*, *7*(3-5), 123–93.

Morales, J. A. (2022). Tide-dominated systems ii: Tidal flats and wetlands. In *Coastal geology* (pp. 289–307). Springer.

Mullarney, J. C., Henderson, S. M., Norris, B. K., Bryan, K. R., Fricke, A. T., Sandwell, D. R., & Culling, D. P. (2017). A question of scale: How turbulence around aerial roots shapes the seabed morphology in mangrove forests of the mekong delta. *Oceanography*, *30*(3), 34–47.

Nardin, W., Locatelli, S., Pasquarella, V., Rulli, M. C., Woodcock, C. E., & Fagherazzi, S. (2016). Dynamics of a fringe mangrove forest detected by landsat images in the mekong river delta, vietnam. *Earth Surface Processes and Landforms*, *41*(14), 2024–2037.

National Office of Statistic and Information. (2017). *Anuario estadístico de cuba 2016. capítulo, vol. 1, territorio*.

Ndurya, M. (2017, February). Community carbon offset project shines in kenya's south coast. https://www.talkafrica.co.ke/community-carbon-offset-project-shines-in-kenyas-south-coast/

Nguyen, L. T. M., Hoang, H. T., Choi, E., & Park, P. S. (2023). Distribution of mangroves with different aerial root morphologies at accretion and erosion sites in ca mau province, vietnam. *Estuarine, Coastal and Shelf Science*, *287*, 108324. https://doi.org/https://doi.org/10.1016/j.ecss.2023.108324

Nidzieko, N. J. (2010). Tidal asymmetry in estuaries with mixed semidiurnal/diurnal tides. *Journal of Geophysical Research: Oceans*, *115*(C8).

Nurkin, B. (1994). Degradation of mangrove forests in south sulawesi, indonesia. *Hydrobiologia*, *285*(1–3), 271–276. https://doi.org/10.1007/bf00005673

of Australasia, M. E. S. (2015). Mangroves of australia. http://www.mesa.edu.au/mangroves/mangroves06.asp

Ohimain, E. I. (2003). Environmental impacts of oil mining activities in the niger delta mangrove ecosystem. *Proceedings of the 8th International Mine Water Association (IMWA) Conference, International Mine Water Association (IMWA), Sandton*, 503–517.

Ohira, W., Honda, K., Nagai, M., & Ratanasuwan, A. (2013). Mangrove stilt root morphology modeling for estimating hydraulic drag in tsunami inundation simulation. *Trees*, *27*, 141–148.

Ong, J., & Gong, W. (2013). Structure, function and management of mangrove ecosystems. *ISME Mangrove educational book series*, (2), 81.

online coastal information, A. (n.d.). Changes in mangrove areas. https://ozcoasts.org.au/indicators/biophysical-indicators/mangrove_areas/

OpenStreetMap. (2021). Coastlines.

Owen, M. (2014, August). *Red mangrove*. https://www.flickr.com/photos/74538007@N07/15460947200

Parelle, J., Brendel, O., Bodénès, C., Berveiller, D., Dizengremel, P., Jolivet, Y., & Dreyer, E. (2006). Differences in morphological and physiological responses to water-logging between two sympatric oak species (quercus petraea [matt.] liebl., quercus robur l.) *Annals of Forest Science*, *63*(8), 849–859.

Pernetta, J. (1993). *Mangrove forests, climate change and sea level rise: Hydrological influences on community structure and survival, with examples from the indo-west pacific*. IUCN.

Pethick, J. (1980). Velocity surges and asymmetry in tidal channels. *Estuarine and Coastal Marine Science*, *11*(3), 331–345.

Polidoro, B. A., Carpenter, K. E., Collins, L., Duke, N. C., Ellison, A. M., Ellison, J. C., Farnsworth, E. J., Fernando, E. S., Kathiresan, K., Koedam, N. E., Livingstone, S. R., Miyagi, T., Moore, G. E., Ngoc Nam, V., Ong, J. E., Primavera, J. H., Salmo, S. G., III, Sanciangco, J. C., Sukardjo, S., … Yong, J. W. H. (2010). The loss of species: Mangrove extinction risk and geographic areas of global concern. *PLOS ONE*, *5*(4), 1–10. https://doi.org/10.1371/journal.pone.0010095

Polidoro, B. A., Carpenter, K. E., Dahdouh-Guebas, F., Ellison, J. C., Koedam, N. E., & Yong, J. W. (2014). Global patterns of mangrove extinction risk: Implications for ecosystem services and biodiversity loss. *Coastal conservation*, *19*(1), 15–36.

Popkin, G. (2020, September). Mangrove loss has fallen dramatically, but the forests are still in danger. https://www.washingtonpost.com/science/mangrove-forest-loss-protection/2020/09/11/e722652a-d694-11ea-9c3b-dfc394c03988_story.html

Postma, H. (1961). Transport and accumulation of suspended matter in the dutch wadden sea. *Netherlands Journal of Sea Research*, *1*(1-2), 148–190.

Postma, H. (1954). Hydrography of the dutch wadden sea. *Arch. Neerl. Zool*, *10*, 405–511.

”Rahman, M. A. A., & Asmawi, M. Z. (2016). Recognizing the urgency of coastal stabilization: The role of a national task force committee for mangrove and coastal planting operations. *Procedia - Social and Behavioral Sciences*, *235*, 222–226. https://doi.org/10.1016/j.sbspro.2016.05.222

Rehem, B. C., Bertolde, F. Z., & de Almeida, A.-A. F. (2012). Regulation of gene expression in response to abiotic stress in plants. *InTech: London, UK*, 13–38.

Reineck, H.-E., & Singh, I. B. (2012). *Depositional sedimentary environments: With reference to terrigenous clastics*. Springer Science & Business Media.

Ren, M. (1986). Tidal mud flat. *Modern sedimentation in the coastal and nearshore zones of China. China Ocean Press, Beijing*, 78–127.

Ren, M.-e. (1985). Modern sedimentation in coastal and nearshore zone of china. *Bejing: China Ocean Press, 495p*.

Renshun, Z. (1992). Suspended sediment transport processes on tidal mud flat in jiangsu province, china. *Estuarine, Coastal and Shelf Science*, *35*(3), 225–233.

Richards, D. R., & Friess, D. A. (2016). Rates and drivers of mangrove deforestation in southeast asia, 2000–2012. *Proceedings of the National Academy of Sciences*, *113*(2), 344–349.

Rinaldi, M., & Casagli, N. (1999). Stability of streambanks formed in partially saturated soils and effects of negative pore water pressures: The sieve river (italy). *Geomorphology*, *26*(4), 253–277. https://doi.org/https://doi.org/10.1016/S0169-555X(98)00069-5

Rogers, K., & Saintilan, N. (2008). Relationships between surface elevation and groundwater in mangrove forests of southeast australia. *Journal of Coastal Research*, (24), 63–69.

Rogers, K., Saintilan, N., & Cahoon, D. (2005). Surface elevation dynamics in a regenerating mangrove forest at homebush bay, australia. *Wetlands Ecology and Management*, *13*, 587–598.

Romañach, S. S., DeAngelis, D. L., Koh, H. L., Li, Y., Teh, S. Y., Raja Barizan, R. S., & Zhai, L. (2018). Conservation and restoration of mangroves: Global status, perspectives, and prognosis. *Ocean and Coastal Management*, *154*, 72–82. https://doi.org/https://doi.org/10.1016/j.ocecoaman.2018.01.009

Saad, S., Husain, M. L., Yaacob, R., & Asano, T. (1999). Sediment accretion and variability of sedimentological characteristics of a tropical estuarine mangrove: Kemaman, terengganu, malaysia. *Mangroves and salt marshes*, *3*, 51–58.

Sanderman, J., Hengl, T., Fiske, G., Solvik, K., Adame, M. F., Benson, L., Bukoski, J. J., Carnell, P., Cifuentes-Jara, M., Donato, D., Duncan, C., Eid, E. M., zu Ermgassen, P., Lewis, C. J. E., Macreadie, P. I., Glass, L., Gress, S., Jardine, S. L., Jones, T. G., … Landis, E. (2018). A global map of mangrove forest soil carbon at 30 m spatial resolution. *Environmental Research Letters*, *13*(5), 055002. https://doi.org/10.1088/1748-9326/aabe1c

Schaeffer-Novelli, Y., & Cintron, G. M. (1986). *Guia para estudo de áreas de manguezal: Estrutura, função e flora*.

Schaeffer-Novelli, Y., & Cintron, G. M. (1988). *Expedição nacional aos manguezais do amapá, ilha de maracá* [Unpublished Report].

Scobel, N. (2008, June). *Mangrove swamp*. https://www.flickr.com/photos/michiganherper/3172168780/

Selvam, V., & Karunagaran, V. (2019, May). *Ecology and biology of mangroves orientation guide*.

Semeniuk, V. (1981). Long-term erosion of the tidal flats king sound, north western australia. *Marine Geology*, *43*(1-2), 21–48.

Sevvel. (2017, September). The root system. http://www.happybotanist.com/the-root-system/

Sherman, R. E., Fahey, T. J., & Martinez, P. (2001). Hurricane impacts on a mangrove forest in the dominican republic: Damage patterns and early recovery 1. *Biotropica*, *33*(3), 393–408.

Shi, Z. (1991). Tidal bedding and tidal cyclicities within the intertidal sediments of a microtidal estuary, dyfi river estuary, west wales, u.k. *Sedimentary Geology*, *73*(1), 43–58. https://doi.org/https://doi.org/10.1016/0037-0738(91)90022-6

Silvestri, S., Kershaw, F., et al. (2010). *Framing the flow: Innovative approaches to understand, protect and value ecosystem services across linked habitats*. UNEP Nairobi, Kenya.

Sin, A. (2014, June). *Pneumatophores of the white mangroves*. https://www.flickr.com/photos/10811135@N00/14169762417

Smith, T. J., Robblee, M. B., Wanless, H. R., & Doyle, T. W. (1994). Mangroves, hurricanes, and lightning strikes. *BioScience*, *44*(4), 256–262.

Snedaker, S. C. (1993). Impact on mangroves. *Climate change in the intra-American seas: implications of future climate change on the ecosystems and socio-economic structure of the marine and coastal regimes of the Caribbean Sea, Gulf of Mexico, Bahamas and NE Coast of South America. Edward Arnold, London*, 282–305.

Solomon, S., Qin, D., Manning, M., Alley, R. B., Berntsen, T., Bindoff, N. L., Chen, Z., Chidthaisong, A., Gregory, J. M., Hegerl, G. C., et al. (2007). Technical summary.

Soltanpour, M., & Haghshenas, S. (2009). Fluidization and representative wave transformation on muddy beds [On the dynamics of mud deposits in coastal areas]. *Continental Shelf Research*, *29*(3), 666–675. https://doi.org/https://doi.org/10.1016/j.csr.2008.09.016

Song, D., Wang, X. H., Kiss, A. E., & Bao, X. (2011). The contribution to tidal asymmetry by different combinations of tidal constituents. *Journal of Geophysical Research: Oceans*, *116*(C12).

Spalding, M., Mcivor, A., Tonneijck, F., Tol, S., & van Eijk, P. (2014, January). *Mangroves for coastal defence. guidelines for coastal managers and policy makers*.

Spalding, M. D., Blasco, F., & Field, C. (1997). World mangrove atlas. https://api.semanticscholar.org/CorpusID:126423173

Spalding, M. D., Leal, M., Andradi-Brown, D., Longley-Wood, K., Friess, D., Beck, M., Beeston, M., Bunting, P., Connolly, R., Dahdouh-Guebas, F., Fatoyinbo, L., Gatt, Y., Geselbracht, L., Glass, L., Goldberg, L., Herr, D., Hilarides, L., Lagomasino, D., Landis, E., … Francis, E. (2021, August). *The state of the world's mangroves 2021*.

Spencer, T., M□ller, I., & Reef, R. (2016). Mangrove systems and environments. In *Reference module in earth systems and environmental sciences*. Elsevier.

Srikanth, S., Lum, S. K. Y., & Chen, Z. (2016). Mangrove root: Adaptations and ecological importance. *Trees*, *30*, 451–465.

Steers, J., Chapman, V., Colman, J., & Lofthouse, J. (1940). Sand cays and mangroves in jamaica cambridge university jamaica expedition, 1939 meeting of the society, 15 april 1940. *The Geographical Journal*, *96*(5), 305–328.

Swales, A., Bentley Sr, S. J., & Lovelock, C. E. (2015). Mangrove-forest evolution in a sediment-rich estuarine system: Opportunists or agents of geomorphic change? *Earth Surface Processes and Landforms*, *40*(12), 1672–1687.

Swales, A., Pritchard, M., & McBride, G. B. (2021). Biogeomorphic evolution and expansion of mangrove forests in new zealand's sediment-rich estuarine systems. In *Dynamic sedimentary environments of mangrove coasts* (pp. 3–45). Elsevier.

Tait, J. F., & Griggs, G. B. (1991). *Beach response to the presence of a sea wall: Comparison of field observations* (tech. rep.). USACE.

Te Brake, B., & Van Huijgevoort, M. (2008). *Hydrological characterization of mangrove forests in can gio and ca mau, vietnam* [Master's thesis, Wageningen University, Department of Environmental Sciences, The Netherlands] [Available on: http://www.slideshare.net/BramteBrake/te-brake-and-van-huijgevoort-2008-hydrological-classification-of-mangrove-forests-in-can-gio-and-ca-mau-vietnam].

Testbook. (2023, March). Consolidation of soil - learn about properties, types, process. https://testbook.com/civil-engineering/consolidation-of-soils-meaning-and-types

Thampanya, U., Vermaat, J., Sinsakul, S., & Panapitukkul, N. (2006). Coastal erosion and mangrove progradation of southern thailand. *Estuarine, coastal and shelf science*, *68*(1-2), 75–85.

Thampanya, U. (2006). *Mangroves and sediment dynamics along the coasts of southern thailand*. Wageningen University; Research.

Thom, B. G. (1984). Coastal landforms and geomorphic processes. *Monographs on oceanographic methodology*, *8*, 3–17.

Thomas, N., Lucas, R., Bunting, P., Hardy, A., Rosenqvist, A., & Simard, M. (2017). Distribution and drivers of global mangrove forest change, 1996–2010. *PloS one*, *12*(6), e0179302.

Tian, J., Zhao, X., Gao, S., Wang, X., & Zhang, R. (2021). Progress in research and application of nanofiltration (nf) technology for brackish water treatment. *Membranes*, *11*(9), 662.

Tomlinson, P. B. (2016). *The botany of mangroves* (2nd ed.). Cambridge University Press. https://doi.org/10.1017/CBO9781139946575

Twilley, R. R., & Rivera-Monroy, V. H. (2009). Ecogeomorphic models of nutrient biogeochemistry for mangrove wetlands. *Coastal wetlands: an integrated ecosystem approach*, *1*, 641–684.

Uncles, R. (1981). A note on tidal asymmetry in the severn estuary. *Estuarine, coastal and shelf science*, *13*(4), 419–432.

Valiela, I., Bowen, J. L., & York, J. K. (2001). Mangrove forests: One of the world's threatened major tropical environments: At least 35% of the area of mangrove forests has been lost in the past two decades, losses that exceed those for tropical rain forests and coral reefs, two other well-known threatened environments. *Bioscience*, *51*(10), 807–815.

van Bijsterveldt, C. E., van Wesenbeeck, B. K., van der Wal, D., Afiati, N., Pribadi, R., Brown, B., & Bouma, T. J. (2020). How to restore mangroves for greenbelt creation along eroding coasts with abandoned aquaculture ponds. *Estuarine, Coastal and Shelf Science*, *235*, 106576. https://doi.org/https://doi.org/10.1016/j.ecss.2019.106576

Van de Kreeke, J., & Robaczewska, K. (1993). Tide-induced residual transport of coarse sediment; application to the ems estuary. *Netherlands Journal of Sea Research*, *31*(3), 209–220.

Van der Ham, R., & Winterwerp, J. (2001). Turbulent exchange of fine sediments in a tidal channel in the ems/dollard estuary. part ii. analysis with a 1dv numerical model. *Continental Shelf Research*, *21*(15), 1629–1647.

van Loon, A., Dijksma, R., & van Mensvoort, M. (2007). Hydrological classification in mangrove areas: A case study in can gio, vietnam. *Aquatic Botany*, *87*(1), 80–82. https://doi.org/https://doi.org/10.1016/j.aquabot.2007.02.001

Van Maren, D., & Gerritsen, H. (2012). Residual flow and tidal asymmetry in the singapore strait, with implications for resuspension and residual transport of sediment. *Journal of Geophysical Research: Oceans*, *117*(C4).

van Maren, D., & Winterwerp, J. (2013). The role of flow asymmetry and mud properties on tidal flat sedimentation [Hydrodynamics and sedimentation on mesotidal sand- and mudflats]. *Continental Shelf Research*, *60*, S71–S84. https://doi.org/https://doi.org/10.1016/j.csr.2012.07.010

Van Straaten, L., & Kuenen, P. H. (1957). Accumulation of fine grained sediments in the dutch wadden sea. *Geologie en mijnbouw*, *19*(1954), 329–354.
van Loon, A. F., Te Brake, B., Van Huijgevoort, M. H., & Dijksma, R. (2016). Hydrological classification, a practical tool for mangrove restoration. *PLoS One*, *11*(3), e0150302.
van Maanen, B., Coco, G., & Bryan, K. R. (2013). Modelling the effects of tidal range and initial bathymetry on the morphological evolution of tidal embayments. *Geomorphology*, *191*, 23–34.
Verhagen, H., & Loi, T. T. (2012). The use of mangroves in coastal protection. *The 8th International Conference on Coastal and Port Engineering in Developing Countries (COPEDEC) India*, 20–24.
Viles, H. A. (1988). Biogeomorphology. *(No Title)*.
Wang, Y. P., Zhang, R., & Gao, S. (1999). Velocity variations in salt marsh creeks, jiangsu, china. *Journal of Coastal Research*, 471–477.
Ward, R. D., Friess, D. A., Day, R. H., & Mackenzie, R. A. (2016). Impacts of climate change on mangrove ecosystems: A region by region overview. *Ecosystem Health and sustainability*, *2*(4), e01211.
Watson, J. (1928). Mangrove forests of the malay peninsula. *Malay Forest Records*, *6*, 1–275.
Wells, J. T., & Roberts, H. H. (1980). Fluid mud dynamics and shoreline stabilization: Louisiana chenier plain. In *Coastal engineering 1980* (pp. 1382–1401).
Whelan, K. R. T. (2005). *The successional dynamics of lightning-initiated canopy gaps in the mangrove forests of shark river, everglades national park, usa*. Florida International University.
Whitehouse, R. J., & Mitchener, H. J. (1998). Observations of the morphodynamic behaviour of an intertidal mudflat at different timescales. *Geological Society, London, Special Publications*, *139*(1), 255–271.
Whitten, A. J., & Whitten, J. E. (1982). Preliminary observations of the mentawai macaque on siberut island, indonesia. *International Journal of Primatology*, *3*, 445–459.
Wiberg, P. L., & Sherwood, C. R. (2008). Calculating wave-generated bottom orbital velocities from surface-wave parameters [Predictive Modeling in Sediment Transport and Stratigraphy]. *Computers and Geosciences*, *34*(10), 1243–1262. https://doi.org/https://doi.org/10.1016/j.cageo.2008.02.010
Winterwerp, J. C., Borst, W. G., & De Vries, M. B. (2005). Pilot study on the erosion and rehabilitation of a mangrove mud coast. *Journal of Coastal Research*, *21*(2), 223–230.
Wolanski, E., Jones, M., & Bunt, J. (1980). Hydrodynamics of a tidal creek-mangrove swamp system. *Marine and Freshwater Research*, *31*(4), 431–450.
Woodroffe, C. (1993). Geomorphological and climatic setting and the development of mangrove forests. *Towards the rational use of high salinity tolerant plants: Vol. 1 Deliberations about High Salinity Tolerant Plants and Ecosystems*, 13–20.
Woodroffe, C., & Grime, D. (1999). Storm impact and evolution of a mangrove-fringed chenier plain, shoal bay, darwin, australia. *Marine Geology*, *159*(1-4), 303–321.
Woodroffe, C. (1992). Mangrove sediments and geomorphology. *Tropical mangrove ecosystems*, *41*, 7–41.
Woodroffe, C. D. (1990). The impact of sea-level rise on mangrove shorelines. *Progress in Physical Geography*, *14*(4), 483–520.
Woodroffe, C. D. (1995). Response of tide-dominated mangrove shorelines in northern australia to anticipated sea-level rise. *Earth surface processes and landforms*, *20*(1), 65–85.
Woodroffe, C. D. (2000). Deltaic and estuarine environments and their late quaternary dynamics on the sunda and sahul shelves. *Journal of Asian Earth Sciences*, *18*(4), 393–413. https://doi.org/https://doi.org/10.1016/S1367-9120(99)00074-7
Woodroffe, C. D., & Davies, G. (2009). The morphology and development of tropical coastal wetlands.
Woodroffe, C. D., Rogers, K., McKee, K. L., Lovelock, C. E., Mendelssohn, I., & Saintilan, N. (2016). Mangrove sedimentation and response to relative sea-level rise. *Annual review of marine science*, *8*, 243–266.
Woodroffe, C. D., Thom, B. G., & Chappell, J. (1985). Development of widespread mangrove swamps in mid-holocene times in northern australia. *Nature*, *317*(6039), 711–713.
Worthington, T., & Spalding, M. (2018). Mangrove restoration potential: A global map highlighting a critical opportunity.

Worthington, T. A., Zu Ermgassen, P. S., Friess, D. A., Krauss, K. W., Lovelock, C. E., Thorley, J., Tingey, R., Woodroffe, C. D., Bunting, P., Cormier, N., et al. (2020). A global biophysical typology of mangroves and its relevance for ecosystem structure and deforestation. *Scientific reports*, *10*(1), 14652.

Wright, L. (1985). River deltas. In *Coastal sedimentary environments* (pp. 5–68). Springer.

Wright, L., & Coleman, J. M. (1973). Variations in morphology of major river deltas as functions of ocean wave and river discharge regimes. *AAPG Bulletin*, *57*(2), 370–398.

Wright, L., Coleman, J. M., & Thom, B. G. (1973). Processes of channel development in a high-tide-range environment: Cambridge gulf-ord river delta, western australia. *The Journal of Geology*, *81*(1), 15–41.

Wright, L., Wiseman, W., Bornhold, B., Prior, D., Suhayda, J., Keller, G., Yang, Z.-S., & Fan, Y. (1988). Marine dispersal and deposition of yellow river silts by gravity-driven underflows. *Nature*, *332*(6165), 629–632.

Wu, Y., Falconer, R. A., & Struve, J. (2001). Mathematical modelling of tidal currents in mangrove forests. *Environmental Modelling & Software*, *16*(1), 19–29.

Xiao, H., Su, F., Fu, D., Wang, Q., & Huang, C. (2020). Coastal mangrove response to marine erosion: Evaluating the impacts of spatial distribution and vegetation growth in bangkok bay from 1987 to 2017. *Remote Sensing*, *12*(2), 220.

Xin, J. (2010, April). Plants in the mangrove part 1. http://the-nature-in-us.blogspot.com/2010/04/what-we-learn-in-mangrove.html

Yang, B., Dalrymple, R., & Chun, S. (2005). Sedimentation on a wave-dominated, open-coast tidal flat, south-western korea: Summer tidal flat–winter shoreface. *Sedimentology*, *52*(2), 235–252.

Yang, Y., Wang, Y. P., & Gao, S. (2003). Hydrodynamic processes and suspended sediment transport in salt-marsh creeks, wanggang, jiangsu, china. *Sedimentation in the Yellow Sea Coasts. Hanrimwon Publishing Co., Seoul*, 79–87.

Young, B. M., & Harvey, E. L. (1996). A spatial analysis of the relationship between mangrove (avicennia marinavar. australasica) physiognomy and sediment accretion in the hauraki plains, new zealand. *Estuarine, Coastal and Shelf Science*, *42*(2), 231–246.

Young, T. P., & Perkocha, V. (1994). Treefalls, crown asymmetry, and buttresses. *Journal of Ecology*, 319–324.

Zhang, X., Chua, V. P., & Cheong, H.-F. (2015). Hydrodynamics in mangrove prop roots and their physical properties [Special Issue on Environmental Hydraulics]. *Journal of Hydro-environment Research*, *9*(2), 281–294. https://doi.org/https://doi.org/10.1016/j.jher.2014.07.010

Zhu, Q. (2017). *Sediment dynamics on intertidal mudflats: A study based on in situ measurements and numerical modelling* [Doctoral dissertation, Delft University of Technology]. https://doi.org/10.4233/uuid:5f094e4b-fef9-4216-abbe-3277adc90b28

zu Ermgassen, P. S., Mukherjee, N., Worthington, T. A., Acosta, A., da Rocha Araujo, A. R., Beitl, C. M., Castellanos-Galindo, G. A., Cunha-Lignon, M., Dahdouh-Guebas, F., Diele, K., Parrett, C. L., Dwyer, P. G., Gair, J. R., Johnson, A. F., Kuguru, B., Savio Lobo, A., Loneragan, N. R., Longley-Wood, K., Mendonça, J. T., … Spalding, M. (2020). Fishers who rely on mangroves: Modelling and mapping the global intensity of mangrove-associated fisheries. *Estuarine, Coastal and Shelf Science*, *247*, 106975. https://doi.org/https://doi.org/10.1016/j.ecss.2020.106975